



UNIVERSITAT ROVIRA I VIRGILI

CONTRIBUTION TO THE DEVELOPMENT OF MATHEMATICAL PROGRAMMING TOOLS TO ASSIST DECISION-MAKING IN SUSTAINABILITY PROBLEMS

Ángel Galán Martín

ADVERTIMENT. L'accés als continguts d'aquesta tesi doctoral i la seva utilització ha de respectar els drets de la persona autora. Pot ser utilitzada per a consulta o estudi personal, així com en activitats o materials d'investigació i docència en els termes establerts a l'art. 32 del Text Refós de la Llei de Propietat Intel·lectual (RDL 1/1996). Per altres utilitzacions es requereix l'autorització prèvia i expressa de la persona autora. En qualsevol cas, en la utilització dels seus continguts caldrà indicar de forma clara el nom i cognoms de la persona autora i el títol de la tesi doctoral. No s'autoritza la seva reproducció o altres formes d'explotació efectuades amb finalitats de lucre ni la seva comunicació pública des d'un lloc aliè al servei TDX. Tampoc s'autoritza la presentació del seu contingut en una finestra o marc aliè a TDX (framing). Aquesta reserva de drets afecta tant als continguts de la tesi com als seus resums i índexs.

ADVERTENCIA. El acceso a los contenidos de esta tesis doctoral y su utilización debe respetar los derechos de la persona autora. Puede ser utilizada para consulta o estudio personal, así como en actividades o materiales de investigación y docencia en los términos establecidos en el art. 32 del Texto Refundido de la Ley de Propiedad Intelectual (RDL 1/1996). Para otros usos se requiere la autorización previa y expresa de la persona autora. En cualquier caso, en la utilización de sus contenidos se deberá indicar de forma clara el nombre y apellidos de la persona autora y el título de la tesis doctoral. No se autoriza su reproducción u otras formas de explotación efectuadas con fines lucrativos ni su comunicación pública desde un sitio ajeno al servicio TDR. Tampoco se autoriza la presentación de su contenido en una ventana o marco ajeno a TDR (framing). Esta reserva de derechos afecta tanto al contenido de la tesis como a sus resúmenes e índices.

WARNING. Access to the contents of this doctoral thesis and its use must respect the rights of the author. It can be used for reference or private study, as well as research and learning activities or materials in the terms established by the 32nd article of the Spanish Consolidated Copyright Act (RDL 1/1996). Express and previous authorization of the author is required for any other uses. In any case, when using its content, full name of the author and title of the thesis must be clearly indicated. Reproduction or other forms of for profit use or public communication from outside TDX service is not allowed. Presentation of its content in a window or frame external to TDX (framing) is not authorized either. These rights affect both the content of the thesis and its abstracts and indexes.

Contribution to the development of mathematical programming tools to assist decision-making in sustainability problems

Ángel Galán Martín



DOCTORAL THESIS

2018

UNIVERSITAT ROVIRA I VIRGLI

CONTRIBUTION TO THE DEVELOPMENT OF MATHEMATICAL PROGRAMMING TOOLS TO ASSIST DECISION-MAKING
IN SUSTAINABILITY PROBLEMS

Àngel Galán Martín

UNIVERSITAT ROVIRA I VIRGLI

CONTRIBUTION TO THE DEVELOPMENT OF MATHEMATICAL PROGRAMMING TOOLS TO ASSIST DECISION-MAKING
IN SUSTAINABILITY PROBLEMS

Àngel Galán Martín

UNIVERSITAT ROVIRA I VIRGLI

CONTRIBUTION TO THE DEVELOPMENT OF MATHEMATICAL PROGRAMMING TOOLS TO ASSIST DECISION-MAKING
IN SUSTAINABILITY PROBLEMS

Àngel Galán Martín

Ángel Galán Martín

Contribution to the development of mathematical programming tools to assist decision-making in sustainability problems

Doctoral Thesis

Supervised by: Dr. Gonzalo Guillén Gosálbez

Dr. Laureano Jiménez Esteller



DEPARTMENT OF CHEMICAL ENGINEERING

SUSCAPE RESEARCH GROUP



UNIVERSITY ROVIRA I VIRGILI

TARRAGONA

2018

UNIVERSITAT ROVIRA I VIRGLI

CONTRIBUTION TO THE DEVELOPMENT OF MATHEMATICAL PROGRAMMING TOOLS TO ASSIST DECISION-MAKING
IN SUSTAINABILITY PROBLEMS

Àngel Galán Martín



**UNIVERSITAT
ROVIRA I VIRGILI**

We state that the present study, entitled “Contribution to the development of mathematical programming tools to assist decision-making in sustainability problems”, presented by Ángel Galán Martín for the award of the degree of Doctor, has been carried out under our supervision at the Department of Chemical Engineering of this university.

Tarragona, 7th November 2017

Doctoral Thesis Supervisor/s

Dr. Gonzalo Guillén Gosálbez

Dr. Laureano Jiménez Esteller

Agradecimientos

En primer lugar, pido disculpas todas las personas que no aparecen aquí explícitamente, pero que de alguna u otra forma dedicaron su tiempo, esfuerzos, consejos y apoyo contribuyendo a la realización de esta tesis.

Asimismo, me gustaría expresar mi más sincero agradecimiento a mis supervisores, el Dr. Gonzalo Guillén Gosálbez y el Dr. Laureano Jiménez Esteller, tanto por brindarme la oportunidad de llevar a cabo mi doctorado, como por su orientación continua, consejos y todo el conocimiento que me transmitieron. Me gustaría también expresar mi gratitud a todos los miembros del grupo de investigación SUSCAPE, especialmente a aquellos que estuvieron trabajando a mi lado durante este período, por su compañerismo, soporte y paciencia. Además me gustaría expresar mi agradecimiento a todos mis queridos amigos, los viejos y los nuevos, de aquí y de allá, gracias a todos por nuestra amistad, nunca os olvidaré.

Finalmente, me gustaría dedicar esta tesis a mi familia. Primeramente, me gustaría expresar mi profundo sentido de gratitud hacia mis padres, Ángel y Begoña, y a mi hermana Esther, os debo mi vida y lo que soy hoy en día, os estaré eternamente agradecido por vuestro amor y apoyo incondicional a lo largo de mi vida. Unidos somos más fuertes para salir adelante. Gracias también a mi querida tía Arancha, por tu cariño y no faltar nunca. Gracias también a mi abuelo Ángel, maestro de vida, donde quiera que estés, tú me enseñaste con tu ejemplo. Por último, y no por eso menos importante, la familia que yo elegí, Eva, gracias por compartir tu vida conmigo y por permanecer a mi lado para fortalecerme, tú me ayudas a ser mi mejor yo, por lo vivido y lo que nos queda por vivir.

Os debo mucho a todos vosotros. Soy lo que soy gracias a vosotros. Sin duda, sin vosotros, esto no hubiera sido posible. Mil gracias de todo corazón.

Summary

Responding to the ongoing and emerging global sustainability challenges is crucial to promote a sustainable growth and development. Impacts and burdens of human activities are exceeding the Earth's carrying capacity, overstepping the safe limits our planet sets for us, which may lead to abrupt or irreversible environmental changes. At the same time, the unstoppable growth of the world population will lead to increased demands as well as higher pressures on the environment. Without taking actions, issues such as climate change, environmental degradation or resources depletion may create unprecedented and perhaps irreversible situations that pose a serious threat to future human well-being and the environment.

There is no doubt that a shift is needed for sustainability which calls for effective solutions when facing problems contributing to the transition towards a more sustainable development. Unfortunately, sustainability challenges often led to very complex problems, where many interrelated aspects and several conflicting stakeholder's preferences have to be considered simultaneously, for which making good decisions become extremely difficult. In this regard, research-based information facing such problems may play an important role in decision and policy-making support to formulate adequate strategies and policies to accelerate the transition toward a sustainable future. This thesis is devoted to tackle different sustainability issues by developing systematic mathematical programming tools aiming at supporting the sustainable decision and policy-making which ultimately will lead to the development of more efficient mechanisms to foster sustainability.

Against this background, there is a growing attention to the need for structural transformations in the way societies interact with the natural environment as the basis to reconnect the human development to sustained

progress. In particular, this thesis focuses on two key transformations: the “*food security transformation*”, through decoupling the intensification of food production from unsustainable use of resources; and the “*clean energy transformation*”, supporting the shift towards an environmentally friendly economy. Regarding the former transformation, where agricultural sustainability has a key role to play, two mathematical programming models were developed aiming to foster more sustainable agricultural practises. With respect to the latter energy transformation, two mathematical programming models are proposed, one to support transition-makers to select and improve technologies, and, the other to promote the collective actions so that forging ahead with an effective clean energy transition.

Four major contributions are made in this thesis. First, a multi-objective tool is proposed to optimal allocate cropping areas considering simultaneously economic and environmental criteria. Second, a multi-period model is proposed to determine optimal cropping plans and subsidies to promote agricultural practices beneficial to the climate and the environment. Third, a novel data envelopment analysis methodology tailored to perform sustainability assessments is proposed, which allows comparing systems (e.g. electricity technologies) and also provides targets for improvement according to the extent to which they adhere to sustainability principles. Fourth, an optimised cooperative approach is proposed to promote and strengthen international cooperation in the fight against climate change.

In summary, this thesis provides sound systematic mathematical programming tools to support decision and policy-making on the path to sustainability, which are flexible and practical enough to contribute towards a more sustainable agriculture and a more sustainable energy future. Although there will be major sustainability challenges ahead, contributions such as those sought in this thesis, although apparently insignificant, may bring major strides in the transition towards a new era where the economy, society and the environment coexist as key pillars of sustainable development.

Resumen

Dar respuesta a los grandes desafíos de sostenibilidad actuales, emergentes y futuros constituye un gran reto que es necesario enfrentar con el fin de promover y finalmente poder conseguir un crecimiento y desarrollo sostenible. La actividad humana genera impactos ambientales que actualmente exceden la resiliencia de nuestros ecosistemas y en último término la capacidad de carga de la Tierra, es decir, se están violando los límites que nuestro planeta nos ha impuesto, lo cual puede derivar en cambios ambientales bruscos o irrecuperables. Al mismo tiempo, el imparable crecimiento de la población mundial conlleva un aumento de la demanda y por lo tanto una mayor presión sobre el medio ambiente. Si se producen retrasos en la adopción de las medidas adecuadas, problemas ambientales tales como el cambio climático, la degradación del medio ambiente o el agotamiento de los recursos pueden llevarnos a una situación sin precedentes, y tal vez irreversible, que puede suponer una seria amenaza para el futuro bienestar del ser humano y el medio ambiente.

No hay duda de que es imprescindible tomar decisiones drásticas y realizar transformaciones que nos acerquen hacia un estado sostenible, lo cual requiere dar soluciones eficaces cuando se aborden los problemas de sostenibilidad existentes. Desafortunadamente, los retos para alcanzar un desarrollo sostenible generalmente llevan vinculados problemas de sostenibilidad muy complejos en los cuales se deben considerar simultáneamente numerosos aspectos y preferencias de diversos grupos de interés, por lo cual tomar las decisiones adecuadas es extremadamente complicado. En este sentido, la información derivada de la investigación científica, en particular la dedicada al desarrollo de sistemas de apoyo para la toma de decisiones, puede desempeñar un papel fundamental dando soporte a los responsables de la formulación de estrategias y políticas orientadas a acelerar la

transición hacia un futuro sostenible. En esta tesis se han abordado distintos problemas de sostenibilidad y se han desarrollado diferentes herramientas sistemáticas de soporte a las decisiones basadas en modelos matemáticos de optimización con el objetivo de facilitar el proceso de toma de decisiones y de formulación de políticas sostenibles efectivas.

Con este contexto de fondo, cada vez se está prestando más atención a la necesidad de realizar transformaciones estructurales en la forma en que las sociedades interactúan entre sí mismas y con el entorno natural cuyo objetivo es el de volver a conectar el desarrollo humano con el progreso sostenible. En particular, esta tesis se centra en contribuir a dos transformaciones estructurales consideradas clave que son: "la transformación hacia una seguridad alimentaria sostenible" desacoplando la intensificación agrícola del uso insostenible de los recursos; y la "transformación hacia un modelo energético sostenible", apoyando el cambio hacia una economía respetuosa con el medio ambiente. Con respecto a la primera transformación, donde la agricultura juega un papel fundamental, se han desarrollado dos modelos de programación matemática cuyo objetivo es fomentar prácticas agrícolas más sostenibles. Con respecto a la transformación energética sostenible, se propone un nuevo método que permite seleccionar y establecer mejoras en las tecnologías de acuerdo a criterios de sostenibilidad, y también se propone un nuevo enfoque para incentivar una acción colectiva para avanzar de manera efectiva en la transición hacia una energía limpia.

Entrando más en detalles, de esta tesis se derivan cuatro contribuciones principales. En primer lugar, se propone una herramienta de optimización multiobjetivo que permite la asignación de áreas de cultivo óptimas considerando criterios económicos y ambientales simultáneamente. En segundo lugar, se propone un modelo de optimización multiperiodo que permite determinar los planes de cultivo y los subsidios óptimos para promover prácticas agrícolas beneficiosas para el clima y el medio ambiente. En tercer lugar, se propone una nueva metodología de

análisis de la envolvente de datos adaptada para la realización de estudios de evaluación de la sostenibilidad que permite comparar sistemas entre sí (por ejemplo, tecnologías de electricidad) y que además proporciona mejoras potenciales de acuerdo con el grado en que se adhieren a los principios de sostenibilidad. En cuarto lugar, se propone un nuevo enfoque basado en la optimización de acciones cooperativas con el objetivo de promover y fortalecer la cooperación internacional en la lucha efectiva contra el cambio climático.

En resumen, esta tesis proporciona herramientas sólidas, prácticas y flexibles de apoyo a la toma de decisiones y a la formulación de políticas en el camino hacia la sostenibilidad que pueden contribuir a conseguir una agricultura más sostenible y a movernos hacia un futuro energético más respetuoso con el medio ambiente. A pesar de los enormes desafíos de sostenibilidad a los que nos enfrentamos, contribuciones como las derivadas de esta tesis, aunque parezcan insignificantes, pueden ayudar a realizar avances hacia una nueva era donde la economía, la sociedad y el ambiente coexistan como pilares clave del desarrollo sostenible.

TABLE OF CONTENTS

I.	Introduction.....	1
1.1	Background and motivation	1
1.2	General objectives.....	6
1.3	Optimal sustainable decision making framework.....	7
1.4	Mathematical programming: optimisation	11
1.4.1	Single objective constrained optimisation problems.....	12
1.4.2	Multiobjective optimisation problems.....	16
1.4.3	Data envelopment analysis	19
1.4.4	Uncertainty: sensitivity analysis	25
1.4.5	Modelling frameworks	28
1.5	Environmental impact assessment.....	29
1.5.1	Life cycle assessment.....	29
1.6	Outline: problems addressed	35
1.6.1	Sustainable allocation of cropping areas (article 1)	35
1.6.2	Sustainable cropping plan decisions and subsidies (Article 2).....	37
1.6.3	Data envelopment analysis for sustainability assessment (Article 3).....	39
1.6.4	Tackling climate change in cooperation (Article 4)	41
1.7	General conclusions	43
1.8	Future work	45
1.9	References.....	47
II.	Sustainable allocation of cropping areas	59

2.1	Introduction.....	59
2.2	Model description and solution method.....	63
2.1.1	Multi-objective linear programming model.....	63
2.1.2	Solution method: multi-objective optimisation.....	67
2.3	Case study.....	69
2.4	Results and discussion.....	75
2.4.1	3-Dimensional objective space.....	75
2.4.2	2-Dimensional Objectives Spaces.....	78
2.4.3	Optimal rainfed and irrigated cropping areas.....	82
2.4.4	Sensitivity analysis.....	85
2.5	Conclusions.....	89
2.6	Acknowledgements.....	91
2.7	Nomenclature.....	91
2.8	References.....	92
2.9	Appendix: estimation of the crop water requirements.....	99
1.9.1	Wheat water use calculation.....	103
III.	Sustainable cropping plans decisions and subsidies.....	111
3.1	Introduction.....	111
3.2	Problem statement.....	115
3.3	Multi-stage linear programming model.....	118
3.4	Case study.....	121
3.5	Results and discussion.....	128
3.6	Basic value payment adjusted: effective subsidy.....	134
3.7	Conclusions.....	137

3.8	Acknowledgements	138
3.9	References.....	138
3.10	Appendix: optimal cropping plan for the Spanish agricultural regions	142
IV.	DEA for sustainability assessment.....	151
4.1	Introduction.....	151
4.2	Motivating example.....	156
4.3	Methodology	157
4.3.1	Data envelopment analysis	157
4.3.2	Enhanced data envelopment analysis: order of efficiency	164
4.4	Application of the enhanced DEA method to a real case study	173
4.4.1	Efficiency of different sustainability dimensions	176
4.4.2	Overall sustainability efficiency.....	178
4.4.3	Inefficiency assessment.....	179
4.5	Conclusions.....	181
4.6	Acknowledgements	182
4.7	References.....	182
V.	Tacking climate change in cooperation.....	191
5.1	Introduction.....	191
5.2	Emissions Reduction Cooperation Model	194
5.3	Results and discussion.....	198
5.3.1	Benefits of increasing cooperation	198
5.3.2	Implications for electricity supply	200
5.3.3	Implications for carbon mitigation	204
5.3.4	Implications for costs	206

5.3.5	Sharing of cooperation benefits	207
5.3.6	Cooperation benefits under uncertainty.....	210
5.4	Conclusions.....	210
5.5	Acknowledgements	213
5.6	References.....	213
5.7	Appendix: methods, supplementary results and sensitivity analysis..	218
5.7.1	Methods	218
5.7.2	Supplementary results	260
5.7.3	Sensitivity analysis.....	271
5.7.4	Nomenclature.....	277
5.7.5	References.....	279
VI.	APPENDIX	285
5.8	List of publications.....	285
5.8.1	Research articles.....	285
5.8.2	Book chapters.....	286
5.9	Scientific conferences participations.....	286
5.9.1	Oral communications	286
5.9.2	Poster presentations	286

Chapter I

Introduction

UNIVERSITAT ROVIRA I VIRGLI

CONTRIBUTION TO THE DEVELOPMENT OF MATHEMATICAL PROGRAMMING TOOLS TO ASSIST DECISION-MAKING
IN SUSTAINABILITY PROBLEMS

Àngel Galán Martín

I. Introduction

1.1 Background and motivation

Society today is facing a new era of great sustainability challenges. The unstoppable population growth, rising demand pressures and the ecosystems and climate crisis, call for actions that allow us to move towards a more sustainable development. To that end, so as to achieve sustainable future, it is essential *“to meet the needs of the present without compromising the ability of future generations to meet their own needs”* (WCED, 1987), which involve the simultaneous pursuit and balanced satisfaction of economic, environmental, and social goals reflecting the three pillars of sustainability (Pope *et al.*, 2004a; Todorov and Marinova, 2011). There is no doubt that a shift is needed for sustainability which requires taking actions and implementing new concrete decisions, initiatives, strategies, projects, programs, plans and policies in line with such sustainability principles. Unfortunately, this is far from being an easy task since encompassing the three dimensions of sustainability leads to complex multi-stakeholders problems. Prioritisation of efforts to address present and emerging sustainability problems should become of paramount importance that would benefit both the environment and the society by identifying proactive pathways towards sustainability. In this context, research-based information facing such problems may play a major role in decision and policy-making support to accelerate the effective shift toward a sustainable development.

Impacts and burdens derived from human activities are overcoming the resilience of the Earth system (i.e. capacity of buffer changes) putting our future at

risk. In this regard, several scientists have identified nine Earth processes being threatened due to an unsustainable use of natural resources (Rockström et al., 2009; Steffen et al., 2015) which may be identified as the global environmental challenges (Figure I-1) to be tackled which include: i) ecosystems and biodiversity loss; ii) climate change; iii) ocean acidification; iv) land-use change; v) unsustainable freshwater use; vi) perturbation of biogeochemical flows (nitrogen and phosphorus); vii) alteration of atmospheric aerosols; viii) chemical pollution; and ix) stratospheric ozone depletion. Responses, actions and efforts, both at global and local scale, and engaging major groups in the society, need to be directed to these sustainability challenges and new emerging ones, since in case that certain thresholds were surpassed, the Earth systems may change potentially leading to an irreversible situation threaten human well-being and the environment equilibrium (Rockström et al., 2009; Steffen et al., 2015).

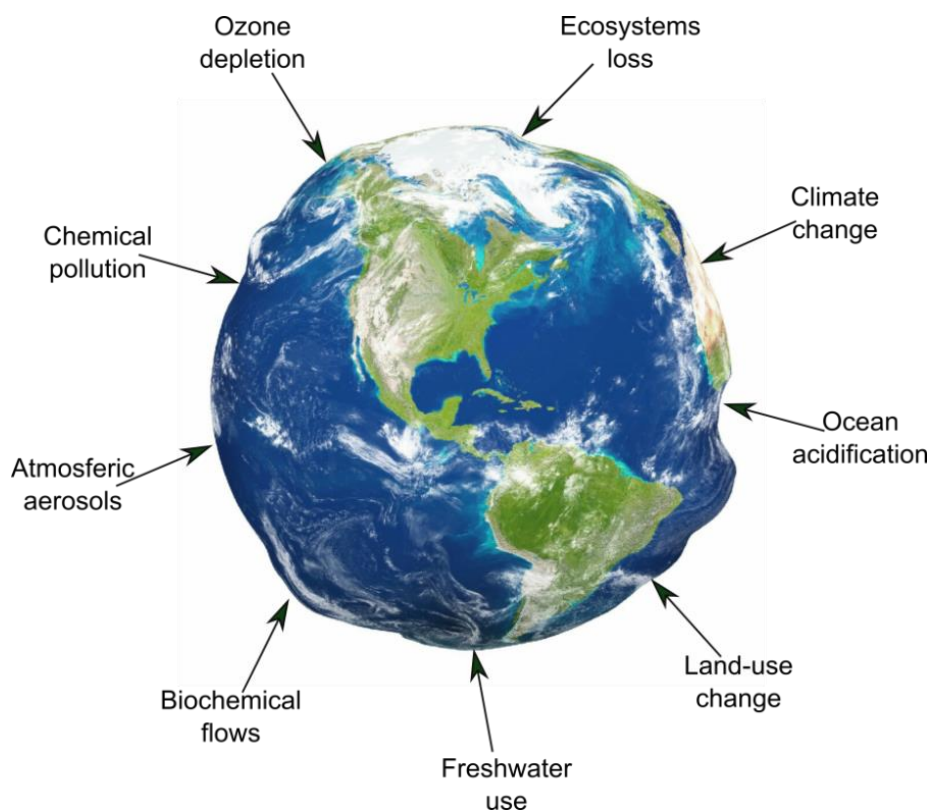


Figure I-1. Global environmental challenges to be addressed for sustainable development.

All actors in the society bear some responsibility in the transition to sustainable development; however, ultimately, all levels of governments and legislative bodies play the key role by designing mechanisms and promoting strategies to foster sustainability (e.g. long-term policies, programs, plans). International institutions, national governments, local administrations and business make silent decisions to such sustainability complex problems that will indeed determine the future. However, making good decisions to such complex problems is extremely difficult since there are large numbers of choices to make, very likely affect different stakeholders with conflicting interests and very often involves several objectives that show conflicting behaviours. These previous difficulties constitute in turn the main motivation of the work presented in this thesis, arises from the need of developing systematic aid tools to facilitate the decision and policy-making process which ultimately will lead to the development of the efficient mechanisms to secure an effective transition towards sustainability.

In particular, this thesis points to two key structural transformations needed to reconnect the human development to sustained progress (Rockström et al., 2013):

- a) *“food security transformation”* (Godfray and Garnett, 2014; Godfray et al., 2010; Tilman et al., 2011), through decoupling the intensification of food production from unsustainable use of resources; and
- b) *“energy transformation”* (Riahi et al., 2012; Tester et al., 2012; van Vuuren et al., 2012), supporting the shift towards an environmentally friendly economy.

The two transformations toward sustainability outlined here require great efforts, detailed strategies/guidelines and, in the end, a continuous problem solving which constitute the basis of the research work developed in this dissertation.

There are multiple approaches to solve the emerging problems, however, in order to find the best solution to them, mathematical programming appears as a powerful tool that has been traditionally used to aid decision-making in many areas of science and engineering (i.e. planning, resource allocation, decision-making, etc...). Also named as mathematical optimisation, it allows modelling a given problem by means of mathematical equations (simplification of the real problem) which can be then solved to select the best alternative from a set of available options to the decision maker (according to one or several criteria). Basically, making a decision corresponds to find the best number to each decision variable that represents the alternative so as the best solution (i.e. alternative) for the problem is selected. In this dissertation, optimisation techniques constitute the methodological basis to develop exact and systematic approaches which allow finding the best-fit solutions when addressing some particular problems contributing to a more sustainable food security and for a more sustainable energy future (see problems in the thesis outline in Figure I-2).

This thesis is devoted to develop decision and policy support optimisation models and methods for tackling complex problems in line with food security and energy transformations contributing to the sustainability transition. The approach is based on the development of mathematical models which represent complex problems to optimise activities contributing to provide tailored solutions for stakeholders and/or decision makers. Regarding the food transformation, giving priority to the agriculture sector, we develop [1] a systematic method to optimal allocate rainfed and irrigated crop production to enhanced food production while simultaneously reducing the environmental impacts of water consumption. Also we present [2] a model to optimise cropping plan decisions by meeting certain environmental requirements which also may be used to determine the adequate subsidy to spur the broad shift towards agricultural practises beneficial for the climate and the environment. Regarding the energy transformation, focusing on the electricity sector, we propose [3] a method to assess the level of sustainability of

system and performed an assessment of different electricity generation technologies, and we propose [4] an approach to enable a resilient collaborative international response in negotiations on climate change mitigation based on quantifying the benefits of curbing CO₂ emissions in cooperation and distributing them among the parties involved in a fair manner so as to spur an effective collective action towards curbing carbon emissions. To this end, we develop a model to optimise the electricity generation curbing the emissions in a cost effective manner considering different level of cooperation among the parties involved.

Figure I-2 summarises the work developed in this thesis, highlighting the four problems addressed and the mathematical programming techniques and methodologies employed to solve each one of them.

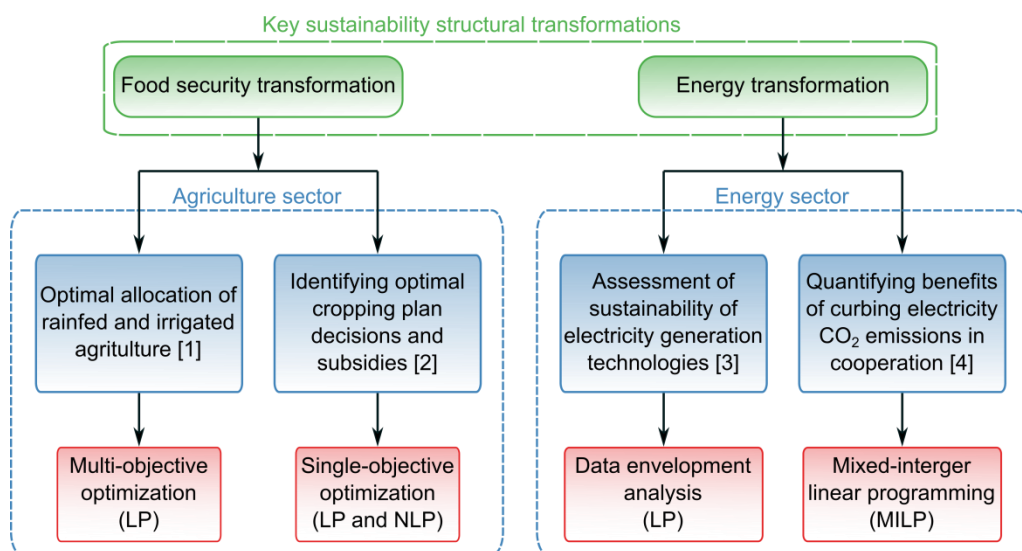


Figure I-2. Thesis roadmap. Green squares depict the key structural sustainability transformations addressed; blue squares correspond to the particular problems tackled, while red squares represent the main mathematical programming techniques used.

The PhD thesis is structured in five main chapters. Chapter I introduces the sustainability challenging problems which motivate this thesis, the main objectives and a general background of the mathematical programming techniques and

environmental assessment methods employed. Then, a brief description of the research works developed is presented, while at the end of the chapter the main conclusions, future work and references are included. The next four chapters (Chapters II-V) include a detailed description of the decision-aided tools developed for each of the sustainability issues addressed. Particularly, Chapter II includes a multi-objective optimisation tool for allocating rainfed and irrigated agricultural areas considering simultaneously both production and environmental criteria. Chapter III includes a multi-stage linear programming model for optimising cropping plan decisions under sustainability conditions. Chapter IV presents an enhanced data envelopment analysis for sustainability assessment and an application to electricity technologies. Finally, Chapter V presents a mathematical model to fight against climate change by optimising the electricity system.

1.2 General objectives

This thesis aims to bring a tiny contribution in the fight against world challenging and emerging sustainability problems. To achieve this, the main goal is to devise decision and policy-making support tools based on mathematical programming optimisation tools to address problems related with food security and energy shifts towards sustainability.

In order to achieve the overall goal, the following particular objectives have to be accomplished:

- To develop a rigorous and systematic multi-objective optimisation tool for allocating rainfed and irrigated cropping areas maximising the crop production simultaneously with the minimisation of the environmental impact on ecosystems and resources.
- To formulate a novel mathematical programming framework capable to assist both policy makers in development of policies that encourage sustainable practices and farmers' cropping plans decisions in response to

sustainable requirements.

- To develop an enhanced data envelopment analysis methodology tailored for sustainability assessment attained by a system.
- To devise an approach to articulate negotiations on climate change mitigation based on quantifying the benefits of cooperating and fair sharing of gains.
- To illustrate the capabilities of the proposed tools and methodologies through their application to real case studies in order to demonstrate how they can support decision and policy makers to design effective strategies towards sustainability.

1.3 Optimal sustainable decision making framework

Management science is the broad ability to solve a problem in order to provide guidelines to make effective decisions. In essence, management science tailored for sustainability constitutes the main goal of this thesis where mathematical programming plays a key role in increasing the managerial effectiveness. In particular, the aim is to develop mathematical programming models and techniques to aid sustainable decision and policy makers thereby effective solving of complex problems with measurable and quantifiable objectives and with less subjectivity as possible.

Integrating sustainability requirements into such mathematical programming models, and therefore into the decision-making process, is critical, since it requires considering simultaneously economic growth, environmental protection and social well-being criteria. This integrated approach requires the consideration and satisfaction of the “Triple Bottom Line” aspects (Savitz and Weber, 2006) (Figure I-3), that is, promoting the balanced integration of the three dimensions of sustainable development so as the state of sustainability is based on understanding the environment as basic need for the economy to meet the social requirements.

Traditionally, optimisation efforts of decision-making problems were focused on maximising an economic criterion, while in the last years other environmental aspects have been incorporated into the models (Azapagic and Clift, 1999a; Azapagic, 1999; Grossmann and Guillén-Gosálbez, 2010a) and the social aspects still are seldom addressed (Cuthill, 2010; Murphy, 2012).



Figure I-3 “Tripple Botton Line” concept of sustainability encompassing economic, environmental and social goals.

To develop a sustainable a decision or a policy-making tool is not an easy task, since it has to provide an easy representation of the decision procedure, but at the same time it requires a full characterisation of the problem under study. The process of solving a decision-making problem is shown schematically in Figure I-4. As can be observed, the general framework comprises three consecutive steps moving from the real world problem to mathematical programming (i.e. model formulation, algorithm and solution method), and finally the decision making analysis. The procedure also includes feedback loops, where some decisions already taken can be re-considered based in new analysis and information.

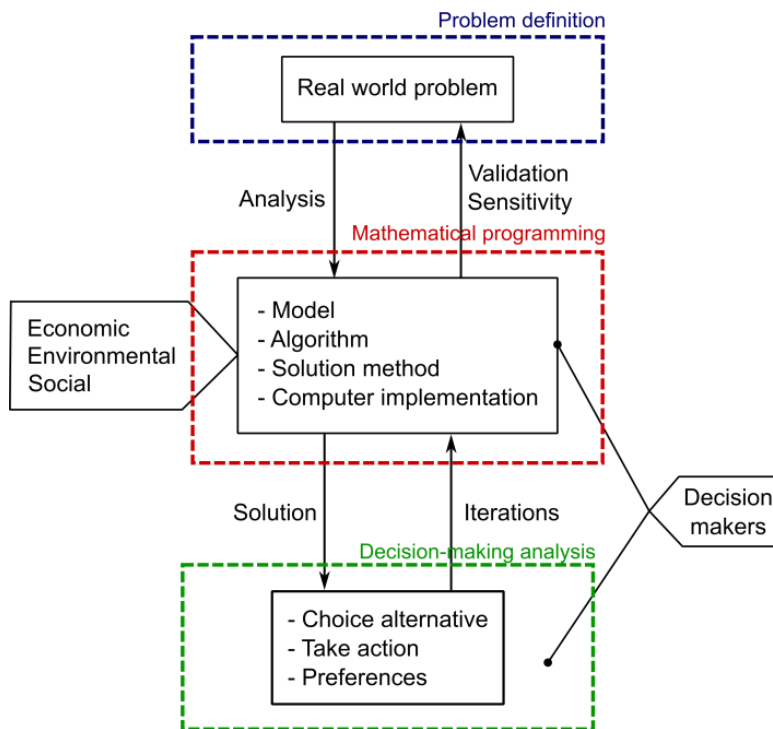


Figure I-4 Methodological framework of the decision-making process.

The steps of the problem formulation are the following:

i. Problem definition: the first step consists of identifying of the *real problem* and analysing and gathering all the information required. Here, the stakeholders' concerns need to be included in order to clearly define and understand the problem. This problem definition is key and its analysis is often extremely valuable providing useful insight on how approach the problem.

ii. Mathematical programming: the next step consists of modelling the problem by means of mathematical functions (*mathematical model building*) containing the decision variables. Problems are usually complex and it is extremely difficult to capture all the details involved. Therefore, models are usually abstractions of the problem since they require simplifications, approximations and assumptions of complex features difficult to handle with mathematics techniques. Either way, the problem under study is represented by means of mathematical

equations including the objective function/s and equality and/or inequality constraints which impose bounds on the decision variables that allow predicting the behaviour of a system. The nature of the optimisation problem is given by the particular combination of parameters, variables and equations it embeds. There are two modelling approaches namely deterministic and stochastic depending on whether the model parameters are considered to be known or parameter are assumed to be uncertain, respectively. Depending on the nature of the objective function/s, constraints and decision variables embedded, the mathematical model can be classified as linear programming (LP), nonlinear programming (NLP), mixed-integer linear programming (MILP) or mixed integer nonlinear programming (MINLP). Depending on the number of objective functions the problem is classified as single-objective optimisation problem (SOO) when only one objective function is considered and multi-objective optimisation (MOO) when more than one objective are considered. Very often, decision makers face the need of considering simultaneously multiple conflicting objectives in the decision process for which the problem is formulated as a MOO. The latter MOO is very common in sustainability assessment since economic, environmental and social objectives may be considered simultaneously. Further details of the mathematical models and optimisation techniques are provided in the ensuing Section 1.4.

For solving the model and to derive the solution, efficient *algorithms* and software systems are available. Several modelling systems and solvers are accessible (either open-sourced or commercial) to assist the *computer implementation* of the optimisation-based modelling process. As examples, common modelling systems are GAMS (Brooke et al., 1998) or AMPL (Fourer et al., 1990) which can use solvers such as CPLEX (IBM, 2009) or BARON (Sahinidis, 1996) devised for mixed-integer linear and nonlinear problems to global optimality, respectively. Finally, as a result of the mathematical programming phase, one (or several) optimal solution(s) is(are) provided which represent(s) the best alternative(s) of the given problem.

After deriving the optimal solution(s), it is very important to check its practical feasibility by coming back to the real problem. To do so, validation is the process to make sure that the solution is appropriate for the real problem and sensitivity analysis check the robustness of the results when changes are performed in the data.

iii. Decision-making analysis: optimal solutions derived from the mathematical programming are then provided to the decision-makers. Usually the solution of the model is not implemented in practical as is, but it provides useful insights to decision and policy makers to combine it with their own knowledge leading to an implementable solution. Often the solution is not feasible in practice and it is necessary to implement modifications into the model several times. Therefore the procedure becomes an iterative process where the decision-maker plays a major role providing information (preferences) to build the model until a satisfactory solution is achieved. Decision-makers' preferences may be incorporated *a priori* or *a posteriori* in the optimal search process depending on whether a unique solution or a set of optimal solutions are desirable (Jaimes et al., 2009). Finally, the most preferred solution obtained following the systematic analysis and modelling approach (Figure I-4) presented here, allows providing help and guidance for decision and policy makers to make effective decisions leading to efficient solutions.

1.4 **Mathematical programming: optimisation**

Mathematical programming consists of building mathematical models that describe complex real-world problem and algorithms to find the optimal solutions to such problems that may be used to assist in taking effective decisions. In other words, mathematical programming is the evaluation of a given problem aiming to minimise or maximise a function by systematically identifying the best values for a continuous or integer variables. Although mathematical programming started as a methodology of academic interest, nowadays it has become a powerful tool broadly applied in many areas of science and engineering both in private and public

decision-making contexts.

The mathematical model for an optimisation problem describing the problem addressed includes one objective function (or several) and constraints (either in the form of equality or inequality) which are formulate via algebraic equations (linear or nonlinear). Each feasible solution of the problem entails a choice of decision variables that satisfies the set of constraints, however, only the *optimal solution* (representing the optimal decision) is a feasible solution which optimises the objective function. The *objective function* is the equation which measures the quality of the solutions, that is, the value to be optimised given a set of constraints and a particular set of variables. This is the goal of the optimisation. The objective function can be an economic criteria (e.g. minimising the cost or maximising the profit), an environmental criteria (e.g. minimising the environmental impact) or a social criteria (e.g. maximising employment). The *constraints* are expressions which impose bounds on the variables, that is, the variables can take certain values but exclude others. The constraints can be equality or inequality equations that must be met (e.g. demand satisfaction, resource limiting or operating requirements).

Next we explain in detail three mathematical programming techniques that constitute the methodological basis of this thesis: single-objective optimisation (SOO), multi-objective optimisation (MOO) and data envelopment analysis (DEA).

1.4.1 *Single objective constrained optimisation problems*

In mathematical programming, a generic single-objective optimisation problem (SOO), is generally stated, in compact form (Grossmann et al., 2000), as minimisation as shown in Eq. I-1:

$$\begin{array}{ll}
 \text{SOO} & \min \quad f(x, y) \\
 & \text{s. t.} \quad h(x, y) = 0 \\
 & \quad \quad g(x, y) \leq 0 \\
 & \quad \quad x \in \mathfrak{R}, y \in \mathbb{Z}
 \end{array}
 \tag{Eq. I-1}$$

where $f(x,y)$ represents the objective function to be minimised ($-f(x,y)$ when the

direction of the optimisation is maximisation); and x and y represent the vectors of continuous and integer decision variables, respectively. Note that widely-used binary variables ($y \in \{0,1\}$) are a particular case of the more general integer ones. The feasible set of solutions (sometimes referred as alternatives, search space or solution space) is defined by the set of constraints imposing restrictions on variables where $h(x,y)$ represents equality constraints whereas $g(x,y)$ refers to inequality constraints.

A point (x,y) satisfying all constraints is a feasible point, that is, a feasible solution to the problem. All feasible points constitute the feasible regions. The aim of the optimisation is to satisfy the optimality criteria, that is, to select the best point from the set of feasible solutions. A point (x^*,y^*) from the feasible region ω is deemed as local minimum if it is the smallest function value in some feasible neighbourhood, that is, there exists a $\delta > 0$ such that $f(x^*,y^*) \leq f(x,y) \forall x,y \in \{\omega: |x - x^*| \leq \delta\}$. Often, in an optimisation problem, there can be many local minima but only one global minimum. A point (x^*,y^*) is a global minimum when it is the smallest function in all the feasible region, that is, $f(x^*,y^*) < f(x,y) \forall x,y \in \omega$. Figure I-5a illustrates the concept of local and global optimum.

There are several properties (e.g. convexity criteria) of the feasible region ω and objective function f which imply that any local optimum is a global optima. If f is convex and the feasible region ω is defined by the equality and inequality constraint is convex, then any local optima will be a global optima. A region ω is convex if and only if for any two points x_1 and x_2 , their linear combination lies in ω , that is, $x = \alpha x_1 + (1 - \alpha)x_2 \in \omega \forall \alpha \in [0,1]$. If $h(x,y)$ is linear and $g(x,y)$ is convex, then the feasible region ω is a convex region. A function f is convex if and only if for any two points x_1 and x_2 the following is satisfied: $f(\alpha x_1 + (1 - \alpha)x_2) \leq \alpha f(x_1) + (1 - \alpha)f(x_2) \forall \alpha \in [0,1]$. Figure I-5 illustrates graphically the concept of optimality (local and global optimum) and the convexity concept.

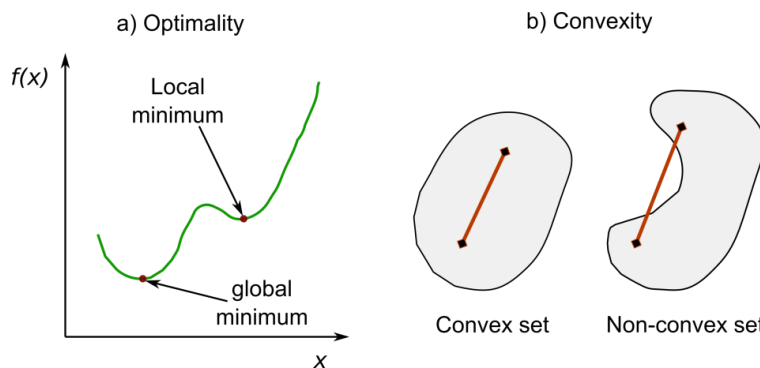


Figure I-5 Graphical representation of (a) optimality and (b) convexity concepts.

Depending on the nature of the objective function and constraints (either linear or nonlinear) and the type of the decision variables embedded (either continuous or binary/integer), the mathematical model can be classified as linear programming (LP), nonlinear programming (NLP), mixed integer linear programming (MILP) or mixed integer nonlinear programming (MINLP). See Figure I-6 for an illustrative representation of these types of problems.

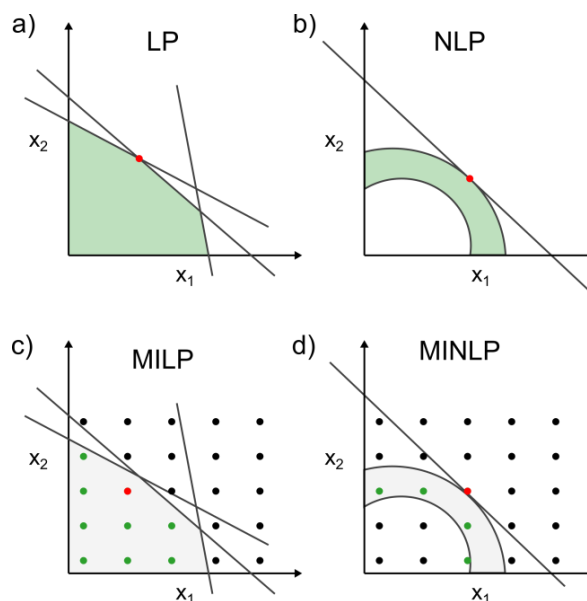


Figure I-6 Graphical representation of the main types of optimisation problems in the variables space (x_1 and x_2). In subplot (a) and (b), grey area represents the feasible region while in subplots (c) and (d) green points represent the feasible region of integer solutions. Red points denote the hypothetical optimal solutions for each type of problem.

A mathematical model takes the form of *LP* when all variables are continuous variables and all algebraic equations are linear. A LP problem could be geometrically represented in Figure I-6a where lines represent the linear equations (both h and g) and the shadow grey area is the corresponding feasible region enclosed within the equality and inequalities. The optimal solution of an LP is a vertex of the feasible polytope that is optimal. The standard method to solve a LP is the simplex method (Dantzig et al., 1955) which consists of performing successive checks along the edges of the feasible region until the best vertex of the objective function is reached. Many improvements and refinements have been developed over the last decades given rise to current commercial optimisers suitable for LP such as CPLEX (IBM, 2009), GUROBI (Optimization, 2012) or LINDO (Schrage, 1995), among others.

When non-linear equations are present in any of the equations (either objective function or constraints) and all variables are continuous the problem becomes *NLP* and its feasible region becomes more sophisticated (Figure I-6b). A key characteristic of a NLP is whether it is convex or non-convex, as the latter might give rise to multiple local optima (i.e. multimodality) where the standard gradient methods may get trapped thereby offering no guarantee to reach the global optima of the problem. If the NLP is convex (feasible region convex, inequality constraint convex and equality constraints linear), then any local optima is a global optima. BARON (Sahinidis, 1996) is a general non-linear optimiser capable of solving nonconvex optimisation problems to global optimality.

A *MILP* is a special case of LP that includes both continuous and integer variables (when all variables are restricted to be integer, they are labelled as integer linear programming, ILP) (Figure I-6c). The standard procedures to solve a MILP are cutting plane methods and the most common is the branch-and-bound algorithm (Land and Doig, 2010). The latter consists of relaxing the original integer variables imposing restrictions over them. The original MILP is divided into several LP sub problems that are solved until all integrality restrictions are satisfied, where the

solution found is an optimal solution of the original MILP. Common commercial solvers that combine those strategies are CPLEX (IBM, 2009), GUROBI (Optimization, 2012) or XPRESS (Optimization, 2007), among others.

Finally, *MINLP* are problems that contains at least one non-linear equation and both continuous and integer variables (Figure I-6d). MINLP problem are hard to solve, however several algorithms (e.g. modified branch-and-bound, outer approximation) and commercial solvers have been developed to tackle with them such as BARON (Sahinidis, 1996), DICOPT (Grossmann et al., 2002) or SBB (Bussieck and Drud, 2001), among others.

In this thesis we address three LP problems ([1], [2] and[3]), one MILP ([4]) and one NLP ([2]) (see problems in Figure I-2 in section 1.1).

1.4.2 Multiobjective optimisation problems

Often, when facing a decision-making problem it may be interesting to consider several criteria simultaneously. In mathematical programming, a generic multi-objective optimisation problem (MOO) consists of the simultaneous optimisation of multiple competing/conflicting criteria (objectives). A MOO is generally stated in compact form as shown in Eq. I-2:

$$\begin{aligned}
 \text{MOO} \quad & \min \quad F = \{f_1, \dots, f_n\} \\
 & \text{s. t.} \quad h(x, y) = 0 \\
 & \quad \quad g(x, y) \leq 0 \\
 & \quad \quad x \in \mathfrak{R}, y \in \mathbb{Z}
 \end{aligned}
 \tag{Eq. I-2}$$

where F represents the vector of n objective functions equations ranging from f_1 to f_n . The solution containing the individual minimum of all objectives is regarded as the utopian point which is in general unattainable (ideal) due to the trade-off existing between the objectives. The counterpart of this ideal point is the nadir point which represents the worse value for all objectives. Instead of a single solution (as in SOO), MOO leads to a set of optimal solutions, called Pareto solutions, with different trade-offs among the conflicting objectives and forming the

Pareto frontier (Ehrgott, 2009). A solution is said to be Pareto optimal when it is impossible to improve one of the objectives without worsening at least another objective. In essence, a set of solution x^* is said to be Pareto optimal for a MOO, if there is no other x in the feasible region such that $f_n(x) \leq f_n(x^*)$ for all $n \in \{1, \dots, n\}$.

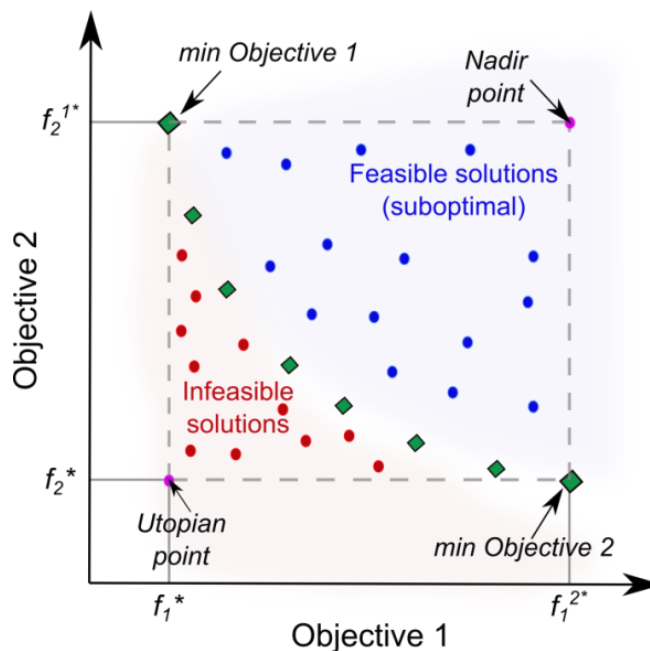


Figure I-7 . Illustration of Pareto optimal frontier of a bi-criteria problem obtainable by multi-objective optimisation method.

Figure I-7 illustrates the concept of Pareto multiobjective optimality for an illustrative optimisation example considering two objectives that we aim to minimise simultaneously (e.g. objective 1 and objective 2). Each solution of the Pareto curve is represented by green points and represents a unique combination of both objectives entailing a particular optimal solution. Any point lying above the curve is sub-optimal since it can be improved in both objectives simultaneously. Region below the curve contains unfeasible solutions, since there is no single point showing better performance than the Pareto solutions simultaneously in both indicators. The anchor points are also represented defined by optimal solutions

considering one single criteria at a time, that is at (f_1^*, f_2^{1*}) and (f_1^{2*}, f_2^*) . Moreover, the utopian point representing the optimal values for each objective function is depicted located at (f_1^*, f_2^*) , whereas the nadir point given by the worse values for each objective is depicted located at (f_1^{2*}, f_2^{1*}) .

There are several approaches to obtain the whole set of Pareto optimal solutions in MOO problems. The most commonly used methods are the weighted sum method, the epsilon constraint method and the normal boundary intersection method. The weighted sum method consists of optimising the weighted sums of all objectives exploring the space of possible weights (Ehrgott, 2006). The epsilon constraint method consists of keeping one objective as a main objective function while the rest are transferred to auxiliary constraints that imposed bounds on the main objective (Ehrgott, 2006; Haimes, Y., Lasdon, L., Wismer, 1971). Normal boundary intersection generates evenly distributed Pareto sets by intersecting the feasible region with a normal to the convex combinations of the optimal solutions for each objective individually in the direction of the utopian point (Das and Dennis, 1998). Without loss of generality, in this work we adopted the epsilon constraint method since it presents several advantages as it is easy to implement, it is not necessary to have the objectives in a common scale and allows exploring the whole feasible region (control of optimal solutions distribution) (Kim and De Weck, 2006; Mavrotas, 2009).

1.4.2.1 Epsilon constraint method

The epsilon constraint (EC) method consists of solving a set of SOO derived from the original MOO, based on formulating an auxiliary model where one objective is kept as a main objective whereas the remaining are transferred to auxiliary constraints that impose bounds (ϵ) on them. In mathematical terms, keeping f_1 as main objective function to be minimised, the problem can be state as follows:

$$\begin{aligned}
 EC \quad & \min f_1(x, y) \\
 \text{s. t.} \quad & f_n(x, y) \leq \varepsilon_n^b \quad \forall n = \{2, \dots, N\}; b = \{1, \dots, B\} \\
 & h(x, y) = 0 \\
 & g(x, y) \leq 0 \\
 & x \in \mathfrak{R}, y \in \mathbb{Z}
 \end{aligned}
 \tag{Eq. I-3}$$

The auxiliary epsilon constraint model is solved for each value of epsilon parameter (ε). The epsilon values for each instance are obtained previously by optimising each objective individually and then dividing the interval defined by the best and worst values for each objective ($[f_n, \bar{f}_n] = [\underline{\varepsilon}, \bar{\varepsilon}]$) into a set of subintervals that will determine the number of optimal solutions obtained. Therefore, by parametrical variation of the ε values, the number of instances to solve the EC problem (Eq. I-3) is defined by all possible combinations of epsilon parameters, that is, B^N instances. However, to simplify this process when many objectives need to be considered, an alternative procedure considering only all bi-objective combinations may be employed, which reduces the problem leading to $\binom{N}{2}B$ iterations.

1.4.3 Data envelopment analysis

Data envelopment analysis (DEA) is a mathematical programming-based technique for the efficiency assessment. In particular, DEA is a non-parametric LP technique that allows quantifying the relative efficiency of a set of comparable decision-making units (DMUs) each one transforming multiple inputs and into multiple outputs (Charnes et al., 1978). DEA analyses each DMU individually by solving an LP model and identifies those that exhibit best performance (i.e. the ones deemed efficient, which form the 'efficient frontier'). Furthermore, DEA measures in turn the level of efficiency of the non-frontier units (inefficient units), identifies sources of inefficiency, and provides specific guidelines on what changes are required to turn inefficient units into efficient.

The original input-oriented DEA CCR model, first proposed by Charnes et al., (1978) based on Farrell's work (Farrell, 1957), is a nonlinear program that measures the efficiency of a DMU as the ratio of the weighted sum of their outputs and

inputs. The aim of this model is to find the optimal weights so as the efficiency of each DMU is maximised separately. In mathematical terms, let us consider a set of $|J|$ DMUs j ($j=1, \dots, |J|$), each using $|I|$ inputs x_{ij} ($i=1, \dots, |I|$) to produce $|R|$ outputs y_{rj} ($r=1, \dots, |R|$), the CCR model defined for each DMU j , the original DEA CCR model is stated as follows (Eq. I-4):

$$\begin{aligned} \max \quad & \theta_j = \frac{\sum_{r \in R} u_r y_{rj}}{\sum_{i \in I} v_i x_{ij}} \\ \text{s.t.} \quad & \sum_{r \in R} u_r y_{rj} - \sum_{i \in I} v_i x_{ij} \leq 0 \quad \forall j \in J \\ & u_r, v_i \geq 0 \quad \forall r \in R, i \in I \end{aligned} \tag{Eq. I-4}$$

where θ_j represents the technical efficiency of the DMU $_j$ and u_r and v_i are free variables denoting the weights (multipliers) given to each output r and input i , respectively. Due to the flexibility in the weights, if a DMU $_j$ satisfies $\theta_j = 1$, it is deemed efficient, and it is considered inefficient when $\theta_j < 1$. The latter implies that the DMU under evaluation is always inferior to other alternatives, even for the most favourable choice of weights (it is possible to reduce any of its inputs without reducing any output).

The previous CCR model is input-oriented, that is, inefficient units are turned efficient through a proportional reduction of inputs while keeping the output constant. In contrast, it is possible to reformulate its equivalent output-oriented model, where an inefficient unit would be turned efficient by increasing its outputs while keeping its inputs constant. Moreover, the CCR model considers constant returns to scale (CRS), as it assumes that DMUs operate at the same scale (i.e. their outputs change proportionally when changes in the inputs are applied). Moreover, the DEA model can also be formulated considering variable return to scale (VRS), known as BCC DEA model (Banker et al., 1984). The choice between the orientation (input or output) and the type of returns to scale depends on the application being addressed; for further discussion on this topics, see Lozano et al. (2009).

As mentioned previously, the original input-oriented CCR DEA model (Charnes et al., 1978) (Eq. I-4) is nonlinear and nonconvex, however, it can be reformulated (from fractional to linear) into the following LP model (Eq. I-5), where the denominator is set to one and the numerator is maximised:

$$\begin{aligned}
 \max \quad & \theta_{j'} = \sum_{r \in R} u_r y_{rj'} \\
 \text{s. t.} \quad & \sum_{i \in I} v_i x_{ij'} = 1 \quad \forall j' \in J \\
 & \sum_{r \in R} u_r y_{rj} - \sum_{i \in I} v_i x_{ij} \leq 0 \quad \forall j \in J \\
 & u_r, v_i \geq 0 \quad \forall r \in R, i \in I
 \end{aligned} \tag{Eq. I-5}$$

where the subscript j' denotes the specific DMU being assessed.

Moreover, for this primal LP problem it is possible to formulate a dual partner problem (duality), which provides the same information as the primal model (Eq. I-5) (i.e. efficiency scores) but calculates in turn targets for the inefficient DMUs so as to become efficient. The LP DEA dual model (Eq. I-6) is formulated by assigning one dual variable to each constraint in the primal model (Cooper et al., 2004) as follows:

$$\begin{aligned}
 \min \quad & Z = \theta_o - \varepsilon \left(\sum_{r \in R} S_r^+ + \sum_{i \in I} S_i^- \right) \\
 \text{s. t.} \quad & \sum_{j \in J} \lambda_j x_{ij} + S_i^- = \theta_o x_{io} \quad \forall i \in I \\
 & \sum_{j \in J} \lambda_j y_{rj} - S_r^+ = y_{ro} \quad \forall r \in R \\
 & \lambda_j, S_i^-, S_r^+ \geq 0 \quad \forall j \in J, i \in I, r \in R
 \end{aligned} \tag{Eq. I-6}$$

where ε is a non-Archimedean infinitesimal value enforcing strict positivity on variables, θ_o is an unconstrained variable that measures the efficiency of the DMU_o under consideration and, therefore, it is lower than or equal to 1 ($\theta_o \leq 1$). S_r^+ and S_i^- denotes the slack variables representing the extra amount by which an input (or output) should be reduced (or increased) to become strong efficient. Note that the values of the slacks are all zero (S_r^+ and $S_i^- = 0$) in the efficient units ($\theta_o = 1$), and strictly positive in the inefficient ones ($\theta_o < 1$). λ_j represents the dual variable that is the weight assigned to each efficient DMU (belonging to the reference set of an inefficient unit) to form a composite non-existing efficient unit that could be used as a benchmark to improve the particular inefficient unit. This hypothetical composite unit is obtained by projecting radially the inefficient unit on the efficient frontier, which is the piece-wise linear function connecting all the efficient DMUs (those with an efficiency score of 1). The BCC dual model can be formulated by adding a convexity constraint to Eq. I-6 which ensures $\sum_{j \in J} \lambda_j = 1$. To illustrate the previous DEA concepts, Figure I-8 provides a graphical representation of two DEA examples considering one single input and one single output case, while Figure I-9 illustrates an example of two inputs and one output.

Figure I-8 provides an illustration of a single input and single output case. Under the CRS assumption, DMU A presents the best efficiency (ratio between output and input) thus A is considered as the referent set for the remaining DMUs. The line connecting the origin and A represents the CRS efficiency frontier (green line) and measures the efficiency of others by deviations from it. The efficiency of A equals to one, while the efficiencies of the remaining DMUs are strictly lower than one. Taking as example the inefficient DMU F, depending on the model orientation followed, its relative efficiency is performed in two different ways: in the input-oriented model (i.e. horizontal projection), the efficiency of F is performed as the ratio between the segments p and q; while in the output-oriented model the inefficiency of F is performed as the ratio of r and s (i.e. vertical projection). Furthermore, in Figure I-8 it is also depicted the VRS efficiency frontier which is the

red line connecting \overline{FABC} . From unit F to A constitutes the increasing returns to scale portion of the frontier, while unit A is experiencing constant returns to scale and from A to the right (segments \overline{AB} and \overline{BC}) make up the decreasing returns to scale portion of the frontier. As seen, depending on whether a CRS or VRS assumption is considered, the results of DEA are completely different since the efficiency frontier varies as does the efficiency score of the inefficient DMUs. For instance, unit B is deemed inefficient under CRS but efficient under VRS and the hypothetical efficient unit for E under CRS would be “e” while under VRS is “e”.

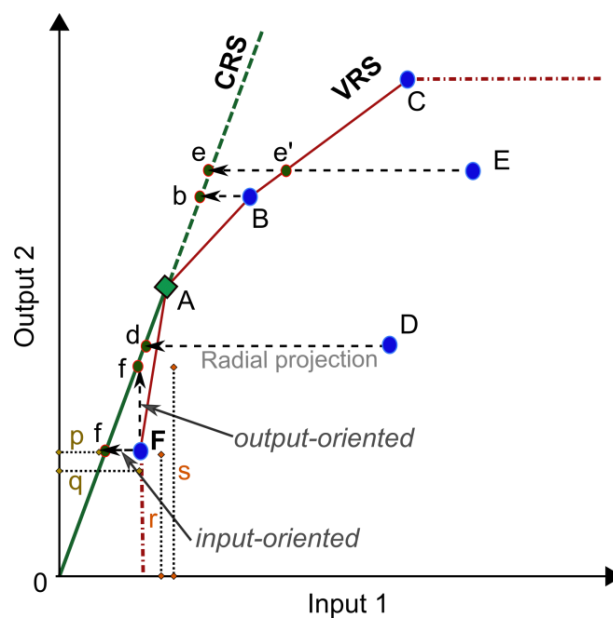


Figure I-8 Graphical representation of a DEA example of a single input and single output using both CRS and VRS approaches.

Figure I-9 provides an illustrative example of two inputs and one output. The efficient DMUs are denoted by green diamonds and determine the efficient frontier, which is the convex envelope depicted in green (\overline{ABC}). Inefficient units are represented by blue circles (D, E and F), while their hypothetical efficient units obtained by means of the radial projections on the frontier are depicted by green circles (d, e and f). As observed, A, B and C present lower input values for the same output and are thus identified as efficient units (i.e. efficiency score equals to 1).

The line connecting them determines the piece-wise linear efficient frontier. On the other hand, D, E, F are deemed inefficient because their efficiency score θ_j is lower than 1 (they produce the same level of output with higher inputs). DEA also quantifies the magnitude of inefficiency by referring to the efficient frontier. For instance, the efficiency of technology E is obtained from the ratio between two segments, the one that goes from zero to the intersecting point between the efficient frontier and the radial projection (e); and the one that connects zero and E. The efficiency score represents the extent to which all the inputs should be proportionally reduced to reach the frontier. Point e (which represents the hypothetical efficient unit for E) is generated by a linear combination of A and B, which is the reference set (peer group), using linear weights equal to λ_1 and λ_2 , respectively, which are provided by the DEA model. Similarly, all inefficient DMUs can be projected onto the efficiency frontier, but in doing so we may sometimes obtain weakly-efficient composite units, as it happens with unit d (weakly-efficient unit for D), which shows a slack in the cost given by the distance \overline{dA} . However, d would remain inferior since technology A has the same input 1 but lower input 2. Therefore, technology D presents a slack or excess in input 2, which implies extra reduction equals to \overline{dA} in order to become strongly efficient, thereby reaching point d^* with the same input 1 and output than unit A.

For further information about DEA models and extensions the reader is referred to Cook and Seiford, (2009), Cooper et al., (2004) and Hosseinzadeh Lotfi et al., (2013).

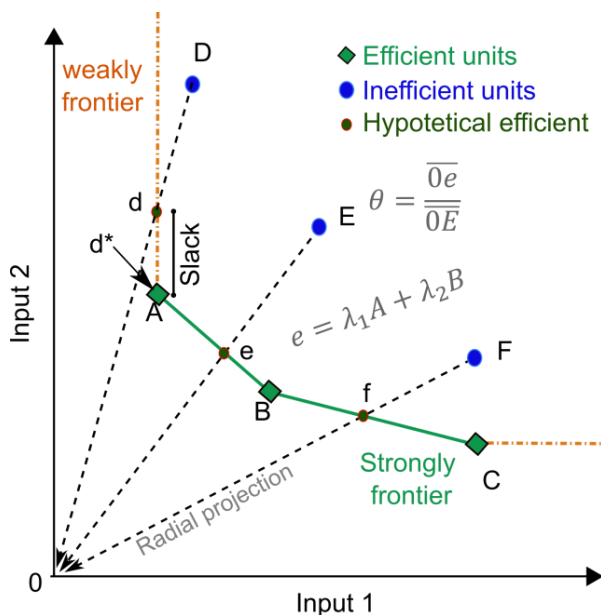


Figure I-9 Graphical representation of a DEA example considering two inputs and one output.

1.4.4 Uncertainty: sensitivity analysis

Despite optimisation is well recognised as a powerful tool to aid decision and policy making, the applicability of the results is in practise more complex, especially because very often the mathematical models entail many sources of uncertainty that need to be considered to ensure the quality of the solution and even its practical feasibility. Most mathematical models are deterministic in nature, that is, assume that all the parameters are perfectly known and show no variability thereby neglecting the uncertainty involved. However, in order to get robust solutions and make good decisions, uncertainties and variability need to be captured in the outcome of the optimisation providing information about the robustness of the solution (Grossmann, 2014). Therefore, accounting for parameter uncertainty is key part of decision-making before using the results to make the best decision (Bilcke et al., 2011).

There are two main approaches to address an optimisation problem under uncertainty, namely preventive and reactive approaches. *Preventive approaches*

consist of modelling optimisation problems by incorporating uncertainties into the models and the main frameworks are stochastic mathematical programming and fuzzy programming, being the former the most commonly used (Heyman and Sobel, 2003; Sahinidis, 2004). These approaches consider all the possible values for the uncertain parameters and find the solution which best fits for all cases. However, despite the advantage of considering uncertainty *a priori* of deriving the optimal solution, these approaches are computationally more expensive and practitioners have more difficulties assessing and interpreting the results since the objective function is replaced by complex risk metrics (e.g. risk, worse case) (Guillén-Gosálbez and Grossmann, 2010; Sabio et al., 2014). On the other hand, *reactive approaches* are based on modifying the deterministic formulation to adjust it to modifications or alternations taking place. The main reactive approaches are rolling-horizons, multiparametric programming and sensitivity analysis. Rolling-horizons approach consists of solving iteratively the deterministic problem by moving forward the optimisation horizon (Kopanos and Pistikopoulos, 2014). Multiparametric programming is based on sensitivity analysis and allows generating a complete map of the optimal solutions in the space of the uncertain parameters. Finally, sensitivity analysis, which is the simplest approach, is employed to provide the range of solutions in the neighbourhood of the nominal value of the uncertain parameters.

In this thesis, all mathematical programming models developed are deterministic in nature, that is, parameters are assumed to be known and show no variability. However, some parameters fed into the models are inherently uncertain which may lead to different decisions or management strategies when small changes on the uncertain parameters are performed. To further investigate the effect of the uncertainty, for simplicity in this thesis we perform sensitivity analysis in order to determine the robustness of the models proposed and get more insightful results. The information provided by the sensitivity analysis is extremely valuable in making decisions since provides insights on: how robust the optimal solution is and under what circumstances the solution would change and how much

worse would be a decision ignoring the uncertainty. In case that the optimal solution is robust (low sensitive to changes in parameters), it is reasonable to adopt decisions based on the solution anyway, since it would be confidence. On the other hand, if the optimal solution is not robust, the deterministic solution may not be acceptable because it is risky but it helps to identify the most critical circumstances and ultimately to identify a strategy that performs well in all circumstances.

The models developed in this thesis are small enough to be solved in a reasonable computational time, so we employed the brute force approach for the sensitivity analysis which consists of changing the initial parameter values and solving the model repeatedly to understand how these uncertainties affect the outcome of the optimisation. The optimisation model is solved iteratively for different potential values of the uncertain parameters (i.e. scenarios), which can be modelled based on known upper and lower bounds or by using probability distributions (e.g. normal, triangular, and uniform). In any case, each parameter value accounting for a different realisation of the uncertain parameter which defines one scenario which are generated (discretized) by applying sampling methods on the probability distributions (e.g. Monte Carlo or Geometric Brownian Motion). More number of scenarios leads to better approximations but also to larger CPU times. To determine the minimum number of scenarios to ensure a specific confidence level of the results, the test proposed by Law and Kelton can be employed (Law and Kelton, 2000). Finally, the set of optimal solutions, derived by solving the set of scenarios (i.e. scenario tree), should be provided to improve the decision and policy maker's knowledge and understanding of the problem to finally take the best decision (Figure I-10). In order to facilitate the interpretation of the results from the sensitivity analysis, they can be provided visually by means of scatter plots, box plots, cumulative distribution or heat maps among other plots.

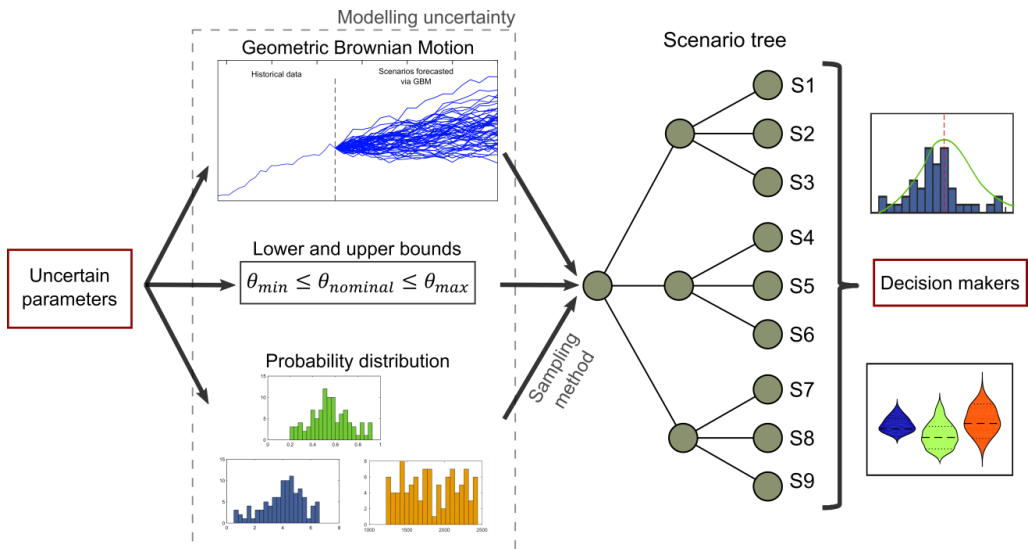


Figure I-10. Sensitivity and uncertainty process tailored to decision-making.

1.4.5 Modelling frameworks

Several algebraic modelling languages (AMLs) have been developed aiming to allow users to express a given problem via algebraic mathematical expressions such as Matlab (Grant et al., 2008), AMPL (Fourer et al., 1990), AIMMS (Bisschop and Roelofs, 2006) and GAMS (Brooke and D Meeraus, 1996). In this thesis we have employed GAMS as modelling framework to implement the mathematical models since it is the most used optimisation software in the Process System Engineering (PSE) field and offers multiple solvers options to derive the solution of the model.

There are several optimisation algorithms implemented and available in GAMS (subject to the proper license), each solver developed to tackle a specific type of problem (i.e. LP, NLP, MILP, MINLP, etc). Without loss of generality, in this thesis, we have employed CPLEX optimisation solver package (IBM, 2009) and BARON solver (Sahinidis, 1996). CPLEX is capable of solving with high performance linear, mixed integer and quadratic constrained programming problems while BARON is devised for the global optimality of nonlinear and mixed-integer nonlinear programs.

1.5 Environmental impact assessment

The environmental dimension of the sustainability challenge is addressed in this thesis by appending the environmental impact as a criterion in the optimisation mathematical models either as an additional objective function or as constraints (see section 1.3). So far, there is no general agreement on how to determine the effects of a system on the environment. Environmental impact assessment has traditionally constituted the methodological basis both in the scientific and political spheres to systematically identify and evaluate the potential impacts that a system may have on the environment. Among the wide range of environmental impact assessment methodologies, Life Cycle Assessment (LCA) has become the predominant methodology that is broadly applied both in private and public environmental decision-making contexts (Azapagic and Clift, 1999a, 1999b; Grossmann, 2004; Hellweg and Milà i Canals, 2014; Pieragostini et al., 2012).

1.5.1 *Life cycle assessment*

LCA is a methodology that aims at quantifying and assessing the inputs and outputs and potential environmental impacts/burdens (on a wide range of environmental issues such as climate change, land use, etc...) of products and processes throughout its entire life cycle (Guinée, 2001; ISO, 2006). In practice, LCA has been typically devised, both in the scientific and political spheres, to improve product systems, to map key drivers of impact on corporate strategies, to provide hotspot analysis of consumption life styles patterns and to pinpoint crucial areas either of consumption or production at regional/country/international level (Hellweg and Milà i Canals, 2014).

Integration of LCA and mathematical programming is worldwide recognised as a powerful tool to aid sustainable decision-making that allows incorporating environmental protection criteria into the decision process. Optimisation on environmental models has been traditionally applied since the middle of 1990s (Azapagic and Clift, 1995) in many areas of sciences and engineering. The reader is

referred to review applications on this topic to the article by Pieragostini et al., (2012). Their tailored combination to the common goal to guide practitioners improving the environmental performance, allows providing useful insights for both decision and policy makers resulted from the strengthen and complementarities of the combined approach (Azapagic and Clift, 1999a, 1999b; Grossmann and Guillén-Gosálbez, 2010b; Grossmann, 2004; Hellweg and Milà i Canals, 2014; Pieragostini et al., 2012). Particularly, LCA allows quantitatively assessing the environmental impact associated to goods and services along its entire life cycle, meanwhile mathematical programming incorporates the former LCA burden and impact quantitative data into the models that are solved identifying in a systematic way the best alternatives (i.e. optimum) according to such as environmental criteria (or in addition to others technical, economic or social criteria). In this context, accounting for the environmental dimension in the sustainable decision-making optimisation framework comprises two consecutive steps. First, an LCA study needs to be carried out to determine the burdens and impacts along the entire life cycle that are then treated as inputs (i.e. parameters) of the optimisation model in the second step. See Figure I-11 for a general overview of the combined approach of mathematical programming and LCA.

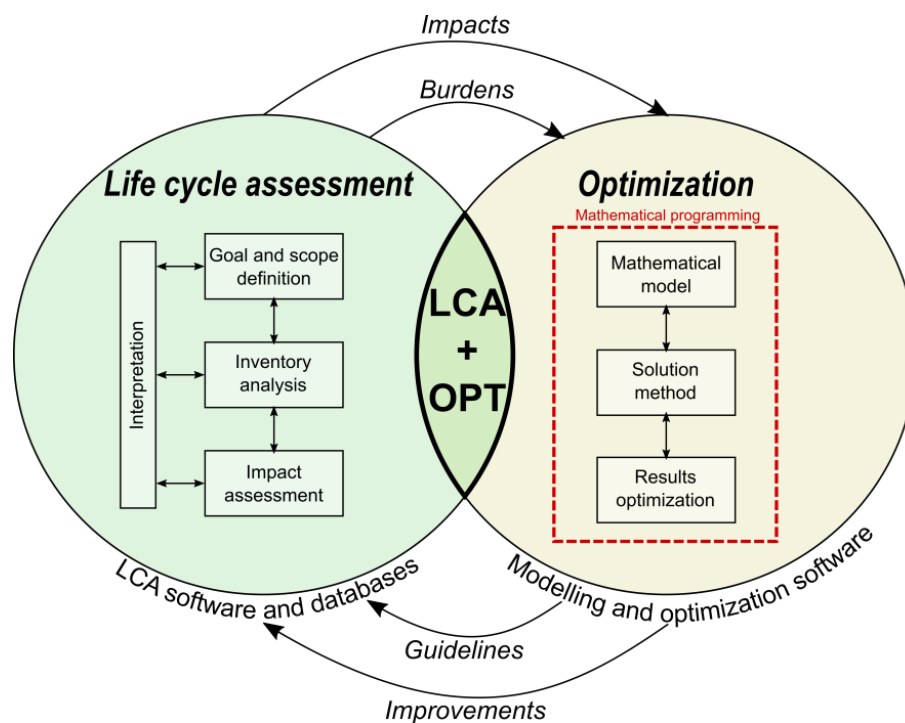


Figure I-11 General overview of the optimisation and LCA combined approach.

As mentioned previously, performing an LCA study allows quantifying the burdens and impacts that are then incorporated as parameters into the mathematical programming models representing the problem addressed. Carrying out a LCA study typically entails four phases: i) description of the goal and scope, ii) inventory, iii) impact assessment, and iv) interpretation. Further details on the principles and framework of LCA are given in the ISO:14044 standards for LCA (ISO, 2006). Conducting the whole LCA study is a time expensive and hard task. To facilitate this process commercial software and models have been developed such as the two leading software used for LCA studies: SimaPro (Goedkoop et al., 2008; Pre-sustainability, 2017) and GaBi (PE-international, 2017). However, even in the case that such tools are employed, the process requires great efforts. To overcome these limitations, several LCA databases are available and become an important data source, being the most popular Ecoinvent (Frischknecht and Rebitzer, 2005). Unfortunately most of software and databases are not open sources since setting

up and maintaining them is economically expensive that limits its widespread accessibility (Hellweg and Milà i Canals, 2014).

The four phases of a LCA study process are described next into details:

1. The first phase consists of the goal definition and scoping that determine and guide the entire process. Many decisions need to be taken throughout this stage that will determine the results of the study. At this stage, the goal and spatial and temporal scope of the study are set and also the functional unit and system boundaries are defined. Furthermore, it is required to choose between attributional or consequential modelling approaches since it influences the next step (i.e. life cycle inventory), system boundaries and other methodological choices (Finnveden et al., 2009; Frischknecht and Stucki, 2010). So far attributional is the most commonly used LCA approach, which assigns responsibilities for a set of impacts. There are two methods to partition the environmental burdens among different products of the same process, namely system expansion and allocation. The former considers products and co-products as different alternatives to assign the environmental burdens. System expansion is the recommended approach (ISO, 2006) and when system expansion is not possible, the allocation approach can be applied by apportion the impacts according to weights (e.g. mass, economic or energy allocation).

2. The second phase of the LCA process consists of the life cycle inventory analysis (LCI) where all inputs and outputs of the system are compiled (measured, estimated or sourced) and tracked along the life cycle. This stage usually requires an iterative process with the scope and goal definition to refine boundaries and allocations. The system is broken down into small units where all inputs and outputs are usually compiled from different sources. Large amount of data need to be accounted at these stage which ultimately leads to variability and uncertainty. The process of the inventory can be mathematically expressed as follows (Eq. I-7):

$$LCI_i^{TOT} = \sum_j LCI_{i,j} \quad \forall i \quad \text{Eq. I-7}$$

where LCI_i^{TOT} represent the total amount of a specific flow i which is computed as the summation of all the flows i for all the system units j $LCI_{i,j}$.

3. The third phase consists of the life cycle impact assessment (LCIA) where all burdens are translated into impacts by multiplying by factors referring to environmental impacts. Here, all emissions and resources previously collected in the inventory are clustered into impact categories and converted into environmental impacts using characterisation factors. Several LCIA methodologies are available that differ in the impact categories covered, the impact indicators and the geographical focus. We refer the reader to JRC (2011) that describes the indicators and models employed providing general choice recommendations. After the characterisation is performed, optional steps are normalisation and weighting. Normalisation allows all impact indicators to be in a common metric and therefore comparable while weighting is used to group different impact categories based on subjective valuations (but agreed in the scientific community). The way to proceed for the impact characterisation is summarise as follows. First, The LCI data are transformed into impact referring to the midpoint categories by means of Eq. I-8.

$$I_m = \sum_i C_{mi} \cdot LCI_i^{TOT} \quad \forall m \quad \text{Eq. I-8}$$

where C_{mi} denotes the characterisation factor that relates the flow i with the midpoint impact category m . As a result I_m represent the indicator for the midpoint category m . Then, taking the midpoint category indicators can be aggregated into the endpoint damage categories as stated in Eq. I-9:

$$I_e = \sum_m N_{me} \cdot I_m \quad \forall e \quad \text{Eq. I-9}$$

where N_{me} denotes the normalisation factors that relates the midpoint categories m with the endpoint category e allowing aggregating them into the endpoint

categories indicators e (I_e). Finally, the endpoint category indicators can be aggregated into a single final score (S) as follows Eq. I-10 :

$$S = \sum_e W_e \cdot I_e \quad \text{Eq. I-10}$$

where the endpoint indicators I_e are multiplied by weighting factors W_e that allows to convert them into same units (i.e. points) that can be summed given rise the weighted impact score S .

Finally, along this impact conversion instrument the indicator resulted can be chosen either at midpoint or endpoint level or as a weighted unique score. There is no guideline about whether a midpoint or an endpoint output should be considered. Midpoint approach provides impact information in several impact categories, while endpoint approach provides impact information aggregated in three areas of protection (i.e. ecosystem quality, human health and resource depletion) that could be appealing for stakeholders who require lower level of environmental impact detail. The choice between midpoint or endpoint categories has to be taken according to the nature of the case study bearing in mind that the higher the aggregation level the lower certainty and more information is lost, however, in some cases it is more relevant for decision-makers.

4. The last phase of the LCA study consists of the interpretation of the results. Here, conclusions of the study are drawn in order to provide recommendations for the decision-making process. Results are very useful to pinpoint where efforts should be made in order to minimise the environmental impact, however, no targets and clear guidelines are provide to achieve the optimal reduction. Moreover, very often the environmental decision problems becomes very complex since it is necessary to compare several alternatives, considering various conflicting objectives (i.e. different impact categories) in many different scenarios. Furthermore, the interdisciplinary nature of the problems requires high number of stakeholders that makes the decision-making very challenging. To overcome these

limitations, LCA outcomes can be incorporated into mathematical programming models that allow identifying in a systematic manner the best ones according to the environmental principles. Once the burdens and impacts along the entire life cycle are either quantified following the previous four phases or collected from an LCA database, they are subsequently fed as parameters into the optimisation model where the problem under study is modelled by means of mathematical equations and solved in order to find the optimal solution.

1.6 Outline: problems addressed

The use of mathematical programming to address global sustainability problems has a great potential and will be a major focus of research to aid decision and policy makers towards making effective actions for a sustainable future. Below a brief summary of the four problems addressed in this thesis (Figure I-2) is shown that will be then developed in details in the ensuing Chapters II, III, IV and V.

1.6.1 *Sustainable allocation of cropping areas (article 1)*

Water scarcity is a major environmental problem worldwide with a large impact on the degradation of ecosystems and depletion of resources (Núñez et al., 2013; Rijsberman, 2006; Rockström et al., 2009; Steffen et al., 2015). Particularly, in arid and semiarid countries freshwater consumption causes significant environmental impacts on natural resources and ecosystems that, at the end, will affect human well-being and health. Most production systems create water shortages which affect natural systems and, in particular, the agricultural sector represents more than two-thirds of the global water use (FAO, 2014; Garrido et al., 2010; Núñez et al., 2013; UNEP, 2007). In this backdrop, appropriate strategies and policies are needed in the agricultural sector in order to achieve a more sustainable agricultural production system, thereby contributing to the required food security transformation.

Previous research has concentrated on quantifying the environmental impact of water consumption without proposing specific measures to solve/minimise the

problem (Hoekstra et al., 2011; Pfister et al., 2009). However, to achieve a more sustainable agricultural production, it is necessary to integrate these descriptive metrics with tailored decision-making tools. Mathematical programming tools can assist decision-making in this field. In particular, the combined use of multi-objective optimisation with life cycle assessment principles is a well suited approach to address environmental issues when production objectives must be optimised without neglecting the environmental concerns.

This work presents a systematic multi-objective optimisation tool for optimising rainfed and irrigated areas considering economic and environmental criteria (Á Galán-Martín et al., 2016). The reader is referred to chapter II for further detailed description on this work. The tool developed is based on a linear programming model that integrates water footprint data and life cycle assessment principles. The water footprint methodology is used to estimate the crop water requirements for green, blue and grey water in a specific location, while the life cycle assessment methodology determines the potential environmental impact on ecosystems and resources. The solution of the multi-objective linear programming model developed is given by a set of optimal Pareto alternatives, each showing a unique combination of objectives values and entailing specific optimal rainfed and irrigated cropping areas.

The capabilities of the proposed approach have been demonstrated through its application to the real case study of wheat (*Triticum aestivum* L.) production in Spain. Results show that significant reductions in the damage to ecosystems and resources can be attained while still maintaining or even increasing the wheat production by an adequate distribution of the rainfed and irrigated wheat areas in the Spanish watersheds. Moreover, some of the Pareto solutions found, each one entailing specific optimal crop areas in each watershed, improve the current situation simultaneously in the two objectives considered. From the set of Pareto solutions, decision and policy makers should select the best one according to their

economic and environmental preferences and considering the views of the farmers and stakeholders (social concerns). Therefore, these optimal solutions represent a useful guide to define appropriate strategies and policies that will ensure a more sustainable agriculture system, minimise the environmental damage and ensuring food security

Figure I-12 shows a graphical summary of the main finding of article 1.

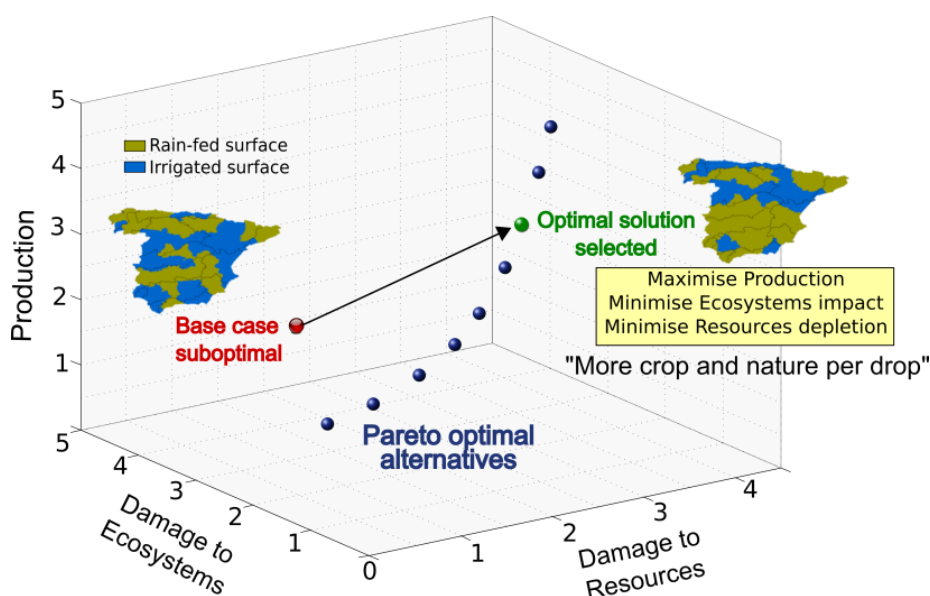


Figure I-12 Graphical abstract of article 1: Multi-objective optimisation of rainfed and irrigated agricultural areas considering production and environmental criteria: A case study of wheat production in Spain.

1.6.2 Sustainable cropping plan decisions and subsidies (Article 2)

The new European Union's Common Agricultural Policy (CAP) covers the period from 2015 to 2020 (European Commission, 2011). Significant novelties in the payment scheme have been introduced which may potentially encourage farmers to implement changes at the farm level by meeting certain environmental requirements in return for new support payments. The mandatory requirements, commonly known as 'greening rules', consist of crop diversification, maintenance of permanent grassland and establishment of an ecological focus area which arise as

key strategies to move towards a more sustainable agricultural production. Several EU farms will fulfil these greening measures without having to make major changes. However, very likely, many farmers will have to make land use decisions bearing in mind the new greening rules which will in turn imply significant changes at the farm level. In this context, decision support models based on mathematical programming techniques may play an important role in order to aid farmers on the farm management facing the new CAP reform.

This work presents a decision-support tool based on a multi-stage linear programming model that identifies optimal cropping plan decisions under the new Common Agricultural Policy (Galán-Martín et al., 2015). Furthermore, by slightly modifying the mathematical formulation, the model proposed is capable of identifying the effective subsidies to spur the broad applicability of the agricultural practises beneficial both for the world's climate and environment. In that sense, the model aims at supporting both EU farmers and EU governments in response to the new CAP reform. A detail description of this work is included in Chapter III.

The capabilities of the tool developed are illustrated through its application to the Spanish payment regionalisation CAP model, which divides the territory in several agricultural regions defined according with similarities on agronomic and socio-economic characteristics. Without loss of generality, six rainfed crops were considered (i.e. wheat, barley, rye, oat, dried peas and sunflower) with particular selling prices, exploitation costs and yields determined based on historical data. The model allows identifying the optimal cropping plans (i.e. crops to be grown and their acreage each year during the reform horizon) that maximises the farmer's net return in each Spanish region by simultaneously meeting the sustainability requirements. The results show that the optimal cropping plans during the policy horizon vary greatly across regions as well as the farmer's net economic return. Additionally, the results suggest that several regions may not fulfill the CAP greening rules because the economic incentive is too small to compensate farmers for the

loss in profit they incur from the implementation of the greening requirements. In consequence, the model is used to calculate the minimum subsidy value that would make the implementation of greening rules economically appealing in all Spanish agricultural regions, thereby acting as a mechanism to promote the shift towards more sustainable agricultural practises. The tool proposed in this work may contribute to the effective transition towards agricultural practises beneficial for the world's climate and environment.

Figure I-13 shows a graphical representation of article 2.

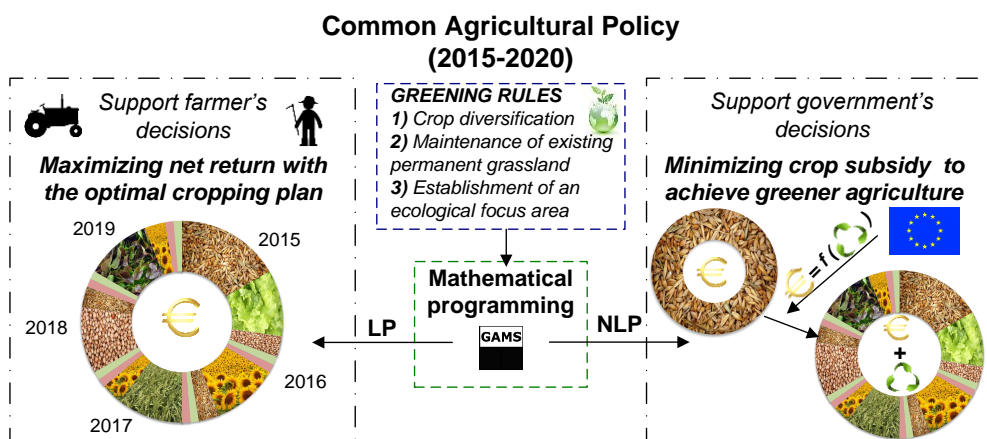


Figure I-13 Graphical abstract of article 2: Multi-stage linear programming model for optimising cropping plan decisions under the new Common Agricultural Policy.

1.6.3 Data envelopment analysis for sustainability assessment (Article 3)

So far no general agreement has been reached on how to assess the level of sustainability of a system (Azapagic and Perdan, 2000; Pope et al., 2004b). This task is challenging, since in sustainability assessment economic, environmental and social aspects need to be considered simultaneously. In this work we explore the use of data envelopment analysis (DEA) (Charnes et al., 1978; Cook and Seiford, 2009), a tool widely used to measure the efficiency of comparable systems, to assess the extent to which a system adheres to sustainability principles. Unfortunately, the standard DEA approach shows two major limitations particularly critical when it is applied for sustainability assessment: it makes no distinction

between the units deemed efficient, and does not offer information regarding each sustainability dimension and the results are very sensitive to the set of input and output considered.

In this work, we proposed an enhanced DEA to overcome the limitations of the standard DEA by integrating the latter with the concept of order of efficiency (Á. Galán-Martín et al., 2016). A detailed description of this work is shown in Chapter IV. In essence, the idea is to repeat the calculation for all the possible combinations of inputs and outputs within each of the sustainability and providing sustainability efficiency metrics. Our enhanced DEA approach presents the following advantages: (i) it considers each sustainability dimension separately, thereby providing more information; (ii) it can handle a large number of economic, environmental and social criteria; (iii) it enables ranking of alternatives according to the extent to which they adhere to defined sustainability principles; and (iv) it provides clear quantitative targets for the inefficient systems to improve their sustainability.

The capabilities of the approach are illustrated through its application to the assessment of electricity generation technologies in United Kingdom, which are expected to play a major role in the future electricity mix. Several economic, environmental and social indicators calculated following a life a cycle approach were considered. The enhanced DEA allowed ranking the technologies according to their sustainability level and provided as well targets for the least sustainable technologies that would make them more sustainable. Our analysis revealed that gas, nuclear and wind are the most sustainable technologies. Coal and solar photovoltaic should improve their environmental and social performance in order to increase their sustainability efficiency. Biomass, either with *Miscanthus sp.* or wood pellets, is equitable but environmentally inefficient, while coal with carbon capture and storage is a bearable technology but economically inefficient.

The enhanced DEA is a useful tool for decision and policy makers, as it allows identifying the main sources of inefficiency, setting in turn targets for future

attainment in order to move towards a more sustainable development. Figure I-14 shows a graphical summary of article 3.

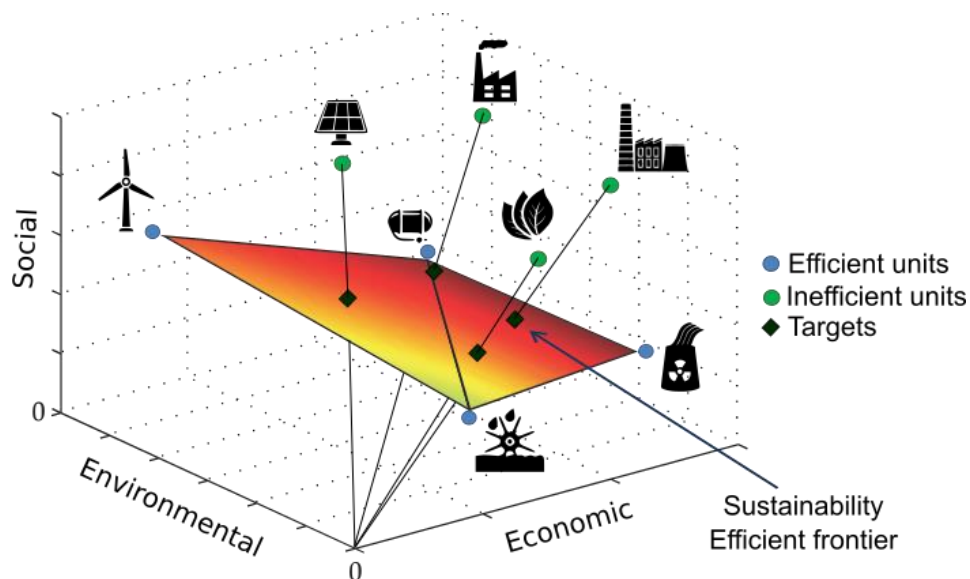


Figure I-14 Graphical abstract of article 3: Enhanced data envelopment analysis for sustainability assessment: A novel methodology and application to electricity technologies.

1.6.4 Tackling climate change in cooperation (Article 4)

Climate change is one of the main challenges facing the world today which has been in the international political agenda as a collective commitment since the United Nations Framework Convention on Climate Change entered into force more than twenty years ago (UNFCCC, 2017). Despite the efforts made so far, the current impasse in climate change negotiations together with the recent withdrawal of U.S. from the Paris Agreement call for new cooperative mechanisms to enable resilient international response (EPA, 2015; Keohane and Victor, 2016; Sandler, 2004; Schmidt, 2015). In this contribution we envision an approach to aid such negotiations based on quantifying the benefits of interregional cooperation and allocating them among the participants in a fair manner (Galan-Martin et al., 2017). The approach is underpinned by advanced optimisation techniques that allow identifying the most cost-effective solutions for meeting emission targets for differing levels of cooperation among the parties involved. The reader is referred to

Chapter V for a detailed description of this work.

To illustrate how our approach would work in practice we consider the U.S. Clean Power Plan (EPA, 2015), a related act in the U.S. aiming to curb the electricity carbon emissions but also being withdrawn, which was the very first step of U.S. that seeks to curb CO₂ emissions by 35% from the power sector. To do so, the plan establishes state individual targets based on three building blocks: switching from coal-powered to natural gas power plants, increasing the share of zero emitting renewable energy generation and improving plant efficiency. To carry out our analysis we have developed a mixed integer mathematical programming named ERCOM (as an acronym for Emission Reduction Cooperation Model) which determines the most cost-effective solution for meeting the electricity demand for different levels of cooperation while not exceeding the total CO₂ emissions ceiling imposed by the U.S. Clean Power Plan. Our approach is underpinned by robust optimisation techniques that automate the screening of millions of alternatives for differing levels of cooperation, ultimately identifying the most cost-effective solutions for meeting emission targets.

The results of the analysis reveal that significant benefits can be attained for low levels of cooperation since, with only half of states cooperating, the cost of electricity generation could be reduced by US\$41 billion per year, while simultaneously cutting carbon emissions by 68% below 2012 levels. These economic and environmental gains arise from sharing the emissions targets and trading electricity thereby exploiting regional advantages. However, this collective gain of cooperation, despite necessary, may be not sufficient, since it also entails an asymmetric distribution of efforts where some states can be penalised when moving towards the partnership. Therefore, efficient mechanisms need to be developed to engage all states through the collective action. Fair sharing of cooperation dividends may be used as a key driver to spur cooperation since the global action to mitigate climate change becomes beneficial for all participants.

We argue that the proposed approach may be used as starting point to break the impasse in the climate change negotiations that could be used in greater future international challenges. Even if global cooperation remains elusive, it is worth trying since the mere cooperation of a few states leads to significant benefits both for the U.S. economy and the climate. These findings call on U.S. to reconsider its withdrawal from the Paris Agreement but also boost individual states to take initiative even in the absence of federal action. Figure I-15 shows a graphical summary of article 4.

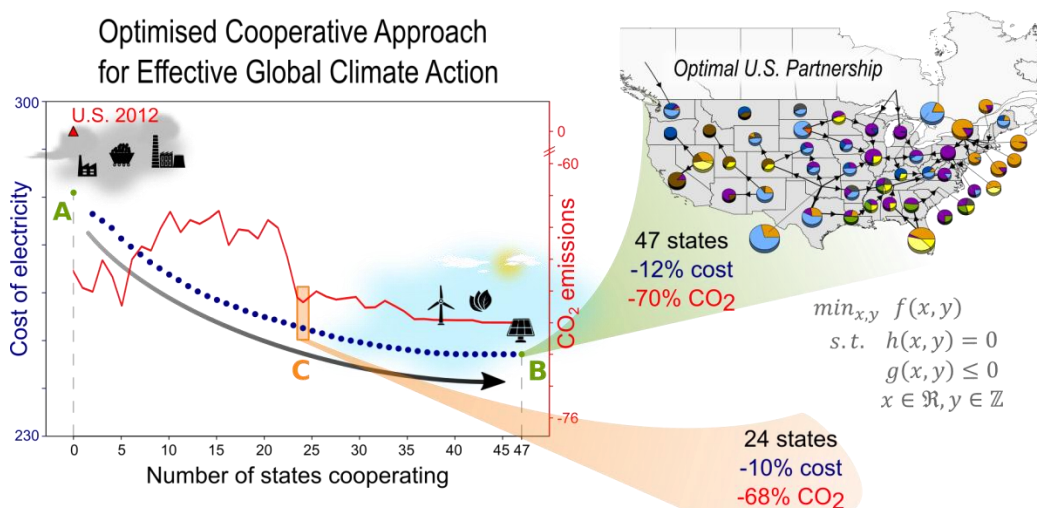


Figure I-15 Graphical abstract of article 4: Time for global action: An optimised cooperative approach towards effective climate change mitigation

1.7 General conclusions

This thesis has been devoted to develop mathematical programming models and methods to support sustainable decision and policy making. Different mathematical programming models have been developed to tackle some sustainability challenges with emphasis on sustainable agricultural planning and sustainable energy systems modelling. We next present a summary of the knowledge derived from the study of the four problems addressed in this thesis. Note that further discussions and particular conclusions can be found in each corresponding chapter. The general conclusions are listed below:

- A systematic multi-objective optimisation tool to optimal allocating rainfed and irrigated crop areas considering simultaneously both economic and environmental criteria have been developed. The tool integrates life cycle assessment principles and water footprint accounting with mathematical programming techniques which allows identifying optimal allocations patterns that simultaneously maximise the crop production and minimise impact on environment. The tool is intended to support decision and policy makers to promote a more sustainable agriculture.
- A multi-stage mathematical programming model for crop planning facing the new Common Agricultural Policy reform has been developed. The applicability of the support-tool is twofold, since it may be used to support farmers' decisions facing the new greening measures but also to support governments proposing an adequate subsidy to potentially engage all farmers towards the sustainable agricultural practices.
- An enhanced data envelopment analysis tailored to perform sustainability assessments has been proposed. The method allows ranking systems according to sustainability principles and also allows in turn pinpointing in a systematic manner the main sources of inefficiency and set improvement targets to become sustainable.
- A novel approach to enable a resilient collaborative international response in negotiations on climate change mitigation is proposed. This approach is based on quantifying the benefits of curbing CO₂ emissions in cooperation using rigorous optimisation tools and distributing them among the parties involved in a fair manner so as to spur an effective collective action.
- The capabilities of the decision and policy making support tools developed in this thesis have been tested by applying them to real world case studies, therefore demonstrating that they could actually be used in the real context guiding us towards more sustainable decisions.

- New tools to reconnect the human development to sustained progress are and will be needed. We have demonstrated that we have the tools to develop new decision and policy making support mechanisms based on optimisation models and methods that might make a key contribution towards the sustainability transition.

1.8 Future work

A wide range of issues as well as potential improvements and new ideas have been revealed in the course of this thesis that may be focus of further investigation. Here we present some of the potential research lines to be explored in future work:

- This thesis was devoted to two key structural transformations (sustainable food security and sustainable energy transformation) contributing to the much-needed transition towards sustainability. Particularly, the optimisation tools developed make a contribution to tackle four out of the nine global environmental challenges currently highlighted, namely, ecosystem loss, climate change, land use change and freshwater use. In the future further attention may be pay to other problems contributing to the remaining global environmental challenges and others emerging ones (e.g. biodiversity loss or chemical production).
- Other key structural transformations towards sustainability to be tackled in the future may be the “Urban sustainability transformation” since urbanisation is increasing extremely rapidly in all developing countries. Sustainable optimisation problems may be addressees related with buildings, smart power grids or transportation.
- So far traditional approaches to sustainability have been concentrated on the production side (i.e. production-based approaches), that is, all the responsibility and environmental burdens are allocated to producers. However, it can be arguably unfair since consumers should also bear some

responsibility about that. Consumers have a key role in the transition towards sustainability. Adopting consumption-based approaches to address problems may constitute a major focus of future research as towards optimising and modifying consumption patterns (e.g. energy consumption or diet). Initiatives supported by mathematical programming models to promote more sustainable lifestyles may play a key role towards sustainable development.

- Social indicators were almost neglected in our approach. Enlarge the scope of the sustainability encompassing more social aspects together with the economic and environmental criteria will be a major focus for future research. Although it might prove challenging from the parameter gathering perspective, there are some emerging methodologies recently proposed (i.e. Social Life Cycle Assessment initiative) that may be used to include social aspects.
- Further work can be focused on the introduction of uncertainties into the models in order to provide more robust solutions. Formulations can be extended to other proactive and preventive approaches such as rolling horizons or stochastic programming.
- Regarding the sustainable food security challenge, the formulation presented in Chapter II may be extended considering agricultural production disturbances under climate change and considering the unstoppable population growth, in line with initiatives such as “The challenge of feeding 10 billion people” with minimum environmental impact (Godfray et al., 2010; Priefer et al., 2013).
- In order to provide more tailored information for decision and policy-makers it may be interesting further extend the formulations incorporating stakeholders’ preferences by means of *a priori* articulation methods such as

bi-level optimisation. Furthermore, development of software tools implementing the models developed herein would be crucial to widen their applicability.

1.9 References

Azapagic, A., 1999. Life cycle assessment and its application to process selection, design and optimisation. *Chem. Eng. J.* 73, 1–21. doi:10.1016/S1385-8947(99)00042-X

Azapagic, A., Clift, R., 1999a. Life cycle assessment and multiobjective optimisation. *J. Clean. Prod.* 7, 135–143. doi:10.1016/S0959-6526(98)00051-1

Azapagic, A., Clift, R., 1999b. The application of life cycle assessment to process optimisation. *Comput. Chem. Eng.* 23, 1509–1526. doi:10.1016/S0098-1354(99)00308-7

Azapagic, A., Clift, R., 1995. Life cycle assessment and linear programming environmental optimisation of product system-. *Comput. Chem. Eng.* 19, 229–234. doi:10.1016/0098-1354(95)87041-5

Azapagic, A., Perdan, S., 2000. Indicators of sustainable development for industry: A general framework. *Process Saf. Environ. Prot.* 78, 243–261.

Banker, R.D., Charnes, A., Cooper, W.W., 1984. Some models for estimating technical and scale inefficiencies in data envelopment analysis. *Manage. Sci.*

Bilcke, J., Beutels, P., Brisson, M., Jit, M., 2011. Accounting for methodological, structural, and parameter uncertainty in decision-analytic models: a practical guide. *Med. Decis. Mak.* 31, 675–692.

Bisschop, J., Roelofs, M., 2006. AIMMS language reference. Lulu. com.

Brooke, A., Kendrick, D., Meeraus, A., Raman, R., America, U., 1998. The general algebraic modeling system. GAMS Dev. Corp.

Brooke, A.K., D Meeraus, A., 1996. GAMS release 2.25; a user's guide. GAMS Development Corporation, Washington, DC (EUA).

Bussieck, M.R., Drud, A., 2001. SBB: A new solver for mixed integer nonlinear programming. GAMS Dev. Corp.

Charnes, A., Cooper, W.W., Rhodes, E., 1978. Measuring the efficiency of decision making units. *Eur. J. Oper. Res.* 2, 429–444. doi:10.1016/0377-2217(78)90138-8

Cook, W.D., Seiford, L.M., 2009. Data envelopment analysis (DEA) – Thirty years on. *Eur. J. Oper. Res.* 192, 1–17. doi:10.1016/j.ejor.2008.01.032

Cooper, W.W., Seiford, L.M., Zhu, J., 2004. *Data Envelopment Analysis: History, models and interpretations*. Kluwer Academic Publishers, Boston.

Cuthill, M., 2010. Strengthening the “social” in sustainable development: Developing a conceptual framework for social sustainability in a rapid urban growth region in Australia. *Sustain. Dev.* 18, 362–373.

Dantzig, G.B., Orden, A., Wolfe, P., 1955. The generalized simplex method for minimizing a linear form under linear inequality restraints. *Pacific J. Math.* 5, 183–195.

Das, I., Dennis, J.E., 1998. Normal-boundary intersection: A new method for generating the Pareto surface in nonlinear multicriteria optimization problems. *SIAM J. Optim.* 8, 631–657.

Ehrgott, M., 2009. Multiobjective Optimization. *AI Mag.* 29, 47. doi:10.1609/aimag.v29i4.2198

Ehrgott, M., 2006. *Multicriteria optimization*. Springer Science & Business Media.

EPA, 2015. Clean Power Plan for existing Power Plants. Environmental Protection Agency.

European Commission, 2011. Proposal for a Regulation of the European Parliament and of the Council Establishing Rules for Direct Payments to Farmers Under Support Schemes Within the Framework of the Common Agricultural Policy, COM(2011) 627 Final/2.

FAO, 2014. AQUASTAT-FAO's information system on water and agriculture [WWW Document]. Organ. las Nac. Unidas para la Aliment. y la Agric. URL <http://www.fao.org/nr/water/aquastat/main/index.stm> (accessed 3.4.14).

Farrell, M.J., 1957. The measurement of productive efficiency. *J. R. Stat. Soc. Series A*, 253–281.

Finnveden, G., Hauschild, M.Z., Ekvall, T., Guinée, J., Heijungs, R., Hellweg, S., Koehler, A., Pennington, D., Suh, S., 2009. Recent developments in Life Cycle Assessment. *J. Environ. Manage.* 91, 1–21. doi:10.1016/j.jenvman.2009.06.018

Fourer, R., Gay, D.M., Kernighan, B.W., 1990. A modeling language for mathematical programming. *Manage. Sci.* 36, 519–554.

Frischknecht, R., Rebitzer, G., 2005. The ecoinvent database system: a comprehensive web-based LCA database. *J. Clean. Prod.* 13, 1337–1343. doi:<http://dx.doi.org/10.1016/j.jclepro.2005.05.002>

Frischknecht, R., Stucki, M., 2010. Scope-dependent modelling of electricity supply in life cycle assessments. *Int. J. Life Cycle Assess.* 15, 806–816. doi:10.1007/s11367-010-0200-7

Galán-Martín, Á., Guillén-Gosálbez, G., Stamford, L., Azapagic, A., 2016. Enhanced data envelopment analysis for sustainability assessment: A novel methodology and application to electricity technologies. *Comput. Chem. Eng.* 90.

doi:10.1016/j.compchemeng.2016.04.022

Galan-Martin, A., Pozo, C., Azapagic, A., Grossmann, I.E., Mac Dowell, N., Guillen-Gosalbez, G., 2017. Time for global action: an optimised cooperative approach towards effective climate change mitigation. *Energy Environ. Sci.* doi:10.1039/C7EE02278F

Galán-Martín, A., Pozo, C., Guillén-Gosálbez, G., Antón Vallejo, A., Jiménez Esteller, L., 2015. Multi-stage linear programming model for optimizing cropping plan decisions under the new Common Agricultural Policy. *Land use policy* 48. doi:10.1016/j.landusepol.2015.06.022

Galán-Martín, Á., Vaskan, P., Antón, A., Esteller, L.J., Guillén-Gosálbez, G., 2016. Multi-objective optimization of rainfed and irrigated agricultural areas considering production and environmental criteria: A case study of wheat production in Spain. *J. Clean. Prod.* doi:10.1016/j.jclepro.2016.06.099

Garrido, A., Llamas, M., Varela-Ortega, C., Novo, P., Rodríguez-Casado, R., Aldaya, M., 2010. *Water Footprint and Virtual Water Trade in Spain: Policy Implications*. La Fundación Marcelino Botín-Sanz de Sautuola y López, New York, NY.

Godfray, H.C.J., Beddington, J.R., Crute, I.R., Haddad, L., Lawrence, D., Muir, J.F., Pretty, J., Robinson, S., Thomas, S.M., Toulmin, C., 2010. Food security: the challenge of feeding 9 billion people. *Science* (80-.). 327, 812–818.

Godfray, H.C.J., Garnett, T., 2014. Food security and sustainable intensification. *Phil. Trans. R. Soc. B* 369, 20120273.

Goedkoop, M., De Schryver, A., Oele, M., Durksz, S., de Roest, D., 2008. *Introduction to LCA with SimaPro 7*. PRé Consult. Netherlands.

Grant, M., Boyd, S., Ye, Y., 2008. *CVX: Matlab software for disciplined convex programming*.

Grossmann, I., 2014. Challenges in the application of mathematical programming in the enterprise-wide optimization of process industries. *Theor. Found. Chem. Eng.* 48.

Grossmann, I.E., 2004. Challenges in the new millennium: product discovery and design, enterprise and supply chain optimization, global life cycle assessment. *Comput. Chem. Eng.* 29, 29–39. doi:10.1016/j.compchemeng.2004.07.016

Grossmann, I.E., Caballero, J.A., Yeomans, H., 2000. Advances in mathematical programming for the synthesis of process systems. *Lat. Am. Appl. Res.* 30, 263–284.

Grossmann, I.E., Guillén-Gosálbez, G., 2010a. Scope for the application of mathematical programming techniques in the synthesis and planning of sustainable processes. *Comput. Chem. Eng.* 34, 1365–1376. doi:10.1016/j.compchemeng.2009.11.012

Grossmann, I.E., Guillén-Gosálbez, G., 2010b. Scope for the application of mathematical programming techniques in the synthesis and planning of sustainable processes. *Comput. Chem. Eng.* 34, 1365–1376. doi:10.1016/j.compchemeng.2009.11.012

Grossmann, I.E., Viswanathan, J., Vecchiotti, A., Raman, R., Kalvelagen, E., 2002. GAMS/DICOPT: A discrete continuous optimization package. GAMS Corp. Inc.

Guillén-Gosálbez, G., Grossmann, I., 2010. A global optimization strategy for the environmentally conscious design of chemical supply chains under uncertainty in the damage assessment model. *Comput. Chem. Eng.* 34, 42–58.

Guinée, J., 2001. Handbook on life cycle assessment — operational guide to the ISO standards. *Int. J. Life Cycle Assess.* 6, 255. doi:10.1007/BF02978784

Haimes, Y., Lasdon, L., Wismer, D., 1971. On a bi-criterion formulation of the

problems of integrated system identification and system optimization. *IEEE Trans. Syst. Man Cybern.* 1 (3), 296–297.

Hellweg, S., Milà i Canals, L., 2014. Emerging approaches, challenges and opportunities in life cycle assessment. *Science* (80-.). 344, 1109 LP – 1113.

Heyman, D.P., Sobel, M.J., 2003. *Stochastic models in operations research: stochastic optimization*. Courier Corporation.

Hoekstra, A.Y., Chapagain, A.K., Aldaya, M., Mekonnen, M.M., 2011. *The water footprint assessment manual: setting the global standard*. Earthscan, London ; Washington, DC.

Hosseinzadeh Lotfi, F., Jahanshahloo, G.R., Khodabakhshi, M., Rostamy-Malkhlifeh, M., Moghaddas, Z., Vaez-Ghasemi, M., 2013. A Review of Ranking Models in Data Envelopment Analysis. *J. Appl. Math.* 2013, 1–20. doi:10.1155/2013/492421

IBM, 2009. V12. 1: User's Manual for CPLEX. *Int. Bus. Mach. Corp.* 46, 157.

ISO, 2006. *Standardization, International Organization for Standardization. The New International Standards for Life Cycle Assessment: ISO 14040 and ISO 14044*. Geneva, Switzerland.

Jaimes, A.L., Martinez, S.Z., Coello, C.A.C., 2009. An introduction to multiobjective optimization techniques. *Optim. Polym. Process.* 29–57.

JRC, 2011. *ILCD Handbook: Recommendations for Life Cycle Impact Assessment in the European context, First Edit.* ed. Luxemburg.

Keohane, R.O., Victor, D.G., 2016. Cooperation and discord in global climate policy. *Nat. Clim. Chang.* 6, 570–575.

Kim, I.Y., De Weck, O.L., 2006. Adaptive weighted sum method for

multiobjective optimization: a new method for Pareto front generation. *Struct. Multidiscip. Optim.* 31, 105–116.

Kopanos, G.M., Pistikopoulos, E.N., 2014. Reactive scheduling by a multiparametric programming rolling horizon framework: a case of a network of combined heat and power units. *Ind. Eng. Chem. Res.* 53, 4366–4386.

Land, A.H., Doig, A.G., 2010. An automatic method for solving discrete programming problems. *50 Years Integer Program. 1958-2008* 105–132.

Law, A., Kelton, D., 2000. *Simulation modeling and analysis*. Ser. *Ind. Eng. Manag. Sci.*

Lozano, S., Iribarren, D., Moreira, M.T., Feijoo, G., 2009. The link between operational efficiency and environmental impacts. A joint application of Life Cycle Assessment and Data Envelopment Analysis. *Sci. Total Environ.* 407, 1744–54. doi:10.1016/j.scitotenv.2008.10.062

Mavrotas, G., 2009. Effective implementation of the ϵ -constraint method in multi-objective mathematical programming problems. *Appl. Math. Comput.* 213, 455–465.

Murphy, K., 2012. The social pillar of sustainable development: a literature review and framework for policy analysis. *Sustain. Sci. Pract. Policy* 8.

Núñez, M., Pfister, S., Antón, A., Muñoz, P., Hellweg, S., Koehler, A., Rieradevall, J., 2013. Assessing the Environmental Impact of Water Consumption by Energy Crops Grown in Spain. *J. Ind. Ecol.* 17, 90–102. doi:10.1111/j.1530-9290.2011.00449.x

Optimization, D., 2007. *Xpress-optimizer reference manual*. Dash Optim. Ltd., Englewood Cliffs, NJ.

Optimization, G., 2012. *Gurobi optimizer reference manual*. URL <http://www>.

gurobi. com 2, 1–3.

PE-international, 2017. GaBi-product sustainability software [WWW Document]. URL <http://www.gabi-software.com>. (accessed 7.10.17).

Pfister, S., Koehler, A., Hellweg, S., 2009. Assessing the Environmental Impacts of Freshwater Consumption in LCA. *Environ. Sci. Technol.* 43, 4098–4104. doi:10.1021/es802423e

Pieragostini, C., Mussati, M.C., Aguirre, P., 2012. On process optimization considering LCA methodology. *J. Environ. Manage.* 96, 43–54. doi:10.1016/j.jenvman.2011.10.014

Pope, J., Annandale, D., Morrison-Saunders, A., 2004a. Conceptualising sustainability assessment. *Environ. Impact Assess. Rev.* 24, 595–616. doi:<https://doi.org/10.1016/j.eiar.2004.03.001>

Pope, J., Annandale, D., Morrison-Saunders, A., 2004b. Conceptualising sustainability assessment. *Environ. Impact Assess. Rev.* 24, 595–616. doi:10.1016/j.eiar.2004.03.001

Pre-sustainability, 2017. No Title [WWW Document]. About SimaPro. PRé Sustain. Amersfoort, Netherl. URL <http://www.pre-sustainability.com/simapro-lca-software>. (accessed 7.10.17).

Priefer, C., Jörisen, J., Bräutigam, K.R., 2013. Technology options for feeding 10 billion people. Options for Cutting Food Waste. *Sci. Technol. Options Assessment*, Eur. Parliam. Brussels, Belgium.

Riahi, K., Dentener, F., Gielen, D., Grubler, A., Jewell, J., Klimont, Z., Krey, V., McCollum, D.L., Pachauri, S., Rao, S., 2012. Energy pathways for sustainable development.

Rijsberman, F.R., 2006. Water scarcity: Fact or fiction? *Agric. Water Manag.*

80, 5–22. doi:10.1016/j.agwat.2005.07.001

Rockström, J., Sachs, J.D., Öhman, M.C., Schmidt-Traub, G., 2013. Sustainable Development and Planetary Boundaries. Backgr. Res. Pap. Submitt. to High Lev. Panel Post-2015 Dev. Agenda. Paris, New York Sustain. Dev. Solut. Netw.

Rockström, J., Steffen, W., Noone, K., Persson, Å., Chapin, F.S., Lambin, E., Lenton, T.M., Scheffer, M., Folke, C., Schellnhuber, H.J., Nykvist, B., de Wit, C.A., Hughes, T., van der Leeuw, S., Rodhe, H., Sörlin, S., Snyder, P.K., Costanza, R., Svedin, U., Falkenmark, M., Karlberg, L., Corell, R.W., Fabry, V.J., Hansen, J., Walker, B., Liverman, D., Richardson, K., Crutzen, P., Foley, J., 2009. Planetary boundaries: Exploring the safe operating space for humanity. *Ecol. Soc.* 14.

Sabio, N., Pozo, C., Guillén-Gosálbez, G., Jiménez, L., Karuppiah, R., Vasudevan, V., Sawaya, N., Farrell, J.T., 2014. Multiobjective optimization under uncertainty of the economic and life-cycle environmental performance of industrial processes. *AIChE J.* 60, 2098–2121.

Sahinidis, N. V., 1996. BARON: A general purpose global optimization software package. *J. Glob. Optim.* 8, 201–205.

Sahinidis, N. V., 2004. Optimization under uncertainty: state-of-the-art and opportunities. *Comput. Chem. Eng.* 28, 971–983.
doi:10.1016/j.compchemeng.2003.09.017

Sandler, T., 2004. *Global Collective Action*. Cambridge University Press.

Savitz, A.W., Weber, K., 2006. *The triple bottom line*. San Fr. Jossey-Boss 320.

Schmidt, R.C., 2015. A balanced-efforts approach for climate cooperation. *Nat. Clim. Chang.* 5, 10–12.

Schrage, L., 1995. *LINDO: Optimization software for linear programming*. Lindo Syst. Inc., Chicago,.

Steffen, W., Richardson, K., Rockstrom, J., Cornell, S.E., Fetzer, I., Bennett, E.M., Biggs, R., Carpenter, S.R., de Vries, W., de Wit, C.A., Folke, C., Gerten, D., Heinke, J., Mace, G.M., Persson, L.M., Ramanathan, V., Reyers, B., Sorlin, S., 2015. Planetary boundaries: Guiding human development on a changing planet. *Science* (80-.). 347. doi:10.1126/science.1259855

Tester, J.W., Drake, E.M., Driscoll, M.J., Golay, M.W., Peters, W.A., 2012. *Sustainable energy: choosing among options*. MIT press.

Tilman, D., Balzer, C., Hill, J., Befort, B.L., 2011. Global food demand and the sustainable intensification of agriculture. *Proc. Natl. Acad. Sci.* 108, 20260–20264.

Todorov, V., Marinova, D., 2011. Modelling sustainability. *Math. Comput. Simul.* 81, 1397–1408. doi:10.1016/j.matcom.2010.05.022

UNEP, 2007. *Global Environment Outlook – Geo 4: Environment for Development*. United Nations Environment Programme. Valletta, Malta.

UNFCCC, 2017. *United Nations Framework Convention on Climate Change -- 20 Years of Effort and Achievement Key Milestones in the Evolution of International Climate Policy* [WWW Document]. URL <http://unfccc.int/timeline/> (accessed 7.11.17).

Van Vuuren, D., Nakicenovic, N., Riahi, K., Brew-Hammond, A., Kammen, D., Modi, V., Nilsson, M., Smith, K., 2012. An energy vision: the transformation towards sustainability—interconnected challenges and solutions. *Curr. Opin. Environ. Sustain.* 4, 18–34. doi:10.1016/j.cosust.2012.01.004

WCED, 1987. *Our Common Future – The Brundtland Report*. World Commission on Environment and Development. Geneva.

Chapter II

Sustainable allocation of cropping areas

UNIVERSITAT ROVIRA I VIRGLI

CONTRIBUTION TO THE DEVELOPMENT OF MATHEMATICAL PROGRAMMING TOOLS TO ASSIST DECISION-MAKING
IN SUSTAINABILITY PROBLEMS

Àngel Galán Martín



II. Sustainable allocation of cropping areas

Multi-objective optimisation of rainfed and irrigated agricultural areas considering production and environmental criteria: A case study of wheat production in Spain

Àngel Galán Martín^a, Pavel Vaskan^a, Assumpció Antón Vallejo^{a,c}, Laureano Jiménez Esteller^a, Gonzalo Guillén-Gosálbez^{a,b*}

^a*Departament d'Enginyeria Química, Universitat Rovira i Virgili, Av. Països Catalans 26, 43007 Tarragona (Spain).*

^b*Centre for Process Systems Engineering, Imperial College London, SW7 2AZ London (United Kingdom).*

^c*Institut de Recerca i Tecnologia Agroalimentàries (IRTA), Ctra Cabrils, km 2, 08348 Cabrils Barcelona (Spain)*

KEYWORDS: Multi-objective optimisation; Agriculture; Linear programming; Water footprint; Life cycle assessment; Decision-making tool

2.1 Introduction

Unsustainable use of freshwater is a major issue that can potentially generate unacceptable environmental changes at the global as well as local scales (Rockström et al., 2009; Steffen et al., 2015). Freshwater resource availability is rapidly decreasing and experts expect that more than two-thirds of the world's population will be affected by water scarcity over the next decades (Rijsberman, 2006).

In practise, agriculture is by far the largest consumer of freshwater worldwide (FAO, 2014; UNEP, 2007). In particular, irrigated agriculture accounts for more than

70% of freshwater withdrawals from rivers, lakes and aquifers (Garrido et al., 2010), while rainfed agriculture is the largest consumer of water from precipitation (Liu et al., 2009; Postel et al., 1996). Overall, water consumption in global crop production is causing significant environmental impacts on natural resources, ecosystem quality and human health (Núñez et al., 2013) that cannot be ignored. In this backdrop, future agriculture will face a great challenge: meeting the growing food demand while simultaneously reducing freshwater consumption and the associated environmental impact.

Hence, managing water resources in the agricultural sector in an efficient manner becomes a critical issue to look at when moving towards a sustainable economy (Ridoutt and Pfister, 2010). To manage water resources efficiently and minimise the impact of water consumption, it is necessary to define appropriate metrics and integrate them into tailored systematic decision-support tools. Research efforts in this area have been devoted mainly to assess the environmental impact of water consumption through descriptive metrics based on two main approaches: water footprint (WF) and life cycle assessment (LCA) (Boulay et al., 2015; Jefferies et al., 2012). In contrast, the literature on decision- support tools for the sustainable management of water and crops in agriculture is still quite scarce.

The WF concept, which was originally introduced by Hoekstra (Hoekstra, 2003), is a descriptive indicator that quantifies the total volume of freshwater used per unit of mass produced during the entire crop production growing period (Hoekstra et al., 2011). On the other hand, LCA is a tool which measures the environmental impact caused by products along their entire life cycle (Finnveden et al., 2009). The impact of water consumption was traditionally neglected in LCA studies (Milà i Canals et al., 2008), but several attempts have been recently made to overcome this limitation (Berger and Finkbeiner, 2010). For instance, Milà i Canals et al. (2008) introduced the concept of freshwater ecosystem impact as an indicator of the effects of direct water consumption on ecosystem health, while Hospido et al.

(2012) applied this indicator to estimate the impact of irrigated products in Spain. Other authors employed both WF and LCA approaches to assess the potential impacts of different crops, such as tea and margarine (Jefferies et al., 2012) as well as tomatoes (Chapagain and Orr, 2009). These authors argue that classical LCA could benefit from WF methods by integrating water assessment with other environmental indicators. Recently, the WF concept has been combined with the LCA approach to quantify the impact of water consumption on all of the stages in the life cycle of a product (Pacetti et al., 2015; Pfister et al., 2009). Pfister et al. (2009) developed a method based on the WaterGAP2 model (Alcamo et al., 2003) that combines WF and LCA. This approach was later applied by Pfister and Bayer (2013) to assess 160 crops worldwide. Moreover, Pacetti et al. (2015) analysed the environmental performance of biogas production from energy crops through the integration of WF and LCA.

The integration of WF and LCA enables a comprehensive assessment of the environmental impact derived from water consumption. Despite its benefits, the approaches mentioned above are still descriptive in nature. That is, they quantify the environmental impact of water consumption, but offer no guidelines on how to minimise such an impact. Obtaining “more crop and nature per drop”, that is, maintaining or even increasing the productivity while minimising the environmental impact is the paradigm to be achieved in agriculture (Aldaya et al., 2009). This goal cannot be addressed using exclusively descriptive approaches. It is necessary to resort to optimisation methods that can generate in a systematic manner a large number of alternatives and identify the best ones among them. Despite their high potential, however, the use of optimisation in the field of agriculture has been quite scarce. The few approaches proposed so far based on optimisation have concentrated primarily on optimising water resources (Singh, 2012a) and cropping patterns (Singh, 2012b) according to economic criteria, thereby disregarding the environmental impact of water use.

Multi-objective optimisation (MOO) allows optimising systems according to different criteria, including environmental and economic aspects (Azapagic, 1999). In particular, MOO (Chankong and Haimes, 1983; Ehrgott, 2000) can treat environmental concerns as decision-making objectives rather than as constraints imposed on the system (García et al., 2014; Grossmann and Guillén-Gosálbez, 2010; Guillen-Gosalbez et al., 2007). MOO generates a set of alternatives (called Pareto optimal solutions) which are non-dominated (none of the objectives in a Pareto optimal point can be improved in value by any other feasible solution without worsening at least another objective value). The analysis of these solutions provides insight into the trade-off between objectives (Azapagic and Perdan, 2005; Branke et al., 2008). In a seminar work, Azapagic and Clift (Azapagic and Clift, 1999; Azapagic, 1999) proposed to combine LCA and MOO into a single framework. This approach has been applied in a plethora of engineering problems in order to automate the search for more sustainable alternatives (Grossmann and Guillén-Gosálbez, 2010; Pieragostini et al., 2012; Yue et al., 2016).

In the agricultural area, MOO has been successfully employed in the management of resources in arid and semiarid areas. Along these lines, Xevi and Khan (2005) applied MOO to optimise reservoir operations and water allocation for irrigation, while Chen et al. (2013) used MOO to realise the optimum allocation of multiple reservoirs in a basin. MOO has also been employed to analyse crop planning problems, most of them focusing either on economic criteria (Dury et al., 2011; Sarker and Ray, 2009; Zeng et al., 2010) or on environmental objectives (Khoshnevisan et al., 2015). To the best of our knowledge, however, MOO and LCA have never been integrated into a single unified framework in the context of agriculture.

In this work we develop a tool to optimise the allocation of crops, an area that offers large potential for enhancing food availability and reducing the environmental impact of agriculture (Foley et al., 2011). A systematic MOO tool is

presented which integrates a descriptive LCA-based methodology (that quantifies the impact of water consumption) with an MOO optimisation model that identifies optimal cropping patterns (i.e. optimal rainfed and irrigated agricultural areas in a specific region of interest) that simultaneously maximise the productivity and minimise the environmental impact of water consumption. The capabilities of the proposed tool are illustrated through its application to a real case study based on wheat production in Spain.

2.2 Model description and solution method

In this section we present the mathematical model for solving the rainfed and irrigated cropping areas allocation problem, followed by the solution procedure.

2.1.1 Multi-objective linear programming model

The problem addressed in the paper is formulated in mathematical terms using a linear programming model (LP) containing four sets of equations: objective function equations, demand satisfaction constraints, capacity limitations constraints and water demand constraints. These equations are described in detail next.

Objective functions equations

The model seeks to minimise the environmental impact while simultaneously maximising the amount of crop produced. This general goal is expressed through the following three objective functions: maximise production (Eq. II-1), minimise damage to ecosystem quality (Eq. II-2), and minimise damage to resources (Eq. II-3).

The total crop production is calculated via Eq. II-1 as the summation of the amount of crop produced in the rainfed and irrigated areas in each watershed j (expressed in tons [t]).

$$\begin{aligned}
 Production = \sum_j [(Yield_j^{DRY} \cdot Surface_j^{DRY}) \\
 + (Yield_j^{IRR} \cdot Surface_j^{IRR})]
 \end{aligned}
 \tag{Eq. II-1}$$

where $Surface_j^{DRY}$ and $Surface_j^{IRR}$ are continuous variables that represent, respectively, the rainfed and irrigated areas in each watershed j devoted to a given crop (expressed in hectare [ha]). In the same equation, $Yield_j^{DRY}$ and $Yield_j^{IRR}$ are production rate parameters associated with the rainfed and irrigated areas within each watershed j (i.e. the ratio between amount of crop produced per unit of land area expressed in tons per hectare [$t \cdot ha^{-1}$]).

The environmental impact derived from water consumption is determined mathematically via Eq. II-2 and Eq. II-3, where EQ represents the damage to ecosystem quality (quantified in square metres per year as land occupation [$m^2 \cdot year$]), and RD represents the damage to resources depletion (expressed in surplus of energy [M]).

$$EQ = \sum_j [CF_j^{EQ} \cdot CWR_j] \tag{Eq. II-2}$$

$$RD = \sum_j [CF_j^{RD} \cdot CWR_j] \tag{Eq. II-3}$$

Here CF_j^{EQ} and CF_j^{RD} are parameters denoting, respectively, the environmental damage in ecosystems and resources caused by water consumption; and CWR_j is a variable that represents the total crop water requirements in each watershed j (expressed in cubic metre [m^3]). CF_j^{EQ} and CF_j^{RD} are environmental damage factors taken from Pfister et al. (2009), which in our case were calculated following LCA principles, using a 0.5° grid cell resolution and aggregating the watersheds by country. CF_j^{EQ} is the ecosystem quality damage factor that represents the surface that suffers the environmental damage caused by water consumption during one year (expressed in square metre-year per cubic metre [$m^2 \cdot year \cdot m^{-3}$]) (note that this approach is similar to the concept of land use

impact). CF_j^{RD} is the characterization factor for freshwater depletion and represents the surplus of energy needed to extract the same amount of water in the future (expressed in mega joules per cubic metre [$\text{MJ} \cdot \text{m}^{-3}$]). For further details on these metrics, the reader is referred to (Pfister et al., 2009).

Demand satisfaction constraint

As already mentioned, the model seeks to maximise the crop production rate. However, there is a minimum production that should be attained in order to ensure that a minimum demand is met. This condition is enforced using the following equation (Eq. II-4):

$$\text{Production} \geq \text{Demand} \quad \text{Eq. II-4}$$

where *Demand* is a parameter (expressed in tons [t]) that represents the minimum amount of crop that needs to be produced.

Capacity limitation constraints

To ensure that the solution found by the algorithm can be implemented in practice, Eq. II-5 forces the optimal surfaces in each watershed j to be below the available surface in the watershed j (parameter $\text{Surface}_j^{\text{AVA}}$).

$$\text{Surface}_j^{\text{DRY}} + \text{Surface}_j^{\text{IRR}} \leq \text{Surface}_j^{\text{AVA}} \quad \forall j \quad \text{Eq. II-5}$$

The available surface for one crop in each watershed j should be limited to the current harvested areas dedicated to this crop (Eq. II-6). Hence, this constraint ensures that the optimal areas are suitable and available for the crop growth, that is, they meet the soil and climate conditions for the crop. Therefore, the available surface is obtained as the summation of the current cultivated rainfed and irrigated areas, denoted by parameters SR_j^{DRY} and SR_j^{IRR} , respectively. The reader should not confuse these parameters with the continuous variables $\text{Surface}_j^{\text{DRY}}$ and $\text{Surface}_j^{\text{IRR}}$.

$$\text{Surface}_j^{\text{AVA}} = \text{SR}_j^{\text{DRY}} + \text{SR}_j^{\text{IRR}} \quad \forall j \quad \text{Eq. II-6}$$

In addition, the rainfed and irrigated surfaces in each watershed j (denoted by continuous variables $\text{Surface}_j^{\text{DRY}}$ and $\text{Surface}_j^{\text{IRR}}$) are constrained within lower and upper bounds, as shown in Eq. II-7 and Eq. II-8.

$$\underline{\text{SR}_j^{\text{DRY}}} \leq \text{Surface}_j^{\text{DRY}} \leq \overline{\text{SR}_j^{\text{DRY}}} \quad \forall j \quad \text{Eq. II-7}$$

$$\underline{\text{SR}_j^{\text{IRR}}} \leq \text{Surface}_j^{\text{IRR}} \leq \overline{\text{SR}_j^{\text{IRR}}} \quad \forall j \quad \text{Eq. II-8}$$

where $\underline{\text{SR}_j^{\text{DRY}}}$ and $\overline{\text{SR}_j^{\text{DRY}}}$ denote, respectively, the lower and upper bounds imposed on the rainfed areas; and $\underline{\text{SR}_j^{\text{IRR}}}$ and $\overline{\text{SR}_j^{\text{IRR}}}$ the corresponding bounds on the irrigated areas. These bounds are calculated as a percentage change with respect to the current areas cultivated in each watershed j .

Agricultural water demand constraints

The crop water requirements in each watershed are determined via Eq. II-9 as the summation of its individual components (i.e. green, blue and grey water):

$$\text{CWR}_j = W_j^{\text{GREEN}} + W_j^{\text{BLUE}} + W_j^{\text{GREY}} \quad \forall j \quad \text{Eq. II-9}$$

where W_j^{GREEN} represents the total volume of green water (i.e. rainfall water) consumed by the rainfed and irrigated surfaces in each watershed j (expressed in cubic metre [m^3]). W_j^{BLUE} represents the total volume of blue water (i.e. irrigation water) consumed by the irrigated surfaces in each watershed j (expressed in cubic metre [m^3]). W_j^{GREY} represents the total volume of grey water consumed (i.e. water needed to assimilate the pollutants) in each watershed j (expressed in cubic metre [m^3]).

The total green, blue and grey water consumed are calculated via Eq. II-10, Eq. II-11 and Eq. II-12.

$$W_j^{GREEN} = CWU_j^{GREEN} \cdot [Surface_j^{DRY} + Surface_j^{IRR}] \quad \forall j \quad \text{Eq. II-10}$$

$$W_j^{BLUE} = CWU_j^{BLUE} \cdot Surface_j^{IRR} \quad \forall j \quad \text{Eq. II-11}$$

$$W_j^{GREY} = CWU_j^{GREY} \cdot [Surface_j^{DRY} + Surface_j^{IRR}] \quad \forall j \quad \text{Eq. II-12}$$

where CWU_j^{GREEN} , CWU_j^{BLUE} and CWU_j^{GREY} are parameters which represent the green, blue and grey water crop requirements in a specific watershed j (expressed in cubic metre [$\text{m}^3 \cdot \text{ha}^{-1}$]). As defined by Hoekstra et al., (2011), the CWU_j^{GREEN} refers to the consumption of the green water resources that are available for the crop in the soil (rainwater insofar as it does not become run-off), CWU_j^{BLUE} refers to the consumption of blue water resources (surface and groundwater consumed/extracted for irrigation), and CWU_j^{GREY} refers to the volume of freshwater that is required to assimilate the load of pollutants (considering natural background concentrations and existing ambient water quality standards).

The crop water requirements can be either determined based on real/experimental data or estimated following the WF assessment method proposed by Hoekstra et al. (2011) and implemented in the CROPWAT 8.0 software developed by the Food and Agriculture Organisation (Allen Richard et al., 1998; FAO, 2010). Note that for rainfed crop production, CWU_j^{BLUE} is zero (no irrigated water), while for irrigated crop production, CWU_j^{GREEN} is assumed to be equal to the rainfed crop production (see details of the method in Appendix A).

2.1.2 Solution method: multi-objective optimisation

The overall problem can be formulated as a multi-objective linear programming model that is expressed in compact form as follows:

$$\begin{aligned}
 \min \quad & F = \{f_1, f_2, f_3\} \\
 \text{s. t.} \quad & \text{Eqs. 4 – 12} \\
 & x \in \mathfrak{R}
 \end{aligned}
 \tag{Eq. II-13}$$

Where function f_1 is the production (Eq. II-1), f_2 is the damage to ecosystem quality (Eq. II-2), and f_3 is the damage to resources depletion (Eq. II-3) (note that minimising the negative of a function is equivalent to maximising the same function). Continuous decision variables x represent the rainfed and irrigated harvested areas in each watershed. We aim to minimise simultaneously the three objective functions subject to the constraints imposed by Eqs. II4-II12.

The multi-objective LP is solved using the epsilon-constraint method (Ehrgott, 2008), which is based on formulating an auxiliary model in which one objective is kept as main objective and the remaining ones are transferred to auxiliary constraints that impose epsilon bounds (ϵ) on their values. This method generates single objective sub-problems by systematically varying the ϵ -constraint bounds imposed on the auxiliary objectives (Chankong and Haimes, 1983; Haimes et al., 1971). Further details on this method can be found elsewhere (Ehrgott, 2008). Therefore, the auxiliary single-objective models are expressed in compact form as follows:

$$\begin{aligned}
 \max \quad & f_1(x) \\
 \text{s. t.} \quad & f_2(x) \leq \epsilon_2 \\
 & f_3(x) \leq \epsilon_3 \\
 & \text{Eqs. 4 – 12} \\
 & x \in \mathfrak{R}
 \end{aligned}
 \tag{Eq. II-14}$$

These models are solved for different epsilon values, thereby generating in each run a different Pareto solution. Therefore, the solution of the multi-objective problem is given by a set of Pareto alternatives that represent the optimal trade-off between the objectives. These solutions cannot be improved in one of the objectives without necessarily worsening at least another criterion. The set of Pareto alternatives forms the Pareto set, which contains all the non-inferior or non-dominated solutions.

Figure II-1 illustrates the concept of Pareto optimality for a simple case with two objectives (e.g. production and environmental impact). Points lying above the curve are sub-optimal solutions that can be improved in both criteria simultaneously. The region below the Pareto curve contains unfeasible solutions, since there is no single point showing better performance than the Pareto solutions simultaneously in both indicators.

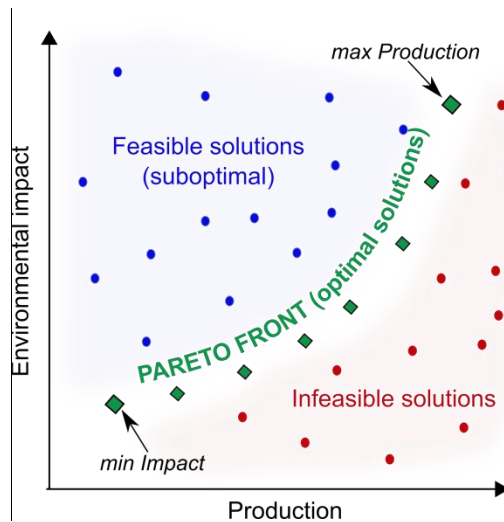


Figure II-1 Pareto Front of a bi-criteria problem obtainable by the multi-objective optimisation method.

Each solution of the Pareto curve is optimal and represents a unique combination of both objectives entailing a particular rainfed and irrigated area in each watershed. Decision and policy-makers will select a solution from the Pareto set that will reflect, in the best manner possible, the stakeholders' preferences.

2.3 Case study

The capabilities of the approach presented are demonstrated through its application to a real case study based on wheat (*Triticum aestivum* L.) production in Spain. Note that this crop is used for illustrative purposes. Our model is indeed general enough to assess any other crop in any other region.

We focus on wheat production because it is one of the most widely used

cultivated grain cereals with a major role in feeding people and livestock. Furthermore, we select the Spanish territory because it is the driest country in Europe, with a high climate variability along its territory located in one climate change hotspot (Giorgi, 2006).

Wheat dominates the Spanish cropping system and it is one of the crops most critically affected by water scarcity and climate change (Karrou and Oweis, 2012; Ortiz et al., 2008). Agronomic practises differ largely along the Spanish territory owing to the different climate, topography, soil and social conditions (Rharrabti et al., 2003). In Spain, rainfed wheat land has traditionally occupied more than 85% of the total wheat arable land, while irrigated land produces more than 20% of the nation's wheat grain. Further details on historical wheat production data over Spain can be found in the Agriculture Statistics of Spanish Ministry of Agriculture, Food and Environment (MAGRAMA, 2014).

Considering as base case the spatial location of the wheat harvested in Spain for 2011, the goal is to apply the proposed approach to optimise wheat rainfed and irrigated cropping areas along the Spanish territory. The region of interest (i.e. the whole area of Spain) is divided into a number of watersheds (regarded as autonomous regions of environmental management and economic development). Figure II-2 shows the 16 Spanish watersheds considered in this study, 15 in the Peninsula and one in the Balearic Islands.



Figure II-2 Study area divided into 16 watersheds.

Two areas of environmental protection are considered: ecosystem quality and resources. We consider the environmental characterisation factors estimated by Pfister et al. (2009) based on the Eco-Indicator-99 LCA method (Goedkoop and Spriensma, 2001) (for further details on these metrics refer to (Pfister et al., 2009)). The characterisation factors for each Spanish watershed are shown in Table II-1. Higher values of the characterisation factors imply greater levels of vulnerability in the watershed concerning the effects of water consumption.

Table II-1 Characterisation environmental factors for ecosystem quality and resources depletion specific for each watershed (Pfister et al., 2009).

Watershed	Ecosystem quality ($\text{m}^2\text{year}\cdot\text{m}^{-3}$)	Resource depletion ($\text{MJ}\cdot\text{m}^{-3}$)
Galicia Costa	0.115	0.000
Miño-Sil	0.107	0.000
Cantábrico Occidental	0.159	0.000
Cantábrico Oriental	0.121	0.000
Ebro	0.270	0.000
Cuencas internas de Cataluña	0.314	2.605
Duero	0.271	0.000
Tajo	0.348	0.000

Júcar	0.545	0.000
Guadiana	0.638	0.000
Tinto, Odiel y Piedras	0.240	0.000
Guadalquivir	0.496	2.978
Guadalete y Barbate	0.112	0.000
Cuenca Mediterránea Andaluza	0.398	3.301
Segura	0.574	9.651
Islas Baleares	0.276	0.000

The current wheat rainfed and irrigated surface and yield parameters corresponding to each watershed (Table II-2) were estimated using historical data regionalised at the province level sourced from the Agricultural Statistics Yearbooks of the Spanish Ministry of Agriculture, Food and Environment for the year 2011 (MAGRAMA, 2014). The province data were aggregated at the watershed level using conversion factors, as shown in Eqs. II-15 to II-18.

$$SR_j^{DRY} = \sum_k [CS_k^{DRY} \cdot f_{k,j}] \quad \forall j \quad \text{Eq. II-15}$$

$$SR_j^{IRR} = \sum_k [CS_k^{IRR} \cdot f_{k,j}] \quad \forall j \quad \text{Eq. II-16}$$

$$Yield_j^{DRY} = \sum_k [YP_k^{DRY} \cdot CS_k^{DRY} \cdot f_{k,j}] / SR_j^{DRY} \quad \forall j \quad \text{Eq. II-17}$$

$$Yield_j^{IRR} = \sum_k [YP_k^{IRR} \cdot CS_k^{IRR} \cdot f_{k,j}] / SR_j^{IRR} \quad \forall j \quad \text{Eq. II-18}$$

where SR_j^{DRY} and SR_j^{IRR} denote the estimated rainfed and irrigated surfaces corresponding to each watershed j ; CS_k^{DRY} and CS_k^{IRR} are the real crop harvested surfaces under rainfed and irrigated conditions in province k ; and $f_{k,j}$ represents the fraction of province k in the watershed j (i.e. area of province k belonging to the watershed j divided by the total area of province k). $Yield_j^{DRY}$ and $Yield_j^{IRR}$ denote the production rate parameter for each watershed j ; while YP_k^{DRY} and YP_k^{IRR} are

rainfed and irrigated crop yield in province k .

We also assume that the wheat demand to be satisfied is equal to 6,888,147 tonnes which corresponds to the total wheat production in Spain for 2011 (MAGRAMA, 2014).

Due to the lack of real data, the wheat water requirements in each watershed (i.e. green, blue and grey denoted by CWU_j^{GREEN} , CWU_j^{BLUE} and CWU_j^{GREY} , respectively) were estimated using the framework proposed by Hoekstra et al. (2011) and the CROPWAT 8.0 software developed by the Food and Agriculture Organisation (Allen Richard et al., 1998; FAO, 2010). The wheat water requirements were first estimated for 67 meteorological stations spread across all watersheds, and then aggregated at the watershed level. Climate data for each meteorological station (temperature, precipitation, humidity, sunshine hours and wind speed) correspond to the average value for the period 1981-2010 (AEMET, 2014) (see details on this method and the estimation in Appendix 2.9). We assume that the theoretical wheat water use (Table II-3) may be overestimated since farmers may not irrigate at the optimum level.

Table II-4 shows the parameters regionalised at the watershed level fed into the model: wheat surface and yield for rainfed and irrigated areas and wheat water requirement for green, blue and grey water. Note that we assume that the rainfed and irrigated yields can be attained with the theoretical water requirements that are estimated. For rainfed areas, CWU_j^{BLUE} is zero (no irrigated water); while for irrigated areas, CWU_j^{GREEN} is equal to the rainfed production, and CWU_j^{BLUE} is the theoretical irrigation needed to achieve the irrigated yield ($Yield_j^{IRR}$) assuming that farmers irrigate at the optimum level.

Table II-4 Wheat yield ($t \cdot ha^{-1}$), available surface (ha) and water use ($m^3 \cdot ha^{-1}$) for green, blue and grey water in each watershed.

Watershed	Rainfed		Irrigated		Crop Water Use		
	Yield	Surface	Yield	Surface	Green	Blue	Grey
Galicia Costa	5.94	2847.70	-	-	3781.75	2495.25	285.00
Miño-Sil	2.51	17548.65	5.65	5302.26	3320.25	4237.75	285.00
Cantábrico Occidental	2.26	1732.64	5.65	362.91	4037.67	1682.67	285.00
Cantábrico Oriental	4.67	15040.09	5.34	1884.29	4478.00	1423.50	285.00
Ebro	3.27	453705.38	4.84	96464.47	2620.38	6098.25	285.00
Cuencas internas de Cataluña	3.88	39787.44	4.98	6734.49	3014.00	4823.00	285.00
Duero	3.80	536016.96	5.24	66792.57	2305.78	6331.89	285.00
Tajo	2.89	144233.87	4.81	12320.69	2049.63	7874.00	285.00
Júcar	2.72	57607.40	5.58	14621.28	2103.50	6968.00	285.00
Guadiana	2.45	140166.92	4.10	12869.88	1885.00	8416.50	285.00
Tinto, Odiel y Piedras	3.41	6247.32	4.68	362.00	1800.00	8178.00	285.00
Guadalquivir	2.62	203516.31	4.29	33060.84	1921.75	7965.75	285.00
Guadalete y Barbate	2.89	45809.96	4.02	4956.49	1824.50	6789.50	285.00
Cuenca Mediterránea Andaluza	2.46	33023.85	4.22	3668.76	1345.50	8037.50	285.00
Segura	2.21	25152.56	5.17	10756.00	1538.67	8189.67	285.00
Islas Baleares	3.40	3612.00	5.10	446.00	1934.00	6531.33	285.00

All the parameters employed in the model are assumed to be deterministic, that is, we assume nominal values for them. However, the crop yield and water requirements highly depend on soil conditions, climate and agronomic practises; while the LCA calculations are also affected by several uncertainty sources, particularly concerning the environmental characterisation factors. As will be later discussed during the article, to deal with these uncertainties we carry out a sensitivity analysis.

It is assumed that the rainfed and irrigated surfaces cannot be altered by more than 20% from their current values (base case). These lower and upper bounds on the variables can be easily modified, and we can even considering replacing crops by others requiring similar conditions. It is also assumed that the water employed in the base case (i.e. for the real wheat harvested rainfed and irrigated areas in 2011 in Spain), corresponds to the theoretical water requirements shown in Table II-4.

2.4 Results and discussion

The LP model was implemented in the General Algebraic Modelling System (GAMS) (Brooke et al., 1998) software version 24.2.1 and solved with the CPLEX 12.6.1.0 solver using an AMD A8-5500 APU with Raedon 3.20 Ghz and 8.0 GB RAM. The model features 55 continuous variables and 42 equations. The solution time varied depending on the instance being solved, but was always within the range 0.5 to 1.3 CPU seconds in the aforementioned computer.

2.4.1 3-Dimensional objective space

We first generated the Pareto set for the original problem containing three objective functions, that is, maximising the production while simultaneously minimising the damage to ecosystems quality and to resources. Figure II-3 shows the set of 3D Pareto points (depicted in blue colour) produced by running 100 iterations of the epsilon constraint method (Ehrgott, 2009). In each of the iterations, production is maximised as a single objective, while the damage to ecosystem

quality and resources are transferred to auxiliary constraints. To generate the ε -constraint bounds imposed on the environmental functions, we first calculated the individual optimum for each objective. Then, we defined the range within which each objective function should fall. Next, we divided this interval into 9 equal intervals, thereby generating 10 ε -constraint bounds for each environmental objective function. Finally, the LP model was recursively solved for each possible combination of the ε -constraint values (i.e. 100 possible combinations).

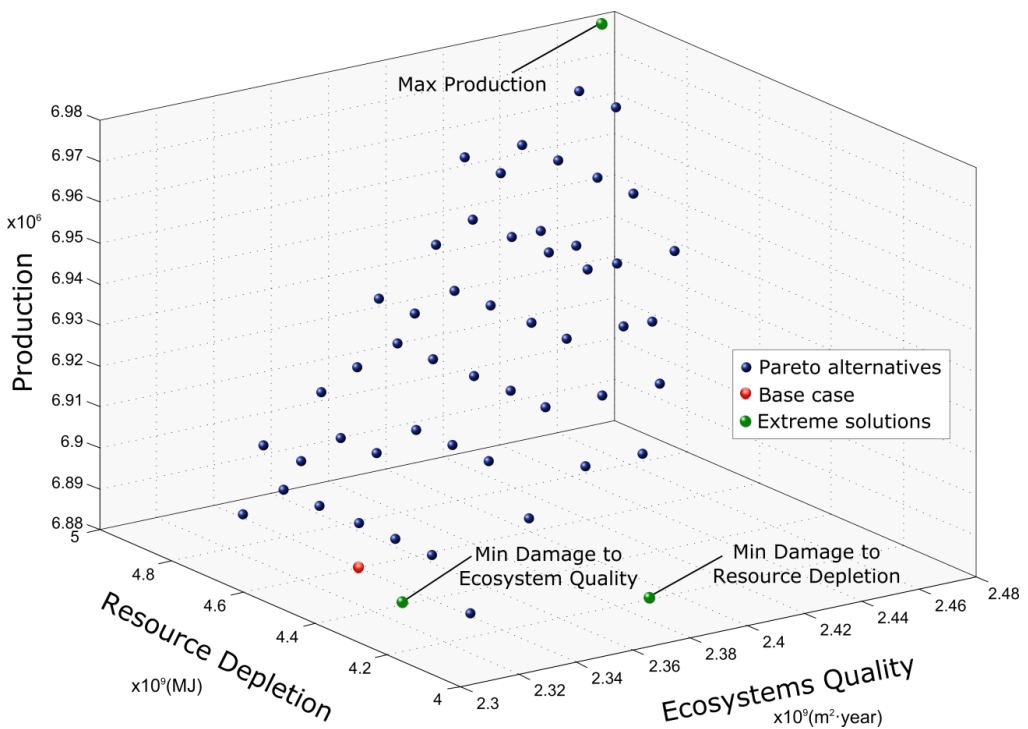


Figure II-3 Pareto set of solutions for the three-criteria multi-objective optimisation problem (3-Dimensional visualisation).

Each point in the 3D Pareto set represents an optimal alternative achieving a unique combination of objectives values (entailing specific rainfed and irrigated surface areas in each watershed). Therefore, each optimal alternative involves replacing (to a certain extent) rainfed by irrigated surfaces or vice-versa in each watershed (compared to the base case). Additionally, Figure II-3 depicts the extreme solutions (in green colour), as well as the base case (in red colour).

The assessment of the 3D Pareto optimal solutions and their comparison with the base case are challenging. To get further insight into the inherent trade-offs between objectives, the solutions are represented in Figure II-4 in the form of a parallel coordinates plot in which each 3D solution is equivalent to a polyline. Each polyline intersects in a specific position the three vertical axes representing the objective functions (production, damage to ecosystem quality and damage to resource depletion). The position where a solution crosses a vertical axis indicates its value in this specific objective. The values were normalised by subtracting the minimum from each element (or by subtracting the value from the maximum, depending on whether the objective is maximised or minimised), and then dividing by the difference maximum-minimum, so that a value of 1 represents the best value for the objective.

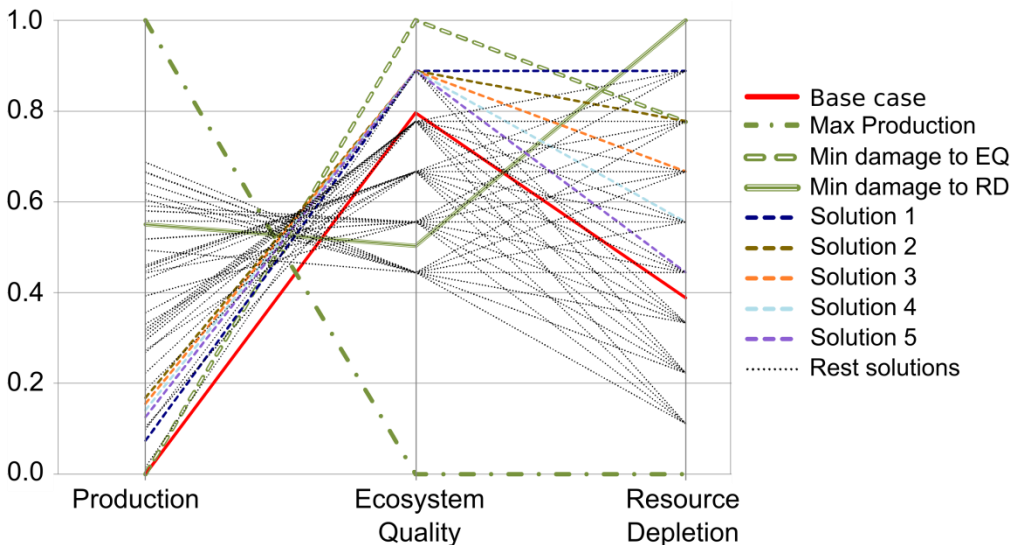


Figure II-4 Parallel coordinates plot of the 3D Pareto set of solutions: extreme solutions for each objective (green polylines), solutions 1 to 5 that improve the base case in the three objectives (dashed polylines), other solutions that improve the base case in at least one objective (dotted polylines), and base case (solid red polyline).

As observed in Figure II-4, the base case (red polyline) is clearly suboptimal, as there are at least 5 Pareto solutions (depicted by dashed coloured polylines) that are better simultaneously in the three objectives. Regarding the extreme solutions,

the minimisation of the damage to ecosystem quality leads to a solution showing better performance than the base case in the three objectives. Maximising the production worsens the environmental objectives, while minimising the damage to resource improves the production yield and worsens the damage to ecosystem quality (with respect to the base case). Additionally, Figure II-4 shows the remaining 3D solutions (depicted by dotted black polylines) that are better than the base case in at least in one objective.

The interpretation of the 3D plot (Figure II-3) and subsequent selection of a preferred Pareto solution are not straightforward. Additionally, the visualisation of a large set of solutions in the parallel coordinates plot (Figure II-4) may be unclear given the dense nature of the cloud of Pareto points. To facilitate this task and get further insight into inherent trade-offs between pairs of objectives, we projected the Pareto points onto 2D plots. Furthermore, we generated a set of optimal Pareto solutions for subspaces of two objectives and compared them with the points resulting from solving the problem in the original space of three objectives. Note that the solutions generated for the 2D cases are guaranteed to be optimal in the 3D space, while the converse is not true.

2.4.2 2-Dimensional Objectives Spaces

The 2D Pareto points were obtained by solving three different bi-criteria LPs, in each of which we minimise each objective against one of the others (*resource depletion vs production*, *ecosystems quality vs production* and *resource depletion vs ecosystem quality*). More precisely, we ran 10 iterations of the epsilon constraint method for each such problem, generating 10 optimal solutions for each 2D space problem. Figure II-5, Figure II-6 and Figure II-7 show the projections onto the subspaces *resource depletion vs production*, *ecosystem quality vs production* and *ecosystems quality vs resource depletion*, respectively. The following points are plotted in the figures: the original set of 3D Pareto optimal solutions projected onto the corresponding 2D subspace (unfilled blue points), the optimal points generated

in the 2D subspace itself (filled blue points) and the base case (red colour point). As observed in Figure II-5 and Figure II-6, there is a clear trade-off between each environmental impact and the production rate (an improvement in the latter implies worsening the former). Furthermore, the base case (depicted in red) is suboptimal in the space of either pair of two objectives.

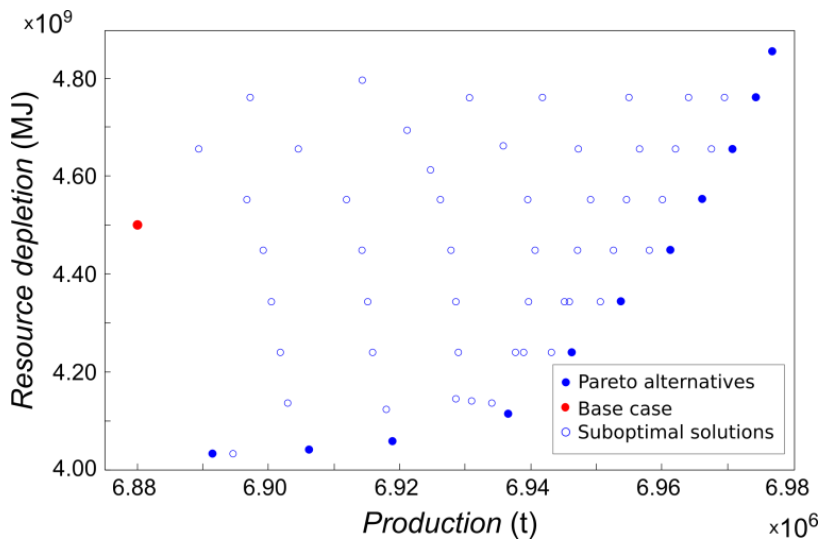


Figure II-5 Set of Pareto optimal solutions for the bi-criteria problem resource depletion vs production.

As can be observed in Figure II-5, there are six optimal solutions in the space *resource depletion vs production* (the first ones starting from the left-hand side of the Pareto set) showing lower damage to resources and higher production rates than the base case (i.e. dominating the base case solution). Additionally, the slope of the Pareto curve is small in the first three points and then increases significantly thereafter, implying that larger improvements in production can be attained by increasing marginally the damage to resources depletion (making such solutions appealing for decision-makers).

On the other hand, the slope of the Pareto set in Figure II-6 (trade-off between ecosystems quality and production) is almost constant. Again, from point 1 to 3 (starting from the left-hand side of the Pareto set), it is possible to improve the

base case simultaneously in both objectives.

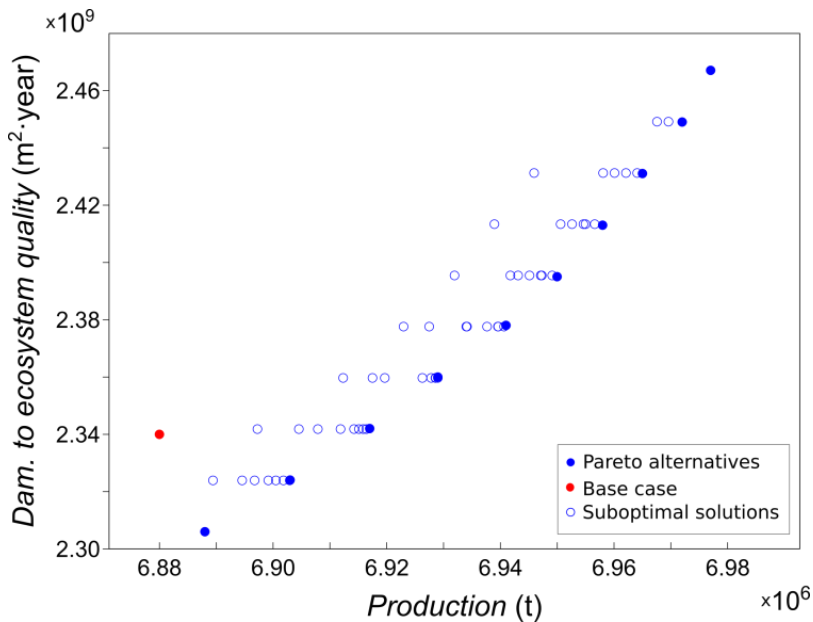


Figure II-6 Set of Pareto optimal solutions for the bi-criteria problem damage to ecosystems quality vs production.

Finally, we analysed the trade-off between both environmental objectives (*damage to ecosystem quality vs resource depletion*) (see Figure II-7). As observed in Figure II-7, there is a clear trade-off between both impacts, as an improvement in one criterion is only possible by worsening the other one, that is, reductions in the minimum damage to ecosystem quality are only possible by increasing the minimum damage to resources.

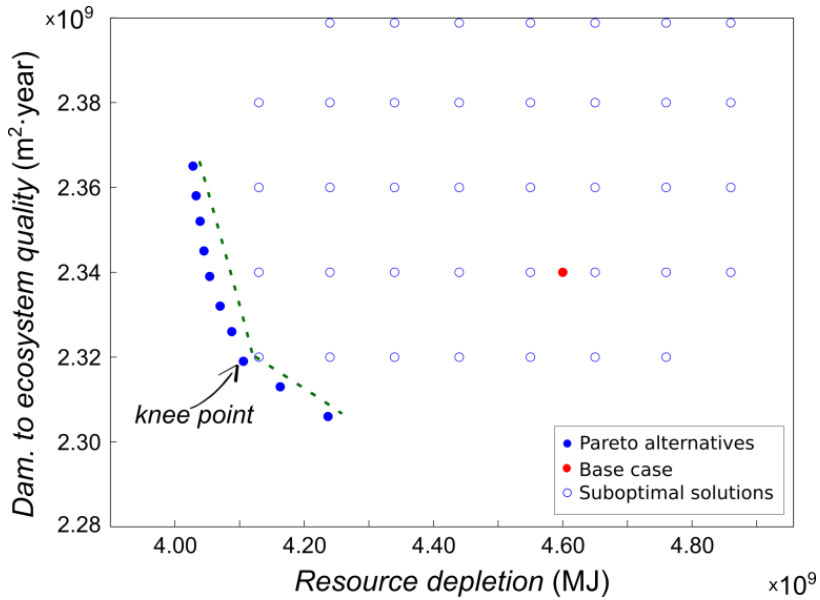


Figure II-7 Set of Pareto optimal solutions for the bi-criteria problem damage to ecosystems quality vs resource depletion.

Remarkably, the base case (depicted in red in Figure II-7) is sub-optimal in the 2D subspace *damage to ecosystems quality vs resource depletion*, as it can be improved simultaneously in both objectives by some points lying in the Pareto front. As observed, all the Pareto solutions generated in the space *damage to ecosystems quality vs resource depletion* show less damage to resources than the base case, and there are six solutions which are also better in terms of damage to ecosystems quality. Starting from the top solution, the slope of the curve decreases sharply, so reductions in damage to ecosystem quality can be attained by increasing the damage to resources depletion marginally, while from point 8 the slope shows a low rate of decrease. Point 8 is identified as a “knee point”, in which the slope of the curve changes significantly, and it may be particularly appealing for decision and policy makers.

2.4.3 *Optimal rainfed and irrigated cropping areas*

Any Pareto point could be chosen by decision and policy-makers as they all represent optimal alternatives achieving a unique combination of objectives values implying a particular rainfed and irrigated area in each watershed. The selection of the most preferred Pareto solution should be made by an expert panel considering the farmers' and other stakeholders' preferences. A priori and posteriori approaches are available for multi-criteria decision-making (further information on this topic can be found in Figueira et al., (2005)). In this work, we provide the set of optimal alternatives without giving any weight/priority to the objectives (i.e. no ranking of Pareto points is provided), so we avoid subjective value judgements.

For illustrative purposes, Figure II-8 shows the surface changes that need to be implemented (with respect to the base case) in the extreme solutions and in the knee point solution identified in Figure II-7. Each watershed is coloured according to the change in hectares assigned to the rainfed and irrigated surfaces (yellow colour for rainfed and blue colour for irrigated). Light and dark shades indicate low and high changes, respectively. Note that changes with respect to the base case imply that rainfed areas are replaced by irrigated surfaces or vice-versa, that is, only changes between rainfed and irrigated areas are allowed (Galicia watershed remains unchanged in all of the solutions, since wheat is only grown under rainfed conditions).

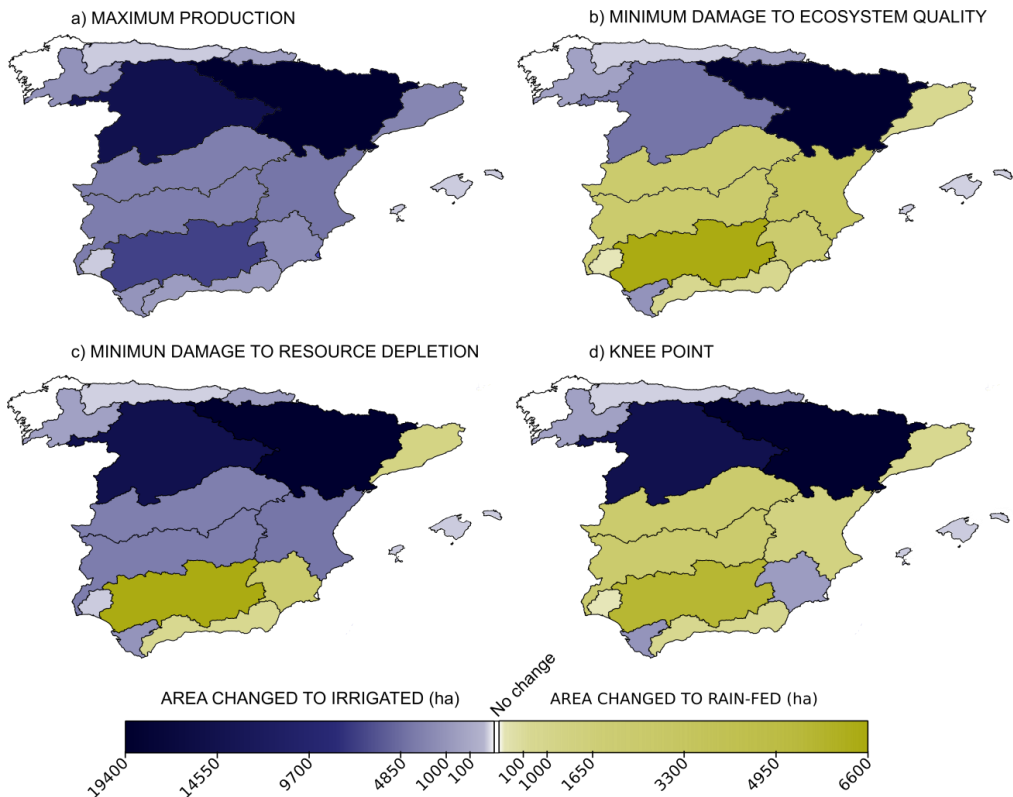


Figure II-8 Optimal changes between rainfed and irrigated areas in each watershed corresponding to the following solutions: (a) maximum production, (b) minimum damage to ecosystem quality, (c) minimum damage to resource depletion and (d) knee point solution identified contrasting ecosystems quality vs resource depletion.

As observed in Figure II-8a, the model maximises the production by increasing the irrigated areas in all of the watersheds, that is, the solution replaces rainfed areas by irrigated ones, since yields are higher in irrigated areas compared to non-irrigated areas that usually suffer water deficiencies. Compared to the base case, the maximum production solution increases the production by 1.1% (92328 t), but this leads to a significant worsening of the environmental objectives, especially in resource depletion (the impact increases by 7.8% in resource depletion and by 4.5% in ecosystem quality).

Figure II-8b shows the optimal changes in the minimum damage to ecosystems quality solution. A clear difference between the northern and the

southern Spanish watersheds is observed. More precisely, in most of the southern watersheds, with high vulnerability to suffer ecosystem damage due to water consumption, the irrigated areas are replaced by rainfed exploitation. The production deficit generated by implementing this plan is offset by replacing rainfed areas by irrigation systems in the northern watershed as well as in Duero, Ebro, Guadalete and Barbate, and Balearic Islands. Comparing to the base case, the minimum damage to ecosystem quality solution preserves 3263 ha from degradation every year and reduces the amount of water consumed by 1.1 % (in turn, this solution also reduces the damage to resource depletion by 7.9% while maintaining the production).

Figure II-8c represents the optimal changes corresponding to the minimum damage to resource depletion solution. As can be observed in the map (Figure II-8c), the irrigated areas are reduced in Cuencas internas de Cataluña, Guadalquivir, Cuenca Mediterránea Andaluza and Segura watersheds, as these regions show the highest vulnerability to resources depletion (see Table II-1). In order to offset the significant production loss taking place when these changes are implemented, the model replaces in the other watersheds rainfed areas by irrigated ones. Compared to the base case, the minimum damage to resource depletion solution decreases by 572 million MJ the energy required to extract water resources in the future (reduction of 12.5%), worsening the impact in ecosystem quality by 2.0% and increasing the production by 0.7%.

Finally, Figure II-8d shows the optimal changes that should be implemented in the knee solution identified in Figure II-7 (trade-off between ecosystems quality and resource depletion). Two clear patterns are identified in the northern and southern Spanish watersheds. More precisely, in many southern watersheds (with high vulnerability in ecosystem damage and resource depletion), the irrigated areas are replaced by rainfed exploitation. However, this reduction of irrigated areas (with higher yields than rainfed ones) generates a production deficit, which is offset

by replacing rainfed areas by irrigation systems in other watersheds, including Duero, Ebro, Guadalete and Barbate, Segura and Balearic Islands. Compared to base case, the knee point solution allows decreasing the damage to ecosystem quality and the damage to resource depletion by 0.9% and 10.7% respectively, while the production is maintained at the same level as in the base case.

2.4.4 Sensitivity analysis

A sensitivity analysis was carried out to investigate the robustness of the deterministic model considering two uncertain parameters: blue water requirements and crop yield. The irrigation requirements may be overestimated in the model, as farmers may not irrigate at the optimum level. On the other hand, the crop yield may be affected by several factors, including weather variations, climate change, soil responses, management practises or pests. Furthermore, we have investigated how the optimal solution changes for different lower and upper bounds imposed on the surfaces.

The results of the sensitivity analysis are summarised in the form of heat maps (Figure II-9 and Figure II-10), which show how the extreme solutions (those obtained in the scalar optimisation of each separate objective) change when the irrigation requirements and crop yields are modified. Each heat map cell is coloured according to the percentage change in the objective function with respect to the nominal case. Red colours indicate worse values, while green colours indicate better values. The x-axis corresponds to different bounds on variables from 0% (no change allowed) to 100% (all rainfed areas can be substituted by irrigated or vice versa). Note that we consider that each uncertain parameter is modified simultaneously in all of the watersheds to the same proportion. The base case (BC) and the nominal case (NC) are also shown to facilitate comparisons.

Changing the irrigation water requirements from 100% to 40% for a fixed yield: as observed in Figure II-9, when maintaining the irrigation as in the nominal case (100% case, as shown in the vertical axis) and changing the bounds on the

areas from 20% to 100% (horizontal axis), the production can increase by 5% at most (Figure II-9a, cell 1.05), the damage to ecosystems can decrease by no more than 6% (Figure II-9b, cell 0.94) and the damage to resources can drop by as much as 58% (Figure II-9c, cell 0.42). On the other hand, when the dose of irrigation is reduced to 40% of its value in the nominal case (vertical axis) and bounds on areas are fixed to 20% (as in the nominal case), the maximum production remains constant, while the damage to ecosystems and the damage to resources can be reduced by as much as 16% (Figure II-9b, cell 0.84) and 22% (Figure II-9c, cell 0.78), respectively, compared to the nominal case.

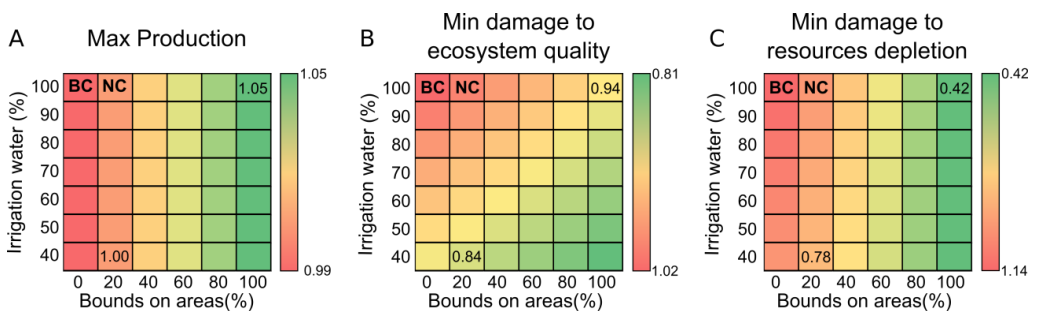


Figure II-9 Sensitivity analysis of the extreme optimal solutions to changes in the irrigation parameter. BC stands for base case and NC for nominal case. The value of each cell represents the percentage change with respect the nominal case.

Changing the yields from 103% to 97% for fixed irrigation requirements: as seen in Figure II-10, when maintaining the yield equal as in the nominal case and changing the bound on areas from 20% to 100%, the production can increase by 5% at most (Figure II-10a, cell 1.05), the damage to ecosystems quality can decrease by 6% (Figure II-10b, cell 0.94) and the damage to resources can decrease by no more than 58% (Figure II-10c, cell 0.42). On the other hand, when the wheat yield is increased by 3% (103% with respect to the nominal case) while maintaining the bounds fixed to 20% (like in the nominal case), the crop production increases in the same proportion (Figure II-10a, cell 1.03), the damage to ecosystems can be reduced by 7% (Figure II-10b, cell 0.93), and the damage to resources can decrease by 8% (Figure II-10c, cell 0.92). When the yield is decreased by 3% and the bounds

on the areas are the same as in the nominal case, then the problem renders infeasible (non-coloured cells appearing in the heat map indicate infeasible solutions), since the demand satisfaction constraint is violated. This is because the demand is kept as in the nominal case and even increasing the irrigated areas until they hit their upper bound is not sufficient to offset the decrease in production.

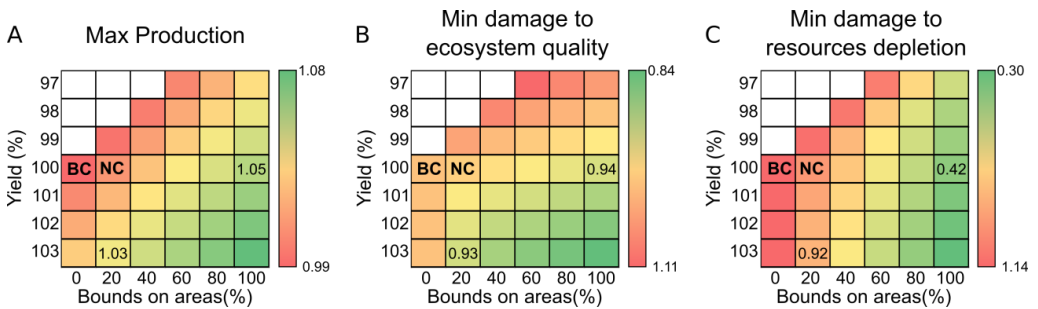


Figure II-10 Sensitivity analysis of the extreme optimal solutions to changes in the crop yield parameter. BC stands for base case and NC for nominal case. The value of each cell represents the percentage change with respect the nominal case.

The changes in the optimal areas are summarised in Figure II-11 and Figure II-12 in the form of radar charts in which each axis corresponds to a watershed (see watersheds codes in Figure II-2) and the ring with value 1 represents the nominal case.

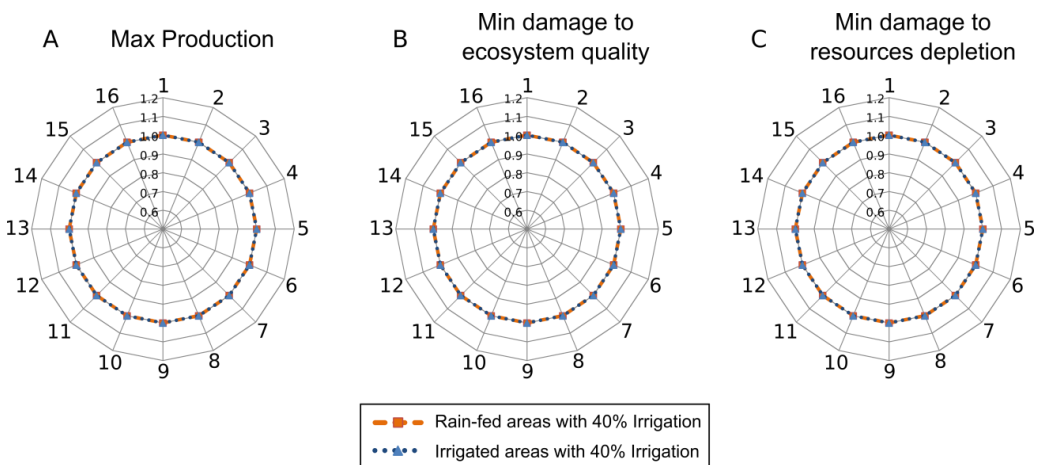


Figure II-11 Sensitivity analysis of the optimal rainfed and irrigated areas to changes in the irrigation.

Changes in the irrigation requirements: as seen in Figure II-11, when the irrigation is reduced to 40% and the bounds fixed to 20% (like in the nominal case), the optimal rainfed and irrigated areas remain the same as in the nominal case in the three objectives regardless of the dose of irrigation. When the production is maximised (Figure II-11a), the irrigated areas are increased in all of the watersheds until they hit the bound imposed (20% of change); and when the damage to ecosystems (Figure II-11b) and the damage to resources (Figure II-11c) are minimised, the optimal areas are allocated based on the vulnerability of watersheds to the water consumption (i.e. based on the environmental characterisation factors specific for each watershed), which remains the same. Therefore, these changes have no impact on the optimal areas.

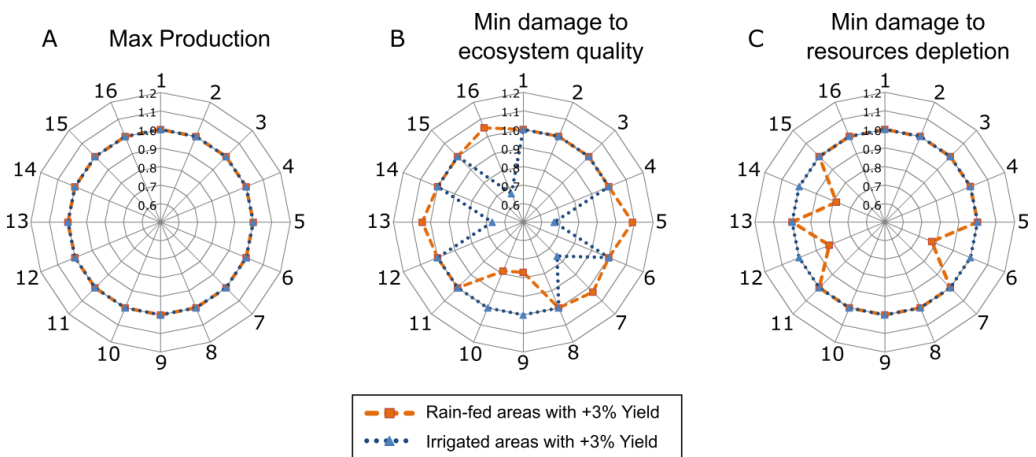


Figure II-12 Sensitivity analysis of the optimal rainfed and irrigated areas to changes in the yield.

Changes in the yield: Figure II-12 shows how the optimal areas change for a 3% increment in the yield maintaining the bounds as in the nominal case. When the production is maximised, the optimal cropping areas remain the same regardless of the value of the yield (Figure II-12a), since irrigated areas (which present higher yield) are increased until they hit their upper bound. When the damage to ecosystems quality is minimised (Figure II-12b), the optimal rainfed and irrigated areas vary greatly in many of the watersheds comparing with the nominal case

(from 8% increase in rainfed area in Ebro, to 33% reduction in irrigated areas in Ebro, Guadalete y Barbarte and Islas Baleares). On the other hand, when the damage to resources is minimised (Figure II-12c), the irrigated optimal areas remain the same as in the nominal case in all of the watersheds, while the rainfed areas are decreased in Cuenca Mediterránea, Guadalquivir and Cuencas internas de Cataluña.

2.5 Conclusions

An optimised allocation of rainfed and irrigated cropping areas is identified as a potential pathway to reduce the environmental impact of water consumption in the transition towards a more sustainable agricultural production system. To address this problem, we have developed a novel systematic decision-support tool that integrates WF and LCA principles with mathematical programming techniques. The task of identifying optimal rainfed and irrigated areas in a watershed was mathematically formulated as a multi-objective linear programming problem that seeks to optimise simultaneously the production and environmental impact of water consumption.

The capabilities of our approach were tested through its application to a case study based on wheat production in Spain. Results show that significant reductions in environmental impact can be attained by properly allocating the rainfed and irrigated cropping areas while still maintaining or even increasing the current production. We found that some of the optimal solutions identified by the optimisation algorithm represent win-win scenarios that improve the base case (current scenario identified as sub-optimal) simultaneously in all of the objectives (i.e. production targets and environmental impacts). Unlike rules of thumb or heuristics, our approach avoids sub-optimal solutions by guaranteeing convergence to the global optimum. The analysis indicates that the systematic tool presented here, which combines MOO with LCA and WF, can be potentially employed for optimally allocating rainfed and irrigated crops in order to reduce the environmental impact of water consumption in agriculture while enhancing food

availability.

Concerning the robustness of the model, the sensitivity analysis performed shows that: (i) water requirements have a significant impact on the environmental objectives (changes in blue water requirements from 100% to 40% can reduce the damage to ecosystems quality by no more than 16%, and the damage to resources in 22%); (ii) changes in the yield can also affect significantly all of the objectives and can even make the model unfeasible for some values (a 3% increment in the yield can increase the production in 3%, and reduce the damage to ecosystems by 7%, and the damage to resources by 8%); (iii) the impact of the bounds on areas is also significant, making it possible to attain larger economic and environmental improvements by widening them (i.e. small lower bounds and bigger upper bounds); (iv) concerning the optimal areas in each watershed, they are sensitive to small changes in yields, which may lead to quite different solutions in each case. The results of the sensitivity analysis highlight the opportunity to extend the deterministic model proposed herein by integrating the uncertainties related to potential changes in climate conditions.

Our systematic decision-support tool is intended to support decision and policy making by providing a set of optimal alternatives and useful guidelines to formulate appropriate regulations and policy responses for the challenge of sustainable agriculture. Note, however, that these policies can only succeed if social and economic costs associated with the transition process are compensated through a set of effective incentives (farmers need to be compensated for the extra costs and income losses incurred). Our framework can contribute to the development of more sustainable agricultural production patterns, enhancing food security and mitigating the problems of water scarcity and environmental degradation.

2.6 Acknowledgements

The authors wish to acknowledge the financial support of this research work from the Spanish Ministry of Education and Science (Projects CTQ2012-37039-C02, DPI2012-37154-C02-02).

2.7 Nomenclature

Indices

J	set for watersheds indexed by j
K	set for provinces indexed by k

Parameters

Demand	Minimum demand satisfaction level of the crop (t)
$\text{Yield}_j^{\text{DRY}}$	productivity in rainfed farmland in watershed j ($\text{t}\cdot\text{ha}^{-1}$)
$\text{Yield}_j^{\text{IRR}}$	productivity in irrigated farmland in watershed j ($\text{t}\cdot\text{ha}^{-1}$)
CF_j^{EQ}	characterisation factor for ecosystem quality in watershed j ($\text{m}^2\cdot\text{year}\cdot\text{m}^{-3}$)
CF_j^{RD}	characterisation factor for resource depletion in watershed j ($\text{MJ}\cdot\text{m}^{-3}$)
$\text{Surface}_j^{\text{AVA}}$	surface available in watershed j (ha)
SR_j^{DRY}	current harvested rainfed surface in watershed j (ha)
SR_j^{IRR}	current harvested irrigated surface in watershed j (ha)
$\text{CWU}_j^{\text{GREEN}}$	green water crop requirements in watershed j ($\text{m}^3\cdot\text{ha}^{-1}$)
$\text{CWU}_j^{\text{BLUE}}$	blue water crop requirements in watershed j ($\text{m}^3\cdot\text{ha}^{-1}$)
$\text{CWU}_j^{\text{GREY}}$	grey water crop requirements in watershed j ($\text{m}^3\cdot\text{ha}^{-1}$)
CS_k^{DRY}	real crop harvested area under rainfed conditions in province k (ha)
CS_k^{IRR}	real crop harvested area under irrigated conditions in province k (ha)
$f_{k,j}$	area fraction of province k in the watershed j (dimensionless)
YP_k^{DRY}	real rainfed crop yield in province k ($\text{t}\cdot\text{ha}^{-1}$)

$Y P_k^{IRR}$ real irrigated crop yield in province k ($t \cdot ha^{-1}$)

Variables

$Surface_j^{DRY}$ rainfed surface in watershed j (ha)

$Surface_j^{IRR}$ irrigated surface in watershed (ha)

$Production$ total production of the crop (tonnes)

EQ damage to ecosystem quality ($m^2 \cdot year$)

RD damage to resources depletion (MJ)

CWR_j crop water requirement in the watershed j (m^3)

W_j^{GREEN} volume of green water consumed by the crop in each watershed j (m^3)

W_j^{BLUE} volume of blue water consumed by the crop in each watershed j (m^3)

W_j^{GREY} volume of grey water consumed by the crop in each watershed j (m^3)

2.8 References

AEMET, 2014. Valores climatológicos normales - Agencia Estatal de Meteorología - AEMET. Gobierno de España [WWW Document]. URL <http://www.aemet.es/es/serviciosclimaticos/datosclimatologicos/valoresclimatologicos> (accessed 1.27.14).

Alcamo, J., Döll, P., Henrichs, T., Kaspar, F., Lehner, B., Rösch, T., Siebert, S., 2003. Development and testing of the WaterGAP 2 global model of water use and availability. *Hydrol. Sci. J.* 48, 317–337. doi:10.1623/hysj.48.3.317.45290

Aldaya, M.M., Martínez-Santos, P., Llamas, M.R., 2009. Incorporating the Water Footprint and Virtual Water into Policy: Reflections from the Mancha Occidental Region, Spain. *Water Resour. Manag.* 24, 941–958. doi:10.1007/s11269-009-9480-8

Allen Richard, G., Pereira, L.S., Raes, D., Smith, M., 1998. *Crop Evapotranspiration, Guidelines for Computing Crop Water Requirements.*, Edición:

R. ed. Fao, Rome.

Azapagic, A., 1999. Life cycle assessment and its application to process selection, design and optimisation. *Chem. Eng. J.* 73, 1–21. doi:10.1016/S1385-8947(99)00042-X

Azapagic, A., Clift, R., 1999. Life cycle assessment and multiobjective optimisation. *J. Clean. Prod.* 7, 135–143. doi:10.1016/S0959-6526(98)00051-1

Azapagic, A., Perdan, S., 2005. An integrated sustainability decision-support framework Part II: Problem analysis. *Int. J. Sustain. Dev. World Ecol.* 12, 112–131.

Berger, M., Finkbeiner, M., 2010. Water Footprinting: How to Address Water Use in Life Cycle Assessment? *Sustainability* 2, 919–944. doi:10.3390/su2040919

Boulay, A.-M., Bayart, J.-B., Bulle, C., Franceschini, H., Motoshita, M., Muñoz, I., Pfister, S., Margni, M., 2015. Analysis of water use impact assessment methods (part B): applicability for water footprinting and decision making with a laundry case study. *Int. J. Life Cycle Assess.* 20, 865–879. doi:10.1007/s11367-015-0868-9

Branke, J., Deb, K., Miettinen, K., Slowinski, R., 2008. Multiobjective Optimization. Interactive and Evolutionary Approaches. Springer, Verlag Berlin Heidelberg.

Brooke, A., Kendrick, D., Meeraus, A., Raman, R., 1998. GAMS—A User's Manual. GAMS Development Corporation, Washington, DC.

Chankong, V., Haimes, Y.Y., 1983. Multiobjective Decision Making: Theory and Methodology. Elsevier-North Holland, New Yoek.

Chapagain, A.K., Orr, S., 2009. An improved water footprint methodology linking global consumption to local water resources: a case of Spanish tomatoes. *J. Environ. Manage.* 90, 1219–28. doi:10.1016/j.jenvman.2008.06.006

Chen, Z.J., Cheng, Z.J., Yan, X.Q., 2013. Multiobjective Optimization Problem of Multireservoir System in Semiarid Areas. *Math. Probl. Eng.* 2013, 1–8. doi:10.1155/2013/354206

Dury, J., Schaller, N., Garcia, F., Reynaud, A., Bergez, J.E., 2011. Models to support cropping plan and crop rotation decisions. A review. *Agron. Sustain. Dev.* 32, 567–580. doi:10.1007/s13593-011-0037-x

Ehrgott, M., 2000. *Multicriteria optimization*. Springer.

Ehrgott, M., 2008. Multiobjective optimization. *AI Mag.* 29, 47–57.

Ehrgott, M., 2009. Multiobjective Optimization. *AI Mag.* 29, 47. doi:10.1609/aimag.v29i4.2198

FAO, 2010. “CROPWAT 8.0” Water Development and Management Unit - Information Resources - Databases [WWW Document]. URL http://www.fao.org/nr/water/infores_databases_cropwat.html

FAO, 2014. AQUASTAT-FAO’s information system on water and agriculture [WWW Document]. Organ. las Nac. Unidas para la Aliment. y la Agric. URL <http://www.fao.org/nr/water/aquastat/main/index.stm> (accessed 3.4.14).

Figueira, J., Greco, S., Ehrgott, M., 2005. *Multiple Criteria Decision Analysis: State of the Art Surveys*. Springer-Verlag New York.

Finnveden, G., Hauschild, M.Z., Ekvall, T., Guinée, J., Heijungs, R., Hellweg, S., Koehler, A., Pennington, D., Suh, S., 2009. Recent developments in Life Cycle Assessment. *J. Environ. Manage.* 91, 1–21. doi:10.1016/j.jenvman.2009.06.018

Foley, J.A., Ramankutty, N., Brauman, K.A., Cassidy, E.S., Gerber, J.S., Johnston, M., Mueller, N.D., O’Connell, C., Ray, D.K., West, P.C., Balzer, C., Bennett, E.M., Carpenter, S.R., Hill, J., Monfreda, C., Polasky, S., Rockström, J., Sheehan, J., Siebert, S., Tilman, D., Zaks, D.P.M., 2011. Solutions for a cultivated planet. *Nature*

478, 337–42. doi:10.1038/nature10452

García, N., Fernández-Torres, M.J., Caballero, J.A., 2014. Simultaneous environmental and economic process synthesis of isobutane alkylation. *J. Clean. Prod.* 81, 270–280. doi:10.1016/j.jclepro.2014.06.016

Garrido, A., Llamas, M., Varela-Ortega, C., Novo, P., Rodríguez-Casado, R., Aldaya, M., 2010. Water Footprint and Virtual Water Trade in Spain: Policy Implications. La Fundación Marcelino Botín-Sanz de Sautuola y López, New York, NY.

Giorgi, F., 2006. Climate change hot-spots. *Geophys. Res. Lett.* 33, L08707. doi:10.1029/2006GL025734

Goedkoop, M., Spriensma, R., 2001. The Eco-Indicator 99: a Damage Oriented Method for Life Cycle Impact Assessment: Methodology Report, Publikatiereeks produktenbeleid; nr. 36A; Ministerie van Volkshuisvesting, Ruimtelijke Ordening en Milieubeheer: Den Haag.

Grossmann, I.E., Guillén-Gosálbez, G., 2010. Scope for the application of mathematical programming techniques in the synthesis and planning of sustainable processes. *Comput. Chem. Eng.* 34, 1365–1376. doi:10.1016/j.compchemeng.2009.11.012

Guillen-Gosalbez, G., Caballero, J. #x ; A., Esteller, L.J., Gadalla, M., 2007. 17th European Symposium on Computer Aided Process Engineering, Computer Aided Chemical Engineering, Computer Aided Chemical Engineering. Elsevier. doi:10.1016/S1570-7946(07)80218-5

Haimes, Y., Lasdon, L.S., Wismer, D.A., 1971. On a bicriterion formulation of the problems of integrated system identification and system optimization. *IEEE Trans. Syst. Man, Cybern.* 3, 296–271.

Hoekstra, A.Y., 2003. Virtual water trade: Proceedings of the International

Expert Meeting on Virtual Water Trade', 12–13 December 2002, Value of Water Research Report Series No 12, UNESCO-IHE, Delft, Netherlands.

Hoekstra, A.Y., Chapagain, A.K., Aldaya, M., Mekonnen, M.M., 2011. The water footprint assessment manual: setting the global standard. Earthscan, London ; Washington, DC.

Hospido, A., Núñez, M., Antón, A., 2012. Irrigation mix: how to include water sources when assessing freshwater consumption impacts associated to crops. *Int. J. Life Cycle Assess.* 18, 881–890. doi:10.1007/s11367-012-0523-7

Jefferies, D., Muñoz, I., Hodges, J., King, V.J., Aldaya, M., Ercin, A.E., Milà i Canals, L., Hoekstra, A.Y., 2012. Water Footprint and Life Cycle Assessment as approaches to assess potential impacts of products on water consumption. Key learning points from pilot studies on tea and margarine. *J. Clean. Prod.* 33, 155–166. doi:10.1016/j.jclepro.2012.04.015

Karrou, M., Oweis, T., 2012. Water and land productivities of wheat and food legumes with deficit supplemental irrigation in a Mediterranean environment. *Agric. Water Manag.* 107, 94–103. doi:10.1016/j.agwat.2012.01.014

Khoshnevisan, B., Bolandnazar, E., Shamshirband, S., Shariati, H.M., Anuar, N.B., Mat Kiah, M.L., 2015. Decreasing environmental impacts of cropping systems using life cycle assessment (LCA) and multi-objective genetic algorithm. *J. Clean. Prod.* 86, 67–77. doi:10.1016/j.jclepro.2014.08.062

Liu, J., Zehnder, A.J.B., Yang, H., 2009. Global consumptive water use for crop production: The importance of green water and virtual water. *Water Resour. Res.* 45, n/a–n/a. doi:10.1029/2007WR006051

MAGRAMA, 2014. Agriculture Statistics [WWW Document]. URL <http://www.magrama.gob.es/es/estadistica/temas/estadisticas-agrarias/agricultura/>

Milà i Canals, L., Chenoweth, J., Chapagain, A., Orr, S., Antón, A., Clift, R., 2008. Assessing freshwater use impacts in LCA: Part I—inventory modelling and characterisation factors for the main impact pathways. *Int. J. Life Cycle Assess.* 14, 28–42. doi:10.1007/s11367-008-0030-z

Núñez, M., Pfister, S., Antón, A., Muñoz, P., Hellweg, S., Koehler, A., Rieradevall, J., 2013. Assessing the Environmental Impact of Water Consumption by Energy Crops Grown in Spain. *J. Ind. Ecol.* 17, 90–102. doi:10.1111/j.1530-9290.2011.00449.x

Ortiz, R., Sayre, K.D., Govaerts, B., Gupta, R., Subbarao, G.V., Ban, T., Hodson, D., Dixon, J.M., Iván Ortiz-Monasterio, J., Reynolds, M., 2008. Climate change: Can wheat beat the heat? *Agric. Ecosyst. Environ.* 126, 46–58. doi:10.1016/j.agee.2008.01.019

Pacetti, T., Lombardi, L., Federici, G., 2015. Water–energy Nexus: a case of biogas production from energy crops evaluated by Water Footprint and Life Cycle Assessment (LCA) methods. *J. Clean. Prod.* 101, 278–291. doi:10.1016/j.jclepro.2015.03.084

Pfister, S., Bayer, P., 2013. Monthly water stress: spatially and temporally explicit consumptive water footprint of global crop production. *J. Clean. Prod.* doi:10.1016/j.jclepro.2013.11.031

Pfister, S., Koehler, A., Hellweg, S., 2009. Assessing the Environmental Impacts of Freshwater Consumption in LCA. *Environ. Sci. Technol.* 43, 4098–4104. doi:10.1021/es802423e

Pieragostini, C., Mussati, M.C., Aguirre, P., 2012. On process optimization considering LCA methodology. *J. Environ. Manage.* 96, 43–54. doi:10.1016/j.jenvman.2011.10.014

Postel, S.L., Daily, G.C., Ehrlich, P.R., 1996. Human appropriation of renewable

fresh water. *Science* (80-). 271, 785–788.

Rharrabti, Y., Royo, C., Villegas, D., Aparicio, N., García del Moral, L., 2003. Durum wheat quality in Mediterranean environments. *F. Crop. Res.* 80, 123–131. doi:10.1016/S0378-4290(02)00176-4

Ridoutt, B.G., Pfister, S., 2010. A revised approach to water footprinting to make transparent the impacts of consumption and production on global freshwater scarcity. *Glob. Environ. Chang.* 20, 113–120. doi:10.1016/j.gloenvcha.2009.08.003

Rijsberman, F.R., 2006. Water scarcity: Fact or fiction? *Agric. Water Manag.* 80, 5–22. doi:10.1016/j.agwat.2005.07.001

Rockström, J., Steffen, W., Noone, K., Persson, Å., Chapin, F.S., Lambin, E., Lenton, T.M., Scheffer, M., Folke, C., Schellnhuber, H.J., Nykvist, B., de Wit, C.A., Hughes, T., van der Leeuw, S., Rodhe, H., Sörlin, S., Snyder, P.K., Costanza, R., Svedin, U., Falkenmark, M., Karlberg, L., Corell, R.W., Fabry, V.J., Hansen, J., Walker, B., Liverman, D., Richardson, K., Crutzen, P., Foley, J., 2009. Planetary boundaries: Exploring the safe operating space for humanity. *Ecol. Soc.* 14.

Sarker, R., Ray, T., 2009. An improved evolutionary algorithm for solving multi-objective crop planning models. *Comput. Electron. Agric.* 68, 191–199. doi:10.1016/j.compag.2009.06.002

Singh, A., 2012a. Optimal Allocation of Resources for the Maximization of Net Agricultural Return. *J. Irrig. Drain. Eng.* 138, 830–836. doi:10.1061/(ASCE)IR.1943-4774.0000474

Singh, A., 2012b. An overview of the optimization modelling applications. *J. Hydrol.* 466-467, 167–182. doi:10.1016/j.jhydrol.2012.08.004

Steffen, W., Richardson, K., Rockstrom, J., Cornell, S.E., Fetzer, I., Bennett, E.M., Biggs, R., Carpenter, S.R., de Vries, W., de Wit, C.A., Folke, C., Gerten, D.,

Heinke, J., Mace, G.M., Persson, L.M., Ramanathan, V., Reyers, B., Sorlin, S., 2015. Planetary boundaries: Guiding human development on a changing planet. *Science* (80-.). 347. doi:10.1126/science.1259855

UNEP, 2007. Global Environment Outlook – Geo 4: Environment for Development. United Nations Environment Programme. Valletta, Malta.

Xevi, E., Khan, S., 2005. A multi-objective optimisation approach to water management. *J. Environ. Manage.* 77, 269–77. doi:10.1016/j.jenvman.2005.06.013

Yue, D., Pandya, S., You, F., 2016. Integrating Hybrid Life Cycle Assessment with Multi-objective Optimization: A Modeling Framework. *Environ. Sci. Technol.* 50, 1501–1509. doi:10.1021/acs.est.5b04279

Zeng, X., Kang, S., Li, F., Zhang, L., Guo, P., 2010. Fuzzy multi-objective linear programming applying to crop area planning. *Agric. Water Manag.* 98, 134–142. doi:10.1016/j.agwat.2010.08.010

2.9 Appendix: estimation of the crop water requirements

From a strategic perspective, it is important to better understand the water requirements of crops in order to determine areas better suited for production. This task requires the explicit consideration of both rainfall and water availability data (Milà i Canals et al., 2010). In this appendix we show the methodology used to estimate the crop water use (CWU_j) in each watershed j . The CWU [$m^3 \cdot ha^{-1}$] is the amount of water to be supplied to the crop in order to compensate for losses caused by evapotranspiration and achieve adequate growth and development (Allen Richard et al., 1998).

The water requirements of a crop (i.e. water footprint can be broken down into three components, green, blue and grey water use, which are in turn defined as parameters in the linear programming model developed in this work. The green water is the portion of the precipitation that does not runoff. It is available on the

soil as soil moisture and can be taken up by a crop. The blue water represents the volume of surface and groundwater consumed/extracted for irrigation. The grey water is the volume of water required to assimilate the pollutants used in agriculture. The green water use (CWU_j^{GREEN}) represents the total rainwater evaporated from the field during the growing period, the blue water use (CWU_j^{BLUE}) represents the irrigation water evaporated from the field, while the grey water use (CWU_j^{GREY}) represents the amount of water required to assimilate the pollutants.

In ascertaining the crop water use (for the three components) within each watershed, we employ the methodology based on the framework proposed by Hoekstra et al. (2011) and the CROPWAT 8.0 software developed by the Food and Agriculture Organisation (Allen Richard et al., 1998; FAO, 2010). The overall methodology flow to estimate the wheat water use for green water (CWU^{GREEN}), blue water (CWU^{BLUE}) and grey water (CWU^{GREY}) is summarised in Figure II-A1.

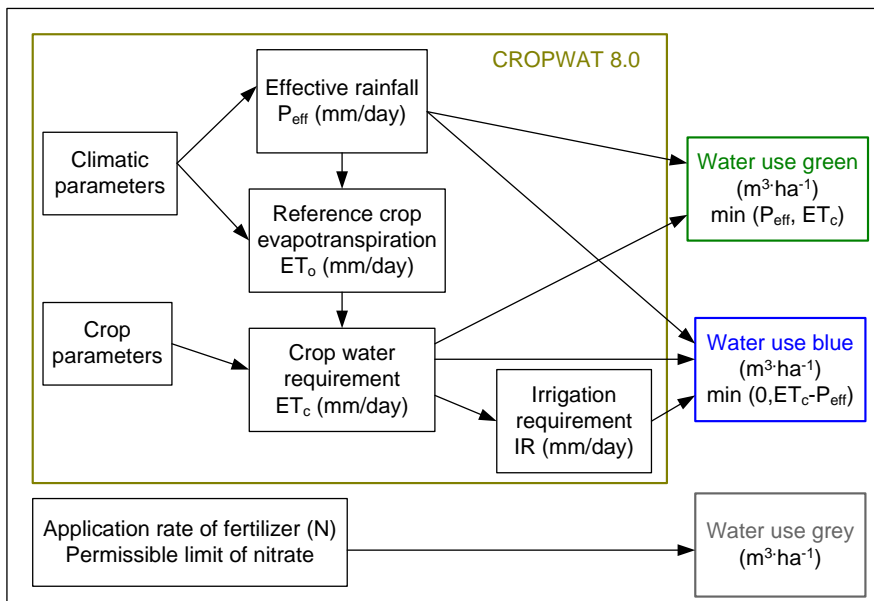


Figure II-A1 Methodology used to estimate the crop water use of a crop.

The CROPWAT software requires several data, mainly climate data and crop

parameters. Climate data could be obtained from weather stations or any agro climatic data base. The weather parameters affecting evapotranspiration are radiation, air temperature, humidity, wind speed and precipitation. The crop parameters are taken from the Food and Agricultural Organisation Book nº56 (Allen Richard et al., 1998). The crop inputs of the CROPWAT software are: first and last planting date, first and last harvesting date, length of individual growing stages, crop factor, rooting depth, allowable depletion levels and yield response factors.

This CROPWAT software allows estimating the evapotranspiration of the crop (ET_c) based on soil, climate and crop data fed into the software. The ET_c , assumed to be equal to the total crop water requirements, depends on factors that affect the evaporation and evapotranspiration, such as, weather parameters, crop characteristics, and management and environmental aspects. The ET_c is the water used for evapotranspiration under ideal growth conditions from planting to harvest. Basically, the ET_c is calculated by multiplying the reference crop evapotranspiration (ET_o) by the crop coefficient (K_c) (Eq. II-A1). The ET_o depends only on climatic parameters and it is calculated by the CROPWAT model according to the FAO Penman-Monteith equation (Allen Richard et al., 1998). K_c over the length of the growing period can be taken from the literature.

$$ET_c = K_c \cdot ET_o \quad \text{Eq. II-A1}$$

CROPWAT software also allows estimating the effective rainfall (P_{eff}) based on climate data, that is, the proportion of the rainfall already available than can be effectively used by the crop after losses due to runoff and percolation. There are four methods available in CROPWAT 8.0 to account for the losses due to runoff or percolation.

Once the ET_c and the P_{eff} are estimated using the CROPWAT software, the next step consists of estimating the green and blue water evapotranspiration (ET_{green} and ET_{blue}). As shown in Eq. II-A2, ET_{green} is calculated as the minimum of the ET_c and the P_{eff} . The CROPWAT model assumes that the crop water requirements are fully

met, so the actual crop evapotranspiration (ET_c) equals the crop water requirements. The ET_{blue} (field evapotranspiration of irrigation water) is calculated as the difference between the ET_c and the P_{eff} as shown in Eq. II-A3. The irrigation requirement is zero if the effective rainfall is larger than the crop water requirements.

$$ET_{green} = \min(ET_c, P_{eff}) \quad \text{Eq. II-A2}$$

$$ET_{blue} = \max(0, ET_c - P_{eff}) \quad \text{Eq. II-A3}$$

Finally, the CWU^{GREEN} , CWU^{BLUE} and CWU^{GREY} are calculate via Eq. II-A4, Eq. II-A5 and Eq. II-A6 respectively. We assume that there are no water limitations on crop growth. The CWU [$m^3 ha^{-1}$] takes into account the total accumulation of the daily evapotranspiration [$mm day^{-1}$] over the complete growing period. The summation is done from the day of planting (day 1) to the day of harvest (l_{gp} denotes the length of the growing period in days).

$$CWU_{green} = 10 \cdot \sum_{d=1}^{l_{gp}} ET_{green} \quad \text{Eq. II-A4}$$

$$CWU_{blue} = 10 \cdot \sum_{d=1}^{l_{gp}} ET_{blue} \quad \text{Eq. II-A5}$$

The CWU^{GREY} is estimated based on a simplified approach proposed by Mekonnen and Hoekstra (2011) (further details of the methodology are described in “The Water Footprint Assessment Manual” (Hoekstra et al., 2011)). The CWU^{GREY} is estimated using Eq. II-A6 based on the crop application rate of nitrogen (AR) [$kg ha^{-1}$] multiplied with the leaching-runoff fraction (δ %) and dividing this by the difference between the maximum acceptable amount of nitrogen (C_{max}) [$kg ha^{-1}$] defined by the water quality standards and its natural concentration (C_{nat}) [$kg ha^{-1}$].

$$CWU_{grey} = (\delta - AR)/(C_{max} - C_{nat}) \quad \text{Eq. II-A6}$$

1.9.1 *Wheat water use calculation*

We employed the methodology explained before (Allen Richard et al., 1998; FAO, 2010; Hoekstra et al., 2011) to estimate the wheat water use for green, blue and grey water in each watershed j (CWU_j^{GREEN} , CWU_j^{BLUE} and CWU_j^{GREY}), which were defined as parameters in the linear programming model.

The wheat water use was first calculated for each meteorological station, and the data were then aggregated at the watershed level as the average of the values of the meteorological stations in each watershed.

Climate data were obtained from the State Meteorological Agency (AEMET, 2014) of the Spanish Ministry of Agriculture, Food and Environment. We used data from 67 meteorological stations located in the watersheds. The data (temperature, precipitation, humidity, sunshine hours and wind speed) corresponded to the average normal value from period 1981-2010.

Wheat parameters, like crop coefficients and crop patterns (first and last planting date, first and last harvesting date, length of individual growing stages, crop factor, rooting depth, allowable depletion levels and yield response factors), were taken from the FAO nº56 (Allen et al., 1998) for winter wheat in the Mediterranean region.

In order to determine the Peff, we employed the USDA Soil Conservation Service Method from the United State Department of Agriculture, Soil Conservation Service.

The wheat grey water use was calculated assuming a crop application rate of nitrogen of $95 \text{ kg}\cdot\text{ha}^{-1}$ and that on average 15% of the nitrogen fertiliser is lost through leaching or runoff, following Mekonnen and Hoekstra (2010). We also have assumed a maximum acceptable concentration of nitrates of $0.05 \text{ kg}\cdot\text{m}^{-3}$ (following the Spanish water quality standards), and a natural nitrogen concentration of zero (due to lack of data).

Table II-A1 shows the wheat water used estimated for each meteorological station. These data were aggregated into the watershed level taking the average of the values of the meteorological station located in the watershed. We defined these specific values for each watershed as parameters in the mathematical model developed.

Table II-A1 Wheat water use ($\text{m}^3 \cdot \text{ha}^{-1}$) for green, blue and grey water for each meteorological station.

Watershed	Meteorological Station	CWU _{green}	CWU _{blue}	CWU _{grey}
Galicia Costa	A Coruña	3440	2591	285
	A Coruña aeropuerto	3261	2212	285
	Santiago aeropuerto	4062	2218	285
	Pontevedra	4364	2960	285
Miño-Sil	Lugo aeropuerto	3514	3011	285
	Vigo aeropuerto	4050	2790	285
	Orense	3036	5167	285
	Ponferrada	2681	5983	285
Cantábrico occidental	Asturias aeropuerto	3773	1500	285
	Oviedo	4326	1695	285
	Santander	4014	1853	285
Cantábrico oriental	Bilbao aeropuerto	4174	2262	285
	San Sebastian Igueldo	4782	585	285
Ebro	Vitoria aeropuerto	3642	3333	285
	Logroño aeropuerto	2435	5897	285
	Pamplona aeropuerto	3299	4609	285
	Daroca	2483	6459	285
	Zaragoza aeropuerto	1965	7575	285
	Huesca aeropuerto	2606	6594	285

	Lleida	1948	7631	285
	Tortosa	2585	6688	285
Cuencas internas de Catalunya	Reus aeropuerto	2557	5547	285
	Barcelona aeropuerto	2912	4712	285
	Barcelona Fabra	2990	4675	285
	Girona aeropuerto	3597	4358	285
Duero	León aeropuerto	2426	5771	285
	Zamora	1880	7127	285
	Salamanca aeropuerto	1968	7020	285
	Valladolid aeropuerto	2096	6533	285
	Valladolid	2109	7017	285
	Ávila	2158	6487	285
	Segovia	2547	6562	285
	Burgos aeropuerto	2737	4954	285
	Soria	2831	5516	285
Tajo	Cáceres	2136	8244	285
	Toledo	1779	8663	285
	Molina de Aragón	2797	5911	285
	Madrid Getafe	1807	8314	285
	Madrid Cuatrovientos	2065	7907	285
	Madrid	2026	7680	285
	Madrid aeropuerto	1857	8227	285
	Madrid Torrejón	1930	8046	285
Júcar	Cuenca	2606	6750	285
	Albacete base aérea	2036	7722	285
	Teruel	2621	6471	285
	Castellón de la Plana	2277	6400	285
	Valencia	2251	6268	285

	Valencia aeropuerto	2152	6872	285
	Alicante	1513	7425	285
	Alicante aeropuerto	1372	7836	285
Guadiana	Ciudad Real	1945	8197	285
	Badajoz aeropuerto	1825	8636	285
Tinto, Odiel y Piedras	Huelva Ronda este	1800	8178	285
Guadalquivir	Sevilla aeropuerto	1826	5175	285
	Morón de la Frontera	2058	8600	285
	Córdoba aeropuerto	2169	8895	285
	Granada aeropuerto	1634	9193	285
Guadalete y Barbate	Jerez de la Frontera	1805	8358	285
	Tarifa	1844	5221	285
Cuenca Mediterránea Andaluzá	Málaga aeropuerto	1804	7616	285
	Almería	887	8459	285
Segura	San Javier aeropuerto	1436	6736	285
	Murcia Alcantarilla	1599	8877	285
	Murcia	1581	8956	285
Islas Baleares	Ibiza	1834	6568	285
	Palma de Mallorca	1841	6941	285
	Menorca aeropuerto	2127	6085	285

1.9.1.1 References

AEMET, 2014. Valores climatológicos normales - Agencia Estatal de Meteorología - AEMET. Gobierno de España [WWW Document]. URL <http://www.aemet.es/es/serviciosclimaticos/datosclimatologicos/valoresclimatologicos> (accessed 1.27.14).

Allen Richard, G., Pereira, L.S., Raes, D., Smith, M., 1998. Crop Evapotranspiration, Guidelines for Computing Crop Water Requirements., Edición:

R. ed. Fao, Rome.

FAO, 2010. "CROPWAT 8.0" Water Development and Management Unit - Information Resources - Databases [WWW Document]. URL http://www.fao.org/nr/water/infores_databases_cropwat.html

Hoekstra, A.Y., Chapagain, A.K., Aldaya, M., Mekonnen, M.M., 2011. The water footprint assessment manual: setting the global standard. Earthscan, London ; Washington, DC.

Mekonnen, M.M., Hoekstra, A.Y., 2010. A global and high-resolution assessment of the green, blue and grey water footprint of wheat. *Hydrol. Earth Syst. Sci.* 14, 1259–1276.

Mekonnen, M.M., Hoekstra, A.Y., 2011. The green, blue and grey water footprint of crops and derived crop products. *Hydrol. Earth Syst. Sci.* 15, 1577–1600. doi:10.5194/hess-15-1577-2011

Milà i Canals, L., Chapagain, A., Orr, S., Chenoweth, J., Anton, A., Clift, R., 2010. Assessing freshwater use impacts in LCA, part 2: case study of broccoli production in the UK and Spain. *Int. J. Life Cycle Assess.* 15, 598–607. doi:10.1007/s11367-010-0187-0

Chapter III

Sustainable cropping plan decisions and subsidies

UNIVERSITAT ROVIRA I VIRGLI

CONTRIBUTION TO THE DEVELOPMENT OF MATHEMATICAL PROGRAMMING TOOLS TO ASSIST DECISION-MAKING
IN SUSTAINABILITY PROBLEMS

Àngel Galán Martín



III. Sustainable cropping plans decisions and subsidies

Multi-stage linear programming model for optimising cropping plan decisions under the new Common Agricultural Policy

Àngel Galán-Martín^a, Carlos Pozo^a, Gonzalo Guillén-Gosálbez^{a,b*}, Assumpció Antón

Vallejo^{a,c}, Laureano Jiménez Esteller^a

^a*Departament d'Enginyeria Química, Universitat Rovira i Virgili, Av. Països Catalans 26, 43007 Tarragona (Spain).*

^b*School of Chemical Engineering and Analytical Science, University of Manchester, Mill, Sackville Street, Manchester M13 9PL (United Kingdom).*

^c*Institut de Recerca i Tecnologia Agroalimentàries (IRTA), Ctra Cabrils, km 2, 08348 Cabrils Barcelona (Spain)*

KEYWORDS: Optimal cropping plan, Decision and policy support tool, Common Agricultural Policy, greening rules

3.1 Introduction

The Common Agricultural Policy (CAP) is the agricultural policy of the European Union (EU) that aims to improve the agricultural productivity ensuring both a fair standard of living of the EU farmers and reasonable food prices without compromising the availability of supplies for consumers. This EU CAP has always been updated to respond the challenges of its time and recently a new reform has come into force as from 1th January 2014 entitled “The CAP towards 2020: Meeting the food, natural resources and territorial challenges of the future”

(European Commission, 2011).

This new EU's CAP, which will be active from 2015 to 2020, introduces a new payment scheme that will potentially induce changes at the individual farm level. The main objective of this new payment scheme is to redistribute the subsidies both between and within EU Member States and farmers in an equity manner so as to move towards a more sustainable agricultural production, that is, to spur the broad application of more sustainable agricultural practises. All EU Member States are therefore expected to implement in the short term this new payment scheme based on a uniform payment per hectare by adopting a national or regional approach (based on administrative or agronomic criteria) (European Parliament and European Council, 2013). Basically, the previous "Single Payment Scheme" is replaced in this reform by a new "Basic Payment Scheme" and also a new "greening payment" is introduced to compensate farmers following a specified set of mandatory sustainable farm practices. Broadly similar to the single payment, the Basic Payment is also a direct payment per hectare to active farmers based on their entitlements, which correspond to the eligible hectares. On the other hand, the main novelty of the new CAP reform is the introduction a new component of the subsidy, namely "Payment for agricultural which are beneficial for the climate and the environment", commonly known as "greening payment", which represents also an additional direct aid per hectare rewarding agricultural sustainable practices. The new greening payment may potentially encourage farmers to meet certain environmental requirements in return for governmental support payments which are expected to offset the cost of providing environmental public goods that are not remunerated by the market. Basically, this greening component rewards farmers complying three basic EU sustainable measures (or equivalent practices) which consist of (1) crop diversification, (2) maintenance of existing permanent grassland and (3) establishment of an ecological focus area on arable land.

In this context, several EU farms will fulfil these greening measures without

having to make major changes to their current cropping acreage. However, many farmers will have to make land use decisions bearing in mind the new greening rules which will in turn imply significant changes at the farm level. These decisions to be taken, known as cropping plan decisions, involve the choice of crops to be grown, their acreage and their allocation among others (Nevo et al., 1994).

A cropping plan decision is the result of a decision-making process subject to various objectives and constraints fitted into different spatial and temporal dynamics (Dury et al., 2011). These decisions on the farming system (e.g. cropping plan or crop rotation) are crucial for farmers since they modify the productivity and profitability on the short and long-term of the farm management. Therefore, it is of paramount importance for the farmers to establish a new cropping plan for the next five years which must satisfy the policy constraints while at the same time maximise the farmer's profit (e.g. maximum gross margin, annual profit or net benefit). In this sense, decision support models can be an important tool to aid farmers on the farm management.

Mathematical programming can provide valuable decision-support in agriculture (Butterworth, 1985). A wide variety of approaches have been developed for supporting cropping plan decisions. An excellent review of cropping plans decision models was provided by Dury et al. (2011). Among them, linear programming (LP) is the most common optimisation approach employed for solving such models due to its simplicity. Mixed integer linear programming (MILP) has also been used to plan the crop rotation problem (Dogliotti et al., 2006) and even evolutionary algorithms were employed to identify optimal cropping plan decisions at the farm level (Sarker and Ray, 2009). In the modelling approaches reviewed, the cropping plan problem was optimised within a given context and considering different objectives. The models were optimised considering either a single objective (e.g. the farmer's profit) or several ones (e.g. environmental and economic objectives) (Bartolini et al., 2007) in response to challenges related to

economic sustainability, resources use and environment protection. In some cases, as happens in the work presented here, these challenges are imposed by policy reforms that force farmers to adapt their practices (Louhichi et al., 2010; Oñate et al., 2007). The overwhelming majority of the mathematical models to support cropping plan decisions assume a single time period and steady state operation, that is, they provide a single set of decisions for a given period, typically one year. In practice, however, a cropping plan contains several time periods, so the underlying decision-making problem is multi-stage in nature and the decisions have to be made over multi-year periods. Dynamic programming (DP) has been applied to identify the optimal management of agricultural resources over planning horizons (Kennedy, 1986), and also for optimising agricultural management problems that are decomposed into sub problems (Janová, 2011; Parsons et al., 2009; Sartra et al., 2013).

This paper proposes a mathematical programming model to support farmers' cropping plan decisions in response to the new CAP reform. The decision-making tool developed herein takes the form of a multi-stage linear programming model (LP) that identifies the optimal cropping plan at the farm level that maximises the farmer's net return in the CAP reform horizon (i.e. from 2015 to 2020). The model provides insight into whether farmers should adopt the greening measures (i.e. policy constraints) and therefore receive the subsidy as compensation to production of environmental public goods, or, in contract, they should grow the most profitable crop without meeting the greening rules. In the latter case, if the sustainable practices were not appealing for the farmers, by slightly modifying the mathematical model, it can also be employed to support policy-makers by determining the minimum subsidy that would ensure the economic viability of greening rules, thereby acting as a mechanism to promote the effective transition towards more sustainable agricultural practises which constitutes in turn the main goal of the new CAP. The capabilities of our approach are illustrated through its application to the Spanish payment CAP regionalisation model, determining the

optimal cropping plan for rainfed farms in each agricultural Spanish region and the minimum subsidy required in each region to spur the broad application of the CAP greening measures.

The remaining of the article is organised as follows. Section 2 describes the problem statement which motivates the development of the mathematical model to support farmers in cropping plan decisions facing the CAP reform. This model is then described in detail in Section 3 and applied to the Spanish agricultural regularisation in Section 4. Finally, the results are shown and discussed in Section 5, whereas the main conclusions of the study are drawn in Section 6.

3.2 Problem statement

We consider an active farmer from an EU Member State who needs to decide whether to adapt his cropping plan in order to fulfil the CAP reform greening measures and therefore to receive the greening subsidy. The farmer seeks to maximise his/her revenues over the CAP reform horizon, that is, the farmer wants to make cropping plan decisions for the next five years maximising his net return regardless of whether their practises are sustainable or not.

As mentioned before, the three basic greening rules of the CAP reform (i.e. agricultural practices beneficial for the climate and the environment) to be fulfilled by the farmer in order to receive the greening subsidy are: (1) crop diversification, (2) maintenance of permanent grassland and (3) establishment of ecological focus areas. The constraints/requirements imposed by each greening rule vary depending on the size of arable land (see Table III-1).

Table III-1 Greening rules of the CAP reform to be fulfilled in order to receive the greening subsidy.

Greening rules	10 ha > Arable land > 30 ha	Arable land > 30 ha
Crop diversification	At least two different crops must be cultivated every year.	At least three different crops must be cultivated every year.
	The main crop shall not cover more than 75 % of the arable land.	The largest crop must not cover more than 75% of the arable land.
		The two largest crops together must not cover more than 95% of the arable land.
Maintenance of permanent grassland	Area of permanent grassland shall be at least 5% of the total arable land.	Area of permanent grassland shall be at least 5% of the total arable land.
Establishment of ecological focus areas	At least 5% of the total arable land shall be ecological focus area.	At least 5% of the total arable land shall be ecological focus area.
	This percentage shall be increased from 5% to 7% from 2017 onwards.	This percentage shall be increased from 5% to 7% from 2017 onwards.

To derive our approach, let us consider that the active farmer owns a piece of arable land of A hectares on which i different crops may be grown. We consider a planning period of t years (i.e. 5 years of the CAP reform horizon), and one growing season per year. We are also given the crop yields and the cost of exploitation of each crop. Moreover, the price received by farmers for each crop and the value of the CAP basic payment are available.

Additionally, it is assumed that there are no constraints to crop conversion and rotations regarding the major rules of crop rotations (Castellazzi et al., 2008). The following assumptions are made when building the model:

- A minimum return period between the same crop is considered.
- There are no agronomic limitations to crop successions. Benefits and risks of successions are not considered.
- The timing of sowing and harvesting between consecutive crops is compatible.
- There are no work limitations and no change in machinery equipment.

The goal of this work is to determine the optimal cropping plan by choosing the crops to be grown every year and their acreage in order to maximise the farmer's economic net return over the CAP reform horizon. However, as mentioned in the introduction, our analysis might reveal that there are agricultural regions where it is more profitable for the farmer not to meet the CAP greening rules. If this is the case, an additional analysis would be then carried out to support governments in order to determine a more equitable and efficient basic payment between farmers and regions that will eventually encourage all farmers to move towards more sustainable agricultural practices by implementing the greening CAP measures. Therefore, in that sense, our mathematical model described into details in the next section 3.3, is aimed at supporting both farmers and governments to ensure the broad applicability of more sustainable agricultural practises. Figure III-1 illustrates graphically the approach proposed, which is described in more details in the ensuing sections of the article.

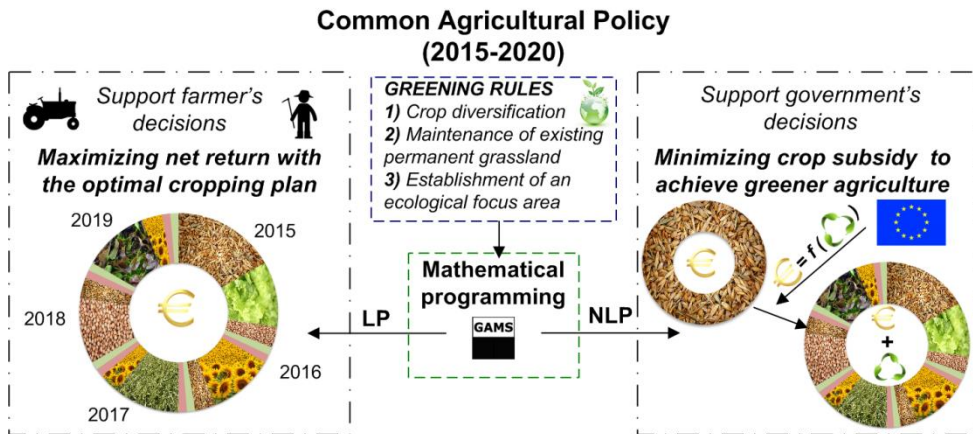


Figure III-2 General overview of proposed framework.

3.3 Multi-stage linear programming model

In this section, we present a multi-stage LP model that determines the optimal cropping plan (i.e. crops to be grown and their acreage) in each agricultural region, which might or might not meet the CAP greening rules, in order to maximise the farmer's economic net return during the planning horizon. The model consists of a linear objective function that determines the net present value and a set of linear constraints, which represent the greening rules of the CAP reform.

Objective function

The objective function is defined via Eq. III-1 where NPV represents the net present value of the farmer's net return (€) during the complete planning horizon.

$$NPV = \sum_{t=1}^5 \frac{Z_t}{(1 + ta)^{t-1}} \quad \forall t \quad \text{Eq. III-1}$$

In Eq. III-1, Z_t denotes the net return (€) in a particular agricultural region in time period t . Note that for the calculation of the NPV , each Z_t is discounted back to its present value using the discount rate ta . The value of Z_t is obtained via Eq. III-2:

$$Z_t = \sum_i [(Y_i \cdot P_{it}) + BP_i + GP_i - C_{it}] \cdot A_{it} \quad \forall t \quad \text{Eq. III-2}$$

where Y_i is a parameter that represents the yield of each crop i in a particular agricultural region ($\text{t} \cdot \text{ha}^{-1}$), P_{it} is a parameter that denotes the price received by the farmer in the market for crop i in period t ($\text{€} \cdot \text{t}^{-1}$) whereas BP_i and GP_i are parameters that account for the basic payment and the greening payment of the CAP for crop i in the agricultural region ($\text{€} \cdot \text{ha}^{-1}$) and C_{it} represents the production cost of the crop i in period t ($\text{€} \cdot \text{ha}^{-1}$). A_{it} is a continuous variable denoting the area of region cultivated with crop i in year t .

The greening payment, GP_i , is a given percentage α of the value of BP_i calculated via Eq. III-3 and will only be received by the farmer if it fulfils the greening rules:

$$GP_i = \alpha \cdot BP_i \quad \forall i \quad \text{Eq. III-3}$$

Model constraints

The maximisation of the objective function (Eq. III-1) in each region is subject to a set of CAP greening constraints which vary depending on the surface of arable land:

Arable land. The land allocated to the crops, the permanent grassland area and the ecological focus area must not exceed the total farm arable land each year.

$$TS_t \geq GRA_t + ECO_t + \sum_i A_{it} \quad \forall t \quad \text{Eq. III-4}$$

In Eq. III-4 TS_t represents the total surface of the arable land, GRA_t represents the permanent grassland area in period t (ha) and ECO_t represents the ecological focus area in period t (ha).

Maintenance of permanent grassland. The permanent grassland has to be at least 5% of the total arable land every year which is modelled via Eq. III-5:

$$GRA_t \geq 0.05 \cdot TS_t \quad \forall t \quad \text{Eq. III-5}$$

Establishment of ecological focus areas. The ecological focus area has to be greater than 5% of the total arable land in the early years (Eq. III-6), and greater than 7% from 2017 onwards (Eq. III-7).

$$ECO_t \geq 0.05 \cdot TS_t \quad \forall t \leq 2 \quad \text{Eq. III-6}$$

$$ECO_t \geq 0.07 \cdot TS_t \quad \forall t \geq 3 \quad \text{Eq. III-7}$$

Crop diversification. The farmer must grow at least two different crops for arable land between 10 ha and 30 ha and at least three different crops for arable land bigger than 30 ha. The main crop (i.e. the crop occupying the largest area) must not cover more than 75% of the total arable land in each period t (Eq. III-8). The two largest crops together must not cover more than 95% of the arable land (Eq. III-9).

$$A_{it} \leq 0.75 \cdot TS_t \quad \forall i, t \quad \text{Eq. III-8}$$

$$A_{it} + A_{ip,t} \leq 0.95 \cdot TS_t \quad \forall i \neq ip, t \quad \text{Eq. III-9}$$

Eq. III-10 enforces the application of crop rotations, that is, the same crop cannot be grown in the same area in sequential seasons. The arable land occupied by one crop in period t should be lower or equal to the surface not occupied by this crop during the previous period.

$$A_{it} \leq TS_t - GRA_t - A_{i,t-1} \quad \forall i, t > 1 \quad \text{Eq. III-10}$$

Non-negativity constraints.

$$A_{it} > 0; GRA_t > 0; ECO_t > 0 \quad \forall i, t \quad \text{Eq. III-11}$$

Taking as a basis the constraints defined above, we define three models that reflect the potential strategies that the farmer can follow during the CAP reform

horizon (see Table III-2). Model I corresponds to not fulfilling the CAP greening measures so that the farmer receives the basic payment but not the greening one. Models II and III illustrate the strategy of fulfilling the greening rules and therefore granting the farmer the greening payment for farms smaller and greater than 30ha, respectively. All the models take the form of an LP. Note that LP models of up to hundreds of thousands of variables and constraints can be efficiently solved on a standard PC using state of the art optimisation packages. Note also that this model can be extended accounting for other technical, agronomic, supply/demand constraints as well as extended to account for risk and uncertainty involved by using stochastic approaches.

3.4 Case study

The capabilities of the multi-stage LP model are demonstrated through a case study that analyses the application of the CAP reform in Spain (BOE, 2014a). In particular, we aim to obtain the optimal cropping plan for 2015 to 2020 in each Spanish agricultural region so as to maximise the farmer's economic net return for a representative rainfed farm. The reason for choosing a rainfed farming systems is two-fold: (i) rainfed agriculture is the predominant farming practice over the Spanish territory, and (ii) the economic feasibility of rainfed crops largely depends on EU CAP subsidies therefore making this case study more attractive (Sánchez-Girón et al., 2007).

Three different scenarios are identified which correspond to the potential strategies that a farmer can follow during the CAP reform horizon. Each potential scenario is represented by one model derived from the LP model explained in Section 3.3. *Model I* corresponds to not fulfilling the CAP greening measures so that the farmer receives the basic payment but not the greening one. *Model II* and *Model III* illustrate the strategy of fulfilling the greening rules and therefore granting the farmer the greening payment for farms smaller and greater than 30 ha, respectively. The overall problem description and the constraints involved in each

potential scenario are those shown in Table III-2.

Table III-2 Description of the three models employed in this study.

Greening rules	Model I	Model II	Model III
Description	Not to meet the greening measures No greening payment	To fulfill the greening measures Arable land 10-30 ha	To fulfill the greening measures Arable land >30 ha
Model*	$\min \{-f_1(x)\}$ s. t. Eq. 4 $x \in \mathfrak{R}$	$\min \{-f_1(x)\}$ s. t. Eqs. 4 – 8, 10 – 11 $x \in \mathfrak{R}$	$\min \{-f_1(x)\}$ s. t. Eqs. 4 – 11 $x \in \mathfrak{R}$

* f_1 is the objective function which represents the net present value and continuous variables x represent the surface of a crop in the arable land in a specific region.

The three models (I, II and III in Table III-2) are then solved considering a rainfed farming system in each of the agricultural regions defined by the Spanish payment regionalisation CAP model (Figure III-4). This allows determining in a systematic manner the optimal cropping plan at the farm level that should be implemented in each particular agricultural region. The optimal strategy to follow by the farmer would correspond to the cropping plan that maximises the farmer's net present value (i.e. farmer's benefit during the CAP reform horizon). Figure III-3 shows the flow chart describing the decision-making process to determine the farmers' optimal cropping plan in each particular agricultural region that maximise their net return. As long as the farmer's net return obtained with Model I is lower or equal than the profit obtained with Model II and Model III, then the greening measures would be appealing for the farmer. Otherwise, the sustainable agricultural practises would not be implemented in practise and therefore the main objective of the CAP reform would be threatened. In the latter case, the LP model will be slightly modified to determine the appropriated subsidy value that would be

required to encourage all farmers to meet the greening rule and therefore to spread the global adoption of sustainable practises (details on this topic will be provided in section 3.6).

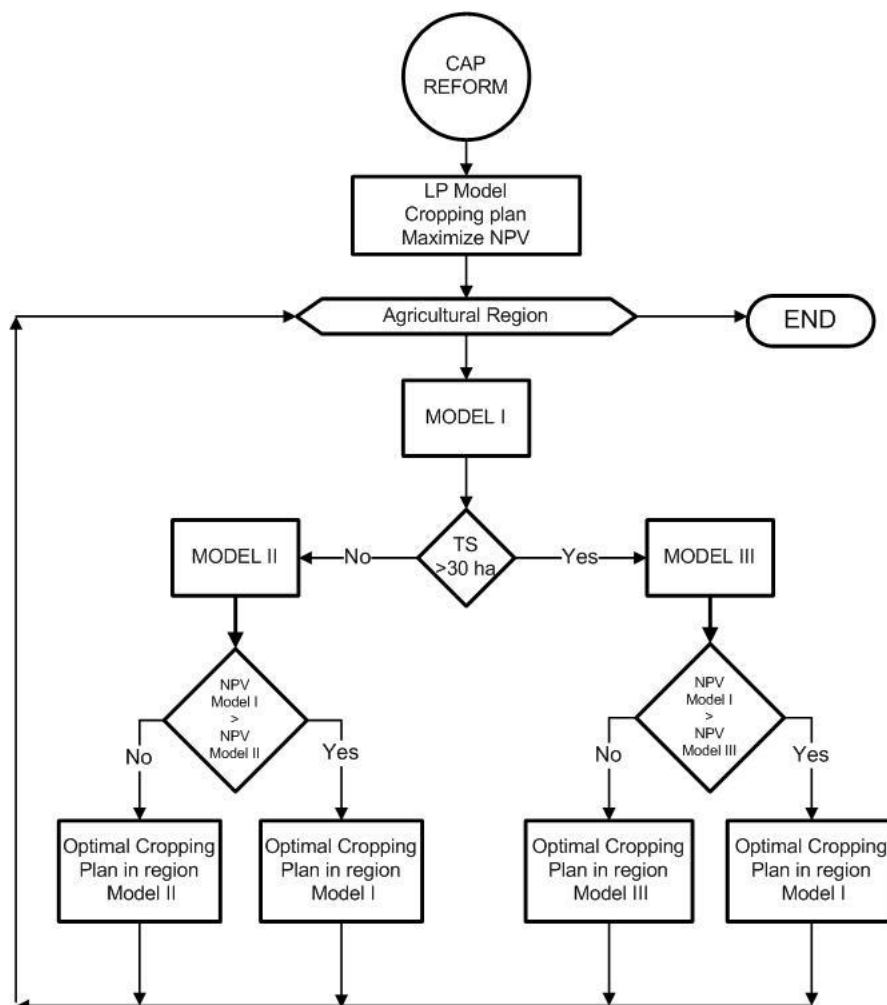


Figure III-3 Flow chart of the decision making process to determine the farmer's optimal cropping plan in each agricultural region during the CAP reform horizon.

We will assume that 6 rainfed crops can be planted each year and that there are no constraints to crop conversion and rotations. Note, however, that the approach presented herein is flexible enough to handle other crops shall they be more suitable according to the farmer's preferences. Table III-3 shows the rainfed crops considered and their selling price and exploitation cost. These crops have

been selected because they represent 70% of the total area dedicated to crops in Spain (MAGRAMA, 2014a). The price received by a farmer per tonne of crop ($\text{€}\cdot\text{t}^{-1}$) corresponds to the national average price from the period 1990 -2012 (MAGRAMA, 2014b), while the production cost for each crop ($\text{€}\cdot\text{ha}^{-1}$) correspond to the average value at the national level in 2011 (MAGRAMA, 2013).

Table III-3 Crops considered in the case study and selling prices and production costs per crop.

i	Crop	Price ($\text{€}\cdot\text{t}^{-1}$)	Cost ($\text{€}\cdot\text{ha}^{-1}$)
1	Wheat	230.1	604.1
2	Barley	194.8	598.1
3	Rye	181.5	377.6
4	Oat	183.6	585.7
5	Dried Pea	223.6	455.6
6	Sunflower	380.1	430.9

The price received by the farmer and the exploitation cost of the crops are capitalised each year during the planning period via Eq. III-12 and Eq. III-13 by recursively updating the current price and cost of the corresponding crop (P_i and C_i , respectively) at an inflation rate (i.e. consumer price index) r (%).

$$P_{it} = P_i(1 + r)^t \quad \forall i, t \quad \text{Eq. III-12}$$

$$C_{it} = C_i(1 + r)^t \quad \forall i, t \quad \text{Eq. III-13}$$

We consider a discount rate of 5% to update the net return in each year during the CAP horizon (parameter ta in Eq. III-1) and a yearly increase inflation rate of 4% for the crop prices and exploitation cost (r in Eq. III-12 and Eq. III-13), which corresponds to the average consumer price index for agriculture in the period 2004-2014 (INE, 2014).

The crop yields (i.e. productivity expressed in $t\cdot ha^{-1}$) were obtained from the Agricultural Statistics Yearbooks (MAGRAMA, 2014b), using the average nominal values in each province (administrative division) of Spain from the period 1997-2012. Then, these data were aggregated at the agricultural region level by considering surface ratios. Table III-4 shows the crop yield in each agricultural region fed as parameters in the LP model.

Table III-4 Crop yield in each agricultural region expressed in tonnes per hectare ($t\cdot ha^{-1}$).

<i>Agricultural Regions</i>	Wheat	Barley	Rye	Oat	Dried Pea	Sunflower
2	2.396	2.334	1.468	1.642	0.811	0.774
3	2.178	2.199	1.300	1.699	0.828	0.710
4	2.132	2.161	1.319	1.562	0.833	0.739
5	2.542	2.407	1.560	1.683	0.986	0.863
6	2.272	2.303	1.609	1.709	1.060	0.882
7	2.991	2.438	1.852	2.259	1.209	1.202
8	3.316	2.993	2.350	2.403	1.147	0.920
9	2.515	2.278	1.043	2.192	1.063	1.136
10	2.255	2.373	0.530	2.372	0.842	1.024
11	1.985	1.879	0.854	1.608	0.792	0.949
12	2.744	2.479	1.643	1.918	0.596	0.414
13	3.395	2.754	2.792	2.001	1.227	1.066
14	3.136	2.558	1.918	2.026	0.355	0.140
15	3.117	3.031	1.597	3.232	1.234	1.159
19	2.593	1.676	1.931	1.509	1.043	1.399
20	5.184	4.924	3.947	4.850	3.073	1.875

Regarding the application of the new basic payment scheme, the Spanish Ministry of Agriculture, Food and Environment has defined a regionalisation model of the subsidies by defining 50 agricultural regions with similar agronomic and

socio-economic characteristics as well as similar agricultural potential. Further details on this topic can be found in Annex II of BOE (2014b). We consider 16 agricultural regions which correspond to the Spanish regions where rainfed crops are cultivated. These regions are geographically shown in the map in Figure III-4. Note that the LP model developed in Section 3.3 will be solved for all agricultural regions since presumably similar cropping plans will be implemented in areas entailing similar agronomic and socio-economic characteristics.

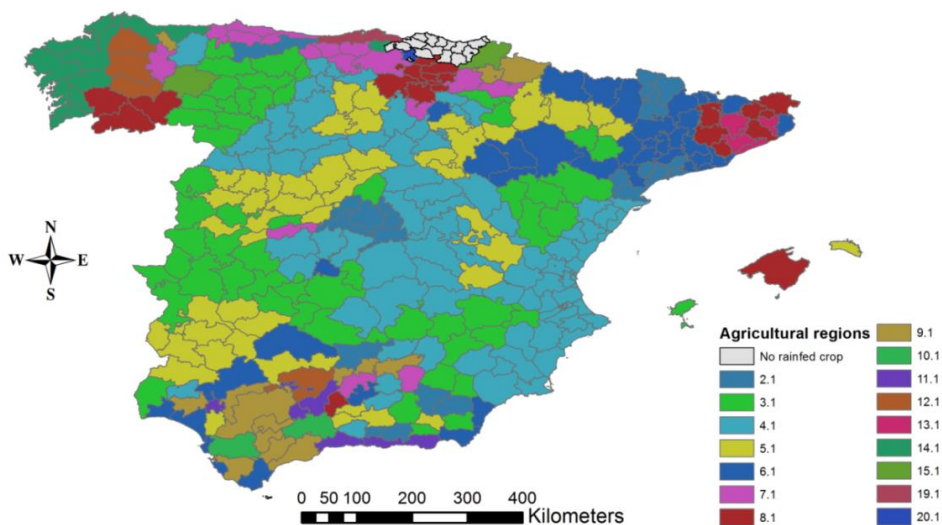


Figure III-4 Agricultural regions for rainfed crops in Spain.

In this regionalised model, the basic payment consists of a fixed subsidy per hectare which is specific for each agricultural region and type of crop (rainfed crops, irrigated crops, livestock and permanent crops). As a general rule, the initial value of the rights of basic payment will be performed by applying a fixed percentage to the amount that the farmer has received in 2014 (BOE, 2014b) and the average value of the basic payment per type of crop in each region will be published at some point during 2015. Due to lack of published data at the time of realisation of this study, here we estimate the average value of the right of basic payment by means of the same methodology that was used to compute the analogue quantities in the previous legislation (i.e. the single payment scheme). Following the derogated

Spanish legislation on the application of the single payment (BOE, 2005, 2004), the average basic payment values are estimated via Eq. III-14.

$$BP_i = Aid_{decoupled} \cdot Percen_{decoupled} \cdot Yield_i + Aid_{coupled} \cdot Yield_i \quad \forall i \quad \text{Eq. III-14}$$

where BP_i denotes the specific basic payment per crop i in agricultural region ($\text{€}\cdot\text{ha}^{-1}$). $Aid_{decoupled}$ represents the direct aid per hectare (i.e. $63\text{€}\cdot\text{t}^{-1}$ for cereals). $Percen_{decoupled}$ is the aid percentage decoupled from the production (i.e. 75% for cereals). $Aid_{coupled}$ represents the direct aid coupled with the production (i.e. $15.75\text{€}\cdot\text{t}^{-1}$ for cereals). $Yield_i$ represents the yield ($\text{t}\cdot\text{ha}^{-1}$) for the crop i in a region (Table III-4). The average value of the basic payment parameter for each crop in each region determined using Eq. III-14 is shown in the next Table III-5. The estimated basic payment for dried peas ($181 \text{€}\cdot\text{ha}^{-1}$) corresponds to the direct payment for legumes according to the derogated Spanish legislation (BOE, 2005, 2004) which assumed to be the same for all agricultural regions.

Table III-5 Basic payment for rainfed crops in each agricultural region ($\text{€}\cdot\text{ha}^{-1}$).

<i>Agricultural regions</i>	Wheat	Barley	Rye	Oat	Dried Pea	Sunflower
2	150.96	147.05	92.46	103.45	181.00	48.73
3	137.24	138.51	81.92	107.06	181.00	44.71
4	134.33	136.16	83.02	98.40	181.00	46.58
5	160.17	151.62	98.26	106.03	181.00	54.39
6	143.16	145.06	101.35	107.68	181.00	55.57
7	188.44	153.57	116.66	142.28	181.00	75.74
8	208.93	188.56	148.03	151.40	181.00	57.97
9	158.43	143.49	65.68	138.06	181.00	71.56
10	142.07	149.51	33.38	149.41	181.00	64.53
11	125.08	118.38	53.78	101.33	181.00	59.80
12	172.90	156.18	103.53	120.84	181.00	26.10

13	213.89	173.50	175.89	126.06	181.00	63.37
14	197.59	161.16	120.85	127.66	181.00	8.83
15	196.34	190.97	100.62	203.62	181.00	73.04
19	163.36	105.61	121.66	95.07	181.00	88.12
20	326.62	310.20	248.63	305.54	181.00	118.11

The "Greening Payment" parameter (i.e. GP_i) is defined as a percentage of the total value of the rights of basic payment that the farmer activates each year. This percentage, slightly above 50%, will be determined annually and published on the website of the Spanish Agrarian Guarantee Fund of the Ministry of Agricultural, Food and Environment (Spanish Ministry of Agricultural Food and Environment, 2015). Due to the lack of this data at the time of performing this study, for the calculations we assumed that this value will be 51.8% of the basic payment.

3.5 Results and discussion

The multi-stage LP model presented in Section 3.3 was implemented in the General Algebraic Modelling System (GAMS) (Brooke et al., 1998) software version 24.2.1 and was solved with the CPLEX 12.6.0.0 solver using an AMD A8-5500 APU with Raedon 3.20 Ghz and 8.0 GB RAM. The LP *Model I* features 36 continuous variables and 41 equations, whereas *Model II* and *Model III* contain 46 continuous variables and 225 equations, respectively. The solution time varied depending on the instance being solved, but was always within the range 8 to 9 CPU seconds in the aforementioned computer.

The solution of the LP model for each scenario in each agricultural region is given by an optimal cropping plan that maximises the farmer's net return per hectare in the CAP reform horizon. The optimal cropping plan in all the agricultural regions when the greening rules are not fulfilled consists of growing wheat every year in all the arable land except for regions 11 and 19, which grow sunflower. The optimal cropping plans fulfilling the greening rules are provided in detail in the

Appendix (Figure III-A1 and Figure III-A2), whereas the resulting net returns per hectare in each agricultural region for each scenario are shown in Table III-6.

As observed in Table III-6, the farmer's net economic return varies greatly between regions, even when the same strategy (I, II and III) is followed. The new basic payment scheme introduced by the CAP reform might not be equitable, since it might benefit certain agricultural regions with high productivity, whereas many regions that are more dependent on supports might receive only a small share of the basic payment. Furthermore, in all the agricultural regions, the farmers' net return in Model II is larger than in Model III. This is because in arable lands above 30 ha it is mandatory to grow an additional third crop that is less profitable than the two others selected by the model. This suggests that setting specific subsidy values for each scenario would result in a more equitable situation.

Table III-6 Optimal farmer's net present value per hectare ($\text{€}\cdot\text{ha}^{-1}$) in each agricultural region for each case scenario. The best strategy for the farmer is highlighted in bold.

<i>Agricultural regions</i>	Model I	Model II	Model III
2	434.33	496.55	487.38
3	128.15	252.86	244.62
4	63.23	196.00	191.38
5	639.82	651.08	642.82
6	260.16	387.08	386.22
7	1270.84	1119.10	1115.00
8	1728.23	1582.31	1580.59
9	601.11	676.33	662.71
10	235.87	400.48	397.59
11	-47.20	91.63	81.99
12	924.06	851.29	843.46
13	1839.06	1851.77	1810.15

14	1475.24	1235.44	1232.22
15	1447.33	1478.73	1471.96
19	921.92	964.45	947.27
20	4355.09	4033.73	4019.85

The highest net return for the farmer in each agricultural region, highlighted in bold in Table III-6, represents the best possible strategy that could be implemented. As can be observed, there are some agricultural regions where the farmer's net return per hectare is bigger in Model I compared to Model II and Model III. This implies that the best strategy consists of not complying with the greening rules (and therefore not receiving the corresponding greening payment). This is the case of farmers owning an arable land between 10 ha and 30 ha in regions 7, 8, 12, 14 and 20, and for farmers owning an arable land bigger than 30 ha in regions 7, 8, 12, 13, 14 and 20. These regions are therefore not moving toward agricultural practises beneficial for the climate and the environment so that the main goal of the CAP reform will be threatened and might not be achieved.

In all these regions (where the best strategy consists of not fulfilling the greening rules) the optimal cropping plan consists of growing wheat every year in all the arable land, as illustrated in Figure III-5. However, this agricultural practice of cropping a single crop year after year on the same land (i.e. mono-cropping) might lead to major shortcomings. Particularly, it might decline yields and might lead as well to the appearance of some diseases, among other drawbacks.

Conversely, in the regions where the farmer's economic net return per hectare is bigger in Model II and/or Model III than in Model I, the best strategy consists of fulfilling the greening rules and therefore the farmer would receive the compensation for the sustainable practises. This is for instance the case in Region 3, in which complying with the greening rules would increase the profit in 124.71€ per ha (for an arable land between 10 ha and 30 ha) and in 116.47€ per ha (arable land

above 30 ha). The optimal cropping plans in Region 3 for scenario II and scenario III are shown in Figure III-6 and Figure III-7, respectively. In these figures, the surfaces occupied are expressed as a percentage of the total surface of arable land

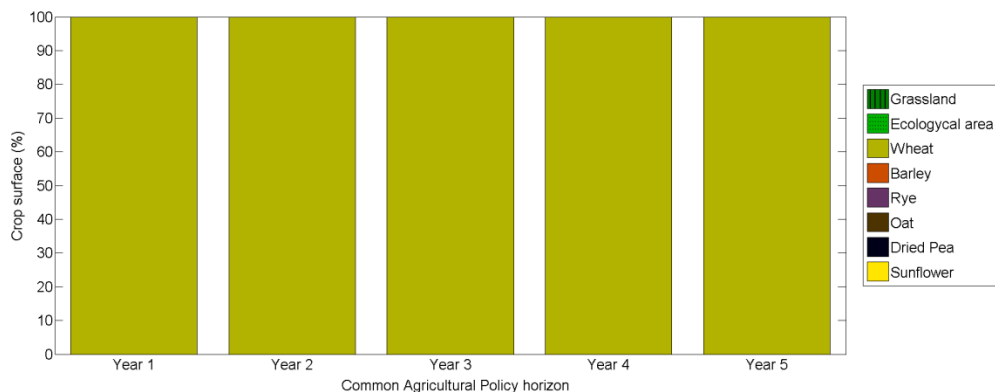


Figure III-5 Optimal cropping plan in agricultural regions without fulfilling the greening rules (those for which Model I provides the maximum NPV).

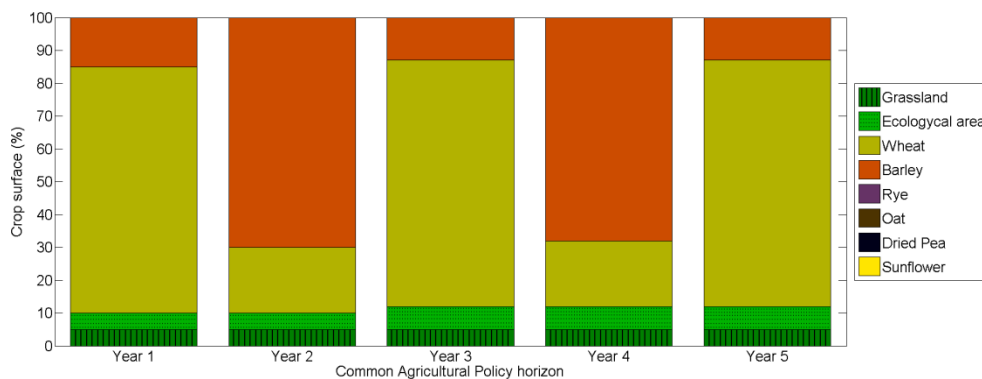


Figure III-6 Optimal cropping plan in Region 3 for arable land between 10 ha and 30 ha.

As observed in Figure III-6, in the cropping plan that maximises the farmer's economic net return, 5% of the total arable land is permanent grassland and 5% ecological focus area (note that the latter percentage is increased to 7% from the third year onwards). The crops selected to be cultivated are wheat and barley. Wheat occupies 75%, 20%, 75%, 20% and 75% of the total arable land each year

during the CAP reform horizon, whereas barley is cultivated in 15%, 70%, 13%, 68% and 13% of the total arable land. This optimal solution allows making crop rotations over the total arable land by growing different crops selected in the same area during sequential seasons (each one at a time). Note that this crop rotation can only be achieved if ecological focus areas are allocated to different surfaces of land in consecutive years. For instance, wheat can only be cultivated in 20% of the arable land in the second year, if all arable land dedicated to other crops in the previous year (15% cultivated with barley and 5% of ecological focus area) is now cultivated with wheat. Crop rotations on the arable land constitute an appropriate farm land management to improve the sustainability of agriculture. This strategy benefits in turn the producer, since it increases crop yields by increasing nitrogen supply, soil organic matter and water availability. In addition, it improves soil conditions and reduces pest, diseases and weed competition (Castellazzi et al., 2008).

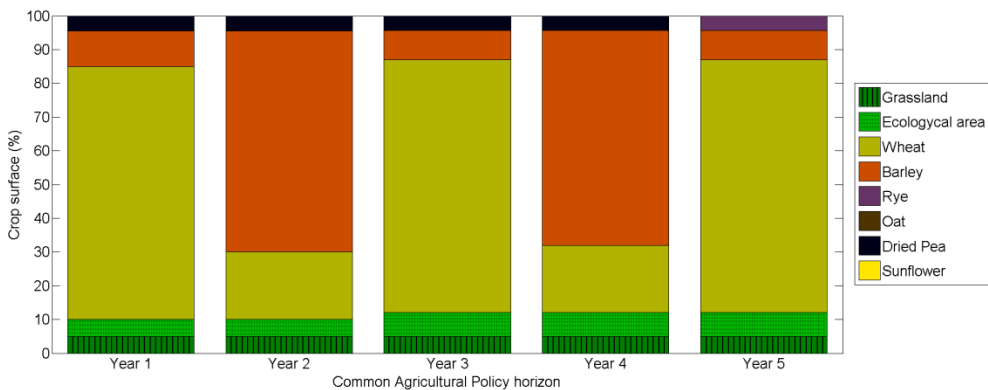


Figure III-7 Optimal cropping plan in Region 3 for arable land bigger than 30 ha.

Figure III-7 shows the cropping plan in region 3, which maximises the farmer's economic net return for arable land bigger than 30 ha. Again, the surface reserved to permanent grassland is 5% of the total arable land during the policy horizon, whereas the ecological focus area is 5% during the first two years and 7% during the latest three. Now, three different crops are selected to be grown each year during the CAP reform horizon. Wheat is grown in 75%, 20%, 75%, 20% and 75% of the

arable land each year; barley is cultivated in 10.5%, 65.5%, 8.6%, 63.6% and 8.6%; whereas dried pea is grown the first four years in 4.5%, 4.5%, 4.4% and 4.4% of the arable land; and rye in 4.4% of the arable land the last year. Recall that this solution also requires ecological focus areas to be allocated in different portions of land in consecutive years in order to ensure crops rotation.

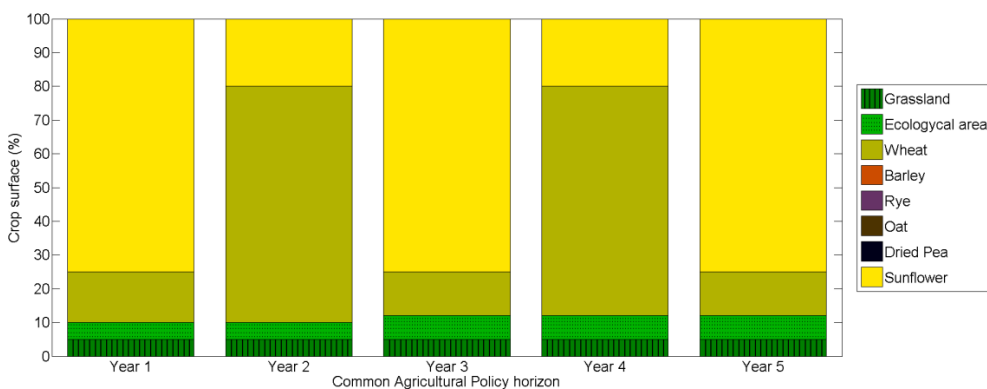


Figure III-8 Optimal cropping plan in Region 19 for arable land between 10 ha and 30 ha.

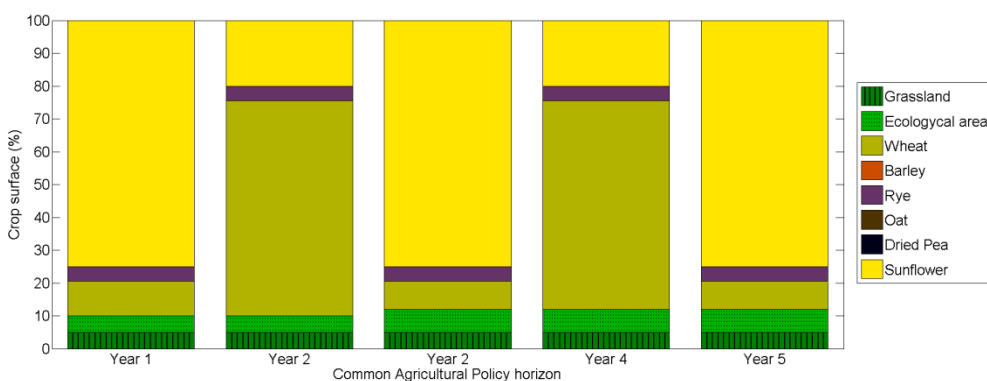


Figure III-9 Optimal cropping plan in Region 19 for arable land bigger than 30 ha.

The whole set of optimal cropping plans for each agricultural region are provided in the Appendix in Table III A1 and Table III A2. The optimal cropping plans tend to involve different crops in every region as do the climate and agronomic conditions. As an example, Figure III-8 and Figure III-9 show the plans in region 19

for cases II and III, respectively. These cropping plans involve sunflower, wheat and rye, whereas the optimal cropping plans in region 3 (Figure III-6 and Figure III-7) relay on barley and wheat. The fact that each agricultural region presents particular optimal cropping plans involving different crops and different acreages reserved to them reveals the importance of assisting farmers in making the new decisions facing the CAP reform.

3.6 Basic value payment adjusted: effective subsidy

As previously discussed, there are certain agricultural regions in which the best strategy to maximise the farmer's benefit consists of not fulfilling the greening rules and therefore not receiving the greening additional payment. This finding highlights that the main goal of the CAP reform (i.e. the broad applicability of the sustainable practises) might be threatened. Furthermore, the farmers' net return varies greatly from one region to another and therefore the more equitable distribution of the income support might also fail.

To overcome these limitations, it could be possible to establish an adequate basic payment for each region to encourage all farmers to meet the greening rules and to ensure the more equitable distribution. The establishment of an appropriate payment value is hence essential to ensure the widespread adoption of more sustainable agricultural patterns. The initial value of the right of basic payment specific to each Spanish region has not been published yet. Hence, an analysis of the optimal values that should be defined in each region in order to attain the environmental targets sought would be very useful for policy makers.

This minimum value of the subsidy that would encourage all farmers to fulfill the greening rules in all the agricultural regions can be obtained by slightly modifying the mathematical model proposed in this manuscript in section 3.3. The basic idea is that the subsidy identified by the model should be large enough to compensate for the losses derived from the implementation of the greening rules imposed by the CAP reform policy.

First, the net present value originally defined as a variable, should be now redefined as a parameter equal to the values obtained previously in each region with Model I, that is, to the net present value obtained when the greening rules were not met (see Table III-6). On the contrary, the basic payment in each region, which was originally treated as a parameter, must now be redefined as a continuous variable. The, a bilinear term appear in the model and therefore the modified model takes the form of a non-linear programming formulation (NLP) that allows providing as output the minimum basic payment per hectare in each agricultural region that makes the net present value equal to the one obtained when the greening rules are not met. Unfortunately, this model is non convex, which means that standard software packages might get trapped in local optima during the search. To avoid this, a global optimisation package is used to guarantee convergence to the global optimum within an epsilon tolerance in a finite number of iterations. Note that the solution of the NLP could also be obtained by solving the original LP model iteratively for different values of the subsidy and then selecting as final value the one that makes the objective function equal to the net present value of Model I.

The NLP model obtained was implemented in the General Algebraic Modeling System (GAMS) software version 24.2.1 and solved with BARON version 12.7.3 solver (Tawarmalani and Sahinidis, 2005) using an AMD A8-5500 APU with Raedon 3.20 Ghz and 8.0 GB RAM. The NLP model for strategy II features 47 continuous variables and 76 equations and the solution time ranges between 26 and 29 CPU seconds. For strategy III, the NLP model features 47 continuous variables and 226 equations and the solution time varies within the range 30 to 36 CPU seconds in the aforementioned computer.

Table III-7 Minimum subsidy ($\text{€}\cdot\text{ha}^{-1}$) for each agricultural region to encourage farmers to meet the greening requirements.

<i>Agricultural regions</i>	Model II	Model III
2	104.35	121.22
3	90.30	100.62
4	83.69	91.82
5	112.47	135.08
6	85.95	96.82
7	116.95	161.58
8	139.59	198.03
9	96.44	104.22
10	97.38	75.99
11	104.35	49.99
12	125.99	158.32
13	123.35	189.75
14	146.30	197.11
15	132.12	179.72
19	129.72	102.99
20	213.08	352.20

The minimum subsidy per hectare in each agricultural region that would encourage all farmers to implement the greening requirements are shown in Table III-7. Note that there is just one basic payment value proposed in each agricultural region. This is because all of the crops considered in the case study are rainfed crops and therefore they present the same basic payment. The subsidy values for these rainfed crops should compensate for the loss of income resulting from the implementation of greening rules. Therefore, higher values than the proposed ones would ensure the adoption of greening strategies beneficial for the climate and the

environment. As observed, the minimum basic payment to encourage all farmers to fulfil the greening rules differs significantly from one region to another. For instance, in region 11 the minimum basic payment should be above $49.99 \text{ €}\cdot\text{ha}^{-1}$, whereas in region 20 it should be higher than $352.20 \text{ €}\cdot\text{ha}^{-1}$. These results reveal that there are regions with higher agricultural potential requiring lower subsidy to be economically profitable and to achieve a more equitable distribution of the CAP's payments.

3.7 Conclusions

The new CAP offers incentives for farmers to modify their cropping plan at the farm level in order to receive the greening payment. The objective of this CAP reform is twofold; to spur the broad implementation of agricultural practises beneficial for the climate and the environment and to distribute the payments in a more equitable manner. This work introduced a multi-stage LP model that identifies the cropping plan that maximises the net return over a given time horizon. Our model provides decision support for cropping planning considering the new CAP reform greening requirements.

The capabilities of our tool were tested through its application to the regionalised agricultural model of Spain. The optimal cropping plan for each agricultural region in Spain was obtained maximising the farmer's net return. Results show that each region optimises its profit by implementing particular cropping plans entailing different crops and acreages reserved to them. We find that the establishment of an adequate basic payment value is essential to ensure an equitable distribution among farmers since the farmer's profit varies greatly from one region to another. Furthermore, several regions may not fulfill the CAP greening rules because the economic incentive is too small to compensate farmers for the loss in profit they incur from the implementation of the greening requirements. For each of them, a minimum subsidy value was determined that makes the greening measures economically appealing. These values vary from one

region to another, which suggests that specific subsidies should be defined for each separate region in order to ensure a more effective transition towards agricultural practises beneficial for the world's climate and environment.

3.8 Acknowledgements

The authors wish to acknowledge the financial support of this research work from the Spanish Ministry of Education and Science (Projects CTQ2012-37039-C02, DPI2012-37154-C02-02)

3.9 References

Bartolini, F., Bazzani, G.M., Gallerani, V., Raggi, M., Viaggi, D., 2007. The impact of water and agriculture policy scenarios on irrigated farming systems in Italy: An analysis based on farm level multi-attribute linear programming models. *Agric. Syst.* 93, 90–114. doi:10.1016/j.agsy.2006.04.006

BOE, 2004. Royal Decree 2352/2004, of 23 December, regarding the implementation of cross compliance as regards direct support within the common agricultural policy framework. *Boletín Oficial del Estado* No. 309, 24/12/2004. [In Spanish].

BOE, 2005. Royal Decree 1618/2005, of 30 December, on implementation of the single payment scheme and other direct support on agriculture and livestock farming. *Boletín Oficial del Estado* No. 313, 31/12/2005. [In Spanish].

BOE, 2014a. Royal Decree 1075/2014, of 19 December, on implementation from 2015 of direct payments to agriculture and livestock and other aid schemes, as well as on the management and control of direct payments and payments to rural development.

BOE, 2014b. Royal Decree 1076/2014, of 19 December, on the assignment of rights basic payment scheme of the Common Agricultural Policy.

Brooke, A., Kendrick, D., Meeraus, A., Raman, R., 1998. GAMS—A User's Manual. GAMS Development Corporation, Washington, DC.

Butterworth, K., 1985. PRACTICAL APPLICATION OF LINEAR/INTEGER PROGRAMMING IN AGRICULTURE. *J. Oper. Res. Soc.* 36, 99–107.

Castellazzi, M.S., Wood, G.A., Burgess, P.J., Morris, J., Conrad, K.F., Perry, J.N., 2008. A systematic representation of crop rotations. *Agric. Syst.* 97, 26–33. doi:10.1016/j.agry.2007.10.006

Dogliotti, S., van Ittersum, M.K., Rossing, W.A.H., 2006. Influence of farm resource endowment on possibilities for sustainable development: a case study for vegetable farms in South Uruguay. *J. Environ. Manage.* 78, 305–15. doi:10.1016/j.jenvman.2005.04.025

Dury, J., Schaller, N., Garcia, F., Reynaud, A., Bergez, J.E., 2011. Models to support cropping plan and crop rotation decisions. A review. *Agron. Sustain. Dev.* 32, 567–580. doi:10.1007/s13593-011-0037-x

European Commission, 2011. Proposal for a Regulation of the European Parliament and of the Council Establishing Rules for Direct Payments to Farmers Under Support Schemes Within the Framework of the Common Agricultural Policy, COM(2011) 627 Final/2.

European Parliament and European Council, 2013. REGULATION (EU) No 1307/2013 OF THE EUROPEAN PARLIAMENT AND OF THE COUNCIL of 17 december 2013 establishing rules for direct payments to farmers under support schemes within the framework of the common agricultural policy and repealing Council Regulation Of. *J. Eur. Union* 56, 487–548.

INE, 2014. Instituto Nacional de Estadística. Índice de precios de consumo armonizado. [WWW Document]. URL <http://www.ine.es/jaxiT3/Datos.htm?t=2529> (accessed 10.3.14).

Janová, J., 2011. The dynamic programming approach to long term production planning in agriculture. *Acta Univ. Agric. Silvic. Mendelianae Brun.* 59, 129–136.

Kennedy, J.O.S., 1986. *Dynamic Programming Applications to Agriculture and Natural Resources*, 1st ed. ed. Springer Netherlands, Dordrecht.

Louhichi, K., Kanellopoulos, A., Janssen, S., Flichman, G., Blanco, M., Hengsdijk, H., Heckelei, T., Berentsen, P., Lansink, A.O., Ittersum, M. Van, 2010. FSSIM, a bio-economic farm model for simulating the response of EU farming systems to agricultural and environmental policies. *Agric. Syst.* 103, 585–597. doi:10.1016/j.agsy.2010.06.006

MAGRAMA, 2013. Resultados técnico-económicos de Cultivos Hortícolas 2011. Subdirección General de Análisis, Prospectiva y Coordinación, Subsecretaría. Ministerio de Agricultura, Alimentación y Medio Ambiente.

MAGRAMA, 2014a. Spanish Survey of Surfaces and Crop Yields (ESYRCE). Spanish Ministry of Agriculture, Food and the Environment.

MAGRAMA, 2014b. Agriculture Statistics [WWW Document]. URL <http://www.magrama.gob.es/es/estadistica/temas/estadisticas-agrarias/agricultura/> (accessed 10.14.14).

Nevo, A., Oad, R., Podmore, T.H., 1994. An integrated expert system for optimal crop planning. *Agric. Syst.* 45, 73–92. doi:10.1016/S0308-521X(94)90281-X

Oñate, J.J., Atance, I., Bardají, I., Llusia, D., 2007. Modelling the effects of alternative CAP policies for the Spanish high-nature value cereal-steppe farming systems. *Agric. Syst.* 94, 247–260. doi:10.1016/j.agsy.2006.09.003

Parsons, D.J., Benjamin, L.R., Clarke, J., Ginsburg, D., Mayes, A., Milne, A.E., Wilkinson, D.J., 2009. *Weed Manager—A model-based decision support system for*

weed management in arable crops. *Comput. Electron. Agric.* 65, 155–167.
doi:10.1016/j.compag.2008.08.007

Sánchez-Girón, V., Serrano, A., Suárez, M., Hernanz, J.L., Navarrete, L., 2007. Economics of reduced tillage for cereal and legume production on rainfed farm enterprises of different sizes in semiarid conditions. *Soil Tillage Res.* 95, 149–160.
doi:10.1016/j.still.2006.12.007

Sarker, R., Ray, T., 2009. An improved evolutionary algorithm for solving multi-objective crop planning models. *Comput. Electron. Agric.* 68, 191–199.
doi:10.1016/j.compag.2009.06.002

Sarttra, T., Manokuakoon, S., Horadee, S., Choosakulwong, K., 2013. Application of dynamic programming to agricultural land allocation: Case study phutthamonthon district, nakhon pathom province, Thailand, in: *Lecture Notes in Engineering and Computer Science*. pp. 893–897.

Spanish Ministry of Agricultural Food and Environment, 2015. Spanish Agrarian Guarantee Fund [WWW Document]. URL <http://www.fega.es/> (accessed 1.20.15).

Tawarmalani, M., Sahinidis, N. V., 2005. A polyhedral branch-and-cut approach to global optimization. *Math. Program.* 103, 225–249.
doi:10.1007/s10107-005-0581-8

3.10 Appendix: optimal cropping plan for the Spanish agricultural regions

The multi-stage LP model developed allows obtaining the optimal cropping plan for a rainfed farm in each region during the CAP reform horizon which maximises the farmer's economic net return.

Table III-A1 and Table III-A1 show the optimal cropping plan in each region for farms smaller a bigger than 30 ha respectively fulfilling the CAP greening rules and therefore the farmer is rewarded with the greening payment. In these tables crop acreages are expressed as percentage of the total surface of the arable land.

Table III A1 Optimal cropping plan in each agricultural region for an arable land between 10 ha and 30 ha fulfilling the greening rules (Model II).

<i>Region/planning</i>		Perm. Grass.	Eco. area	Wheat	Barley	Rye	Oat	Dry Pea	Sunflower
2	Year 1	5	5	75	15	-	-	-	-
	Year 2	5	5	20	70	-	-	-	-
	Year 3	5	7	75	13	-	-	-	-
	Year 4	5	7	20	68	-	-	-	-
	Year 5	5	7	75	13	-	-	-	-
3	Year 1	5	5	75	15	-	-	-	-
	Year 2	5	5	20	70	-	-	-	-
	Year 3	5	7	75	13	-	-	-	-
	Year 4	5	7	20	68	-	-	-	-
	Year 5	5	7	75	13	-	-	-	-
4	Year 1	5	5	75	15	-	-	-	-
	Year 2	5	5	20	70	-	-	-	-
	Year 3	5	7	75	13	-	-	-	-
	Year 4	5	7	20	68	-	-	-	-

	Year 5	5	7	75	13	-	-	-	-
5	Year 1	5	5	75	15	-	-	-	-
	Year 2	5	5	20	70	-	-	-	-
	Year 3	5	7	75	13	-	-	-	-
	Year 4	5	7	20	68	-	-	-	-
	Year 5	5	7	75	13	-	-	-	-
6	Year 1	5	5	75	-	15	-	-	-
	Year 2	5	5	20	-	70	-	-	-
	Year 3	5	7	75	-	13	-	-	-
	Year 4	5	7	20	-	68	-	-	-
	Year 5	5	7	75	-	13	-	-	-
7	Year 1	5	5	75	-	-	-	-	15
	Year 2	5	5	20	-	-	-	-	70
	Year 3	5	7	75	-	-	-	-	13
	Year 4	5	7	20	-	-	-	-	68
	Year 5	5	7	75	-	-	-	-	13
8	Year 1	5	5	75	-	15	-	-	-
	Year 2	5	5	20	-	70	-	-	-
	Year 3	5	7	75	-	13	-	-	-
	Year 4	5	7	20	-	68	-	-	-
	Year 5	5	7	75	-	13	-	-	-
9	Year 1	5	5	75	-	-	-	-	15
	Year 2	5	5	20	-	-	-	-	70
	Year 3	5	7	75	-	-	-	-	13
	Year 4	5	7	20	-	-	-	-	68
	Year 5	5	7	75	-	-	-	-	13
10	Year 1	5	5	75	15	-	-	-	-

	Year 2	5	5	20	70	-	-	-	-
	Year 3	5	7	75	13	-	-	-	-
	Year 4	5	7	20	68	-	-	-	-
	Year 5	5	7	75	13	-	-	-	-
11	Year 1	5	5	75	-	-	-	-	15
	Year 2	5	5	20	-	-	-	-	70
	Year 3	5	7	75	-	-	-	-	13
	Year 4	5	7	20	-	-	-	-	68
	Year 5	5	7	75	-	-	-	-	13
12	Year 1	5	5	75	15	-	-	-	-
	Year 2	5	5	20	70	-	-	-	-
	Year 3	5	7	75	13	-	-	-	-
	Year 4	5	7	20	68	-	-	-	-
	Year 5	5	7	75	13	-	-	-	-
13	Year 1	5	5	75	-	15	-	-	-
	Year 2	5	5	20	-	70	-	-	-
	Year 3	5	7	75	-	13	-	-	-
	Year 4	5	7	20	-	68	-	-	-
	Year 5	5	7	75	-	13	-	-	-
14	Year 1	5	5	75	-	15	-	-	-
	Year 2	5	5	20	-	70	-	-	-
	Year 3	5	7	75	-	13	-	-	-
	Year 4	5	7	20	-	68	-	-	-
	Year 5	5	7	75	-	13	-	-	-
15	Year 1	5	5	75	-	-	15	-	-
	Year 2	5	5	20	-	-	70	-	-
	Year 3	5	7	75	-	-	13	-	-

	Year 4	5	7	20	-	-	68	-	-
	Year 5	5	7	100	-	-	13	-	-
19	Year 1	5	5	15	-	-	-	-	75
	Year 2	5	5	70	-	-	-	-	20
	Year 3	5	7	13	-	-	-	-	75
	Year 4	5	7	68	-	-	-	-	20
	Year 5	5	7	13	-	-	-	-	75
20	Year 1	5	5	75	15	-	-	-	-
	Year 2	5	5	20	70	-	-	-	-
	Year 3	5	7	75	13	-	-	-	-
	Year 4	5	7	20	68	-	-	-	-
	Year 5	5	7	75	13	-	-	-	-

Table III A2 Optimal cropping plan in each agricultural region for an arable land between 10 ha and 30 ha fulfilling the greening rules (Model II).

<i>Region/planning</i>		Perm. Grass.	Eco. area	Wheat	Barley	Rye	Oat	Dry Pea	Sunflower
2	Year 1	5	5	75	10.5	4.5	-	-	-
	Year 2	5	5	20	65.5	4.5	-	-	-
	Year 3	5	7	75	8.6	4.4	-	-	-
	Year 4	5	7	20	63.6	4.4	-	-	-
	Year 5	5	7	75	8.6	4.4	-	-	-
3	Year 1	5	5	75	10.5	-	-	4.5	-
	Year 2	5	5	20	65.5	-	-	4.5	-
	Year 3	5	7	75	8.6	-	-	4.4	-
	Year 4	5	7	20	63.6	-	-	4.4	-
	Year 5	5	7	75	8.6	4.4	-	-	-

4	Year 1	5	5	75	10.5	-	-	4.5	-
	Year 2	5	5	20	65.5	-	-	4.5	-
	Year 3	5	7	75	8.6	-	-	4.4	-
	Year 4	5	7	20	63.6	-	-	4.4	-
	Year 5	5	7	75	8.6	4.4	-	0	-
5	Year 1	5	5	75	10.5	4.5	-	-	-
	Year 2	5	5	20	65.5	4.5	-	-	-
	Year 3	5	7	75	8.6	4.4	-	-	-
	Year 4	5	7	20	63.6	4.4	-	-	-
	Year 5	5	7	75	8.6	4.4	-	-	-
6	Year 1	5	5	75	4.5	10.5	-	-	-
	Year 2	5	5	20	4.5	65.5	-	-	-
	Year 3	5	7	75	4.4	8.6	-	-	-
	Year 4	5	7	20	4.4	63.6	-	-	-
	Year 5	5	7	75	4.4	8.6	-	-	-
7	Year 1	5	5	75	-	4.5	-	-	10.5
	Year 2	5	5	20	-	4.5	-	-	65.5
	Year 3	5	7	75	-	4.4	-	-	8.6
	Year 4	5	7	20	-	4.4	-	-	63.6
	Year 5	5	7	75	-	4.4	-	-	8.6
8	Year 1	5	5	75	4.5	10.5	-	-	-
	Year 2	5	5	20	4.5	65.5	-	-	-
	Year 3	5	7	75	4.4	8.6	-	-	-
	Year 4	5	7	20	4.4	63.6	-	-	-
	Year 5	5	7	75	4.4	8.6	-	-	-
9	Year 1	5	5	75	-	-	-	4.5	10.5
	Year 2	5	5	20	4.5	-	-	-	65.5

	Year 3	5	7	75	4.4	-	-	-	8.6
	Year 4	5	7	20	4.4	-	-	-	63.6
	Year 5	5	7	75	4.4	-	-	-	8.6
10	Year 1	5	5	75	10.5	-	4.5	-	-
	Year 2	5	5	20	65.5	-	4.5	-	-
	Year 3	5	7	75	8.6	-	4.4	-	-
	Year 4	5	7	20	63.6	-	-	-	4.4
	Year 5	5	7	75	8.6	-	-	-	4.4
11	Year 1	5	5	75	-	-	-	4.5	10.5
	Year 2	5	5	20	-	-	-	4.5	65.5
	Year 3	5	7	75	-	-	-	4.4	8.6
	Year 4	5	7	20	-	-	-	4.4	63.6
	Year 5	5	7	75	-	-	-	4.4	8.6
12	Year 1	5	5	75	10.5	4.5	-	-	-
	Year 2	5	5	20	65.5	4.5	-	-	-
	Year 3	5	7	75	8.6	4.4	-	-	-
	Year 4	5	7	20	63.6	4.4	-	-	-
	Year 5	5	7	75	8.6	4.4	-	-	-
13	Year 1	5	5	75	4.5	10.5	-	-	-
	Year 2	5	5	20	4.5	65.5	-	-	-
	Year 3	5	7	75	4.4	8.6	-	-	-
	Year 4	5	7	20	4.4	63.6	-	-	-
	Year 5	5	7	75	4.4	8.6	-	-	-
14	Year 1	5	5	75	4.5	10.5	-	-	-
	Year 2	5	5	20	4.5	65.5	-	-	-
	Year 3	5	7	75	4.4	8.6	-	-	-
	Year 4	5	7	20	4.4	63.6	-	-	-

	Year 5	5	7	75	4.4	8.6	-	-	-
15	Year 1	5	5	75	4.5	-	10.5	-	-
	Year 2	5	5	20	4.5	-	65.5	-	-
	Year 3	5	7	75	4.4	-	8.6	-	-
	Year 4	5	7	20	4.4	-	63.6	-	-
	Year 5	5	7	75	4.4	-	8.6	-	-
19	Year 1	5	5	10.5	-	4.5	-	-	75
	Year 2	5	5	65.5	-	4.5	-	-	20
	Year 3	5	7	8.6	-	4.4	-	-	75
	Year 4	5	7	63.6	-	4.4	-	-	20
	Year 5	5	7	8.6	-	4.4	-	-	75
20	Year 1	5	5	75	10.5	-	4.5	-	-
	Year 2	5	5	20	65.5	-	4.5	-	-
	Year 3	5	7	75	8.6	-	4.4	-	-
	Year 4	5	7	20	63.6	-	4.4	-	-
	Year 5	5	7	75	8.6	-	4.4	-	-

Chapter IV

DEA for sustainability assessment

UNIVERSITAT ROVIRA I VIRGLI

CONTRIBUTION TO THE DEVELOPMENT OF MATHEMATICAL PROGRAMMING TOOLS TO ASSIST DECISION-MAKING
IN SUSTAINABILITY PROBLEMS

Àngel Galán Martín



IV. DEA for sustainability assessment

Enhanced data envelopment analysis for sustainability assessment: A novel methodology and application to electricity technologies

Àngel Galán-Martín^a, Gonzalo Guillén-Gosálbez^{a,b*}, Laurence Stamford^c, Adisa

Azapagic^c

^a*Departament d'Enginyeria Química, Universitat Rovira i Virgili, Av. Paisos Catalans 26, 43007 Tarragona (Spain).*

^b*Centre for Process Systems Engineering, Imperial College London, SW7 2AZ London (United Kingdom).*

^c*School of Chemical Engineering and Analytical Science, The University of Manchester, Mill, Sackville Street, Manchester M13 9PL (United Kingdom).*

KEYWORDS: Enhanced data envelopment analysis; Order of efficiency; Sustainability efficiency; Life cycle sustainability assessment; Sustainability targets; Electricity generation.

4.1 Introduction

Sustainable development plays a key role in modern societies that seek “to meet the needs of the present without compromising the ability of future generations to meet their own needs” (WCED, 1987). Promoting sustainable development requires implementing concrete actions, projects, programs, plans and policies, which involve the simultaneous pursuit and satisfaction of economic, environmental, and social goals.

Setting sustainability goals and targets requires some knowledge and understanding of the current level of sustainability. This can be attained through sustainability assessments, by considering simultaneously all three ‘pillars of sustainability’ – economic, environmental and social (Azapagic and Perdan, 2000; Pope et al., 2004). A full characterisation and evaluation of a system in these dimensions requires, therefore, the definition of a wide range of economic, environmental and social indicators, thereby leading to complex multi-criteria decision-making problems. A possible way to simplify the assessment is to define an aggregated sustainability metric by expressing preferences and assigning the weights of importance to the economic, environmental and social indicators (Gerdessen and Pascucci, 2013; Martins et al., 2007; Sikdar, 2003). However, while this approach is easy to implement, it is plagued with difficulties at both the philosophical and conceptual levels. This includes the fact that in many cases the value judgements underlying the expression of preferences are incompletely formed or do not exist so that their articulation prior to understanding the trade-offs between different sustainability criteria could be misleading and/or meaningless. This could impede the deliberative process among different stakeholders, which is central to decision making: the discursive mediation of conflicting interests and rival perspectives represents a process whereby the decision can be delivered in an ethically acceptable way (Azapagic and Perdan, 2005). In addition, valuable information on the performance of a system in a particular dimension might be lost during aggregation which could rule out some good alternatives before the trade-offs have been understood and explored by decision-makers.

One of the aims of sustainability assessment is to identify measures to be optimised in order to minimise or avoid adverse impacts (Gibson, 2001). Most sustainability assessment approaches establish a ‘direction to target’(Pope et al., 2004), that is, whether or not a proposed measure in one direction represents a positive, neutral or negative contribution towards the sustainability target. This

approach is limited in scope, as it provides no quantitative guidelines on how to improve the level of sustainability. ‘Distance from target’ approaches are more effective in practice because they measure the extent of progress towards (or away from) sustainability, making it possible to define quantitative targets that ensure a more sustainable development (Jaeger et al., 2011). Furthermore, quantitative methods can be coupled with mathematical programming techniques to automate the search for alternatives with improved environmental performance (Grossmann and Guillén-Gosálbez, 2010).

This paper proposes a novel approach based on data envelopment analysis (DEA) to quantify the level of sustainability attained by a system and identify targets for improvements. DEA is a non-parametric linear programming (LP) technique that measures the efficiency of a set of entities, termed decision-making units (DMUs), each transforming multiple inputs into multiple outputs (Charnes et al., 1978). In addition to calculating the efficiency scores, DEA provides specific guidelines, expressed as quantitative targets, which can be used to improve the efficiency level, in this context related to the level of sustainability.

There has been a substantial body of research on methodological developments and applications of DEA, but these efforts have primarily focused on the assessment of DMUs in areas of science and engineering outside environmental science (Liu et al., 2013, 2015). More recently, DEA was combined with life cycle assessment (LCA) to assess the environmental efficiency of different systems (Hoang and Alauddin, 2011; Iribarren et al., 2013; Lorenzo-Toja et al., 2014; Mohammadi et al., 2014; Vázquez-Rowe and Iribarren, 2014). These studies, however, covered only environmental and economic aspects but disregarded the social dimension of sustainability. Other authors have used DEA to assess the overall level of sustainability, but aggregated the multidimensional metrics into a single indicator (Chang et al., 2013; Khodakarami et al., 2014; Reig-Martínez et al., 2011; Tajbakhsh and Hassini, 2014), an approach that exhibits the limitations of the

aggregation discussed earlier.

Despite its advantages, DEA shows two major limitations that are particularly critical when it is applied for sustainability assessment. First, it answers the question of whether a unit is efficient or not, but makes no distinction between the units deemed efficient (i.e. no ranking of efficient units is provided). Hence, since all the efficient units show the same efficiency score of 1, it is difficult to select a final alternative in the absence of a ranking scheme (Cook and Seiford, 2009). Secondly, efficiency scores are very sensitive to the number of inputs and outputs (i.e. the number of sustainability indicators in this context) as well as to the size of the sample (Bhagavath, 2006). For large sets of inputs and outputs with respect to the number of units, a case that is very likely in sustainability assessments, the lack of ranking leads to a poor discrimination in which many units can be regarded as efficient (Avkiran, 2002).

Improving the discriminatory power of standard DEA with no loss of information has become a major challenge that has attracted a significant research interest. Different approaches have been proposed to deal with the issue of ranking of DMUs in DEA (Adler et al., 2002; F. Hosseinzadeh Lotfi et al., 2013). One important method for ranking the DMUs is based on the cross-efficiency technique (Washio and Yamada, 2013; Wu et al., 2012; Zerafat Angiz et al., 2013), whereby the units are self- and peer-evaluated. Some authors have also used super-efficiency methods (Chen et al., 2011, 2013; Li et al., 2007), based on the idea of excluding the unit under evaluation to analyse the remaining units. Other methodologies are based on finding optimal common weights to discriminate among the units, usually based on value judgements (Jahanshahloo et al., 2005; Wang et al., 2011, 2009). Other ways to rank the units are through benchmarking methods and statistical techniques (Chen and Deng, 2011; Lu and Lo, 2009). Some researchers have combined DEA with multiple-criteria decision-making methodologies in which additional preferential information is required (Farhad Hosseinzadeh Lotfi et al.,

2013; Jablonsky, 2011). However, despite the large number of approaches developed to further discriminate among the DEA units, no single methodology can be considered as a complete solution to the ranking problem.

To overcome the limitations of standard DEA, this work introduces an enhanced DEA methodology that is tailored to carrying out sustainability assessments. This approach integrates standard DEA with the concept of order of efficiency (optimality), as originally proposed by Das (1999) and later used by Antipova et al. (2015) and Pozo et al. (2012). In essence, the idea is to apply standard DEA repeatedly for different combinations of metrics in each sustainability dimension separately so as to determine an overall sustainability efficiency. The capabilities of our methodology are illustrated through a sustainability assessment of electricity-generation technologies in the United Kingdom (UK), which are expected to play a major role in its future electricity mix (Stamford and Azapagic, 2014). The main advantages of the proposed approach are that: (i) it considers each sustainability dimension separately; (ii) it can handle many economic, environmental and social indicators without compromising the discriminatory capabilities of the method; (iii) it provides a clear ranking of units based on their overall performance without the need to define explicit weights on the individual metrics; and iv) it provides clear quantitative targets for the inefficient systems to become efficient.

The rest of the article is organised as follows. A motivating example is presented in Section 2, while in Section 3 we describe the standard and the enhanced DEA methodologies, revisiting in both cases the motivating example to illustrate the differences between the two approaches. A real case study that evaluates the sustainability of electricity technologies in the UK is introduced in Section 4 to demonstrate the capabilities of the proposed methodology. Finally, the conclusions of the work are drawn in Section 5.

4.2 Motivating example

This section introduces a simple example that motivates our methodological approach. Consider a set of units (e.g. technologies, products, processes, etc.), each characterised by multiple economic, environmental and social inputs, synonymous to sustainability decision criteria, and required to produce one unit of output (e.g. 1 kWh). As indicated in Table IV-1, seven technologies (A, B, C, D, E, F and G) are considered, each of which has three economic inputs (I-1, I-2 and I-3), three environmental (I-4, I-5 and I-6), and three social inputs (I-7, I-8 and I-9) to produce one unit of output (O-1). The table shows the values of each input, which are dimensionless for the purposes of this example, but otherwise would be expressed in appropriate units. Lower input levels imply better performance in all of the cases.

Table IV-1 Motivating example: seven technologies with nine inputs to produce one unit of output.

<i>Technology</i>	<i>Economic inputs</i>			<i>Environmental Inputs</i>			<i>Social inputs</i>			<i>Output</i>
	<i>I-1</i>	<i>I-2</i>	<i>I-3</i>	<i>I-4</i>	<i>I-5</i>	<i>I-6</i>	<i>I-7</i>	<i>I-8</i>	<i>I-9</i>	<i>O-1</i>
A	4.0	5.0	2.9	1.0	2.5	3.0	4.2	2.1	1.3	1.0
B	2.5	1.0	3.7	2.0	5.0	2.0	3.1	3.4	4.0	1.0
C	2.0	1.3	1.0	4.5	4.3	1.0	1.3	5.0	2.7	1.0
D	4.5	7.0	8.0	2.0	7.0	8.0	0.5	7.0	7.0	1.0
E	3.0	3.0	1.8	2.5	1.5	5.0	3.0	1.8	3.3	1.0
F	6.5	2.0	2.1	1.3	2.0	4.0	0.8	3.2	2.4	1.0
G	3.0	3.5	1.1	4.0	3.1	3.0	2.0	2.7	1.9	1.0

The goal of the analysis is to assess the level of sustainability attained by each technology in Table IV-1, that is, we aim to address the following points:

- Which technologies are 'more efficient' in terms of sustainability (i.e. perform better considering sustainability principles)?

- For the ones found to be inefficient, how could we improve their level of sustainability?

DEA was not originally devised to assess the level of sustainability, so an enhanced version is required for this purpose. Both standard and enhanced DEA are discussed in the next section.

4.3 Methodology

The fundamentals of standard DEA are presented first before describing the improvements introduced in this work to tailor the method for its use for sustainability assessment.

4.3.1 Data envelopment analysis

As mentioned earlier, DEA is a non-parametric LP technique that quantifies the relative efficiency of a set of comparable DMUs taking into account several inputs and outputs simultaneously (Charnes et al., 1978). DEA analyses each DMU individually by solving an LP model and identifies those that exhibit best performance, i.e. the ones deemed efficient, which form the ‘efficient frontier’. DEA also measures in turn the level of efficiency of the non-frontier units (inefficient units), identifies sources of inefficiency, and provides specific guidelines on what changes are required to turn inefficient units into efficient.

The original input-oriented DEA model, known in the literature as the Charnes, Cooper and Rhodes (CCR) model, first proposed by these authors (Charnes et al., 1978) based on Farrell’s work (Farrell, 1957), is a nonlinear program that measures the efficiency of a unit as the ratio of the weighted sum of their outputs and inputs. The goal of this model is to find the optimal weights that maximise the efficiency of a set of DMUs separately (i.e. for each such DMU, the best weights are found that maximise the outputs/inputs ratio).

Let us consider a set of $|J|$ DMUs j ($j=1, \dots, |J|$), each using $|I|$ inputs x_{ij} ($i=1, \dots, |I|$) to produce $|R|$ outputs y_{rj} ($r=1, \dots, |R|$). The CCR model defined for each

DMU j , is stated as follows:

$$\text{Max } \theta_j = \frac{\sum_{r \in R} u_r y_{rj}}{\sum_{i \in I} v_i x_{ij}} \quad \text{Eq. IV-1}$$

$$\text{s. t. } \sum_{r \in R} u_r y_{rj} - \sum_{i \in I} v_i x_{ij} \leq 0 \quad \forall j \in J \quad \text{Eq. IV-2}$$

$$u_r, v_i \geq 0 \quad \forall r \in R, i \in I \quad \text{Eq. IV-3}$$

where θ_j is the technical efficiency of the DMU $_j$ and u_r and v_i are free variables denoting the weights (multipliers) given to each output r and input i , respectively. Due to the flexibility in the weights, if a DMU $_j$ satisfies $\theta_j = 1$, it is deemed efficient, and it is considered inefficient when $\theta_j < 1$. The latter implies that the DMU under evaluation is always inferior to other alternatives, even for the most favourable choice of weights (it is possible to reduce any of its inputs without reducing any output).

The previous CCR model is input-oriented, that is, an inefficient unit is turned into efficient through a proportional reduction of inputs and keeping the output constant. Moreover, the CCR model considers constant returns to scale (CRS), as it assumes that DMUs operate at the same scale and their outputs change proportionally when changes in the inputs are applied. The original input-oriented CCR DEA model (Charnes et al., 1978), which is nonlinear and nonconvex, can be reformulated into the following LP model (Eq. IV-4, Eq. IV-5, Eq. IV-6 and Eq. IV-7), where the denominator is set to one and the numerator is maximised:

$$\text{Max } \theta_{j'} = \sum_{r \in R} u_r y_{rj'} \quad \text{Eq. IV-4}$$

$$\text{s. t. } \sum_{i \in I} v_i x_{ij'} = 1 \quad \forall j' \in J \quad \text{Eq. IV-5}$$

$$\sum_{r \in R} u_r y_{rj} - \sum_{i \in I} v_i x_{ij} \leq 0 \quad \forall j \in J \quad \text{Eq. IV-6}$$

$$u_r, v_i \geq 0 \quad \forall r \in R, i \in I \quad \text{Eq. IV-7}$$

where the subscript j' denotes the specific DMU being assessed.

For this primal LP problem it is possible to formulate a partner problem (dual), which provides the same information as the primal (i.e. efficiency scores) and calculates in turn targets for the inefficient DMUs so as to become efficient. The LP dual model is formulated by assigning one dual variable to each constraint in the primal model (Cooper et al., 2004) as follows:

$$Z = \min \theta_o - \varepsilon \left(\sum_{r \in R} S_r^+ + \sum_{i \in I} S_i^- \right) \quad \text{Eq. IV-8}$$

$$\text{s. t.} \quad \sum_{j \in J} \lambda_j x_{ij} + S_i^- = \theta_o x_{io} \quad \forall i \in I \quad \text{Eq. IV-9}$$

$$\sum_{j \in J} \lambda_j y_{rj} - S_r^+ = y_{ro} \quad \forall r \in R \quad \text{Eq. IV-10}$$

$$\lambda_j, S_i^-, S_r^+ \geq 0 \quad \forall j \in J, i \in I, r \in R \quad \text{Eq. IV-11}$$

where ε is a non-Archimedean infinitesimal value designed to enforce strict positivity on variables. θ_o is unconstrained and measures the efficiency of the DMU_o under consideration and, therefore, it is less than or equal to 1 ($\theta_o \leq 1$). S_r^+ and S_i^- are slack variables denoting the extra amount by which an input (or output) should be reduced (or increased) to be efficient. Note that the values of the slacks are all zero (S_r^+ and $S_i^- = 0$) in the efficient units ($\theta_o = 1$), and strictly positive in the inefficient ones ($\theta_o < 1$). λ_j is a variable that represents the weight assigned to each efficient DMU (belonging to the reference set of an inefficient unit) to form a composite efficient unit that could be used as a benchmark to improve the inefficient unit. This composite unit is obtained by projecting radially the inefficient unit on the efficient frontier, which is the piece-wise linear function connecting all

the efficient DMUs (those with an efficiency score of 1). To illustrate this, we use below a simplified motivating example described in Section 4.2.

4.3.1.1 An illustrative example for standard DEA

For simplicity, the analysis in the simplified example is restricted to one environmental input (I-1) (environmental impact) and one economic input (I-4) (cost), together with one output (O-1), as shown in Table IV-1. Figure IV-1 provides a graphical representation of the DEA results. The efficient technologies, denoted by the red circles, determine the efficient frontier, which is the convex envelope depicted in blue colour. Inefficient systems are represented by black circles, while their radial projections on the frontier are depicted by green circles.

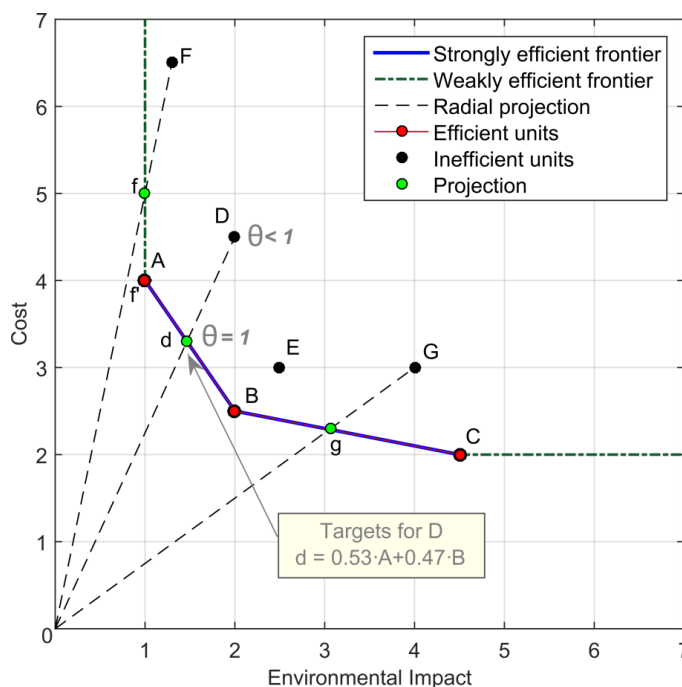


Figure IV-1 Graphical representation of DEA results for the simplified motivating example. The figure shows the two inputs considered in the analysis, cost and environmental impact (note that the output is constant for all of the decision-making units).

As can be observed in Figure IV-1, technologies A, B and C have lower input values for the same output and are thus identified as efficient (i.e. their efficiency equals 1). The line connecting them determines the piece-wise linear efficient

frontier. On the other hand, D, E, F and G are deemed inefficient because their efficiency score θ_j is lower than 1 (they produce the same level of output with higher inputs, that is, they are more expensive and cause greater environmental impact). DEA also quantifies the magnitude of inefficiency by referring to the efficient frontier. For instance, the efficiency of technology D is obtained from the ratio between two segments, the one that goes from zero to the intersecting point between the efficient frontier and the radial projection of D; and the one that connects zero and D (i.e. the ratio between $\overline{0d}$ and $\overline{0D}$ is equal to 0.73 for this case). The efficiency score represents the extent to which all the inputs should be proportionally reduced to reach the frontier; therefore, D should reduce its inputs to 73.33% of its current level in order to be efficient. Point d (which represents the hypothetical efficient unit for D) is generated by a linear combination of A and B, which is the reference set (peer group), using linear weights equal to 0.53 and 0.47 respectively, which are provided by the DEA model.

Similarly, all inefficient DMUs can be projected onto the efficiency frontier, but in doing so we may sometimes obtain weakly-efficient composite units, as it happens with unit f (efficient unit for F), which shows a slack in the cost given by the distance $\overline{f\bar{A}}$. In other words, unit F should reduce its inputs at least by 23.08% (efficiency equals to 76.92%) to be weakly-efficient. However, f would remain inferior since technology A has the same environmental impact but lower cost. Therefore, technology F presents a slack or excess of 1 unit in the cost, which implies an input value of 61.5% of its current level to be strongly efficient. That is, a reduction of 23.08% (from 6.5 to 5.0) in the cost for F is not enough to become strongly efficient. For that, the unit needs to decrease the cost by a further 38.5% (from 6.5 to 4.0), thereby reaching point f' with the same inputs and output than technology A.

Note that the criteria to be considered in DEA (i.e. the economic, environmental and social indicators) might be treated as inputs or outputs

depending on whether they should be minimised or maximised, respectively (i.e. depending on whether lower or higher values imply better performance, respectively). Furthermore, it is possible to define all the indicators as inputs (whose value should be minimised) by carrying out a proper data normalisation. Note also that the data conversion does not affect the results since the radial DEA models are unit invariant, that is, the efficiency scores are independent of the measurement units of the inputs and outputs; further information on this topic can be found in Edelstein and Paradi (2013) and Tone (2001), among others.

4.3.1.2 Standard DEA for sustainability assessment applied to the motivating example

To answer the questions posed in the motivating example, we propose to assess the efficiency in each sustainability dimension separately (i.e. economic, environmental and social) and then aggregate the results into an overall sustainability efficiency. Therefore, a unit will have a sustainability efficiency of 1 if it is efficient simultaneously in all three dimensions of sustainability.

Let θ_j^d be the efficiency of DMU j for the sustainability dimension d , that is, the efficiency calculated by DEA when only the inputs belonging to this dimension are considered. We define an overall sustainability efficiency, denoted by θ_j^{sust} and calculated by Eq. IV-12, as the average of the efficiencies in each sustainability dimension (reflecting a balanced integration of the three dimensions of sustainable development in which all of them are considered equally important):

$$\theta_j^{sust} = \frac{\sum_{d \in D} \theta_j^d}{|D|} \quad \forall j \in J \quad \text{Eq. IV-12}$$

Note that the efficiency scores (θ_j^d and θ_j^{sust}) fall within the range 0-1. As explained before, a DMU j is considered efficient in a specific sustainability dimension if its efficiency score equals 1 ($\theta_j^d = 1$). The higher the dimension's efficiency score, the higher the level of efficiency for that sustainability dimension. Similarly, a DMU j is considered efficient from the sustainability point of view if its

overall sustainability efficiency score equals 1 ($\theta_j^{sust}=1$), that is, if it is efficient for all three sustainability dimensions. The higher the sustainability efficiency scores, the higher the level of sustainability.

We now revisit the motivating example by applying standard DEA. The results are presented in Figure IV-2 which shows the efficiency scores for each sustainability dimension and the overall sustainability efficiency for each technology. Each axis in the radar chart corresponds to a technology and the outermost ring represents an efficiency score of 1. The dashed orange, green and blue lines represent the economic, environmental and social efficiency, respectively, while the purple line represents the overall sustainability efficiency. Moreover, Figure IV-2 displays the efficiency for each technology calculated considering simultaneously all of the inputs given in Table IV-1 (black dotted line) without classifying them according to the sustainability dimension they refer to.

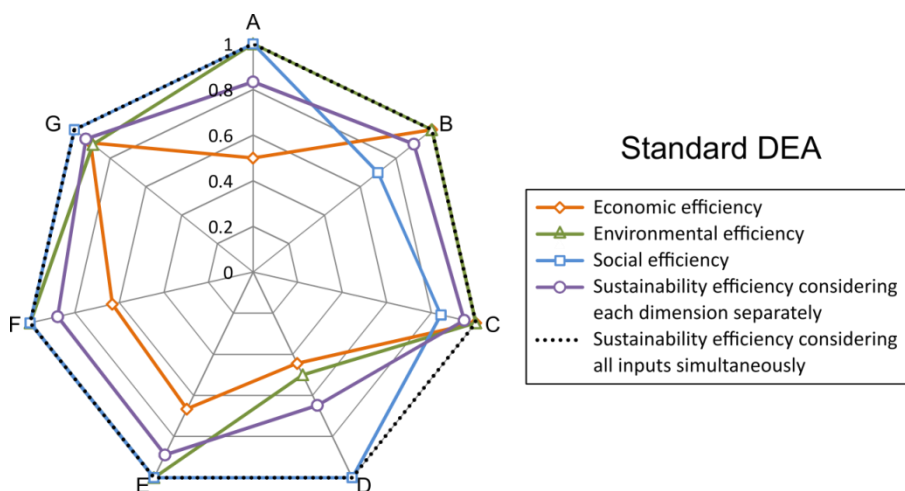


Figure IV-2 Standard DEA results for the motivating example.

As can be seen in Figure IV-2, when considering all inputs simultaneously regardless of the dimension they belong to (black dotted line), all the technologies are deemed efficient (efficiency scores equal 1), thereby leading to a very poor discrimination and loss of information. This is because each technology performs well in at least one indicator, a situation that typically arises in sustainability studies.

For example, an analysis of the input data shows that D is deemed efficient despite performing well for a single social indicator (I-7) and very poorly for the remaining economic and environmental metrics. Thus, the outcome of standard DEA in this case provides little insight into which technologies are more sustainable across the three sustainability dimensions.

By considering each sustainability dimension separately (i.e. applying DEA to each sustainability dimension at a time and then aggregating the results into the overall sustainability efficiency score), we can generate more insightful results. In this case, no single technology is found sustainable overall, since none is efficient simultaneously in all three dimensions. The technology with the highest overall sustainability efficiency is C (sustainability efficiency score of 0.95), followed by G (0.93), while D is the least sustainable (0.65). As observed in the efficiencies attained in each dimension, the discrimination can still be poor even after applying standard DEA to each of them separately. This is because some dimensions require the evaluation of many metrics, and because of this several technologies performing well only in a very small number of them can be deemed efficient within a specific dimension. For instance, technology B and C are both found economically efficient and it is not possible with standard DEA to discriminate between them. The same happens in the environmental and social dimensions, in which several technologies are found efficient, leaving open the question of which one is globally better still. Therefore, there is a need for enhancing standard DEA to overcome these limitations; this is discussed next.

4.3.2 *Enhanced data envelopment analysis: order of efficiency*

This section introduces an enhanced DEA method tailored for sustainability assessment that integrates the concept of 'order of efficiency'. The fundamentals of enhanced DEA are presented first, followed by revisiting the motivating example to demonstrate the capabilities of the approach.

In essence, our method ranks DMUs according to how they perform globally, without the need to define explicit weights for the inputs and outputs. This has at least two advantages: it removes the subjectivity associated with the weighting of decision criteria and eases the burden on decision-makers by avoiding the need for elicitation of preferences. This is achieved by integrating into standard DEA the concept of 'order of efficiency', originally introduced to rank Pareto optimal solutions from a set of many (Das, 1999). A solution is said to be efficient of order k if it is not dominated by any other solution in any of the possible k -elements subsets of objectives. This approach is well suited for cases with a large number of criteria (objectives) (Das, 1999), in which a large number of points might be regarded as Pareto optimal, even if they perform well in only one criterion out of a large number of objectives and poorly in the rest. The order of efficiency determines preferences among optimal solutions by ranking them according to their order of efficiency, whereby lower orders imply higher degrees of efficiency (Das, 1999) and, therefore, higher preferences for those solutions.

On the basis of the original concept, here we adopt the order of efficiency in the context of DEA, so that a DMU is identified as efficient of order k , if and only if, it is found efficient in any of the possible k -elements subsets of inputs. Following this proposed enhanced DEA approach, the calculations of standard DEA are repeated iteratively for all possible combinations of inputs/outputs and then aggregated into an overall efficiency metric (note that in this work, without loss of generality, we only consider combinations of inputs since there is just one output). The enhanced DEA based methodology is summarised in Figure IV-3 and explained in more detail below.

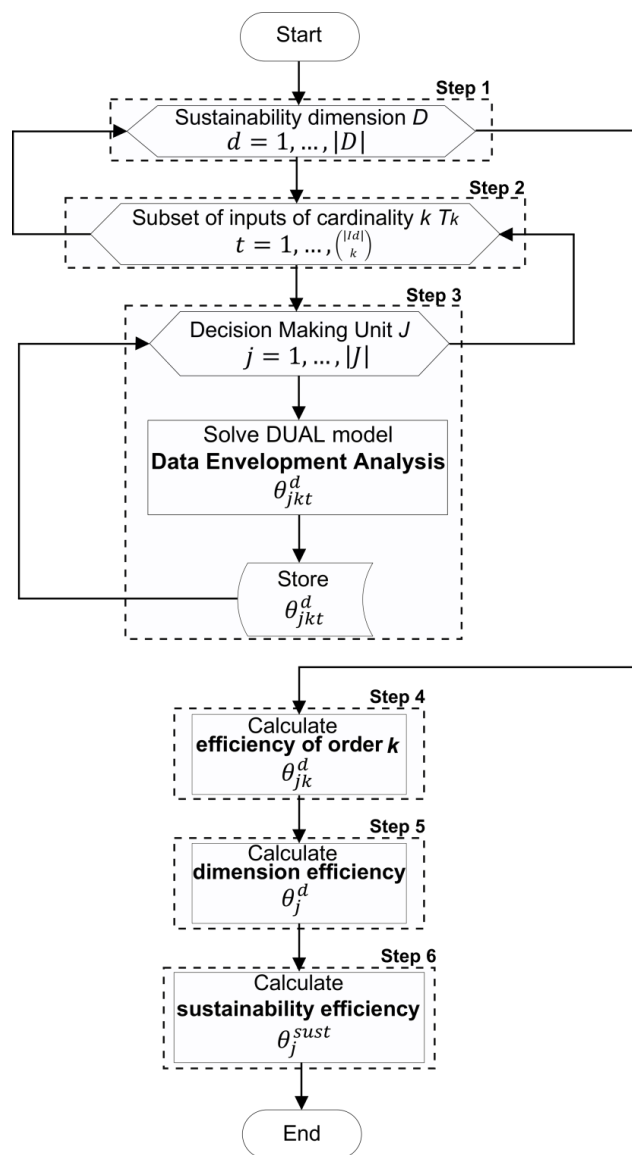


Figure IV-3 Algorithm of the proposed enhanced DEA methodology to assess the sustainability efficiency in the economic, environmental and social dimensions.

Let J be the set of DMUs to be analysed by DEA ($j=1, \dots, |J|$) characterised for a set T of sustainability criteria or indicators. Considering the set D of sustainability dimensions (i.e. economic, environmental and social), the first step requires categorizing the indicators within the sustainability dimension d they belong to, such that each dimension comprises $|I_d|$ sustainability criteria or indicators. These are defined as inputs whose values need to be minimised to produce a unit of

output (fixing the output to 1 and normalizing the inputs accordingly). In the second step (Figure IV-3), within each sustainability dimension d , each and every of the possible combination t of inputs are identified, each containing k inputs out of $|I_d|$, with the total number of combinations given by $\binom{|I_d|}{k}$. In the third step, the DEA model is solved to determine the efficiency score for every DMU j in each combination of inputs t_k (denoted by θ_{jkt}^d).

Then, in step 4, the efficiency of order k (denoted by θ_{jk}^d) can be determined for each DMU j using Eq. IV-13 as the average efficiency in all possible combinations t containing elements of size k belonging to dimension d (note that each and every of the possible subset of inputs needs to be considered).

$$\theta_{jk}^d = \frac{\sum_{t \in T_{kd}} \theta_{jkt}^d}{\binom{|I_d|}{k}} \quad \forall d \in D, j \in J, k \in K_d \quad \text{Eq. IV-13}$$

A DMU j is said to be efficient of order k in a specific sustainability dimension d , if and only if, the efficiency for any subset of inputs t of cardinality k is equal to 1, that is, $\theta_{jkt}^d = 1$ for all $t \in T_k$, where T_k is the set of possible combinations of $|I|$ inputs of size k . Note that if a DMU is efficient of order k , it is also efficient of order $k' > k$. Note also that the utopia point (if attainable) is to be efficient of order 1, that is, to be the best in every input individually. Therefore, as mentioned earlier, lower orders of efficiency reflect a better overall performance, since that implies a more balanced performance in all inputs.

To compute the efficiency of order k , we run the DEA calculations for each and every possible combination of inputs. This approach is equivalent to imposing bounds on the weights (multipliers) in the DEA model, so that inputs i' not included in a specific subset are given a fixed weight equal to 0 ($v_{i'}=0$), while the weights for the other included inputs are considered as free variables. The advantage of our approach is that there is no need to define explicit weights for inputs/outputs. Instead, we solve the DEA models for every combination of inputs.

Furthermore, we define an overall efficiency score in each dimension (i.e. dimension efficiency denoted by θ_j^d) for each DMU j as the average of all of the efficiency scores obtained for all of the orders of efficiency. That is, in the fifth step in Figure IV-3, the dimension efficiency is determined as the average of all of the efficiency scores computed by DEA for all of the possible combinations of inputs within each sustainability dimension d , as given in Eq. IV-14:

$$\theta_j^d = \frac{\sum_{k \in K_d} \sum_{t \in T_{kd}} \theta_{jkt}^d}{\sum_{k \in K_d} \binom{|I_d|}{k}} \quad \forall d \in D, j \in J \quad \text{Eq. IV-14}$$

where d represents the sustainability dimension (i.e. economic, environmental and social) to which the efficiency refers, I_d is the set of inputs (i.e. sustainability criteria or metrics) that quantify different aspects of that dimension, T_{kd} is the set of combinations of order k of these inputs covered by dimension d , and K_d is the set of allowable orders in dimension d (note that $|K_d| = |I_d|$).

The dimension efficiency (θ_j^d) takes values between 0 and 1, where a score of 1 means that the DMU j under consideration is efficient in the sustainability dimension d , that is, efficient in all of the possible subset of inputs – a situation that will take place only if DMU j is the best in all of the inputs simultaneously. In this context, DMUs with greater efficiency scores are considered more efficient within a sustainability dimension.

Finally, with the values of the dimension efficiencies in hand, we can determine in step 6 the overall sustainability efficiency θ_j^{sust} using Eq. (12). The overall sustainability efficiency allows ranking of all the DMUs in terms of their sustainability performance, since greater sustainability efficiency scores reflect better level of sustainability for a given DMU. It should be noted, however, that we refer to sustainability in the context of efficiency so that the solutions found efficient may not necessarily be fully sustainable according to the original Brundtland definition of sustainability (WCED, 1987).

One of the advantages of the DEA model is that it can be implemented in standard software packages and solved very efficiently using LP methods, which can potentially encourage a widespread adoption of the methodology proposed herein. In this work, without loss of generality, we employ the input-oriented CCR DEA model, which considers CRS. However, the methodology could be extended to output-orientation and be formulated as the BCC DEA model (named after Banker, Chames and Cooper (1984)), which considers variable returns to scale. The choice between the two models depends on the application being addressed; for further discussion on this topic, see Lozano et al. (2009). Note, however, that when all the indicators are treated as inputs (by fixing the output to 1 and normalising the data), the selection of either a CCR or BCC model may become irrelevant since all units produce the same output levels.

The inefficiency assessment for every combination of inputs provides a large number of improvement targets that are difficult to interpret. Hence, we propose to establish improvement targets for every unit deemed inefficient in each individual dimension, considering all of the inputs in that dimension simultaneously (i.e. higher order of efficiency), rather than all of the possible combinations of inputs. More precisely, let us denote by E the reference set of efficient DMUs j for an inefficient DMU j' . For each DMU j' found inefficient in a specific dimension d' considering all the inputs within that dimension (i.e. k equals to $|I|$), the corresponding targets that its inputs i (x_{ij}) should achieve to become efficient are given in Eq. IV-15. Note that x_{ij} is a parameter representing the input values of the DMUs in the reference set, while variables $\theta_{j'}$, λ_j and S_i^- are computed by solving the dual DEA model (Eq. IV-8, Eq. IV-9, Eq. IV-10 and Eq. IV-11). Hence, the target value for input i in dimension d' that DMU j' should attain is computed as follows:

$$target_input_{d',j'i} = \sum_{j \in E} \lambda_j x_{ij} = \theta_{j'} x_{ij'} - S_i^- \quad \forall i \in I, d' \in D, j' \in J \quad \text{Eq. IV-15}$$

where λ_j are the linear combination coefficients that multiply the members of the

peer group of j' , θ_j , is the efficiency score of the inefficient unit j' and S_i^- is a slack variable denoting the extra amount by which the input i should be reduced to be strongly efficient.

4.3.2.1 An illustrative example for enhanced DEA

To illustrate the enhanced DEA methodology that integrates the concept of order of efficiency, the example in Table IV-1 is revisited next considering only the economic inputs (i.e. I-1, I-2 and I-3). Figure IV-4 illustrates graphically the concept of efficiency of order k (in this case, efficiency of order 3, as three inputs are considered), where technologies A, B, C, D, E, F and G are represented by coloured lines. The vertical axis shows the efficiency score for each technology when three inputs are considered, while the other axes display the value of each input for each technology.

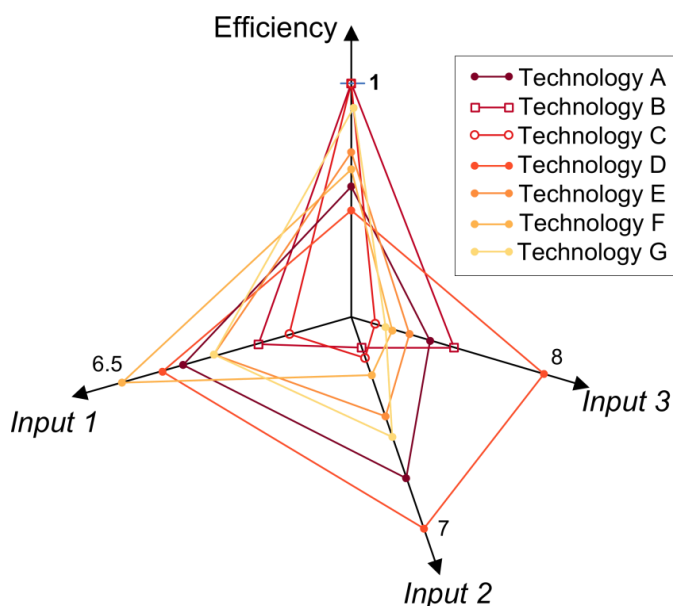


Figure IV-4 An illustrative example for enhanced DEA with the efficiency of order 3. The vertical axis shows the efficiency score for the technologies considering the three inputs simultaneously, while the remaining axes show the amount of inputs for each technology.

As can be seen in Figure IV-4, technologies B and C are found to be efficient of order 3 as their efficiency score is equal to 1, while the other technologies are

inefficient of order 3 (i.e. efficiency scores are below 1). For the latter, an inefficiency assessment can be performed to set targets for reaching the efficiency frontier, as explained in Section 4.3.2.

The efficiency calculations are repeated next for each possible subset of inputs (one subset of order 3, three subsets of order 2 and three subsets of order 1). Figure IV-5 summarises the results for each order of efficiency (i.e. orders 3, 2 and 1), with Figure IV-5a showing the results for the original order of efficiency (order 3), Figure IV-5b and Figure IV-5c give the efficiency scores for each subset of inputs of order 2 and 1, respectively, and Figure IV-5d shows the overall economic efficiency score (orange dotted line) for each technology, determined by Eq. IV-14.

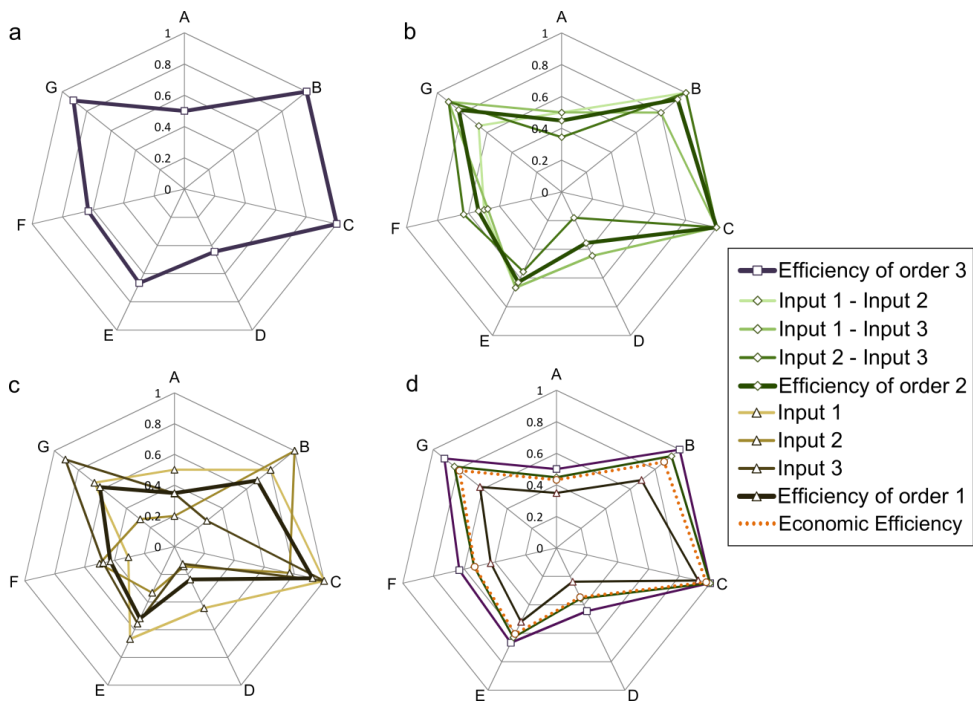


Figure IV-5 Graphical representation of efficiency of order of k (for a given set of economic inputs): (a) economic efficiency of order 3, (b) economic efficiency of order 2, (c) economic efficiency of order 1 and (d) overall economic efficiency.

As can be observed in Figure IV-5a, technologies B and C are identified as efficient of order 3. Technology C is in turn efficient of order 2, since it is efficient

for any combination of two inputs (Figure IV-5b). That is, when input 3 is removed and we consider only {input 1, input 2}, technologies B and C are efficient. The same happens when input 1 is removed from the analysis, to consider only {input 2, input 3}. On the contrary, when input 2 is removed, giving rise to the space {input 1, input 3}, C remains efficient, while B is found inefficient. Hence, B is efficient of order 3, but not of order 2. Furthermore, C is inefficient of order 1 (Figure IV-5c), since it shows the best performance in inputs 1 and 3 but not in input 2. Thus, this analysis reveals that technologies A, D, E, F and G are inefficient of orders 3 to 1, technology B is efficient of order 3, and technology C is efficient of order 2 (and, therefore, of order 3 as well). In addition, in terms of the overall economic efficiency (Figure IV-5d), C is the most economically efficient (score of 0.97) and D the least (0.35).

Therefore, as this simplified example demonstrates, the combined use of DEA and the concept of order of efficiency enables a further discrimination of alternatives. For example, B and C were indistinguishable for the original three inputs considered because they both showed an efficiency of 1. However, after estimating the order of efficiency they could be ranked easily according to the overall economic efficiency scores, which for B is 0.87 and for C 0.97.

4.3.2.2 Enhanced DEA for sustainability assessment applied to the motivating example

We now revisit the motivating example by applying the enhanced DEA approach. Figure IV-6 displays the efficiency in each sustainability dimension along with the overall sustainability efficiency for each technology. Technology A is the best in the environmental and social dimensions (with the efficiency of 0.88 and 0.87, respectively), while technology C is the best for the economic aspect (0.97). After aggregating all the efficiency values, technology C emerges as the most sustainable option, with the highest sustainability efficiency score of 0.78; technology D is the least sustainable, scoring only 0.5.

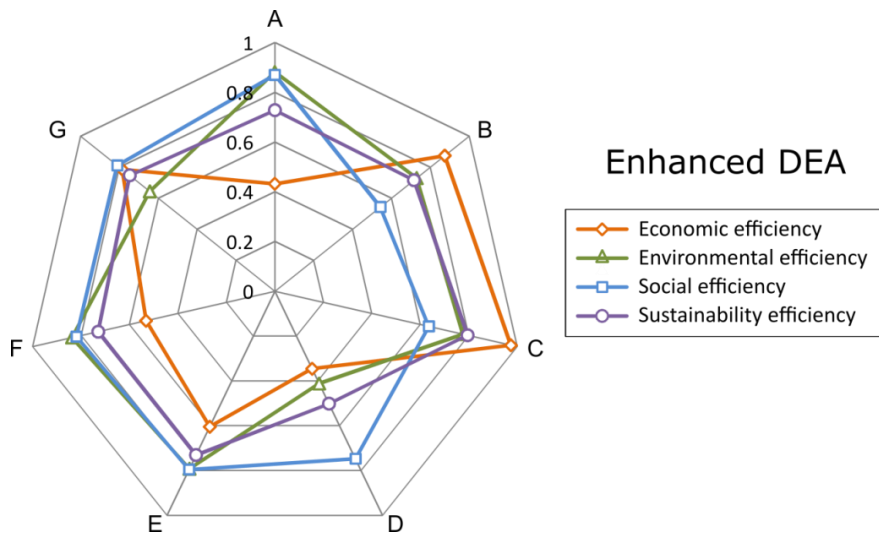


Figure IV-6 Enhanced DEA results for the motivating example.

Comparing the results of enhanced DEA (Figure IV-6) with those obtained with standard DEA (Figure IV-2), it is clear that the former improves the discriminatory capabilities between the technologies, since no single technology now has the same efficiency score as any of the others, thereby enabling their ranking according to the efficiency in each dimension and the overall sustainability efficiency.

4.4 Application of the enhanced DEA method to a real case study

The capabilities of the proposed methodology are illustrated next through its application to a real case study that assesses several electricity-generation technologies expected to play a major role in a future UK electricity mix. The data are sourced from Stamford and Azapagic (2014). Each of these technologies is defined as a DMU that uses a given amount of economic, environmental and social inputs to produce 1 kWh of electricity as an output. The specific technologies studied are: nuclear (pressurised water reactor, PWR), gas (combined cycle gas turbine, CCGT), coal with and without carbon capture and storage (CCS), wind (offshore), solar photovoltaics (PV) and biomass (wood and *Miscanthus* pellets). Stamford and Azapagic assessed 36 inputs (sustainability criteria) for these

technologies following a life cycle approach. To simplify the analysis, we consider 18 inputs here: three economic, nine environmental and six social life cycle sustainability indicators (Table IV-2). For further details on these metrics, see Stamford and Azapagic (2014).

Table IV-2 Sustainability indicators considered as inputs in the enhanced DEA.

<i>Dimension</i>	<i>Sustainability indicators^a</i>	<i>Units^b</i>
Economic	Capital cost	£·kWh ⁻¹
	Operation and maintenance cost	£·kWh ⁻¹
	Fuel cost	£·kWh ⁻¹
Environmental	Freshwater eco-toxicity	kg DCB-eq·kWh ⁻¹
	Marine eco-toxicity	kg DCB-eq·kWh ⁻¹
	Global warming	kg CO ₂ -eq· kWh ⁻¹
	Ozone depletion	kg CFC-11-eq· kWh ⁻¹
	Acidification	kg SO ₂ -eq· kWh ⁻¹
	Eutrophication	kg PO ₄₃ -eq· kWh ⁻¹
	Photochemical smog	kg C ₂ H ₄ -eq· kWh ⁻¹
	Land occupation	m ² yr· kWh ⁻¹
	Land eco-toxicity	kg DCB-eq· kWh ⁻¹
Social	Direct employment	person-yrs·kWh ⁻¹
	Worker injuries	injuries·kWh ⁻¹
	Human toxicity potential	kg DCB-eq·kWh ⁻¹
	Radiation: total	DALY·kWh ⁻¹
	Depletion of elements	kg Sb-eq·kWh ⁻¹
	Depletion of fossil fuels	MJ·kWh ⁻¹

^aFor all the indicators except direct employment, the lower the value, the higher the level of sustainability.

^bDCB: dichlorobenzene. DALY: disability-adjusted lost years.

Note that we treat all sustainability indicators as inputs while holding the output equal to 1 kWh. For all sustainability indicators, lower values mean better

performance, except the direct employment for which a higher value is preferred. The values of the inputs were normalised to a common interval [0.1,0.9] so that 0.1 corresponds to the minimum and 0.9 to the maximum value (opposite for the direct employment indicator).

The DEA dual model (Eq. IV-8, Eq. IV-9, Eq. IV-10 and Eq. IV-11) combined with the order of efficiency concept (see the algorithm in Figure IV-3) were both implemented in the General Algebraic Modelling System (GAMS) version 24.4.1, solving the LP formulations with the solver CPLEX 12.6.1.0 on an AMD A8-5500 APU with Raedon 3.20 GHz and 8.0 GB RAM. The efficiency of each technology was optimised in each of the 581 possible subset of inputs (7 in the economic dimension, 511 in the environmental dimension and 63 in the social dimension), giving rise to a total of 4648 runs. The CPU time was below one second for all of the instances.

Figure IV-7 outlines the steps followed to assess the sustainability of the electricity technologies based on the algorithm in Figure IV-3. The first step requires categorising the indicators as inputs or outputs within the sustainability dimension d they belong to - the indicators are modelled as economic, environmental or social inputs required to produce a certain amount of output. In the second step, each and every of the possible subsets of inputs t for each order of efficiency k are identified (t_k) within each category. In the third step, the DEA model is applied to determine the efficiency score of each electricity technology for each combination of inputs t_k (θ_{jkt}^d). Then, within each dimension d and for each DMU j , the efficiency of each order k (θ_{jk}^d) and the overall dimension efficiency are determined (θ_j^d) in steps 4 and 5, respectively. Finally, the overall sustainability efficiency score (θ_j^{sust}) for each DMU j is computed in step 6.

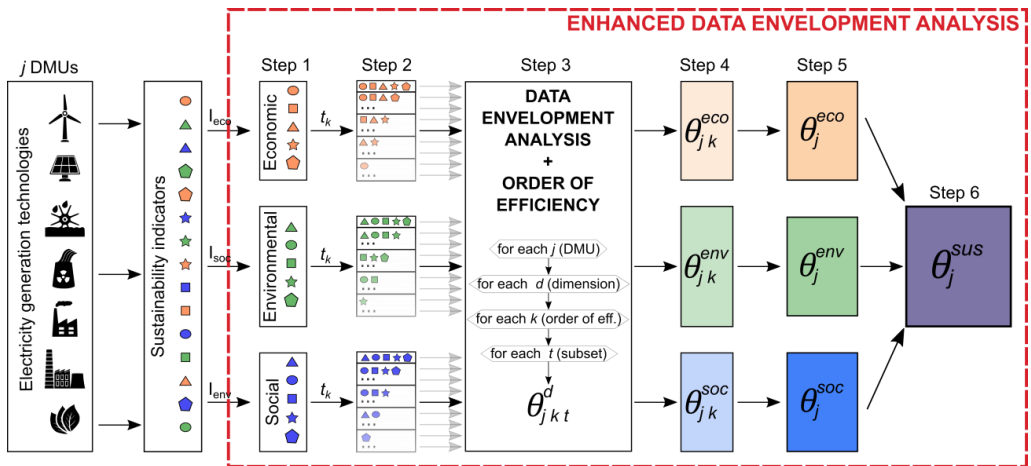


Figure IV-7 Graphical summary of the enhanced DEA method applied to assess the sustainability of the electricity generation technologies.

4.4.1 Efficiency of different sustainability dimensions

The results are summarised in Figure IV-8, Figure IV-9 and Figure IV-10, with each line corresponding to a different order of efficiency. The darkest line represents the overall efficiency in each sustainability dimension calculated by Eq. IV-14.

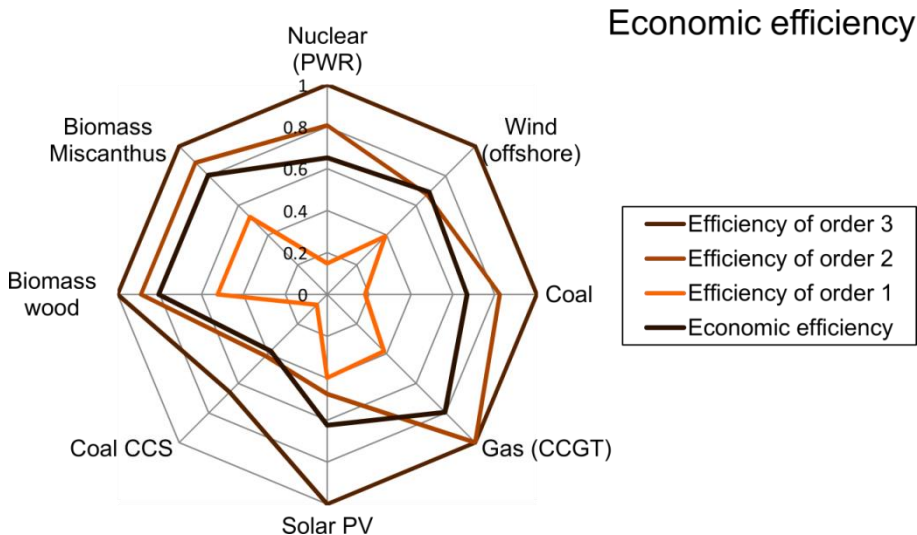


Figure IV-8 Economic efficiency of electricity generation technologies.

The economic efficiency assessment (Figure IV-8) shows that all the technologies except for coal CCS are efficient of order 3. Among them, only gas

electricity is efficient of order 2 (and also of order 3), but no technology is efficient of order 1. The biomass options show the highest overall economic efficiency (0.80), while coal CCS is the least economically efficient technology (with an overall economic efficiency score of 0.38). Note that the technology with the largest efficiency score might not have the lowest efficiency order. This is the case with biomass which has the highest economic efficiency score, while gas shows the best (lowest) efficiency order. This is because gas performs poorly for the fuel cost indicator, while biomass performs well in all of the economic indicators simultaneously. Nevertheless, biomass is economically the most sustainable option, for the economic indicators considered here.

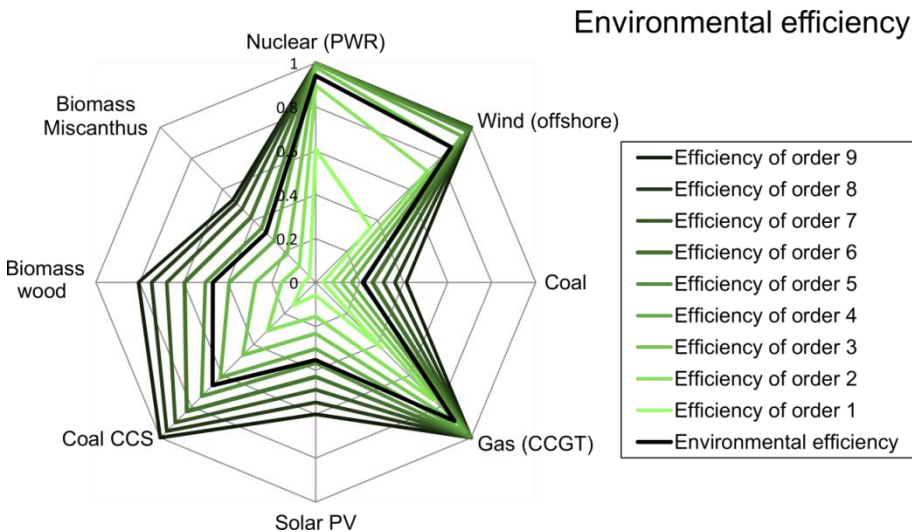


Figure IV-9 Environmental efficiency of electricity technologies.

The results of the environmental efficiency assessment in Figure IV-9 suggest that coal, solar PV and biomass are environmentally inefficient. Offshore wind and coal CCS are efficient of order 9, gas of order 7 (and also of orders 8 and 9), while nuclear is efficient of order 5 (and also of orders 6 to 9). No single technology has an order of efficiency below 5. Nuclear has the best overall environmental efficiency score (0.94), followed by gas, wind and coal CCS (0.89, 0.87, and 0.66, respectively). On the other hand, biomass with wood pellets, solar PV, biomass with *Miscanthus*

pellets and coal are the least environmentally efficient technologies, with the efficiency scores of 0.47, 0.35, 0.32, and 0.22, respectively. Note that, as opposed to the previous case, here the technology with the best overall environmental efficiency score (nuclear) also has the best (lowest) order of efficiency. Thus, based on the inputs (indicators) considered in this case study, nuclear electricity is environmentally the most sustainable option.

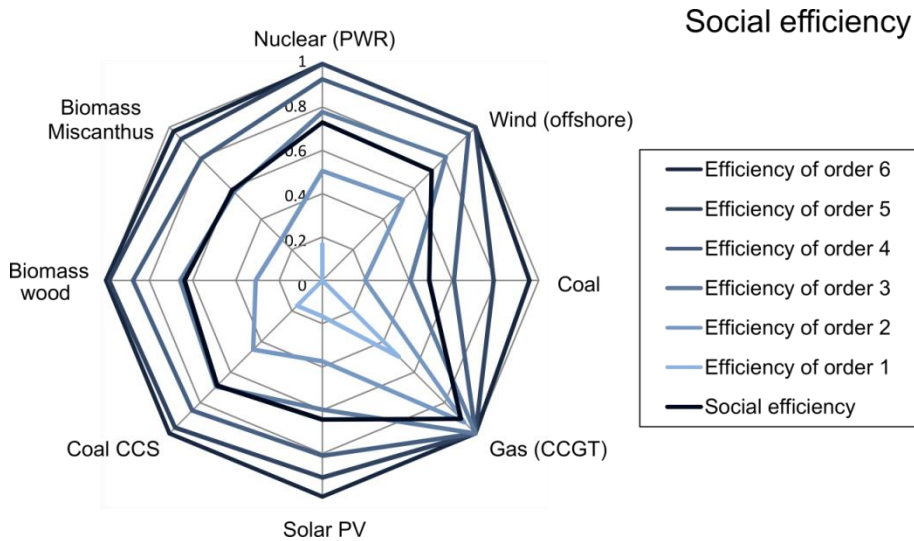


Figure IV-10 Social efficiency of electricity generation technologies.

The social efficiency assessment in Figure IV-10 indicates that all of the technologies, except coal and biomass with *Miscanthus* pellets, are socially efficient of order 6. Nuclear and wind are in turn socially efficient of order 5 while gas is socially efficient of order 2 (and, therefore, also of orders 3 to 6). Moreover, the overall social efficiency score of gas is the largest by far (0.9). Again, the technology with the best efficiency score (i.e. gas) has the best efficiency order. Hence, this technology is clearly the best from a social sustainability perspective.

4.4.2 Overall sustainability efficiency

Figure IV-11 provides the overall sustainability efficiency scores along with the dimension efficiency score for each technology. Gas electricity has the highest overall sustainability efficiency score (0.86), followed by nuclear (0.78) and wind

(0.76). Biomass with wood pellets, coal CCS, and biomass with *Miscanthus* pellets have the sustainability efficiency values of 0.64, 0.58 and 0.57, respectively. Finally, solar PV and coal show the worst scores of 0.54 and 0.45, respectively.

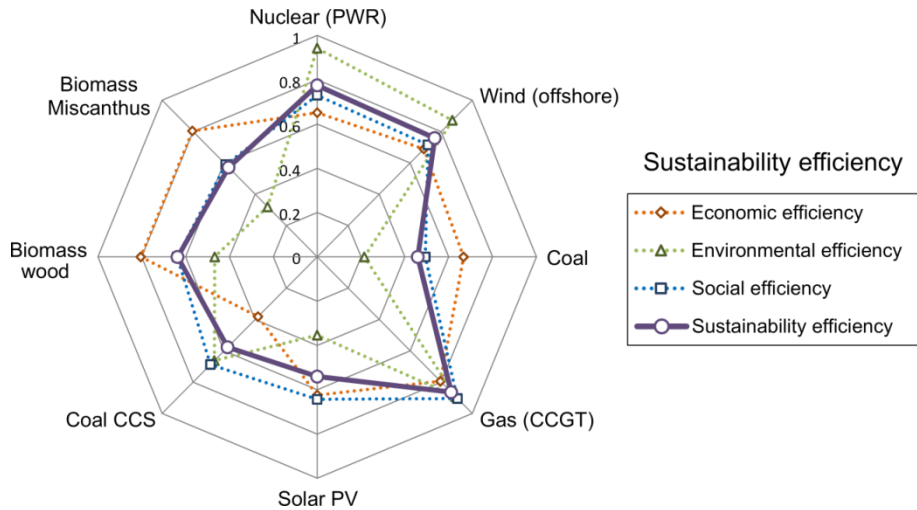


Figure IV-11 Overall sustainability efficiency of the technologies for electricity generation.

4.4.3 Inefficiency assessment

For each technology found inefficient (when all the corresponding inputs within the dimension are considered), the corresponding targets that its inputs should achieve to become efficient were determined using Eq. IV-15. The improvement targets for each technology are summarised in Figure IV-12. The figure shows the percentage reductions in the form of a heat map that should be attained in each current indicator value to make the technology efficient in a given dimension. Each cell is coloured according to the reduction value assigned to each input – the darker the shade, the higher the reduction needed. Note that in the case of the indicator *direct employment*, the target is a positive increment rather than a reduction.

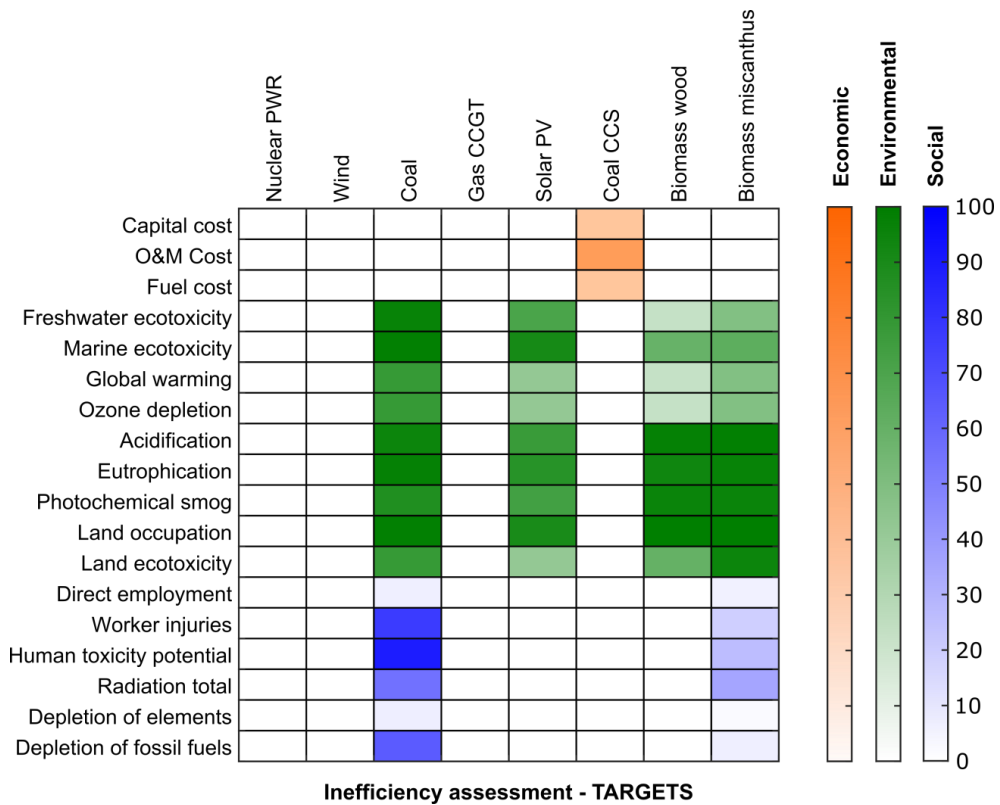


Figure IV-12 Heat map of inputs reductions for the electricity generation technologies required to achieve the economic, environmental and social efficiency.

In the economic dimension, coal CCS is the only inefficient technology. To become efficient, it should reduce its capital and fuel costs by 34%, and its operation and maintenance cost by 62%. These targets can be seen as either pure targets to reach the economic efficiency, or as the level of financial subsidies necessary to make the technology efficient.

As mentioned earlier, coal, solar PV and both biomass options are inefficient in the environmental dimension. The corresponding improvement targets are also shown in Figure IV-12. Among them, coal has the largest improvement targets. One-third of the total UK electricity consumption is generated from coal (DECC, 2015, 2014) and coal is expected to remain in the future UK energy mix to some extent. Hence, minimising its environmental impact may contribute significantly to reducing the environmental footprint of energy generation in the UK. For solar PV the

environmental impacts that require largest reductions are land occupation (89%), marine ecotoxicity (90%), eutrophication (84%) and acidification (77%), which are mainly caused during the manufacture of the solar facilities. Regarding the biomass options, the most critical categories are land occupation (99%), acidification (97%), photochemical smog (95%) and eutrophication (93%). These impacts are primarily driven by biomass cultivation; therefore, the use of second-generation biomass, such as agricultural and forestry residues or waste, could help to achieve the reductions required.

Finally, for the social dimension, coal and biomass with *Miscanthus* pellets are found inefficient. The highest improvements are required for coal in the categories human toxicity potential, workers injuries and depletion of fossil fuels, which should be reduced by 89%, 77% and 62%, respectively. By comparison, the improvements needed for the biomass option are relatively small: radiation, human toxicity potential and worker injures should be reduced respectively by 36%, 23% and 19% to become socially efficient.

4.5 Conclusions

In this work, we have proposed an enhanced DEA methodology for the assessment of the level of sustainability attained by a system. Our approach improves the discriminatory capabilities of standard DEA by grouping the inputs into economic, environmental and social indicators and by integrating the concept of order of efficiency. The latter is in particular powerful as it allows dealing with a large number of economic, environmental and social indicators simultaneously. The main advantages of enhanced DEA are: (i) it considers each sustainability dimension separately; (ii) it can handle a large number of economic, environmental and social criteria; (iii) it enables ranking of alternatives according to the extent to which they adhere to defined sustainability principles without the need to elicit preference weights for the criteria; and iv) it provides clear quantitative targets for the inefficient systems to become efficient, i.e. sustainable.

The capabilities of the methodology have been illustrated by application to a real case study assessing the level of sustainability of different electricity generation technologies. Gas, nuclear and wind electricity have been found efficient in all three dimensions of sustainability simultaneously when all the indicators within each dimension were considered. Gas electricity has the highest overall sustainability efficiency (mainly because of its very good performance in the social dimension), followed by nuclear and wind. Gas is also the most economically and socially efficient (highest economic and social efficiency scores), while nuclear is the best in the environmental dimension.

The proposed methodology can facilitate transition towards a more sustainable society by identifying the most sustainable options. Furthermore, it helps to pinpoint in a systematic manner the main sources of inefficiency and set improvement targets. This information can be useful for industry as an aid for improving technologies and products and for policy makers when designing future policies in accordance with the principles of sustainable development.

4.6 Acknowledgements

The authors wish to acknowledge the financial support for this research from the Spanish Ministry of Education and Science (Projects CTQ2012-37039-C02, DPI2012-37154-C02-02) and UK Engineering and Physical Sciences Research Council (EPSRC, Grant no. EP/K011820/1). We also would like to acknowledge financial support from the Pump-Priming Research Programme of The University of Manchester.

4.7 References

Adler, N., Friedman, L., Sinuany-Stern, Z., 2002. Review of ranking methods in the data envelopment analysis context. *Eur. J. Oper. Res.* 140, 249–265. doi:10.1016/S0377-2217(02)00068-1

Antipova, E., Pozo, C., Guillén-Gosálbez, G., Boer, D., Cabeza, L.F., Jiménez, L.,

2015. On the use of filters to facilitate the post-optimal analysis of the Pareto solutions in multi-objective optimization. *Comput. Chem. Eng.* 74, 48–58. doi:10.1016/j.compchemeng.2014.12.012

Avkiran, N.K., 2002. *Productivity Analysis in the Service Sector with Data Envelopment Analysis*, 2nd Editio. ed. N.K. Avkiran, Camira, Qld.

Azapagic, A., Perdan, S., 2005. An integrated sustainability decision-support framework Part I: Problem structuring. *Int. J. Sustain. Dev. World Ecol.*

Azapagic, A., Perdan, S., 2000. Indicators of sustainable development for industry: A general framework. *Process Saf. Environ. Prot.* 78, 243–261.

Bhagavath, V., 2006. Technical efficiency measurement by data envelopment analysis: An application in transportation. *Alliance J. Bus. Res.*

Chang, D.-S., Kuo, L.R., Chen, Y., 2013. Industrial changes in corporate sustainability performance – an empirical overview using data envelopment analysis. *J. Clean. Prod.* 56, 147–155. doi:10.1016/j.jclepro.2011.09.015

Charnes, A., Cooper, W.W., Rhodes, E., 1978. Measuring the efficiency of decision making units. *Eur. J. Oper. Res.* 2, 429–444. doi:10.1016/0377-2217(78)90138-8

Chen, J.-X., Deng, M., 2011. A cross-dependence based ranking system for efficient and inefficient units in DEA. *Expert Syst. Appl.* 38, 9648–9655. doi:10.1016/j.eswa.2011.01.165

Chen, J.-X., Deng, M., Gingras, S., 2011. A modified super-efficiency measure based on simultaneous input–output projection in data envelopment analysis. *Comput. Oper. Res.* 38, 496–504. doi:10.1016/j.cor.2010.07.008

Chen, Y., Du, J., Huo, J., 2013. Super-efficiency based on a modified directional distance function. *Omega* 41, 621–625.

doi:10.1016/j.omega.2012.06.006

Cook, W.D., Seiford, L.M., 2009. Data envelopment analysis (DEA) – Thirty years on. *Eur. J. Oper. Res.* 192, 1–17. doi:10.1016/j.ejor.2008.01.032

Cooper, W.W., Seiford, L.M., Zhu, J., 2004. *Data Envelopment Analysis: History, models and interpretations*. Kluwer Academic Publishers, Boston.

Das, I., 1999. A preference ordering among various Pareto optimal alternatives. *Struct. Optim.* 18, 30–35.

DECC, 2015. Energy statistics: “UK energy statistics: provisional data 2014”. Department of Energy & Climate Change. London., https://www.gov.uk/government/uploads/system/uploads/attachment_data/file/406993/Press_Notice_Feb_2015.pdf.

DECC, 2014. *Digest of United Kingdom Energy Statistics 2014*. Department of Energy & Climate Change. London.

Edelstein, B., Paradi, J.C., 2013. Ensuring units invariant slack selection in radial data envelopment analysis models, and incorporating slacks into an overall efficiency score. *Omega* 41, 31–40. doi:10.1016/j.omega.2011.09.008

Farrell, M.J., 1957. The measurement of productive efficiency. *J. R. Stat. Soc. Series A*, 253–281.

Gerdessen, J.C., Pascucci, S., 2013. Data Envelopment Analysis of sustainability indicators of European agricultural systems at regional level. *Agric. Syst.* 118, 78–90. doi:10.1016/j.agsy.2013.03.004

Gibson, R.B., 2001. Specification of sustainability-based environmental assessment decision criteria and implications for determining “significance” in environmental assessment.

Grossmann, I.E., Guillén-Gosálbez, G., 2010. Scope for the application of mathematical programming techniques in the synthesis and planning of sustainable processes. *Comput. Chem. Eng.* 34, 1365–1376. doi:10.1016/j.compchemeng.2009.11.012

Hosseinzadeh Lotfi, F., Jahanshahloo, G.R., Khodabakhshi, M., Rostamy-Malkhalifeh, M., Moghaddas, Z., Vaez-Ghasemi, M., 2013. A Review of Ranking Models in Data Envelopment Analysis. *J. Appl. Math.* 2013, 1–20. doi:10.1155/2013/492421

Hosseinzadeh Lotfi, F., Rostamy-Malkhalifeh, M., Aghayi, N., Ghelej Beigi, Z., Gholami, K., 2013. An improved method for ranking alternatives in multiple criteria decision analysis. *Appl. Math. Model.* 37, 25–33. doi:10.1016/j.apm.2011.09.074

Jablonsky, J., 2011. Multicriteria approaches for ranking of efficient units in DEA models. *Cent. Eur. J. Oper. Res.* 20, 435–449. doi:10.1007/s10100-011-0223-6

Jaeger, C. J., Tàbara, D.J., Jaeger, J., 2011. *European Research on Sustainable Development: Volume 1: Transformative Science Approaches for Sustainability.* Springer, Berlin (Germany).

Jahanshahloo, G.R., Memariani, A., Lotfi, F.H., Rezai, H.Z., 2005. A note on some of DEA models and finding efficiency and complete ranking using common set of weights. *Appl. Math. Comput.* 166, 265–281. doi:10.1016/j.amc.2004.04.088

Khodakarami, M., Shabani, A., Farzipoor Saen, R., 2014. A new look at measuring sustainability of industrial parks: a two-stage data envelopment analysis approach. *Clean Technol. Environ. Policy* 16, 1577–1596. doi:10.1007/s10098-014-0733-8

Li, S., Jahanshahloo, G.R., Khodabakhshi, M., 2007. A super-efficiency model for ranking efficient units in data envelopment analysis. *Appl. Math. Comput.* 184, 638–648. doi:10.1016/j.amc.2006.06.063

Liu, J.S., Lu, L.Y.Y., Lu, W.-M., 2015. Research Fronts in data envelopment analysis. *Omega* 58, 33–45. doi:10.1016/j.omega.2015.04.004

Liu, J.S., Lu, L.Y.Y., Lu, W.-M., Lin, B.J.Y., 2013. A survey of DEA applications. *Omega* 41, 893–902. doi:10.1016/j.omega.2012.11.004

Lozano, S., Iribarren, D., Moreira, M.T., Feijoo, G., 2009. The link between operational efficiency and environmental impacts. A joint application of Life Cycle Assessment and Data Envelopment Analysis. *Sci. Total Environ.* 407, 1744–54. doi:10.1016/j.scitotenv.2008.10.062

Lu, W.-M., Lo, S.-F., 2009. An interactive benchmark model ranking performers — Application to financial holding companies. *Math. Comput. Model.* 49, 172–179. doi:10.1016/j.mcm.2008.06.008

Martins, A.A., Mata, T.M., Costa, C.A. V., Sikdar, S.K., 2007. Framework for Sustainability Metrics. *Ind. Eng. Chem. Res.* 46, 2962–2973. doi:10.1021/ie060692l

Mohammadi, A., Rafiee, S., Jafari, A., Keyhani, A., Dalgaard, T., Knudsen, M.T., Nguyen, T.L.T., Borek, R., Hermansen, J.E., 2014. Joint Life Cycle Assessment and Data Envelopment Analysis for the benchmarking of environmental impacts in rice paddy production. *J. Clean. Prod.* doi:10.1016/j.jclepro.2014.05.008

Pope, J., Annandale, D., Morrison-Saunders, A., 2004. Conceptualising sustainability assessment. *Environ. Impact Assess. Rev.* 24, 595–616. doi:10.1016/j.eiar.2004.03.001

Pozo, C., Guillén-Gosálbez, G., Sorribas, A., Jiménez, L., 2012. Identifying the preferred subset of enzymatic profiles in nonlinear kinetic metabolic models via multiobjective global optimization and Pareto filters. *PLoS One* 7, e43487. doi:10.1371/journal.pone.0043487

Reig-Martínez, E., Gómez-Limón, J.A., Picazo-Tadeo, A.J., 2011. Ranking farms

with a composite indicator of sustainability. *Agric. Econ.* 42, 561–575.
doi:10.1111/j.1574-0862.2011.00536.x

Sikdar, S.K., 2003. Sustainable development and sustainability metrics. *AIChE J.* 49, 1928–1932. doi:10.1002/aic.690490802

Stamford, L., Azapagic, A., 2014. Life cycle sustainability assessment of UK electricity scenarios to 2070. *Energy Sustain. Dev.* 23, 194–211.
doi:10.1016/j.esd.2014.09.008

Tajbakhsh, A., Hassini, E., 2014. A data envelopment analysis approach to evaluate sustainability in supply chain networks. *J. Clean. Prod.*
doi:10.1016/j.jclepro.2014.07.054

Tone, K., 2001. A slacks-based measure of efficiency in data envelopment analysis. *Eur. J. Oper. Res.* 130, 498–509. doi:10.1016/S0377-2217(99)00407-5

Vázquez-Rowe, I., Iribarren, D., 2014. Review of Life-Cycle Approaches Coupled with Data Envelopment Analysis: Launching the CFP + DEA Method for Energy Policy Making. *Sci. World J.* 2015 (2015), 10.

Wang, Y.-M., Luo, Y., Lan, Y.-X., 2011. Common weights for fully ranking decision making units by regression analysis. *Expert Syst. Appl.* 38, 9122–9128.
doi:10.1016/j.eswa.2011.01.004

Wang, Y.-M., Luo, Y., Liang, L., 2009. Ranking decision making units by imposing a minimum weight restriction in the data envelopment analysis. *J. Comput. Appl. Math.* 223, 469–484. doi:10.1016/j.cam.2008.01.022

Washio, S., Yamada, S., 2013. Evaluation method based on ranking in data envelopment analysis. *Expert Syst. Appl.* 40, 257–262.
doi:10.1016/j.eswa.2012.07.015

WCED, 1987. *Our Common Future – The Brundtland Report*. World

Commission on Environment and Development. Geneva.

Wu, J., Sun, J., Liang, L., 2012. Cross efficiency evaluation method based on weight-balanced data envelopment analysis model. *Comput. Ind. Eng.* 63, 513–519.
doi:10.1016/j.cie.2012.04.017

Zerafat Angiz, M., Mustafa, A., Kamali, M.J., 2013. Cross-ranking of Decision Making Units in Data Envelopment Analysis. *Appl. Math. Model.* 37, 398–405.
doi:10.1016/j.apm.2012.02.038

Chapter V

Tackling climate change in cooperation

UNIVERSITAT ROVIRA I VIRGLI

CONTRIBUTION TO THE DEVELOPMENT OF MATHEMATICAL PROGRAMMING TOOLS TO ASSIST DECISION-MAKING
IN SUSTAINABILITY PROBLEMS

Àngel Galán Martín



V. Tacking climate change in cooperation

Time for global action: An optimised cooperative approach towards effective climate change mitigation

A. Galán-Martín^a, C. Pozo^a, A. Azapagic^b, I. E. Grossmann^c, N. Mac Dowell^d and G.

Guillén-Gosálbez^{a*}

^a*Centre for Process Systems Engineering, Imperial College London, SW7 2AZ London (United Kingdom).*

^b*School of Chemical Engineering and Analytical Science, The University of Manchester, Mill, Sackville Street, Manchester M13 9PL (United Kingdom).*

^c*Centre for Advanced Process Decision-making. Department of Chemical Engineering, Carnegie Mellon University, Pittsburgh 15213, Pennsylvania (United States).*

^d*Centre for Environmental Policy, Imperial College London, South Kensington*

KEYWORDS: Cooperation; Fair sharing of benefits; Climate change; Optimisation; US Clean Power Plan; Paris Accord; US withdrawal;

5.1 Introduction

Climate change has been in the international political agenda as a collective commitment since the United Nations Framework Convention on Climate Change entered into force more than twenty years ago (UNFCCC, 2017). Despite the efforts made so far, coordinating global actions on climate change mitigation and identifying solutions that satisfy a diverse group of stakeholders is still a major challenge facing the world today (Hallegatte et al., 2016; Keohane and Victor, 2016;

Lenton, 2014; Lewis, 2016; Sandler, 2004; Schmidt, 2015; Tavoni, 2013). The standard negotiation approach of defining regional and national targets, reflecting a 'fair' allocation of responsibilities among the countries involved, has thus far proved ineffective (Hardin, 2009; Höhne et al., 2014; Raupach et al., 2014). Some of the main obstacles in reaching global agreements have been the conflicting interests and competing priorities of different countries, which in turn have determined their willingness to act towards mitigation of climate change (Hallegatte et al., 2016). As a result, the agreed mitigation strategies might not be the most effective but simply those capable of achieving consensus.

Recently, the U.S. announced its withdrawal from the 2015 Paris Climate Agreement, arguing that it was unfair for the U.S. economy. To tackle climate change more successfully (Bahn et al., 1998; Cole, 2015; Dutta and Radner, 2004; Heitzig et al., 2011; Jacobson et al., 2015; Smead et al., 2014) and avoid domino effects of other countries potentially pulling out of the Agreement, alternative approaches will be needed. In this contribution, we argue that quantifying the benefits of cooperation and sharing them fairly through compensation mechanisms could provide a basis for more effective mitigation agreements, allowing implementation of the most cost-efficient technologies in the right places (Bahn et al., 1998; Petrosjan and Zaccour, 2003; Unger and Ekvall, 2003).

To demonstrate how the proposed approach would work, we apply it to the U.S., as an illustrative case of a multi-state region which could be extrapolated at the global level. Action to mitigate climate change remains a controversial topic with high political polarisation in the U.S. Here, we aim to provide sound scientific evidence of the benefits of cooperation in climate change mitigation that could be used in ongoing discussions. Specifically, we quantify the benefits of adopting a centralised global action to reduce CO₂ emissions for different levels of cooperation among states using the targets defined in the Clean Power Plan (EPA, 2015) (CPP), one of the main elements of the Obama Administration's strategy for meeting the

U.S. Paris commitments. The CPP was enacted by the Environmental Protection Agency (EPA) on the 3rd August 2015 and has been the U.S. flagship programme in climate change mitigation until the 28th March 2017, when the current Administration issued an Executive Order (Exec. Ord. No. 13783, 2017) to review the rule so as to suspend, revise or rescind the CPP (82 FR 16329, 2017). As a result of this review, the new Administration has decided to repeal the CPP, which has raised the question of whether the U.S. might still be able to meet its commitments made under the Paris Agreement. Essentially, the CPP aimed to curb CO₂ emissions from the power sector by 35% from 2012 baseline levels by establishing individual CO₂ emissions targets for 47 out of 50 states (Alaska, Hawaii and Vermont are excluded). The targets, which varied greatly across the states, were based on the capacity of each state to implement three mitigation strategies, namely, switching from coal to natural gas power plants; increasing the share of renewables; and improving plant and heat-rate efficiency. The CPP followed the so-called “production-based” approach to climate change mitigation, which considers only direct CO₂ emissions, as opposed to a “consumption-based” method whereby both direct and indirect emissions in the supply chain are taken into account; the latter are also referred to as “embodied” or “cradle to grave” emissions. With the CPP being rescinded, it is timely to investigate how its targets could be attained while benefiting the U.S. economy, the claim to the opposite being the main reason for its withdrawal. This is important not only because the U.S. is the second global emitter of GHG emissions (European Commission-Joint Research Center, 2014), but also because modernising the aging U.S. power system in a cost-effective manner can provide a robust and resilient response to the transformations challenges ahead (e.g. distributed generation, cybersecurity) (DOE, 2015). In this context, elucidating the value of cooperation at local and regional levels can potentially provide a roadmap on how to tackle more complex negotiations at the multi-national level, such as the Paris Agreement.

5.2 Emissions Reduction Cooperation Model

To carry out our analysis, we rely on mathematical programming techniques (also named as optimisation) that aim to find the optimal solution of a model representing a complex problem by means of a set of mathematical equations. The model contains three main elements: first, the objective function whose value needs to be maximised or minimised; second, a set of constraints that the solution sought should satisfy; and third, decision variables whose values are unknown and have to be found to optimise the objective. The type of variables (i.e. continuous and/or discrete) and equations (linear and/or non-linear) provide the class of the model.

In this contribution, we developed a mixed integer linear programming model (MILP) referred to as ERCOM as an acronym of Emission Reduction Cooperation Model. ERCOM is capable of identifying the most cost-effective ways of meeting the electricity demand while not exceeding the total CO₂ emissions ceiling, in this case that imposed by the CPP. In short, given the electricity demand in each U.S. state, costs (power plant construction, operation, maintenance and connection to electricity grid) and CO₂ emissions for each electricity technology and their potential location, ERCOM minimises the cost of electricity generation in the U.S. for the year 2030 (the CPP target year) considering different levels of cooperation among the states. Hence, the MILP model automates the screening of millions of partnership alternatives so as to ultimately identify the most cost-effective collective action towards carbon mitigation for a given level of cooperation. An outline of the model is provided next, while a detailed description of the mathematical formulation, data and assumptions is given in the Appendix 5.7.

In essence, ERCOM contains standard equations to model an energy system designed to meet specific reliability of electricity supply together with a set of constraints that enable assessing the benefits of cooperating when implementing CO₂ abatement strategies. In the non-cooperative approach, each region is forced

to keep its emissions below a specific regional limit, in this case based on the CPP targets for each state. This can be expressed in compact form as follows:

$$\min_x \sum_{i \in I} \sum_{j \in J} c_{ij}^T x_{ij} \quad \text{Eq. V-1}$$

$$\text{s. t. } \sum_{i \in I} em_{ij} x_{ij} \leq \bar{e}_j \quad \forall j \in J \quad \text{Eq. V-2}$$

$$A_{ij} x_{ij} \leq a_{ij} \quad \forall i \in I, j \in J \quad \text{Eq. V-3}$$

$$x \in \mathbb{R} \quad \text{Eq. V-4}$$

where x_{ij} are continuous variables denoting the amount of electricity generated by each technology i in each region j ; c_{ij}^T is a cost vector that multiplies the amount of electricity generated by each technology with its cost level; em_{ij} is the vector containing emission coefficients for each technology i in each region j ; \bar{e}_j is the emission target for region j ; A_{ij} is the technical matrix of constraints to be met by the energy system; while a_{ij} is the corresponding vector of right-hand side parameters, such as the electricity generation potential for each technology i in each region j .

In the cooperative approach, emissions limits can be met either in cooperation or individually. More precisely, by sharing emission targets, each region is allowed to emit above its quota of emissions as long as others compensate for these extra emissions. This multi-regional cooperative approach can be modelled in a simplified manner as follows (see section 5.7.1.2 in Appendix for details on the original formulation of ERCOM):

$$\min_{x,y} \sum_{i \in I} \sum_{j \in J} c_{ij}^T x_{ij} \quad \text{Eq. V-5}$$

$$\text{s. t. } \sum_{i \in I} \sum_{j \in P} em_{ij} x_{ij} \leq \sum_{j \in P} \bar{e}_j \quad \text{Eq. V-6}$$

$$\sum_{i \in I} em_{ij} x_{ij} \leq \bar{e}_j \quad \forall j \notin P \quad \text{Eq. V-7}$$

$$\sum_{j \in J} y_j = CS \quad \text{Eq. V-8}$$

$$A_{ij}x_{ij} + B_j y_j \leq a_{ij} \quad \forall i \in I, j \in J \quad \text{Eq. V-9}$$

$$x \in \mathbb{R}, y \in \{0,1\} \quad \text{Eq. V-10}$$

In the above model we consider two types of regions j , those that belong to the partnership P and meet aggregated targets ($j \in P$) and those outside the partnership, and therefore satisfy individual targets ($j \notin P$). To model the decision to participate in the partnership, we introduce binary variable y_j , which works as follows. When region j belongs to the partnership ($j \in P$), y_j will take a value of one and equation (Eq. V-6) will be enforced for all the members of the partnership, that is, the total emissions of the regions that cooperate should not exceed the summation of their targets (note that some individual targets can be exceeded provided the aggregate is satisfied). If region j does not belong to the partnership ($j \notin P$), y_j will be zero and equation (Eq. V-7) will then force every such region to meet its individual target. It is worth noting that equations Eq. V-6 and Eq. V-7 are simplified expressions, since the definition of set P actually requires reformulated big-M constraints and the linearisation of nonlinear terms (see equations from V-A1 to V-A7 in Appendix 5.7.1.2 for further details). Then, the level of cooperation can be controlled via equation (Eq. V-8), where parameter CS represents the number of regions in the partnership (i.e. the total number of binary variables that can take a value of one). Finally, B_j is an additional matrix that models the practical implications of belonging to the partnership. This matrix includes carbon emission equations (Eqs. V-A1 to V-A8), resources availability constraints (Eqs. V-A9 to V-A14), operational constraints (Eqs. A-A15 to V-A19), transmission and distribution constraints (Eqs. V-A20 to V-A27), a demand satisfaction constraint (Eq. V-A28) and equations related to costs calculations (Eqs. V-A30 to V-A34).

Essentially, ERCOM identifies the most cost effective collective action towards carbon mitigation for different levels of cooperation, each entailing different numbers of regions cooperating in partnerships (from the case in which regions act

independently from each other, $CS = 0$, to the case where all cooperate, $CS = |J|$). The model determines optimal capacities of electric power technologies in each state, inter-state electricity flows (note that inter-state transmissions are only allowed between states within the partnership) and electricity trades with Canada required to potentially meet each state's power demand in 2030 considering region-specific abatement curves for each state (see section 5.7.1.3 of the Appendix for a detailed description of the data). The following electricity sources are included in the model: coal, natural gas (including carbon capture and storage, CCS, for both), nuclear, hydro, solar, wind, geothermal and biomass. Potential use of each resource is limited by its regional availability, but the model allows an exchange of fossil fuels and biomass among states. The reliability of supply is ensured by identifying an optimal mix of base-load and intermittent technologies. The cooperation between the states is established through electricity trading and sharing of their emission targets, allowing one state to exceed its target as long as another offsets its emission excess. By establishing cooperation among states, the model can exploit regional abatements costs, thereby identifying solutions that are more efficient globally. In this way, ERCOM goes beyond other energy systems optimisation models, such as MARKAL/TIMES, NEMS and SWITCH (Fripp, 2012; Loulou et al., 2004; Nelson et al., 2012; Safaei and Keith, 2015; US Energy Information Administration, 2011), to explore the gains of tackling climate change mitigation through cooperation. Note that the motivation for cooperation extends beyond pure economic interests and emissions concerns. Hence, ERCOM could account for alternative criteria embracing other environmental burdens (e.g. damage to human health, biodiversity loss, etc.), social indicators (e.g. jobs created, labour compensation, etc.), as well as reliability and energy security concerns, among others. Without loss of generality, ERCOM focuses only on cost and emissions, centring the analysis and interpretation of its solutions on the value of cooperation. As far as we are aware, this is the first time such an approach has been proposed.

5.3 Results and discussion

5.3.1 *Benefits of increasing cooperation*

We consider a complete range of optimal solutions to explore the benefits of inter-state cooperation, from no cooperation to full cooperation among all the states. In the case of no cooperation, the states act independently from each other, with no trade of electricity among them and each aiming to meet independently the individual emissions reduction target set by the CPP. In this instance, the electricity generation costs are minimised in each state separately. This leads to solution A in Figure V-1, with the total cost of electricity generation in 2030 across all the states being 4% below the actual cost in 2012, despite a 15% higher demand. The total reduction in CO₂ emissions is almost double the overall U.S. CPP reduction target: 67% vs 35%. This is achieved by exploiting the economic competitiveness of low-carbon options (Heuberger et al., 2016; MacDonald et al., 2016; NREL, 2012) which allows curbing of CO₂ emissions while decreasing the overall costs. Further details on this solution can be found in section 5.7.2.1 in Appendix.

At the other end of the scale, we consider cooperation of all the states through electricity trade and emissions sharing, therefore forming a global partnership. In this case, instead of focusing on the individual states and their emission targets, we consider that the U.S. acts as a whole coordinated entity to minimise the total electricity costs, subject to the overall CO₂ reduction target of at least 35% at the country level. The calculated optimal solution is denoted by point B in Figure V-1. As shown, the electricity cost is reduced by 12% compared to solution A, equivalent to a saving of more than US\$33 billion per year. Compared to the actual costs in 2012, the saving amounts to billion US\$46/yr; these savings are discussed further in the next section. Thus, full cooperation guided by optimisation tools such as ERCOM can bring enormous benefits to a national economy, leading to the most cost-effective reduction of CO₂ emissions from the electricity sector. Indeed, the savings attained are of the same order of magnitude as the expected

combined benefits that the implementation of CPP would bring through mitigation of climate change and avoidance of related health impacts, estimated between US\$26 and US\$45 billion in 2030 (EPA, 2015). In addition to the costs reduction, the overall CO₂ emissions are decreased far beyond the 35% target - 70% compared to the base line year. Furthermore, in the case of no-cooperation, CO₂ emissions are reduced by a further 3%. These findings show that, contrary to the claims of the Trump's Administration, pursuing climate change mitigation can bring significant benefits not only for the climate but also for the U.S. economy.

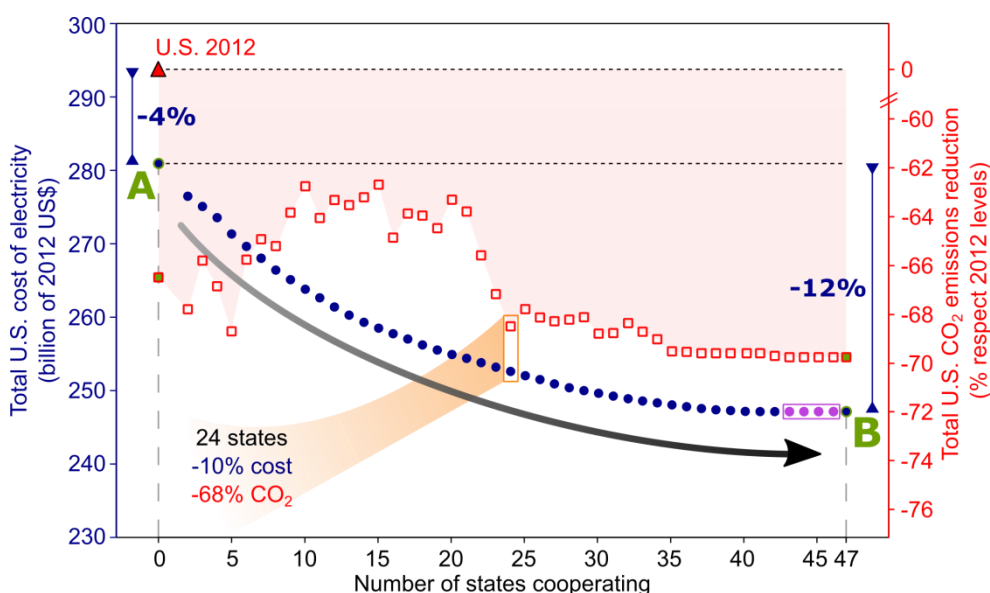


Figure V-1 Optimal cost (primary axis) and emissions (secondary axis) of electricity generation in the U.S. in 2030 as a function of the level of cooperation. Blue dots represent the minimum cost solution obtained with the ERCOM model for each level of cooperation (in 2012 US\$) while red squares and the red-shaded region represent the level of emissions reduction attained (in % with respect to 2012 levels). Solution A corresponds to the case where all states satisfy their CPP targets individually, whereas in solution B all the states cooperate together. The U.S. situation for 2012 is depicted with a red triangle.

We then calculate optimal solutions involving the cooperation of different number of states, obtaining the cooperation curve depicted in Figure V-1. At first, the total electricity cost drops considerably with a small number of states involved in cooperation (~10) and then continues to decline marginally up to the point where 43 states are cooperating (see the cooperation curve in Figure V-1). Beyond this

point, involving the remaining four states (depicted with purple dots in Figure V-1) in the global U.S. partnership incurs no further cost or emission benefits - while they may still participate formally in the electricity trade and emission sharing, in practice they behave independently so neither extra economic or environmental benefits are attained. The cooperation curve divides the search space into two regions, providing a lower bound (i.e. minimum limit) on the total cost that could be attained when a given number of states cooperate. The region below the curve is therefore empty where no feasible solutions exist that entail lower cost than the ones on the curve. The region above the curve contains feasible solutions but they are suboptimal compared to those on the curve. These suboptimal solutions would eventually emerge from decentralised negotiation schemes that may converge towards a Nash equilibrium entailing a certain level of cooperation (Dutta and Radner, 2004; Heitzig et al., 2011; Wood, 2011).

5.3.2 *Implications for electricity supply*

Depending on whether an individualist or a cooperative approach is followed, the optimal U.S. electricity supply system would be different since each approach entails specific compliance options. In solution A, no cooperation is allowed and states would be forced to meet their CPP target individually only by switching to cleaner energy mixes. In solution B (i.e. global U.S. partnership), states are allowed to share targets and exchange electricity which allows for exploiting region-specific abatement costs and availabilities of low-carbon and low-cost sources. Broadly speaking, in both solutions A and B, coal-fired power plants would be almost entirely phased out and natural gas and wind power would become the predominant sources of electricity. At the same time, generation from other renewable sources would be increased while nuclear capacity would be kept constant as specified in the CPP. Overall, the share of renewable sources would increase substantially, contributing 47% of the total U.S. electricity demand in 2030 for solution A and 53% for solution B (Figure V-2).

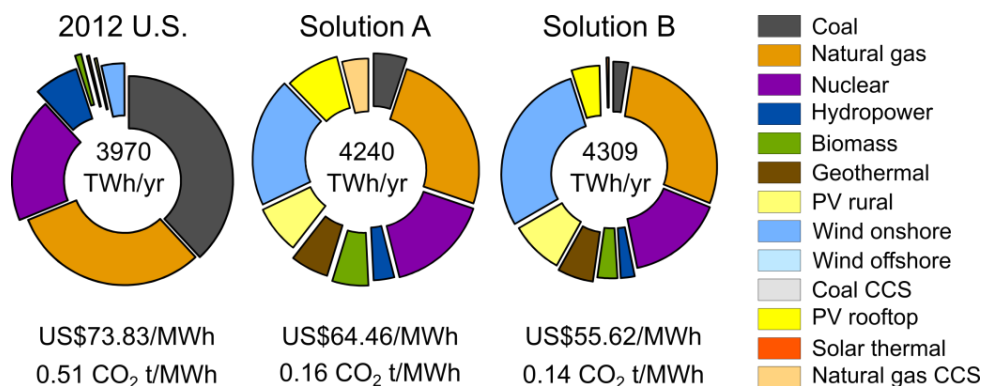


Figure V-2 Global U.S. electricity generation portfolios for 2012 (pie chart on the left), solution A (centre) and solution B (right). Slice colours represent the share of each technology according to the legend. Additionally, the associated levelised cost of electricity (LCOE, in US\$/MWh) and the emissions rate (in CO₂ t/MWh) are depicted together with the pie charts.

Despite similar U.S. electricity portfolios in A and B, the latter entails lower costs and emissions from electricity generation mainly because cooperation allows deploying further low-cost and zero-emitting wind onshore (i.e. 29% in B comparing to 20% in A of the total electricity generation). Conversely, in solution A, more coal, natural gas with CCS and biomass would be required to ensure the system reliability due to the intermittency of wind and solar power used in some states (see section 5.7.2.1 in Appendix for a breakdown by state of the cost-optimal electricity system in solution A). As a result of the compliance advantages emerging from the cooperation, the global U.S. levelised cost of electricity (LCOE) in solution B would be further reduced to US\$55.6/MWh compared to US\$64.46/MWh in solution A; while the global U.S. carbon intensity would be 0.14 CO₂ t/MWh in solution B compared to 0.16 CO₂ t/MWh in solution A.

Further analysis of solution B shows the implications of full cooperation at the state level (Figure V-3). The breakdown of the global U.S. partnership reveals that, although coal electricity would be displaced in most states (from 38% of the total U.S. electricity generation in 2012 to 2% in 2030), it would remain constant in six states (Arkansas, Wyoming, North Carolina, Tennessee and North and South Dakota), where it would be used to back up the intermittent wind and solar PV.

Other states would rely on natural gas and nuclear, which would represent 52% and 24% of the total base-load generation. Natural gas would become the predominant source (more than 80%) in some north-eastern states, such as Rhode Island, Connecticut, Massachusetts, New Jersey, New York and New Hampshire. Nuclear installed capacity would be kept constant in all states, as specified in the CPP, and would represent all the electricity generated in Pennsylvania and almost all (more than 85%) in Michigan, Wisconsin and Virginia. Overall, electricity from renewable sources would supply 53% of the U.S. power needs in 2030, with onshore wind and solar PV generation increasing substantially in many states. Solar PV would grow in Florida, Nevada, Colorado, Utah, Minnesota and Delaware to provide more than one third of their total generation. Onshore wind would be installed in 26 states and become the dominant source of power in Washington, New Mexico, Texas, Oklahoma, Indiana, Maine, Missouri, West Virginia, South Dakota, Nebraska and Wyoming. Additionally, geothermal resources would be exploited in Western states (California, Arizona, Colorado, Idaho, Montana, New Mexico, Nevada, Utah, Washington and Wyoming), while biomass would be deployed in Louisiana, Mississippi, Tennessee, Georgia and South and North Carolina. Concentrated solar thermal would be installed in South Dakota, reaching 10% of the total share, and to a much lesser extent in Florida (less than 1%). The model decides in turn to rule out offshore wind and both coal and natural gas with CCS, which are at present economically less competitive than the other options.

Analysing the electricity trade, four groups of states would emerge: (i) states that would export electricity without importing it (e.g. Florida, Oklahoma, South Dakota, Nevada and Indiana); (ii) states that would import electricity without exporting (e.g. Arizona, California, Illinois and New Jersey); (iii) states that would export and import electricity (e.g. New York, Pennsylvania, Tennessee and Texas); and (iv) states not trading electricity at all (like Maine, Montana and North Dakota, which satisfy their demand with domestically generated electricity). Furthermore, Washington, Michigan and Wisconsin would import hydro-electricity from Canada.

In total, four states would act as key suppliers providing clean and low-cost electricity. Oklahoma and Indiana would increase their generation substantially to provide wind-based electricity while Florida and Nevada would do the same providing solar-rich electricity.

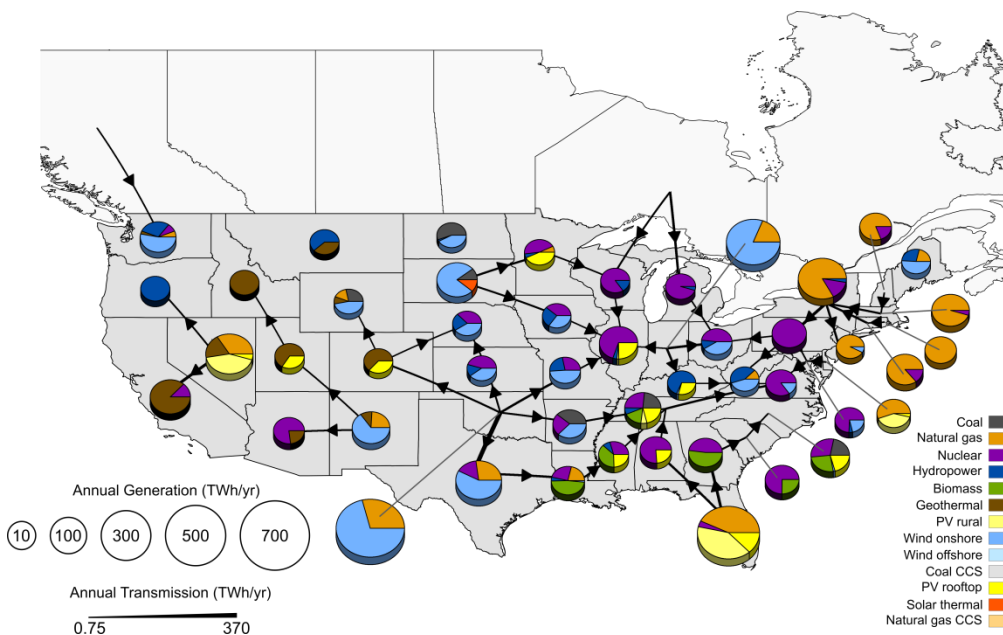


Figure V-3 Geographical breakdown of the U.S. cost-optimal electricity system in 2030 for solution B (full cooperation in Figure V-1). The size of the pie charts is proportional to the electricity generation in each state (MWh/yr) whereas the slice colours denote the technology and the slice sizes represent the associated percentage share. Arrows illustrate the electricity trade between the U.S. states and Canada, with their thickness proportional to the amount of electricity traded.

Note that the cost-optimal cooperative solution shown in Figure V-3 should be understood as a roadmap to guide the most cost-effective path for the transition to a low-carbon electricity sector. Coordinating where and how much infrastructure needs to be built would require further discussions with relevant stakeholders, considering economic, political and social concerns; this is beyond the scope of this paper.

5.3.3 *Implications for carbon mitigation*

In the absence of cooperation, switching to low-carbon electricity options is the only strategy that can reduce carbon emissions, while in the cooperation approach, cross-border imports of electricity and sharing of the emissions cap are also allowed. These mitigation strategies are implemented in solution B. As shown in Figure V-4, the majority of the states would reduce their carbon intensity (41 out of 47) and become net importers of electricity (31), while only a few (11) would emit above their CO₂ target and rely on burden sharing to offset their emission excess. For example, Kentucky would reduce its carbon intensity by 100%, while others, such as New Jersey, would increase its carbon intensity by 78%. Analysing the cross-border electricity flows, some states would emerge as net exporters of electricity while others would be net importers. For instance, Oklahoma would be a net exporter that sells a total of 596 TWh of electricity to Kansas, Colorado, Texas, Missouri and Arkansas, whereas Texas would be a net importer that would purchase more electricity from Oklahoma (328 TWh) than it would sell to Louisiana (102 TWh, a net balance of -226 TWh). The analysis of the emissions reveals that Texas, California, Pennsylvania and Ohio would reduce their territorial emissions beyond their CPP target in order to offset those in the states that exceed theirs (e.g. New York, Oklahoma, Nevada and Florida). This reduction in emissions would not necessarily imply deploying a low-carbon electricity mix, since it could also be the result of reducing electricity generation. The latter would happen in New Jersey, which would increase its carbon intensity by deploying more natural gas (from 44% to 93%) -selected due to its economic competitiveness- but would offset this by decreasing its total domestic electricity generation by almost 20%. In practice, most states would rely on a combination of mitigation strategies. Texas, for instance, would emit below its original CPP target by becoming a net importer of electricity and by implementing a lower-carbon mix. On the contrary, New York would implement a more carbon-intensive mix and become a net exporter of electricity, but would offset its excess of emissions by sharing its carbon burden. Ultimately, all

these strategies would give rise to an imbalance between states emitting below or above their CPP targets, where the overall emissions at the U.S. level would be finally reduced by 70%, instead of the required 35%. Compared to the no cooperation model (solution A in Figure V-1), the overall annual reduction in emissions would amount to 66 Mt CO₂. This reduction would be attained because increasing the share of low-carbon technologies would be economically appealing, despite requiring a base-load capacity to ensure system reliability when intermittent renewables would be used (Heuberger et al., 2016; MacDonald et al., 2016; NREL, 2012). Thus, these results show that the most cost-effective mitigation pathway, emerged from the centralised approach, would ultimately lead to state emissions levels which are totally different from the original targets proposed by the CPP (some states would exceed their original limit while others would compensate for these extra emissions). In addition to this mismatch, there would also be cost implications that are discussed in more detail in the next section.

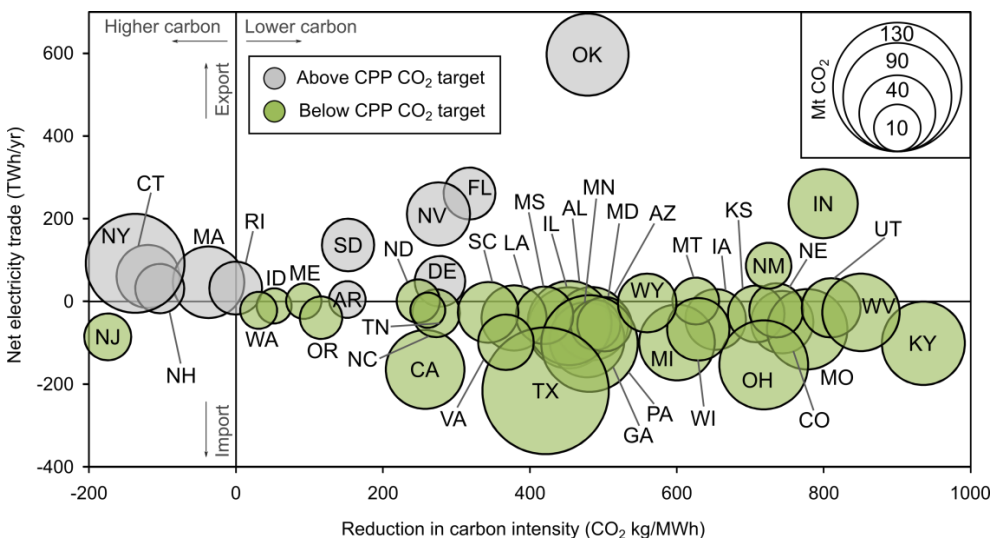


Figure V-4 State mitigation strategies under full cooperation (solution B in Figure V-1). Each bubble corresponds to one state, for which three values are shown: (i) the reduction in carbon intensity relative to the baseline year of 2012 (x-axis); (ii) the net electricity trade (y-axis) (the values for (i) and (ii) are represented by the centre of the bubble); and (iii) the difference in emissions between the CPP target and solution B (denoted by the size of the bubble, with the grey bubbles representing the states emitting above their CPP target and the green the states with the emissions below their target).

5.3.4 *Implications for costs*

We next analyse in detail the distribution of economic efforts resulting from the multiple patterns described previously. To this end, we compare the electricity costs in solutions A and B for every U.S. state (Figure V-5). Thirty states would benefit when moving from A to B, while 14 would be penalised and only three (Montana, North Dakota and Wisconsin) would experience no change. Oklahoma would be the most penalised state when moving from an individualist strategy towards the global U.S. partnership. It would increase its electricity generation by a factor of nine, mainly by deploying a substantial capacity of onshore wind (70% of the electricity portfolio) to supply electricity to neighbouring states. This is due to its significant wind potential (best capacity factor among all states), which would allow the state to provide low-cost and zero-emitting electricity to satisfy the demand of other states. Similarly, Florida and Nevada would also incur extra costs because they would have to increase their electricity generation so as to exploit their solar potential and provide low-carbon power to neighbouring regions. Unlike these states, Texas, California, Kentucky and Ohio would import part of their electricity to satisfy their demand, thereby reducing their investment in domestic facilities. In particular, Ohio would be the state benefitting the most, reducing its generation by six-fold by importing most of its electricity demand. On the other hand, Maine would generate the same amount of electricity in solutions A and B, but it would lose out in the cooperation because it would require replacing natural gas by more expensive onshore wind. By doing so, part of the natural gas potential in Maine would then be used in other states which would otherwise incur a higher levelised cost of electricity (LCOE).

As can be seen, under full cooperation some states would benefit by joining the global U.S. partnership and would therefore be willing to collaborate; however, others would be penalised and would require incentives to prevent them from leaving the global partnership.

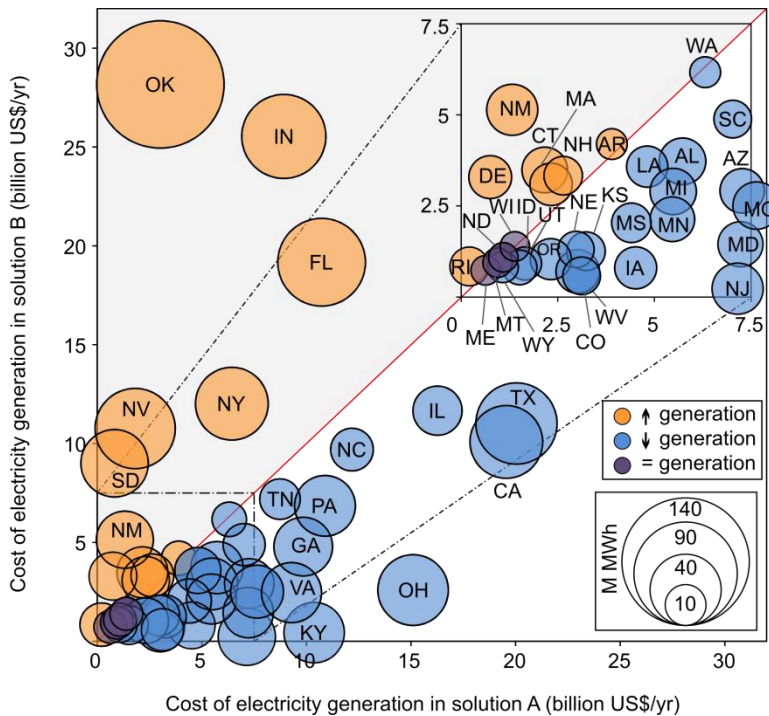


Figure V-5 Comparison of the cost of electricity generation in the different U.S. states for solutions A and B. Each state is depicted by a bubble, where the centre of the bubble represents the cost of electricity generation for solution B (y-axis) and solution A (x-axis). The states on the diagonal (solid red line) have the same electricity generation cost for both solutions; those below the diagonal benefit from cooperation and those above it are penalised. The size of the bubbles indicates the difference in electricity generation between solutions A to B. The colour code is as follows: the orange colour denotes an increase in generation, the blue a decrease and the purple no change. The inset in the top right-hand corner represents the magnified results shown in the bottom left-hand corner of the graph within the dotted square.

5.3.5 *Sharing of cooperation benefits*

The global U.S. partnership would entail an uneven distribution of efforts that might deter the penalised states from participating. Appropriate mechanisms and policies would be therefore required to incentivise cooperation and avoid missing the significant potential benefits of cooperating. These benefits should be shared in a fair manner among all states in order to engage them in a collective action. To harmonise the benefits of participating in the global partnership, each part could receive the same dividend according to the equality principle. Following this premise, costs in the cooperation would be redistributed in such a way that each

state would achieve the same cost reduction when transitioning from solution A (individual) to B (cooperative), which in this case corresponds to a 12% cost reduction. This rule is illustrated in Figure V-6, which can be derived from Figure V-5 after allocating the overall 12% of cost reduction among the U.S. states.

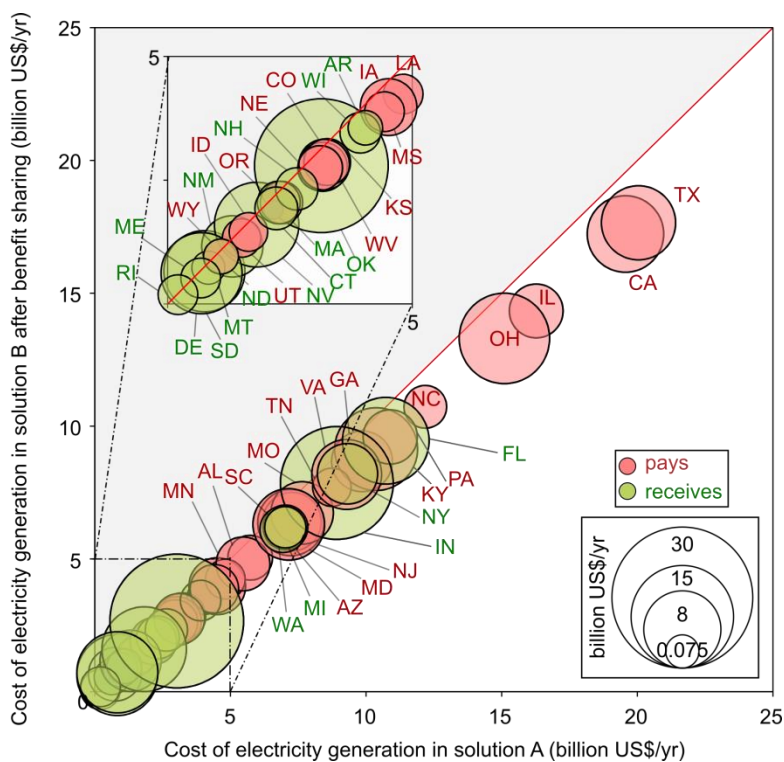


Figure V-6 Costs of electricity generation in different U.S. states after sharing cooperation dividends. Each state is depicted by a bubble, where the centre of the bubble represents the cost of electricity generation for solution B after sharing the benefits (y-axis) and the cost of solution A (x-axis). States on the diagonal (solid red line) have the same electricity generation cost for both solutions; those below the diagonal benefit from the cooperation and those above it are penalised. The size of the bubbles indicates the amount of the compensation payments, where red colour denotes states which contribute to the global partnership and green colour states which receive payments. The inset in the top left-hand corner represents the magnified results shown in the bottom left-hand corner of the graph within the dotted square.

As seen, after splitting the cooperation dividends, all states would benefit in the global partnership (all states would lie below the diagonal). As an example, in solution A, Oklahoma would incur a cost of US\$3.01 billion/yr, while in solution B its cost would be US\$2.66 billion/yr, that is, 12% cheaper. Obviously, the new

distribution of costs would require establishing transfer payments between states originally benefitting and being penalised when cooperating (Figure V-7). Particularly, 28 states would have to contribute to the global partnership (i.e. payments to the central partnership administration), while 19 states would receive compensation payments (i.e. receive payments from the central administration). Within the first set of states, we would find Ohio, deemed as the state benefitting the most from the cooperation, that would have to contribute to the partnership with US\$10.7 billion/yr, resulting in a final total cost of US\$13.3 billion/yr (12% lower than its cost in the individualist strategy). Conversely, Oklahoma, the most penalised state in the global partnership, would receive US\$25.5 billion/yr. To ensure a fair and reliable process, these compensation payments should be managed by the centralised U.S. partnership administration via tailored financial mechanisms.

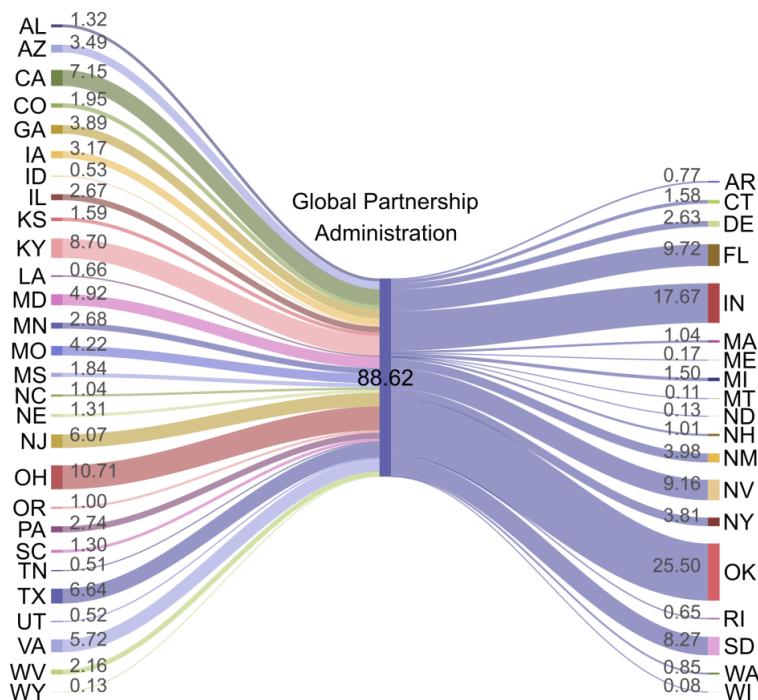


Figure V-7 Compensation payment scheme to spur cooperation. In the Sankey flow diagram, states on the left would contribute (pay) to the global partnership administration, while states on the right would receive compensation payments. The thickness of the flows is proportional to the payment made or received (billion US\$/yr).

Alternative sharing schemes could be applied based on additional fairness principles besides equality (e.g. equity, proportionality, capacity) (Phillips, 1997; Ringius et al., 2002), which would further assess the contributions made by each state, both as a producer and a consumer (see section 5.7.2.2 in Appendix for further discussion on this topic). Designing a sharing scheme perceived as “fully fair” by all participants might be extremely hard and further complicated by the fact that these alternative sharing schemes could incorporate other additional benefits (e.g. jobs creation, energy security and tax revenue) and environmental impacts (e.g. land use, water scarcity and deforestation), in addition to climate change (Laurent and Espinosa, 2015).

5.3.6 *Cooperation benefits under uncertainty*

All the calculations discussed previously were repeated considering the main uncertainties present in the ERCOM model in order to assess their impact on the outcome of the optimisation. To this end, ERCOM was solved iteratively for different potential values (scenarios) of the uncertain parameters (e.g. future electricity demand, capacity factors, potential of each electricity technology, etc.), which were modelled using probability distributions and sampling methods. The additional results of this sensitivity analysis, discussed further in section 5.7.3 of the Appendix show that benefits from cooperation are always high regardless of the scenario analysed, with the cost savings ranging between 11.5% and 17.9% compared to the individualist approach, and the emissions reduction between 43% and 74% with respect to 2012 levels.

5.4 **Conclusions**

The current global context calls for advanced mechanisms to optimise collective actions and articulate cooperation in climate change mitigation. In an ideal world, centralised solutions would be implemented and globally optimal decisions made for the sake of the common action against climate change. In a real world, many conflicting interests exist and consensus must be reached at the

expense of global optimality. We envision herein a scheme underpinned by optimisation tools to aid climate change mitigation in a more cost-effective and transparent manner. Following this approach, a centralised globally optimal solution would be first determined to make individual states aware of the potential benefits of cooperating among them. The opportunity cost of sacrificing global optimality, properly quantified via rigorous tools, should become a major driver to spur cooperation among states. In a second step, the global cooperation benefits should be shared in a fair manner among the parties involved, providing a basis to kick off negotiations for the joint carbon mitigation action.

We applied this approach to a U.S. policy originally aimed at reducing carbon emissions from electricity generation but currently being withdrawn – the Clean Power Plan - to demonstrate how the emission targets could be met while attaining significant reductions in costs, thereby potentially boosting the U.S. economy. This could be accomplished via cooperation, even at low levels of engagement; for example, a 10% reduction in cost would be achieved with only half of the states cooperating while leading to emission reductions nearly double the overall CPP target (68% compared to 35%). Benefits from cooperation would result from sharing emission limits and trading electricity, both of which would lower the abatement costs by implementing the best technologies in the best locations.

The uneven distribution of territorial capacities, which constitutes the basis of the overall cooperation gains, would entail also an asymmetric distribution of efforts, where some states would be economically penalised when moving from an individualist strategy to a cooperative one. Hence, the collective gain of cooperation, albeit necessary, would not be self-sufficient to ensure the participation of all the parties involved. A fair sharing of the cooperation dividends may act as a compensation mechanism to spur the collective action towards carbon mitigation since all states would benefit by joining the global partnership, therefore making such move appealing for all of them. Further analysis of the globally optimal

solution could be carried out including production-based and consumption-based data as well as socio-economic benefits and environmental impacts. In reaching an agreement, states should be flexible and understand that no perfect sharing mechanism might exist that can satisfy fully all the regions involved. Hence, efforts should focus on finding “reasonable” sharing schemes based on optimised solutions where all can benefit from cooperating.

Despite the savings in cost and emissions derived from cooperation, among other potential benefits, translating agreements into practical actions might still be challenging due to the existence of multiple stakeholders with conflicting goals and a wide range of disparate regulations at the regional level. A centralised authority could help in this task by establishing a common harmonised regulatory framework that would align the interests of private and public bodies while being consistent with the optimal roadmap identified via optimisation.

This work thus opens new avenues to develop customised schemes to aid carbon mitigation negotiations. Regardless of the approach followed, we have clearly illustrated that optimised solutions and sharing of the cooperation dividends in a fair manner should be key ingredients in any process aiming at reaching mutually beneficial collective agreements. We show here that we do have the tools available to quantify such benefits in an objective, clear, systematic and transparent manner, and that the potential benefits of cooperation can be significant and fully justify the efforts spent in finding agreements.

Overall, the CPP and similar initiatives for coordinating efforts against climate change in different countries (e.g. Five Years Plans in China, the Brazilian National Plan on Climate Change, the Clean Energy Plan in Australia, the National Climate Change Response Green Paper in South Africa, or the Climate Change Act in the United Kingdom) offer a unique opportunity to test, validate and refine approaches like the one envisioned here, which could ultimately be used at the international level to tackle greater coordination challenges, such as the Paris Agreement.

Today, there seems to be a general scientific consensus on the need to undertake stronger actions against climate change in the short term. In this contribution, we leave aside the controversial politicisation and polarisation of this topic in the U.S. and focus on providing sound scientific evidence of the potential benefits of curbing emissions in cooperation following optimised roadmaps generated with mathematical tools. These results, however, might trigger further fruitful discussions on climate change mitigation and open a deeper debate on whether the U.S. Administration should reconsider its decision to withdraw from the Paris Agreement and join again the partnership for global climate action. Even if full cooperation remains elusive, our proposed approach demonstrates that cooperation of only a few parties can lead to significant economic and environmental benefits which may entice more states to join the new U.S. Climate Alliance, whose members pledge to take climate action regardless of what the federal government decides.

5.5 Acknowledgements

G.GG thanks the Spanish Ministry of Education and Competitiveness (CTQ2016-77968-C3-1-P, MINECO/FEDER) for the financial support received. C.P, G.GG and N.MD thank the financial support from NERC - Natural Environment Research Council (PSD202).

5.6 References

82 FR 16329, 2017. Announcement of review of the Clean Power Plan. Federal Register Volume 82, Issue 63 (April 4, 2017).

Bahn, O., Haurie, A., Kyreos, S., Vial, J. -P., 1998. Advanced mathematical programming modeling to assess the benefits from international CO₂ abatement cooperation. *Environ. Model. Assess.* 3, 107–115. doi:10.1023/A:1019062806256

Cole, D.H., 2015. Advantages of a polycentric approach to climate change policy. *Nat. Clim. Chang.* 5, 114–118.

DOE, 2015. Quadrennial technology review. An assessment of energy technologies and research opportunities. Department of Energy of the United States of America.

Dutta, P.K., Radner, R., 2004. Self-enforcing climate-change treaties. *Proc. Natl. Acad. Sci.* 101, 5174–5179. doi:10.1073/pnas.0400489101

EPA, 2015. Clean Power Plan for existing Power Plants. Environmental Protection Agency.

European Commission-Joint Research Center, 2014. GHG emissions time series 1990-2012 per region/country.

Exec. Ord. No. 13783, 2017. Executive Order No. 13783 “Promoting Energy Independence and Economic Growth” (March 4, 2017).

Fripp, M., 2012. Switch: A Planning Tool for Power Systems with Large Shares of Intermittent Renewable Energy. *Environ. Sci. Technol.* 46, 6371–6378. doi:10.1021/es204645c

Hallegatte, S., Rogelj, J., Allen, M., Clarke, L., Edenhofer, O., Field, C.B., Friedlingstein, P., van Kesteren, L., Knutti, R., Mach, K.J., Mastrandrea, M., Michel, A., Minx, J., Oppenheimer, M., Plattner, G.-K., Riahi, K., Schaeffer, M., Stocker, T.F., van Vuuren, D.P., 2016. Mapping the climate change challenge. *Nat. Clim. Chang.* 6, 663–668.

Hardin, G., 2009. The Tragedy of the Commons*. *J. Nat. Resour. Policy Res.* 1, 243–253.

Heitzig, J., Lessmann, K., Zou, Y., 2011. Self-enforcing strategies to deter free-riding in the climate change mitigation game and other repeated public good games. *Proc. Natl. Acad. Sci. U. S. A.* 108, 15739–15744. doi:10.1073/pnas.1106265108

Heuberger, C.F., Staffell, I., Shah, N., Mac Dowell, N., 2016. Quantifying the value of CCS for the future electricity system. *Energy Environ. Sci.* 9, 2497–2510. doi:10.1039/C6EE01120A

Höhne, N., den Elzen, M., Escalante, D., 2014. Regional GHG reduction targets based on effort sharing: a comparison of studies 14, 122–147. doi:10.1080/14693062.2014.849452

Jacobson, M.Z., Delucchi, M.A., Bazouin, G., Bauer, Z.A.F., Heavey, C.C., Fisher, E., Morris, S.B., Piekutowski, D.J.Y., Vencill, T.A., Yeskoo, T.W., 2015. 100% clean and renewable wind, water, and sunlight (WWS) all-sector energy roadmaps for the 50 United States. *Energy Environ. Sci.* 8, 2093–2117.

Keohane, R.O., Victor, D.G., 2016. Cooperation and discord in global climate policy. *Nat. Clim. Chang.* 6, 570–575.

Laurent, A., Espinosa, N., 2015. Environmental impacts of electricity generation at global, regional and national scales in 1980–2011: what can we learn for future energy planning? *Energy Environ. Sci.* 8, 689–701.

Lenton, T.M., 2014. Game theory: Tipping climate cooperation. *Nat. Clim. Chang.* 4, 14–15.

Lewis, N.S., 2016. Aspects of science and technology in support of legal and policy frameworks associated with a global carbon emissions-control regime. *Energy Environ. Sci.* 9, 2172–2176.

Loulou, R., Goldstein, G., Noble, K., 2004. Documentation for the MARKAL Family of Models. Energy Technology Systems Analysis Programme.

MacDonald, A.E., Clack, C.T.M., Alexander, A., Dunbar, A., Wilczak, J., Xie, Y., 2016. Future cost-competitive electricity systems and their impact on US CO₂ emissions. *Nat. Clim. Chang.* 6, 526–531.

Nelson, J., Johnston, J., Mileva, A., Fripp, M., Hoffman, I., Petros-Good, A., Blanco, C., Kammen, D.M., 2012. High-resolution modeling of the western North American power system demonstrates low-cost and low-carbon futures. *Energy Policy* 43, 436–447. doi:10.1016/j.enpol.2012.01.031

NREL, 2012. National Renewable Energy Laboratory. Renewable Electricity Futures Study Report No. NREL/TP-6A20-52409.

Petrosjan, L., Zaccour, G., 2003. Time-consistent Shapley value allocation of pollution cost reduction. *J. Econ. Dyn. Control* 27, 381–398. doi:10.1016/S0165-1889(01)00053-7

Phillips, R.A., 1997. Stakeholder theory and a principle of fairness. *Bus. Ethics Q.* 7, 51–66.

Raupach, M.R., Davis, S.J., Peters, G.P., Andrew, R.M., Canadell, J.G., Ciais, P., Friedlingstein, P., Jotzo, F., van Vuuren, D.P., Le Quere, C., 2014. Sharing a quota on cumulative carbon emissions. *Nat. Clim. Chang.* 4, 873–879.

Ringius, L., Torvanger, A., Underdal, A., 2002. Burden Sharing and Fairness Principles in International Climate Policy. *Int. Environ. Agreements* 2, 1–22. doi:10.1023/A:1015041613785

Safaei, H., Keith, D.W., 2015. How much bulk energy storage is needed to decarbonize electricity? *Energy Environ. Sci.* 8, 3409–3417.

Sandler, T., 2004. *Global Collective Action*. Cambridge University Press.

Schmidt, R.C., 2015. A balanced-efforts approach for climate cooperation. *Nat. Clim. Chang.* 5, 10–12.

Smead, R., Sandler, R.L., Forber, P., Basl, J., 2014. A bargaining game analysis of international climate negotiations. *Nat. Clim. Chang.* 4, 442–445.

Tavoni, A., 2013. Game theory: Building up cooperation. *Nat. Clim. Chang.* 3, 782–783.

UNFCCC, 2017. United Nations Framework Convention on Climate Change -- 20 Years of Effort and Achievement Key Milestones in the Evolution of International Climate Policy [WWW Document]. URL <http://unfccc.int/timeline/> (accessed 7.11.17).

Unger, T., Ekvall, T., 2003. Benefits from increased cooperation and energy trade under CO₂ commitments—The Nordic case. *Clim. Policy* 3, 279–294.

US Energy Information Administration, 2011. The Electricity Market Module of the National Energy Modeling System: Model Documentation Report Report No. DOE/EIA-M068.

Wood, P.J., 2011. Climate change and game theory. *Ann. N. Y. Acad. Sci.* 1219, 153–170. doi:10.1111/j.1749-6632.2010.05891.x

5.7 Appendix: methods, supplementary results and sensitivity analysis

This section contains the supplemental materials for the article “Time for global action: Optimised cooperative approach towards effective climate change mitigation”. The Appendix is organised as follows. First, the methods are explained including the description of (i) the Emissions Reduction Cooperation Model (ERCOM) (mathematical formulation, data and assumptions), (ii) some additional results are presented and (iii) the results sensitivity analysis applied to handle uncertainties are shown. . Finally, the nomenclature and acronyms are described and the list of references is provided.

5.7.1 *Methods*

5.7.1.1 *Problem statement*

We aim to quantify the benefits of tackling climate change by meeting a set of individual emissions reduction targets acting in cooperation. To do so, we consider as test bed the U.S. Clean Power Plan (EPA, 2015) which establishes individual state emissions reduction targets to curb CO₂ emissions from the U.S. power sector by 35% from 2012 baseline levels.

Essentially, we are given a set of regions (i.e. U.S. states) that need to reduce their CO₂ emissions from electricity generation by acting either as isolated entities or in cooperation. Emissions reduction targets are provided for every state, which can be met individually in every region or in cooperation (i.e. establishing partnerships so that the joint emissions fall below the summation of individual targets, while some regional targets might be exceeded as long as others compensate them). Each region is considered as a load area with a specific electricity demand. We are also given a set of potential technologies for electricity generation for which their carbon intensities and costs data in every region are known. The goal of the analysis is then to determine the optimal portfolio of technologies and electricity trades between regions that satisfy the electricity

demand at minimum cost while not surpassing the emissions targets.

To carry out this analysis, we have developed a mixed-integer linear programming (MILP) model, referred to as ERCOM (Emission Reduction Cooperation Model) that will be described in detail in the ensuing section. ERCOM is capable of systematically identifying the most cost-effective ways of meeting the U.S. electricity demand for different levels of cooperation among states.

5.7.1.2 *ERCOM model*

The model proposed herein minimises the U.S. electricity generation cost while satisfying the emissions targets imposed in the Clean Power Plan (EPA, 2015) (CPP) for different levels of cooperation among states. Specifically, the optimisation is performed for 2030, which is the policy horizon in the CPP. The model, referred to as ERCOM henceforth (as an acronym of Emissions Reduction Cooperation Model), takes the form of a mixed-integer linear program (MILP) where binary variables denote whether states meet their targets in partnerships or acting independently, while continuous ones represent technologies capacities, electricity generation, inter-state electricity flows and electricity trades with Canada. ERCOM considers U.S. states as load demand areas which are interconnected among them by transmission lines. The set of potential options for power generation includes coal, natural gas, nuclear, hydropower, solar, wind, geothermal and biomass. Furthermore, ERCOM ensures the reliability of the system by enforcing the use of back-up generation based on firm technologies (which make up for power drops in power supply from intermittent renewable sources). The cost of both standard and back-up generation is assessed via the levelised cost of electricity (i.e. LCOE), which considers operating and capital costs, annualised over their expected lifetime.

The model provides a lower bound on the U.S. electricity generation cost for a given number of states cooperating in partnerships. For simplicity, we do not calculate the specific partnerships that could be formed (i.e. how many partnerships exist and which states cooperate within each one), but rather assume the existence

of a global partnership encompassing all the states willing to cooperate. This assumption simplifies the combinatorial complexity of the problem. Further details on the model formulation and assumptions are provided in the ensuing sections.

5.7.1.2.1 Mathematical formulation

The ERCOM model comprises three main blocks of equations: those related to carbon emissions, load-meeting constraints and equations required to compute the cost of electricity generation. These blocks of equations are presented and described in detail next. Note that we use italic font to represent variables along the text.

Carbon emissions

The CPP imposes specific reduction targets on the territorial (i.e. production-based) CO₂ emissions of every state j (parameter TARG _{j}). Such targets must be met by every state either individually or by sharing them with those states belonging to the global partnership. To model this, we introduce binary variable Y_j , which takes a value of one if state j belongs to the global partnership and zero otherwise. This binary variable is then used in the following equation (Eq. V-A1):

$$EM_j \leq \text{TARG}_j + Y_j M1 \quad \forall j \quad \text{Eq. V-A1}$$

Here, EM_j is a continuous variable that represents the CO₂ emissions of state j and $M1$ is a sufficiently large parameter. This equation works as follows: when state j addresses the CPP individually, the binary variable is zero and enforces the term $Y_j M1$ to be zero as well, so the corresponding target TARG _{j} is imposed on the states' emissions. Conversely, when state j belongs to the global partnership, the binary variable is one and the term $Y_j M1$ takes a very big positive value (i.e. $M1$), thereby relaxing the constraint so that no bound is effectively imposed on its individual emissions. Furthermore, states belonging to the partnership share their targets in a way such that a global partnership emissions cap must be ultimately satisfied, as imposed via Eq. V-A2.

$$\sum_j Y_j EM_j \leq \sum_j Y_j TARG_j \quad \text{Eq. V-A2}$$

That is, the summation of the emissions of those states belonging to the global partnership must not exceed the summation of targets of its individual members. Note that when a state acts independently, Y_j is zero and therefore its corresponding emissions and target disappear from both sides of the inequality. The product of Y_j and EM_j introduces a nonlinear term into the model. To keep it linear and simplify the calculations, we linearise the nonlinear term through the following equations:

$$\sum_j YEM_j \leq \sum_j Y_j TARG_j \quad \text{Eq. V-A3}$$

$$YEM_j \leq EM_j + M1(1 - Y_j) \quad \forall j \quad \text{Eq. V-A4}$$

$$YEM_j \geq EM_j - M1(1 - Y_j) \quad \forall j \quad \text{Eq. V-A5}$$

$$YEM_j \leq Y_j M1 \quad \forall j \quad \text{Eq. V-A6}$$

Following this approach, the product $Y_j EM_j$ in Eq. V-A2 is replaced by continuous variable YEM_j , which is defined via constraints (Eq. V-A4, V-A5 and V-A6). These equations work as follows: when state j cooperates in the partnership (i.e. $Y_j = 1$), the term $M1(1 - Y_j)$ in Eq. V-A4 and Eq. V-A5 vanishes, thus enforcing YEM_j to be equal to EM_j . Eq. V-A6 is then relaxed and does not impose any additional bound on YEM_j . Conversely, when state j does not cooperate in the partnership, then $Y_j = 0$ and Eq. V-A6 forces YEM_j to be zero, while Eq. V-A4 and Eq. V-A5 are relaxed and do not impose any additional bound. Recall that when $Y_j = 0$, the production-based emissions of state j are bounded via Eq. V-A1.

The number of states belonging to the global partnership (denoted by parameter CS) is controlled via Eq. V-A7.

$$\sum_j Y_j = CS \quad \text{Eq. V-A7}$$

As will be later discussed, the model is solved for different values of CS, thereby reflecting different levels of cooperation.

State emissions are calculated from the electricity generated via technology i in each state j and the associated carbon intensity (parameter $CI_{i,j}$), as given by Eq. V-A8. Note that the amount of electricity generated is modelled via continuous variables $GEN_{i,j}^{ST}$ and $GEN_{i,j}^{BU}$, which account for standard and backup generation, respectively.

$$EM_j = \sum_i GEN_{i,j}^{ST} CI_{i,j} + \sum_i GEN_{i,j}^{BU} CI_{i,j} \quad \forall j \quad \text{Eq. V-A8}$$

Note that our model takes into account the need to resort to firm energy sources as ancillary systems so as to satisfy peaks in demand when facing unfavourable weather conditions. This will be explained in more detail later in this document.

Load-meeting constraints

The total amount of electricity generated in state j with technology i is bounded according to the availability of the associated resource in the state (which is denoted by parameter $GEN_{i,j}^{POT}$), as given by Eq. V-A9.

$$GEN_{i,j}^{ST} + GEN_{i,j}^{BU} \leq GEN_{i,j}^{POT} \quad \forall j, i \quad \text{Eq. V-A9}$$

≠ coal, coal CCS, natural gas, natural gas CCS

Eq. V-A9 applies to all the technologies except for those competing for the same resources. Hence, coal-based technologies (i.e. coal and coal with carbon capture and storage (CCS)) compete for coal and are grouped into set CT (i.e. CT = {coal, coal CCS}), as illustrated in Eq. V-A10.

$$\sum_{i \in CT} (GEN_{i,j}^{ST} + GEN_{i,j}^{BU}) \leq GEN_{i',j}^{POT} \quad \forall j, i' = coal \quad \text{Eq. V-A10}$$

Eq. V-A11 is defined for natural gas-based technologies (i.e. natural gas and natural gas CCS), which form the set NGT (i.e. NGT = {natural gas, natural gas CCS}), and consume natural gas.

$$\sum_{i \in NGT} (GEN_{i,j}^{ST} + GEN_{i,j}^{BU}) \leq GEN_{i',j}^{POT} \quad \forall j, i' = \text{natural gas} \quad \text{Eq. V-A11}$$

Furthermore, country-wise bounds on generation are imposed via parameter GEN_i^{POTGLO} on those technologies which consume resources that can be traded between states (i.e. coal, natural gas, biomass, coal CCS and natural gas CCS). In these cases, besides inland potentials, it is necessary to enforce a global limit on the corresponding resource according to its availability in the whole country (Eq. V-A12, Eq. V-A13 and Eq. V-A14).

$$\sum_j (GEN_{i,j}^{ST} + GEN_{i,j}^{BU}) \leq GEN_i^{POTGLO} \quad \forall i = \text{biomass} \quad \text{Eq. V-A12}$$

$$\sum_j \sum_{i \in CT} (GEN_{i,j}^{ST} + GEN_{i,j}^{BU}) \leq GEN_i^{POTGLO} \quad \forall i' = \text{coal} \quad \text{Eq. V-A13}$$

$$\sum_j \sum_{i \in NGT} (GEN_{i,j}^{ST} + GEN_{i,j}^{BU}) \leq GEN_i^{POTGLO} \quad \forall i' \quad \text{Eq. V-A14}$$

= natural gas

The amount of electricity generated (i.e. MWh) is constrained to be lower than the capacity installed (parameters $CAP_{i,j}^{ST}$ and $CAP_{i,j}^{BU}$, in mw). Capacity and generation are linked through the capacity factor (represented by parameter $CF_{i,j}$) and the annual hours (parameter H), as shown in Eq. V-A15 and Eq. V-A16.

$$GEN_{i,j}^{ST} \leq CAP_{i,j}^{ST} CF_{i,j} H \quad \forall i, j \quad \text{Eq. V-A15}$$

$$GEN_{i,j}^{BU} = CAP_{i,j}^{BU} CF_{i,j} H \quad \forall i, j \quad \text{Eq. V-A16}$$

The capacity factor is the ratio between the actual power output and the potential output at full nameplate capacity. This factor takes into account periods in which the plant is either out of service (e.g. due to plant maintenance or limited resources) or operated below its nominal capacity. Note that the bound on standard generation (Eq. V-A15) can be imposed as an inequality, even if the constraint will always be active in the optimal solution (i.e. satisfied as a strict equality). For back-up systems, the equation must be satisfied as a strict equality (Eq. V-A16), as these

technologies must ensure the system reliability.

The CPP does not contemplate installing additional nuclear facilities as a compliance strategy to reduce CO₂ emissions. To model this, Eq. V-A17 fixes the nuclear capacity, modelled by parameter $CAP_{i,j}^{CUR}$, to its present value.

$$CAP_{i,j}^{ST} + CAP_{i,j}^{BU} = CAP_{i,j}^{CUR} \quad \forall j, i = nuclear \quad \text{Eq. V-A17}$$

The model must ensure that power can be dispatched at any time. We therefore differentiate between dispatchable (i.e. coal w/o CCS, natural gas w/o CCS, nuclear, hydropower, biomass, geothermal and solar thermal) and non-dispatchable (i.e. solar PV rural and rooftop and wind onshore and offshore) technologies. The former can be dispatched according to the power demand, while the latter depend on the availability of intermittent resources. Hence, to ensure system reliability it is necessary to support intermittent renewable energies (IR) with ancillary systems such as back-up generation based on firm technologies (both renewable and non-renewable) or energy storage. Here, we consider the former option, which is modelled via Eq. V-A18, where BUC is a parameter providing the capacity of dispatchable technologies that must be installed for every MW of non-dispatchable intermittent technologies, while IR is the set of non-dispatchable technologies requiring ancillary systems (i.e. $IR = \{solar\ PV\ (rural), solar\ PV\ (rooftop), wind\ onshore, wind\ offshore\}$).

$$\sum_{i \notin IR} CAP_{i,j}^{BU} = BUC \sum_{i \in IR} CAP_{i,j}^{ST} \quad \forall j \quad \text{Eq. V-A18}$$

The back-up capacity of intermittent renewables is set to zero, as imposed by Eq. V-A19. Note, that we consider solar thermal CST as a dispatchable technology, since it incorporates thermal storage that allows maintaining a reliable electric power system with high shares of renewables (Lilliestam et al., 2012; Pfenninger et al., 2014; Usaola, 2012).

$$CAP_{i,j}^{BU} = 0 \quad \forall j, i \in IR \quad \text{Eq. V-A19}$$

Electricity transmission plays a key role in the electricity system optimisation, since it allows exploiting the region-specific abatement costs. Inter-state electricity trade is only allowed between neighbouring states (i.e. states j' included in set NU_j) participating in the global partnership (i.e. those for which $Y_j = 1$). Hence, two conditions must be enforced for two states to exchange electricity: that they are neighbours and that they both belong to the global partnership, as given by Eq. V-A20 and Eq. V-A21.

$$TRD_{j,j'}^{ORIG} \leq Y_j M2 \quad \forall j, j' \in NU_j \quad \text{Eq. V-A20}$$

$$TRD_{j,j'}^{ORIG} \leq Y_{j'} M2 \quad \forall j, j' \in NU_j \quad \text{Eq. V-A21}$$

Here, $TRD_{j,j'}^{ORIG}$ is a continuous variable accounting for the amount of electricity that state j imports from state j' , and $M2$ is a sufficiently large parameter. As seen, when both states belong to the global partnership, then the corresponding binary variables are one (i.e. $Y_j = 1$ and $Y_{j'} = 1$), implying that electricity can be exchanged between both provided it does not surpass the allowable limit $M2$. When any (or both) of the states are not in the partnership, then the electricity flow is set to zero.

Additionally, the electricity is subject to losses during transmissions. We model this via Eq. V-A22, which links the electricity transmitted at origin (continuous variable $TRD_{j,j'}^{ORIG}$) to that received at the final destination ($TRD_{j,j'}^{DEST}$) and the associated losses ($TRD_{j,j'}^{LOSS}$).

$$TRD_{j,j'}^{ORIG} = TRD_{j,j'}^{DEST} + TRD_{j,j'}^{LOSS} \quad \forall j, j' \in NU_j \quad \text{Eq. V-A22}$$

That is, the final amount of electricity that reaches state j coming from state j' ($TRD_{j,j'}^{DEST}$) is equal to the initial amount sent from j' ($TRD_{j,j'}^{ORIG}$) minus the losses taking place in between ($TRD_{j,j'}^{LOSS}$). Here, the transmission losses are considered proportional (parameter TLF) to the distance between states j and j' (parameter $DIST_{j,j'}$) and the amount of electricity transmitted:

$$TRD_{j,j'}^{LOSS} = TRD_{j,j'}^{ORIG} DIST_{j,j'} TLF \quad \forall j, j' \in NU_j \quad \text{Eq. V-A23}$$

Electricity imports from Canada represent a key compliance strategy to curb U.S. CO₂ emissions. We allow electricity trades between the southern Canadian provinces (i.e. British Columbia, Alberta, Saskatchewan, Manitoba, Ontario and Quebec) and neighbouring states, regardless of whether these U.S. states participate or not in the partnership. Electricity imports through these transmission lines suffer from energy losses, which are calculated via Eq. V-A24 and Eq. V-A25.

$$TRDCAN_{j,k}^{ORIG} = TRDCAN_{j,k}^{DEST} + TRDCAN_{j,k}^{LOSS} \quad \forall j, k \in NC_j \quad \text{Eq. V-A24}$$

$$TRDCAN_{j,k}^{LOSS} = TRDCAN_{j,k}^{ORIG} \text{DISTCAN}_{j,k} \text{TLF} \quad \forall j, k \in NC_j \quad \text{Eq. V-A25}$$

Here, $TRDCAN_{j,k}^{ORIG}$, represents the electricity sent from Canadian region k to U.S. state j , $TRDCAN_{j,k}^{DEST}$ denotes the electricity reaching the state and $TRDCAN_{j,k}^{LOSS}$ accounts for the electricity lost during transmission. $\text{DISTCAN}_{j,k}$ is a parameter providing the distance between state j and Canadian region k (note that trade is only allowed between neighbour j - k pairs), while TLF represents the transmission losses factor.

Total electricity imports from Canada cannot exceed a given percentage (denoted by parameter CTB) of the U.S. electricity demand (computed as the summation of the demand in each state DEM_j), as illustrated in Eq. V-A26.

$$\sum_j \sum_{k \in NC_j} TRDCAN_{j,k}^{ORIG} \leq \text{CTB} \sum_j \text{DEM}_j \quad \text{Eq. V-A26}$$

where NC_j denotes the set of Canadian regions k which are neighbours to U.S. state j . Moreover, the amount of electricity imported by every state (i.e. imported from other U.S. states as well as from Canada) is bounded by the electricity demand in the state, as shown in Eq. V-A27. This limits the capacity that a state has to act as a transmission node (i.e. a state is not allowed to import large amounts of electricity to later sell them to other states).

$$\sum_{j' \in NU_j} TRD_{j,j'}^{DEST} + \sum_{k \in NC_j} TRDCAN_{j,k}^{DEST} \leq \text{DEM}_j \quad \forall j \quad \text{Eq. V-A27}$$

The demand satisfaction constraint ensures that the electricity demand of each state j , denoted by parameter DEM_j , must equal the domestic electricity generation plus the input flows of electricity and minus the output flows, as illustrated in Eq. V-A28.

$$\begin{aligned} \sum_i GEN_{i,j}^{ST} + \sum_{i \notin IR} GEN_{i,j}^{BU} + \sum_{j' \in NU_j} TRD_{j,j'}^{DEST} \\ + \sum_{k \in NC_j} TRDCAN_{j,k}^{DEST} - \sum_{j' \in NU_j} TRD_{j',j}^{ORIG} & \quad \text{Eq. V-A28} \\ = DEM_j DSF & \quad \forall j \end{aligned}$$

Here, DSF represents a demand satisfaction factor that is included to warrant the reliability of the system. That is, by forcing the system to cover the demand plus a reserve margin (i.e. $DSF > 1$), electricity supply is ensured even in case of outage. Note that demand and supply are matched annually rather than on an hour-per-hour basis. The hour-per-hour demand match is yet enforced by implementing back up generation systems in the supply.

Cost of electricity generation

The objective function of the ERCOM model seeks to minimise the total cost of electricity generation in U.S., denoted by continuous variable $COST^{TOT}$, which is given by the summation of the individual costs in all of the states, as shown in Eq. V-A29.

$$COST^{TOT} = \sum_j COST_j \quad \text{Eq. V-A29}$$

In turn, the cost of electricity generation in each state j (continuous variable $COST_j$) accounts for the state annualised capital costs (continuous variable $COST_j^{CAP}$), annual fixed and variable operating costs (continuous variables $COST_j^{FIX}$ and $COST_j^{VAR}$, respectively), as well as the costs derived from electricity imports from Canada ($COST_j^{CAN}$):

$$COST_j = COST_j^{CAP} + COST_j^{FIX} + COST_j^{VAR} + COST_j^{CAN} \quad \forall j \quad \text{Eq. V-A30}$$

Note that the costs associated to inter-state trades are not considered in Eq. V-A30, since they would cancel out in Eq. V-A29 (i.e. the money paid by the states purchasing electricity is received by states selling it). State capital costs ($COST_j^{CAP}$) are determined from the installed capacity of both, standard and back-up technologies ($CAP_{i,j}^{ST}$ and $CAP_{i,j}^{BU}$), their unitary capital costs ($CO_{i,j}^{CAP}$), their capacity factor ($CF_{i,j}$) and the total annual hours (H), as given by Eq. V-A31.

$$COST_j^{CAP} = \sum_i [(CAP_{i,j}^{ST} + CAP_{i,j}^{BU})CO_{i,j}^{CAP}CF_{i,j}H] \quad \forall j \quad \text{Eq. V-A31}$$

The fixed operating costs of state j , denoted by continuous variable $COST_j^{FIX}$, are determined from the capacity of standard and back-up technologies i that are installed (represented by variables $CAP_{i,j}^{ST}$ and $CAP_{i,j}^{BU}$, respectively), their unitary annual fixed operating costs ($CO_{i,j}^{FIX}$), the capacity factor of each technology i in state j ($CF_{i,j}$) and the total annual hours (H):

$$COST_j^{FIX} = \sum_i [(CAP_{i,j}^{ST} + CAP_{i,j}^{BU})CO_{i,j}^{FIX}CF_{i,j}H] \quad \forall j \quad \text{Eq. V-A32}$$

Furthermore, the variable operating costs in state j ($COST_j^{VAR}$) are estimated from the electricity generated by each technology i (both standard and back-up, that is, $GEN_{i,j}^{ST}$ and $GEN_{i,j}^{BU}$, respectively), and the unitary variable costs of those technologies in that state ($CO_{i,j}^{VAR}$), as shown in Eq. V-A33.

$$COST_j^{VAR} = \sum_i [(GEN_{i,j}^{ST} + GEN_{i,j}^{BU})CO_{i,j}^{VAR}] \quad \forall j \quad \text{Eq. V-A33}$$

The cost of electricity imports from neighbouring Canadian regions k (continuous variable $TRDCAN_{j,k}^{DEST}$) to state j are determined from the electricity flows imported and a unitary selling price (CO^{CAN}) via Eq. V-A34:

$$COST_j^{CAN} = \sum_{k \in NC_j} TRDCAN_{j,k}^{DEST} CO^{CAN} \quad \forall j \quad \text{Eq. V-A34}$$

Finally model ERCOM can be written in compact form as follows:

$$(MCP) \quad \min \quad COST^{TOT}$$

$$s. t. \quad \text{Eqs. (A1, A3 – A34)}$$

The model is solved for different values of the parameter CS (i.e. varying the number of states in the global partnership), starting from the case where states act independently from each other (CS = 0) and ending in the solution where all of them cooperate in a global partnership (CS = 47).

ERCOM was implemented in the General Algebraic Modelling System (Brooke et al., 1998) (GAMS) version 24.4.1. The model features 11,470 continuous variables, 47 binary variables and 8,167 constraints. The model was solved with CPLEX 24.4.6 on an AMD A8-5500 APU with Raedon 3.20 Ghz and 8.0 GB RAM. The solution time of each instance was below 1 CPU second in the aforementioned computer.

5.7.1.3 Data description and assumptions

This section describes the major assumptions made in ERCOM along with the data fed into the model. We first solved the model assuming deterministic values of the parameters and later on investigated the effects of various uncertainties via sensitivity analysis (see section 5.7.1.5 for the procedure followed and section 5.7.3 for the associated results).

5.7.1.3.1 Clean Power Plan: state targets

The CPP (EPA, 2015) was adopted by the U.S. Environmental Protection Agency (EPA) on the 3th August 2015, becoming the first and very big step in U.S. towards climate change mitigation. The overall goal of the CPP is to curb carbon emissions from the power sector by 32% (from 2005 levels) by 2030 (i.e. equivalent to 35% from 2012 baseline levels). To achieve this overall global target, the CPP establishes individual state-by-state targets. In addition, it provides states with enough flexibility to design strategic plans to meet their targets, either acting individually or cooperating with other states.

To set state-specific goals, EPA analysed affordable strategies for each state based on three building blocks: i) switching from coal-powered plants to natural-gas powered plants, ii) increasing low-carbon energy (i.e. increasing renewable energy generation), and, iii) improving the heat-rate of fossil-fuel fired plants to reduce their overall emissions rate. In practice, states have two compliance options, which translate into two types of CPP targets: (i) those imposed on the carbon intensities (rate-based approach) and (ii) those imposed over the total CO₂ emissions (mass-based approach). Without loss of generality, we use here targets on carbon intensities. These targets vary greatly across states (i.e. from 7% in Connecticut to 48% in South Dakota) owing to different electricity mixes, technological feasibilities and costs and emissions reduction potentials for each particular state.

Figure V-A1 displays the U.S. state specific CPP goals (i.e. parameter $TARG_j^{CI}$, represented as a reduction target in the figure) that should be accomplished in 2030. As observed, four states fall in the range 7-14% of emissions reduction level, five states in the range 14-21%, five states in the range 21-27%, eight states in the range 27-34%, 17 states in the range 34-41% and eight states in the range 41-47%. Further details on the calculation of the CPP emissions targets are provided by the U.S. Environmental Protection Agency (<https://www.epa.gov/cleanpowerplan>). These targets on carbon intensities ($TARG_j^{CI}$) are used to establish the state emissions target in ERCOM (i.e. $TARG_j$) via Eq. V-A35.

$$TARG_j = \sum_i GEN_{i,j}^{CUR} (TARG_j^{CI} CI_{i,j}) \quad \forall j \quad \text{Eq. V-A35}$$

Here, $GEN_{i,j}^{CUR}$ is the amount of electricity generated in 2012 with technology i in state j and $CI_{i,j}$ is the carbon intensity associated to that technology and state.

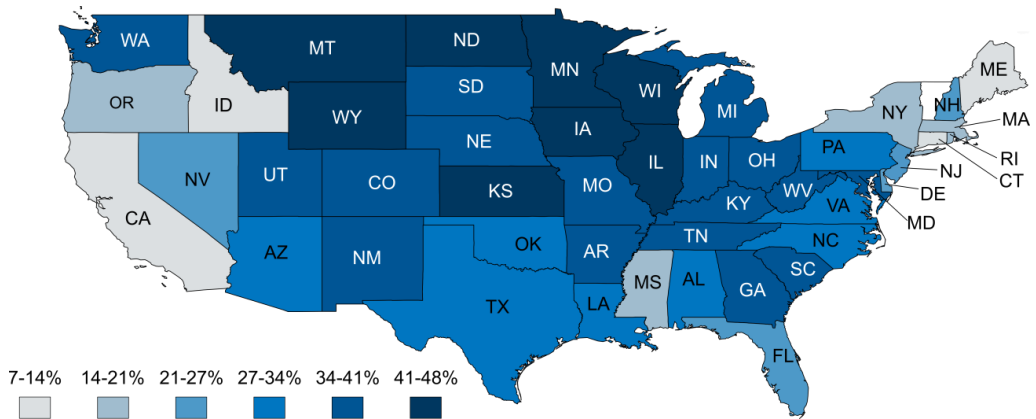


Figure V-A1 State specific emission reduction targets established by the CPP for 2030 referred to 2012 emissions levels. States are coloured according to the scale of emissions reduction targets imposed by the CPP. States labels are in compliance with ISO 3166-2 code.

5.7.1.3.2 Existing technologies capacity and generation

The existing capacities installed in the states along with the annual net generation rates (parameter $GEN_{i,j}^{CUR}$ in Eq. V-A35) for year 2012 were sourced from the Official Energy Statistics of the U.S. Energy Information Administration (EIA) (EIA, 2016a). Pie charts in Figure V-A2 depict the state electricity generation mixes (Subplot V-A2a) as well as the state installed electricity capacity (Subplot V-A2b). As seen, the electricity generation portfolios vary greatly from state to state. Most of the electricity mixes rely on coal, natural gas and nuclear, which are the dominant energy sources of electricity. However, in the Northwest, hydropower has the highest share in the electricity mixes of Washington, Oregon, Idaho, Montana and South Dakota. In addition, wind power (onshore) plays an important role in the northern and central states. Geothermal power is implemented mainly in California and Nevada, while Maine uses large amounts of biomass. Electricity production from Solar PV (both at rural and rooftop levels) is rather low in several states, and the same happens with concentrated solar thermal in Arizona, California and Nevada.

Figure V-A3 shows the global U.S. electricity generation portfolio and capacity for 2012. As can be observed, fossil fuels dominate the U.S. electricity portfolio.

Almost 69% of the electricity in U.S. was generated from fossil coal and natural gas sources, while nuclear represents about 19%. The share of renewables was 11.8%, with hydro power accounting for 7%. As observed, the share of coal and nuclear in terms of power generation is above their share in terms of installed capacity. This is because coal and nuclear technologies provide base load, while natural gas typically covers peak loads and solar and wind renewables are intermittent due to their dependence on climatic conditions.

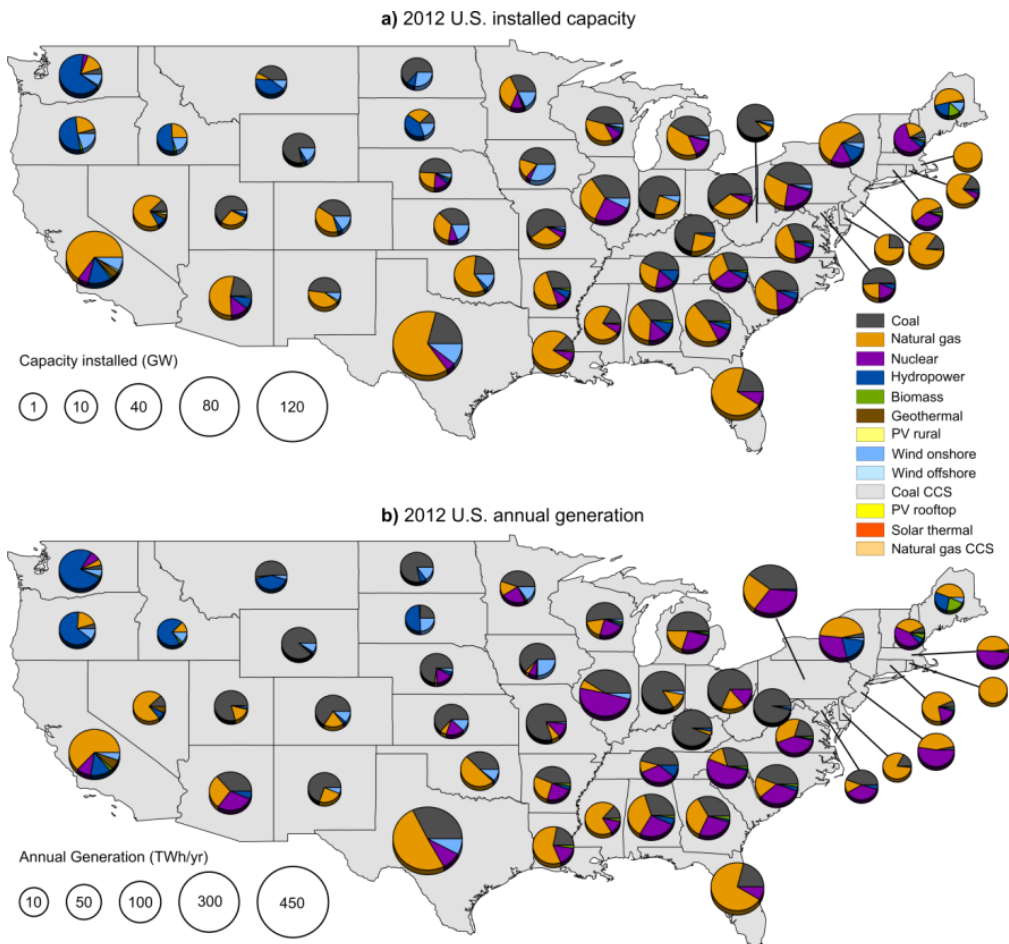


Figure V-A2 U.S. installed capacity and generation for 2012. Subplot V-A2a depicts the installed capacity of each technology in each state in 2012 whereas subplot V-A2b stands for the electricity generation. The size of the pie charts is proportional to the capacity installed and to the electricity generation of each state, respectively, whereas the slice colours denote the technology and the slice sizes represent the associated percentage share.

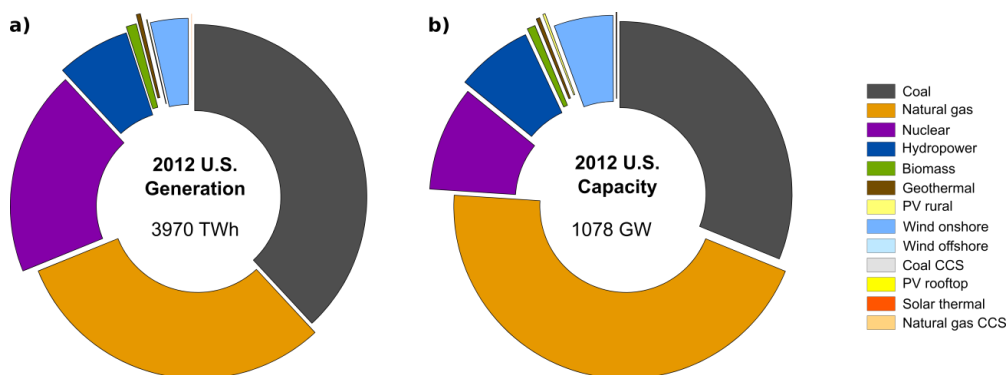


Figure V-A3 Global U.S. generation and installed capacity for 2012. Pie chart on the left (Subplot V-A3a) depicts the global U.S. power generation portfolio while pie chart on the right (Subplot V-A3b) depicts the global U.S. installed capacity. Slice colours represent the share of each technology according to the legend.

5.7.1.3.3 Geospatial and temporal definition: load areas

The U.S. power electricity generation is optimised for 2030, which is the CPP policy horizon. ERCOM is defined at the state level and on an annual basis. Following this approach, the U.S. is divided into 47 load areas corresponding to the states boundaries included in the CPP. Furthermore, we match electricity supply and demand on an annual basis. We consider that the aforementioned geospatial and temporal resolutions are accurate enough for the purposes of our study. In the real operability of the electricity system, however, load and supply need to be balanced on a finer scale. To account for this, we enforce the model to back up the installation of intermittent renewables by means of ancillary systems based on dispatchable technologies, which ensures the reliability of the whole electricity system.

The electricity load (i.e. annual electricity demand) for each state was estimated using the data published by the U.S. Energy Information Administration (EIA) on electricity retail sales by state, which is a good proxy of consumption rates (EIA, 2016a). These data were sourced for the baseline year (i.e. 2012) and forecasted to 2030 by applying a 0.8% average annual growth rate, as projected by the EIA (EIA, 2015). The electricity power demand varies greatly across states

(Figure V-A4), being Texas, California and Florida the states showing the highest electricity demands. Furthermore, we consider a demand satisfaction factor (i.e. parameter DSF) that is set at 1.05 to ensure that the model can cover the electricity demand plus a reserve margin of 5%. This factor further reinforces the reliability of the system (Short et al., 2011).

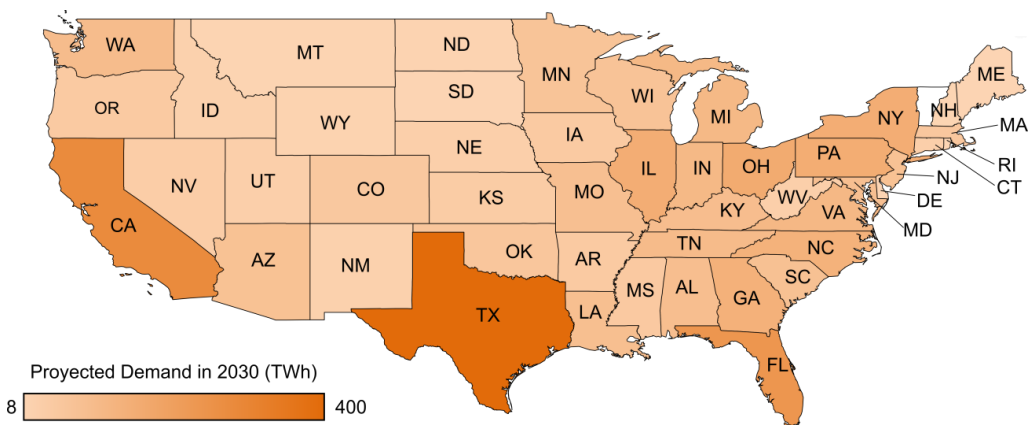


Figure V-A4 Projected annual electricity demands for each load area in 2030. States are coloured according to the scale of the projected electricity demand for 2030 expressed in TWh.

5.7.1.3.4 Transmissions lines

The U.S. electricity transmission network consists of approximately 200,000 miles of high voltage lines that connect generators to distributors in order to transport the electricity to the costumers. Unfortunately, data on the specific location and capacity of all U.S. power lines is missing, as EIA publishes interactive maps of only major electric transmissions lines (>345 kV) in the U.S. territory (see <http://www.eia.gov/state/maps.cfm>). Considering the state spatial resolution, the model assumes that the available U.S. electricity grid connects every U.S. state with its neighbouring states, that is, with those states with which it shares boundaries. Therefore, we model every state as a nodal area connected to neighbouring nodal areas by transmission lines, as depicted in Figure V-A5. Moreover, the CPP enables Canadian imports as a compliance strategy, so international transmission lines between U.S. states and the bordering Canadian provinces are also considered. Line

arcs in the transmission network represent distances between states (parameter $DIST_{ij}$), as calculated with the great circle formula.

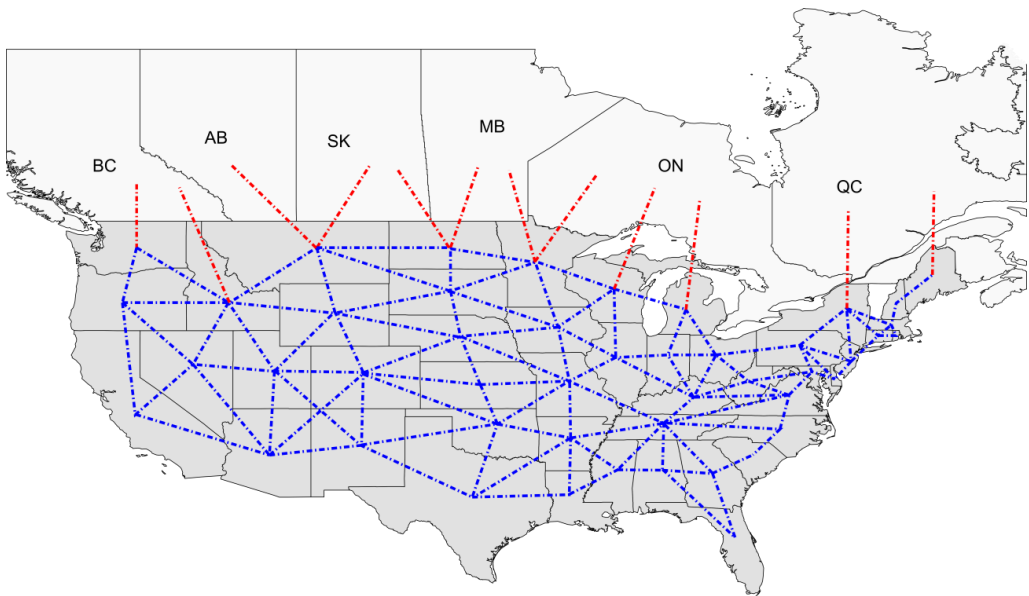


Figure V-A5 U.S. electricity potential transmission network considered in the study. Blue lines represent the transmissions lines whose ends are the nodes that correspond to the U.S. states. Red lines represent the international transmission lines with the Canadian provinces. Canadian provinces are labelled according to the ISO 3166-2 code.

5.7.1.3.5 Power losses during transmission and distribution

The EIA estimates that average annual transmission and distribution losses are roughly 6% of the total amount transmitted (EIA, 2016a). To capture such energy losses, we consider that 0.62% of the transmitted energy is lost every 100 km (Fripp, 2012). ERCOM models these losses via parameter TLF.

5.7.1.3.6 Capacity factors of the electricity generation technologies

Capacity factors (parameter CF_{ij}) affect greatly the electricity generation and the LCOE. Differences in regional resources availability and plant operations lead to great variations of the capacity factor across the U.S. states. Average capacity factors for each technology in each state were calculated from historical data published by the EIA. These data cover the capacity installed and the electricity generated for period 1990-2013 (EIA, 2016a). Data gaps in states not deploying a

given technology in that time period where covered using the average capacity factor of the technology among all the states. There are two exceptions to this rule: (i) states not deploying nuclear power in the baseline year show a capacity factor of zero, since installing additional nuclear facilities is not a CPP compliance option; and (ii) a capacity factor of 0.36 was employed for wind offshore in coasting states, as recommended by the EIA (EIA, 2015), given that this technology is not deployed at all along U.S. in the baseline year. For biomass, we considered the categories “wood and derived fuel from wood” and “other biomass” available in the aforementioned source. Capacity factors for advanced coal and advanced combined cycle with carbon capture and storage (CCS) were assumed to be the same as those for conventional coal and natural gas, respectively. We also assumed that solar PV (both rural and rooftop scale) and solar thermal display the same capacity factor. Figure V-A6 shows the capacity factors. In general terms, we can observe that non-dispatchable technologies (i.e. those tied to an intermittent resource) show lower capacity factors than firm technologies (i.e. those whose output can be varied at will to meet a certain demand).

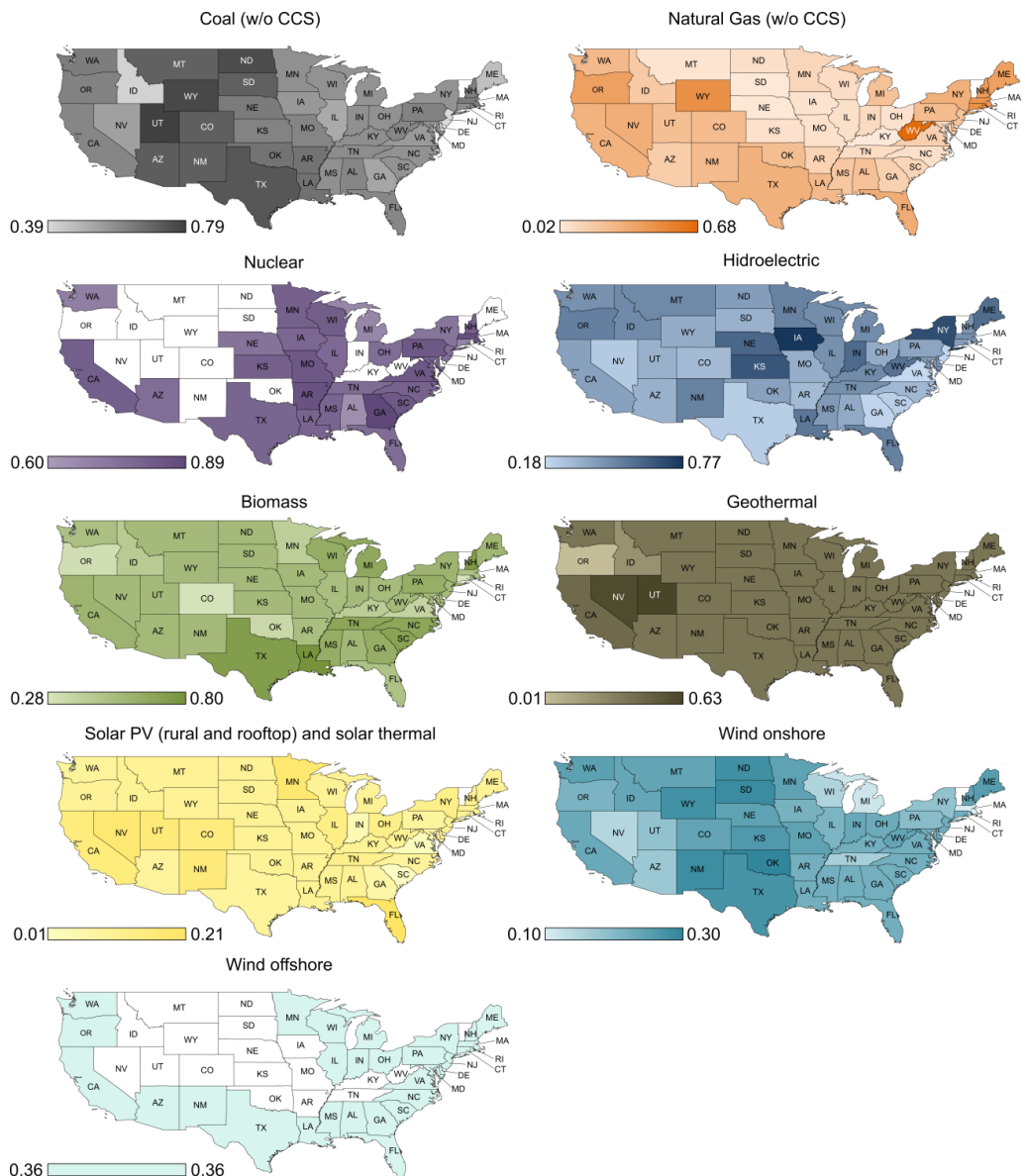


Figure V-A6 Capacity factor for each technology in each state. States are coloured according to the each specific scale so that the darker the shade of the state, the higher the capacity factor.

5.7.1.3.7 Cost of electricity generation technologies

The levelised cost of the electricity (LCOE) is (arguably) a convenient measure of the economic competitiveness of the electricity generation technologies. Costs of electricity generation for each technology were determined from the average

national LCOE for plants entering in service in 2020 following the Annual Energy Outlook 2015 developed by the EIA(EIA, 2015) (see Table V-A1). This report provides capital and transmission lines cost along with fixed and variable operations and maintenance (O&M) costs. The LCOE represents the cost per kWh of building and operating a plant over a given financial life (i.e. 30-year cost recovery period with a tax weighted average cost of capital of 6.1%). This parameter assumes a specific utilisation rate for each plant type (further details on specific assumptions are discussed in <http://www.eia.gov/forecasts/aeo/index.cfm>).

Table V-A1 Average capital and transmission lines costs, and fixed and variable operation and maintenance (O&M) costs for each electricity generation technology (2012 US\$/MWh) (EIA, 2015).

<i>Technology</i>	Costs		
	Capital and lines	Fixed O&M	Variable O&M
Coal	61.6	4.2	29.4
Natural Gas	15.6	1.7	57.8
Nuclear	71.2	11.8	12.2
Hydropower	72.7	3.9	7.0
Biomass	48.3	14.5	37.6
Geothermal	35.5	12.3	0
PV rural	113.9	11.4	0
Wind onshore	60.8	12.8	0
Wind offshore	174.4	22.5	0
Coal CCS	98.5	9.8	36.1
PV rooftop	113.9	11.4	0
Solar Thermal	196.6	42.1	0
Natural Gas CCS	31.3	4.2	64.7

These costs are region-specific due to local labour markets and differences in availability of energy sources. Hence, to capture such differences, costs were

regionalised at the state level using Eq. V-A36, Eq. V-37 and Eq. V-38. These equations make use of the regional capacity factors (Figure V-A6) and state cost adjustment factors compiled by the U.S. Army Corps of Engineers (U.S. Army Corps of Engineers., 2011).

$$CO_{i,j}^{CAP} = CO_i^{CAPAVE} \omega_j \left[\frac{47}{\sum_{j'} 1/CF_{i,j'}} \frac{1}{CF_{i,j}} \right] \quad \forall i, j \quad \text{Eq. V-A36}$$

$$CO_{i,j}^{FIX} = CO_i^{FIXAVE} \omega_j \left[\frac{47}{\sum_{j'} 1/CF_{i,j'}} \frac{1}{CF_{i,j}} \right] \quad \forall i, j \quad \text{Eq. V-A37}$$

$$CO_{i,j}^{VAR} = CO_i^{VARAVE} \omega_j \left[\frac{47}{\sum_{j'} 1/CF_{i,j'}} \frac{1}{CF_{i,j}} \right] \quad \forall i, j \quad \text{Eq. V-38}$$

In these equations, $CO_{i,j}^{CAP}$, $CO_{i,j}^{FIX}$ and $CO_{i,j}^{VAR}$ are parameters denoting the regional capital/transmission lines cost, and fixed and variable O&M costs for each technology i in each state j (2012 US\$/MWh), respectively; CO_i^{CAPAVE} , CO_i^{FIXAVE} and CO_i^{VARAVE} denote the average capital and transmission lines cost, and fixed and variable O&M costs for each electricity generation technology i , respectively (i.e. columns 2-4 in Table V-A1); and ω_j denotes the cost adjustment factor for each state j , where 47 is the number of elements used in the regionalisation (i.e. the number of states).

5.7.1.3.8 Electricity generation potential for each technology

The annual potential generation associated with every technology in each state (parameter $GEN_{i,j}^{POT}$ in ERCOM) is strongly related to the marginal abatement costs that ultimately drive the optimisation results (i.e. optimal electricity mixes and electricity trades). The model considers free trade of fossil fuels between states. We assume that the potential for fossil fuel-fired generation with coal and natural gas (both conventional and with CCS) is five times bigger than its generation in 2012. Regarding nuclear generation, potential levels are irrelevant, since the CPP does not consider new expansion as a compliance option. The potential for generation via

renewables technologies is retrieved from the data published by the U.S. National Renewable Energy Laboratory (NREL) (Lopez et al., 2012). Furthermore, we assume that states can double their published biomass potential by trading resources between them. NREL estimates the technical renewable potential at the state-level based on renewable resources availability and quality, technical system performance, topographic limitations, and environmental, and land-use constraints (further details of the methodology and assumptions for estimating the renewables generation potential can be found in the report “U.S. Renewable Energy Technical Potentials: A GIS-Based Analysis” (Lopez et al., 2012) available online at http://www.nrel.gov/gis/re_potential.html). Figure V-A7 shows the annual potential generation in TWh/yr for each technology and state considered in ERCOM.

Furthermore, global bounds (parameter GEN_i^{POTGLO} in ERCOM) are also imposed on the potential of technologies relying on energy sources that can be traded. Specifically, coal and coal CCS share a global upper bound given by coal-based generation limits in the baseline year. The same applies to natural gas w/o CCS. For biomass, we consider a global upper bound equal to the summation of all the states' potential, as published by NREL.

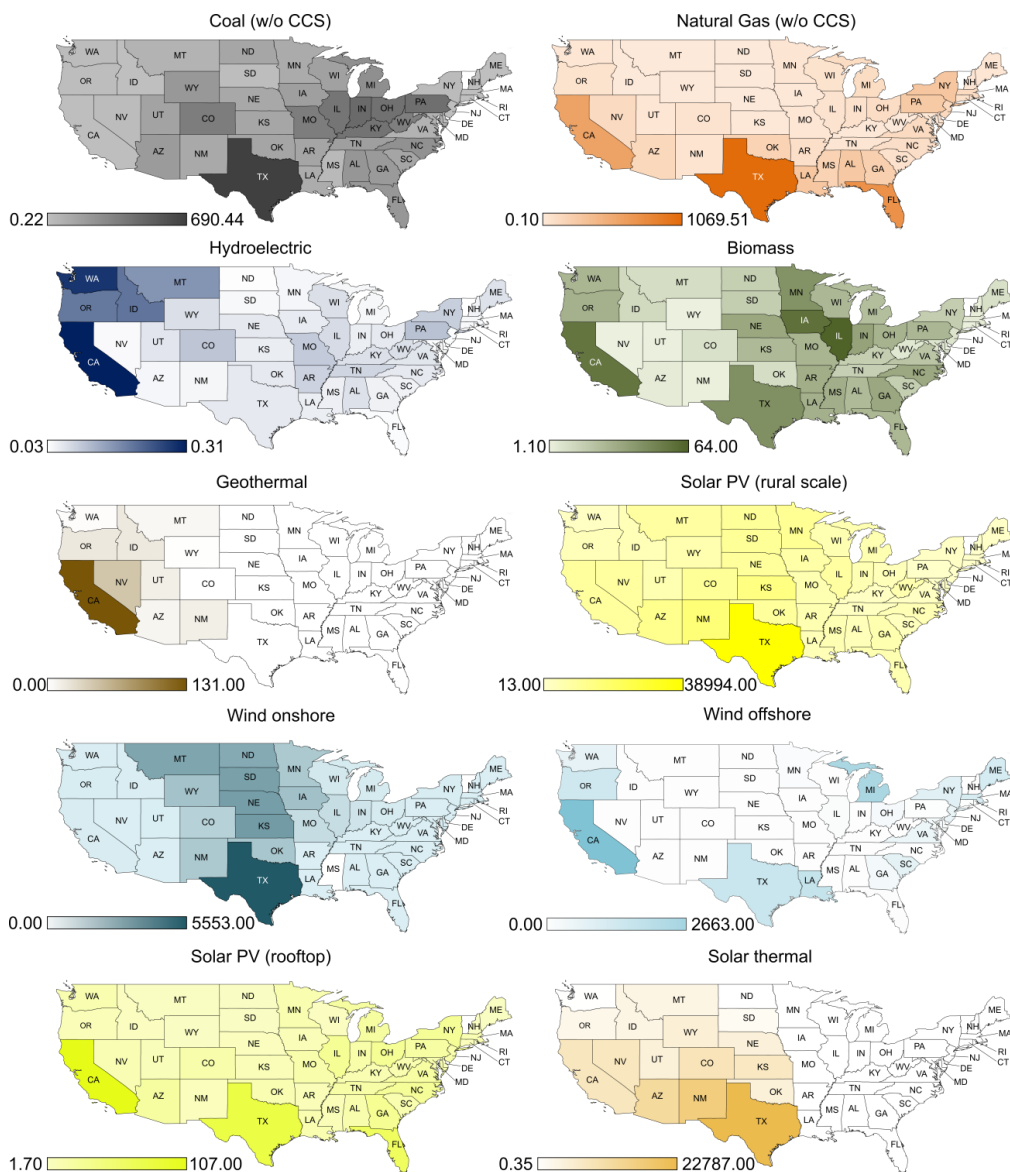


Figure V-A7 Annual electricity generation potential. States are coloured according to their annual electricity generation potential expressed in TWh/yr. The darker the shade, the higher the potential.

5.7.1.3.9 Electricity imports from Canada

We assume that electricity imports from Canadian regions are generated with hydropower and are therefore zero emitting and dispatchable. Electricity import prices (parameter CO^{CAN}) can fluctuate significantly (e.g. from as little as US\$25/MWh to as much as US\$70/MWh) (Antweiler, 2016), but for simplicity we

set a price of US\$39/MWh according to historical data (CEA, 2015).

In 2014, the electricity imported from Canada represented 1.8% of U.S. electricity retail sales, which was almost 10% of the total Canadian generation. In ERCOM, we assume that the electricity imports from Canada cannot exceed 5% of the demand of the U.S. (parameter CTB), which is in line with the expected growth estimated by the North American Electric Reliability Corporation (i.e. three times more compared to 2014 levels) (NERC, 2015).

5.7.1.3.10 Emission levels by technology: carbon intensity

The carbon intensity (parameter Cl_{ij} , expressed in CO_2 kg/MWh) for fossil fuel-fired power plants was sourced from the average regional performance rate included in Appendix 3 of the CPP final rule (EPA, 2015). Such carbon intensities for coal and natural gas were calculated by the EPA as the average of the category-specific performance rates reported by unit levels or plant levels for 2012. Nuclear and renewables technologies are assumed to be zero emitting in the CPP. Regarding both coal and natural gas with CCS, we assume that they capture 90% of the flue gas CO_2 , thereby reducing absolute emissions by 90% (Heuberger et al., 2016). Figure V-A8 shows the carbon intensities of coal and natural gas in each state expressed in kg CO_2 per MWh. Note that carbon intensities from 2012 represent a conservative estimation that overlooks improvements in technology efficiency, which is one of the CPP building blocks.

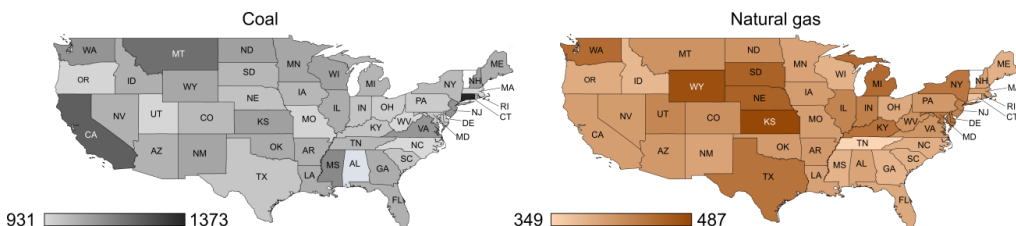


Figure V-A8 Emission performance rates of coal and natural gas by state. States are coloured according to their carbon intensity (CO_2 kg/MWh). The darker the shade, the higher carbon intensity.

5.7.1.3.11 System reliability: backup generation

High penetration of intermittent renewable power (i.e. wind and solar) can compromise the system reliability due to the variability and uncertainty of the sources (i.e. non dispatchable). To circumvent this issue, ancillary systems are installed to back-up the generation of intermittent renewable energies. However, the capacity of dispatchable technologies required to compensate their lack of firmness is still controversial, with very different values available in the literature (e.g. from as little as 15–20% of the intermittent capacity (Gross et al., 2006; Partnership, 2015) to as much as 50–100% (Brown et al., 2014)). A value of 50% for the BUC parameter was therefore set in the ERCOM model. The physical interpretation for this is that each MW installed of an intermittent renewable technology requires the installation of additional 0.5 MW of firm technology to hedge supply in periods with unfavourable weather conditions.

5.7.1.4 Consumption-based allocation

Consumption-based carbon emissions and electricity generation costs are quantified by allocating emissions and costs to end users rather than to producers. At a global U.S. scale, the total consumption-based emissions (and cost) are equal to the production-based ones (recall that the imports from Canada are zero emitting). However, this does not happen on a regional basis due to the exchange of electricity between states. Allocation of emissions is still an open issue in the literature, where several methods were put forward to tackle this problem, particularly in the context of multi-product plants (i.e. how to allocate the total emissions of a plant among the products it manufactures (Tehrani Nejad M, 2007)). As described in more detail next, here we allocate emissions and costs based on mass balances defined for every U.S. state. The allocation method is outlined in Figure V-A9 by means of a simplified example consisting of three states trading electricity. The waterfall plot below shows the breakdown of the consumption-based emissions calculation for state A. As seen, the consumption-based emissions corresponding to state A ($CBEM_A$) are calculated from its production-based emissions (\overline{EM}_A) plus the

emissions embodied in the electricity imported from states B and C (red and green bars with blue contours respectively) minus the emissions embodied in the electricity exported from the state A to the neighbouring states (bars filled with blue colour); where the amount of emissions embodied in the trades are given by the product between the amount of electricity traded ($\overline{\text{TRD}}_{j,j'}^{\text{ORIG}}$) and the consumption-based carbon intensity (i.e. CO₂ kg/MWh) of the supplier state ($\text{CBEM}_j, (\text{DEM}_j, \text{DSF})^{-1}$).

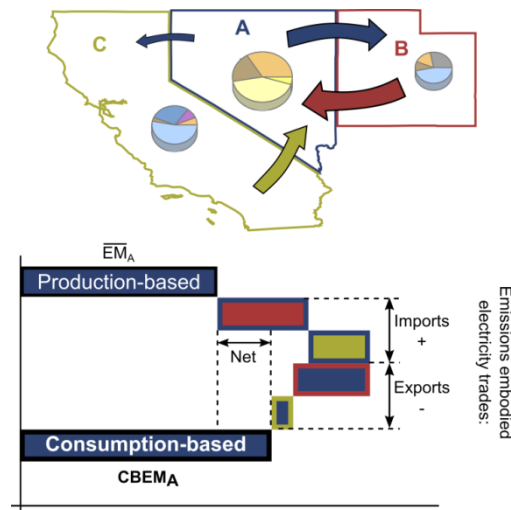


Figure V-A9 Illustration of the consumption-based allocation method. Three states (i.e. A, B and C) trading electricity are considered where arrows represent the emissions embodied in the electricity trades. The waterfall plot below denotes the breakdown of the consumption-based emissions calculation for state A. Length of the bars represents the amount of the emissions and each bar is filled according to the emitter state and contoured according to the receiver state.

5.7.1.4.1 Consumption-based emissions

To quantify the consumption-based emissions of a state in any optimal solution calculated by ERCOM, we derive the following balance on carbon emissions:

$$\text{CBEM}_j = \overline{\text{EM}}_j + \sum_{j' \in \text{NU}_j} \overline{\text{TRD}}_{j,j'}^{\text{ORIG}} \frac{\text{CBEM}_{j'}}{\text{DEM}_{j'} \text{DSF}} - \sum_{j' \in \text{NU}_j} \overline{\text{TRD}}_{j',j}^{\text{ORIG}} \frac{\text{CBEM}_j}{\text{DEM}_j \text{DSF}} \quad \forall j \quad \text{Eq. V-A39}$$

Here, $CBEM_j$ are the consumption-based (footprint) emissions of state j , that is, the kg of CO₂ emitted to satisfy its electricity demand, while \overline{EM}_j are the optimal production-based emissions of state j (the ones calculated by ERCOM), $\overline{TRD}_{j,j'}^{\text{ORIG}}$ represents the optimal trade between states j and j' (calculated also by ERCOM), DEM_j denotes the demand of state j and DSF is the demand satisfaction factor. Note that imports from Canada are zero-carbon and therefore are omitted from the balance. Hence, the equation states that the consumption-based emissions of a state equal its production-based emissions plus the emissions embodied in the electricity imported by the state minus the emissions embodied in the electricity exported from the state to other neighbouring states.

This equation is implicit in $CBEM_j$, as it requires the values of the consumption-based emissions of other states j' (i.e. $CBEM_{j'}$), which may in turn depend on the consumption-based emissions of the state for which the balance is defined. Therefore, Eq. (V-A39) leads to a system of linear equations that need to be solved simultaneously. After running ERCOM, the production-based emissions of every state (\overline{EM}_j) and the inter-state flows ($\overline{TRD}_{j,j'}^{\text{ORIG}}$) become available. With this information at hand, we next build the system of linear equations in Eq. V-A39 and solve it to obtain the values of $CBEM_j$, which provide the consumption-based carbon emissions of every state.

5.7.1.4.2 Consumption-based costs

The cost of the electricity consumed by a state is calculated following a similar approach as before, as shown in Eq. V-A40.

$$CBCOST_j = \overline{COST}_j + \sum_{j' \in NU_j} \overline{TRD}_{j,j'}^{\text{ORIG}} \frac{CBCOST_{j'}}{DEM_{j'} DSF} - \sum_{j' \in NU_j} \overline{TRD}_{j',j}^{\text{ORIG}} \frac{CBCOST_j}{DEM_j DSF} \quad \forall j \quad \text{Eq.V-A40}$$

This equation states that the cost of satisfying the electricity of a state is given by the cost of generating the electricity domestically plus the cost of the imports minus the cost of the exports. Here, $CBCOST_j$ is the cost of satisfying the electricity demand of state j , that is, the global cost of satisfying its electricity

demand, while \overline{COST}_j represents the optimal production-based costs of state j . $\overline{TRD}_{j,j'}^{ORIG}$ denotes the optimal electricity transmitted from state j' to j , DEM_j is the final demand of state j and DSF is the demand satisfaction factor. Costs associated to imports from Canada are not explicitly defined in Eq. V-A40, but rather accounted for by the parameter \overline{COST}_j (see Eq. V-A30 in model ERCOM). Note that this allocation reflects the cost of generating electricity, but not the market price at which the electricity might be sold in the future (which will very likely lie above the former). Eq. V-A40 defines also a system of linear equations that can be built once the optimal solution of ERCOM is identified (values of \overline{COST}_j and $\overline{TRD}_{j,j'}^{ORIG}$). The solution of such system of equations therefore provides the value of $CBCOST_j$.

5.7.1.5 Sensitivity analysis

Some of the parameters in ERCOM are inherently uncertain. We perform a sensitivity analysis to understand how these uncertainties affect the outcome of the optimisation. To this end, the model is solved iteratively for different potential values of the uncertain parameters (i.e. scenarios), which are modelled using probability distributions. These values, each accounting for a different realisation of the uncertain parameter, are generated by applying sampling methods on the underlying probability distributions. After solving ERCOM for every scenario, we finally obtain a probability distribution of the model results (i.e. costs) that can be used to construct confidence intervals for the optimal U.S. electricity cost. In particular, we analyse the following cases:

- **Case 1:** to identify the most critical uncertainties, we first solve the model by varying one single parameter at a time (e.g. \overline{DEM}_j for all states j) while keeping the remaining parameters at their nominal (i.e. deterministic) values. We solve in total 9 NSC instances, where 9 refers to the number of uncertain parameters (see uncertain parameters in section 5.7.1.5; note that we explore the disaggregated LCOE parameters together, rather than separately) and NSC is the number of scenarios.

- **Case 2:** the model is solved considering all the uncertain parameters simultaneously (i.e. NSC times).

In the next section, we introduce the probability distributions used to model the uncertain parameters, whereas in section 5.7.1.5.1 we show how we fit each uncertain parameter to one of these distributions. Finally, in section 5.7.3 we discuss the results of the sensitivity analysis.

5.7.1.5.1 Probabilistic distributions

The probabilistic distributions used in the analysis are next discussed (a generic random variable X is used for simplicity).

Geometric Brownian Motion

Strictly speaking, Geometric Brownian Motion (GBM) is not a probabilistic distribution but rather a continuous-time stochastic process which is used to model unpredictable events occurring during “deterministic” trends (Marathe and Ryan, 2005). Eq. V-A41 describes the GBM differential equation applied to model a stochastic variable X :

$$dX_t = \mu X_t dt + \sigma X_t dW_t \quad \text{Eq. V-A41}$$

where X_t represents the value of stochastic variable X in time instant t , μ denotes the drift parameter, σ is the standard deviation (or volatility) and dW_t is the increment of the Wiener process, modelled as a stochastic variable that follows a standard normal distribution. Therefore, the first term of the equation represents the expected value of the stochastic variable X in time t , whereas the second term adds the stochastic component to the prediction.

Assuming that the natural logarithm of the future realisation of X is normally distributed (i.e. log-normally distributed), the solution to Eq. V-A41 is given by Eq. V-A42.

$$X_{t+\Delta t} = X_t \left[\left(\mu + \frac{\sigma^2}{2} \right) \Delta t + \left(\sigma \sqrt{\Delta t} (N(0,1)) \right) \right] \quad \text{Eq. V-A42}$$

Here, Δt is the time step. Therefore, this equation allows forecasting future values of X (i.e. $X_{t+\tau}$) according to historical data (i.e. X_t), once the drift parameter μ and the volatility σ have been determined.

Triangular distribution

A random variable X following a triangular distribution (i.e. $X \sim T(a,b,c)$) can take values between a lower limit a and an upper limit b , with mode (i.e. peak) c . The probability density function is then given by:

$$f(x) = \begin{cases} \frac{2(x-a)}{(b-a)(c-a)} & a \leq x \leq c \\ \frac{2(b-x)}{(b-a)(b-c)} & c \leq x \leq b \end{cases} \quad \text{Eq. V-A43}$$

Triangular distributions can be used to approximate normal distributions when data is scarce but the minimum (a) and maximum (b) values of the random variable along with its modal (i.e. nominal) value (c) are available.

Uniform distribution

A random variable X following a uniform distribution ($X \sim U(a,b)$) has constant probability within the interval $[a,b]$:

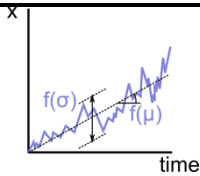
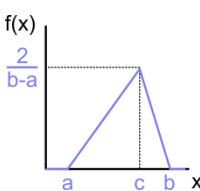
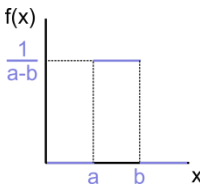
$$f(x) = \begin{cases} \frac{1}{(b-a)} & a \leq x \leq b \\ 0 & \text{otherwise} \end{cases} \quad \text{Eq. V-A44}$$

This is the simplest continuous probability distribution, since it only requires the extremes (a,b) of the support to be fully characterised.

5.7.1.5.2 Uncertain parameters

The uncertain parameters in ERCOM and the probabilistic distributions used to describe them are given in Table V-A2.

Table V-A2 Summary of probabilistic distributions used to describe uncertain parameters in ERCOM.

Uncertain parameter	Probabilistic distribution	Graphical representation	Characteristic parameters
\widetilde{DEM}_j	Geometric Brownian Motion		μ, σ
\widetilde{BUC} \widetilde{CO}^{CAN} $\widetilde{CO}_{i,j}^{CAP}$ $\widetilde{CO}_{i,j}^{FIX}$ $\widetilde{CO}_{i,j}^{VAR}$ \widetilde{CTB}	Triangular		a, b, c
$\widetilde{CF}_{i,j}$ \widetilde{C}_i $\widetilde{GEN}_{i,j}^{POT}$ $\widetilde{GEN}_{i,j}^{POTGLO}$	Uniform		a, b

Scenarios are generated from these distributions via Monte Carlo sampling, assuming in all the cases that the uncertain parameters are uncorrelated. More scenarios lead to better approximations but also to larger CPU times. In our case, 100 scenarios (i.e. $NSC = 100$) are enough to estimate the objective function for a confidence level $\gamma = 95\%$ (i.e. $\alpha = 0.05$) according to Law and Kelton's test (Law and Kelton, 2000). Specifically, for simplicity we apply this test to the results (i.e. total U.S. cost) of Case 2 (considering all uncertainties simultaneously) and use the same number of scenarios in Case 1 as well. The test is applied as follows:

1. We define a number of scenarios.

2. We solve model ERCOM for each of these scenarios, obtaining the electricity cost in each of them (\overline{COST}_s^{TOT}).
3. We calculate the confidence interval half length, $\delta(\text{NSC}, \alpha)$, via Eq. V-A45.

$$\delta(\text{NSC}, \alpha) = t_{\text{NSC}-1, \frac{1-\alpha}{2}} \sqrt{\frac{\text{Var}(\overline{COST}_s^{TOT})}{\text{NSC}}} \quad \text{Eq. V-A45}$$

Here, $t_{\text{NSC}-1, \frac{1-\alpha}{2}}$ is the critical point of the t-distribution and $\text{Var}(\overline{COST}_s^{TOT})$ is the variance of the total cost in the scenarios.

4. We finally check that Eq. V-A41 holds:

$$\frac{\delta(\text{NSC}, \alpha)}{E(\overline{COST}_s^{TOT})} \leq \frac{\gamma}{1 - \gamma} \quad \text{Eq. V-A46}$$

Here, $E(\overline{COST}_s^{TOT})$ is the expected value of the optimal total U.S. cost.

If this condition does not hold, we increase the number of scenarios and go to step 1 until the condition is satisfied.

The interested reader is referred to the original work by Law and Kelton (Law and Kelton, 2000) for further details. We next describe in detail how we fit each parameter to the corresponding distribution.

Electricity demand

Electricity demand is subject to several unforeseen aspects such as market volatility, technology improvements (e.g. development of electric cars), population growth and new policies, among others. Unlike other uncertain parameters considered “constant” over time, we forecast future demands using the GBM approach based on historical data trends. Annual electricity demands for each state were sourced from electricity retail sales (reported to be a good proxy for electricity demand) published by the EIA. Specifically, we use historical retail sales from period 1990-2012(EIA, 2016a), where 2012 was used as the baseline year.

An average annual growth rate of 0.8% projected by the EIA (EIA, 2015) was defined as drift parameter for each state (μ_j), while the volatility was determined using the historical data as follows. Firstly, yearly returns for each state j ($r_{j,t}$) are calculated for each two consecutive time periods via Eq. V-A47, by considering a time step of one year.

$$r_{j,t} = \frac{DEM_{j,t+1}}{DEM_{j,t}} \quad \forall t < T \quad \text{Eq. V-A47}$$

Then, the average of the yearly returns for each state (\bar{r}_j) is determined using Eq. V-A48, whereas the standard deviation of the yearly returns provides the state volatility (σ_j), as given by Eq. V-A49.

$$\bar{r}_j = \frac{\sum_t r_{j,t}}{2012 - 1990} \quad \forall j \quad \text{Eq. V-A48}$$

$$\sigma_j = \sqrt{\frac{1}{2012 - 1990} \sum_t (r_{j,t} - \bar{r}_j)^2} \quad \forall j \quad \text{Eq. V-A49}$$

Once drift and volatility have been determined, Eq. V-A42 allows us to project demands from 2012 onwards up to 2030 (year-per-year) by applying Monte Carlo sampling on the $N(0,1)$ (see Fig. V-A10).

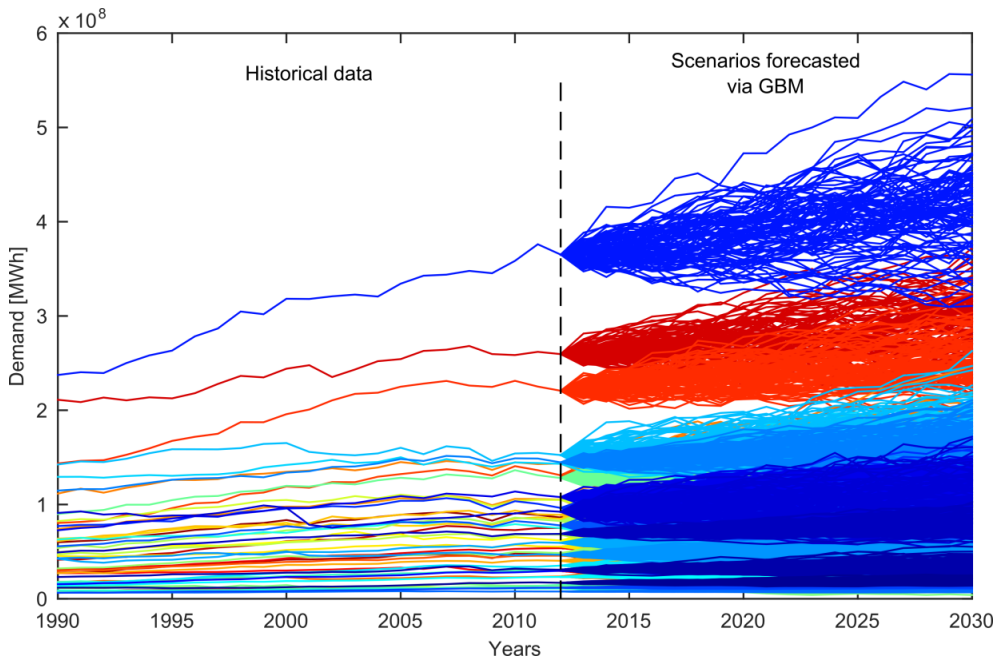


Figure V-A10 Scenarios for electricity demand in each state (MWh). States' demands are forecasted using GBM from 2012 onwards by using historical data from 1990-2012. Each projection represents one scenario with the same probability of occurrence.

Coefficient for back up generation

As previously discussed, firm capacity can range from as little as 15–20% of the intermittent capacity (Gross et al., 2006; Partnership, 2015) to as much as 50–100% (Brown et al., 2014). We use these values to fit a triangular distribution so that $\overline{BUC} \sim T(0.15, 1.00, 0.50)$. Figure V-A11 provides a histogram based on the scenarios generated for this parameter.

Note that a reliable representation of this parameter is of utmost importance, since it greatly influences the outcome of the optimisation. Higher values of this parameter will lead to mixes with less intermittent renewable technologies, whereas low values of BUC allow for larger shares of non-dispatchable resources.

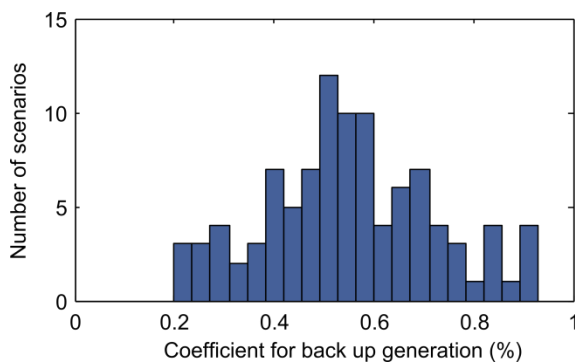


Figure V-A11 Scenarios for the coefficient for back up generation (%). Scenarios for the BUC parameter are generated based on a triangular distribution.

Cost of electricity from Canada

The cost of the electricity purchased from Canada, \widetilde{CO}^{CAN} , is subject to market fluctuations. We fit a triangular distribution where US\$39/MWh is the nominal (i.e. peak) value (CEA, 2015), and with a minimum value $a = \text{US}\$25/\text{MWh}$ and a maximum value $b = \text{US}\$70/\text{MWh}$, which are both defined considering historical electricity price fluctuations (Antweiler, 2016). Therefore, the final distribution is $\widetilde{CO}^{CAN} \sim T(25,70,39)$ (see Figure V-A12).

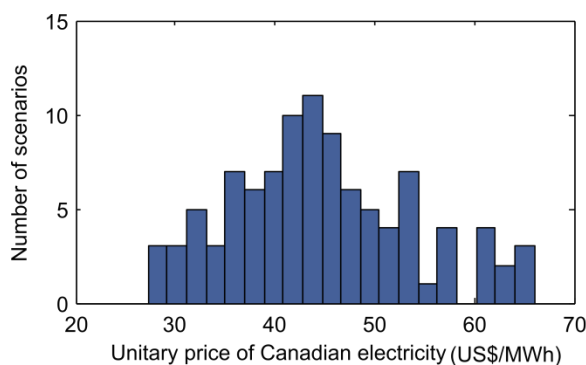


Figure V-A12 Scenarios for the cost of electricity imports from Canada (US\$/MWh). Scenarios for the \widetilde{CO}^{CAN} parameter are generated based on a triangular distribution.

Costs of electricity generation technologies

Capital and transmission lines cost as well as fixed and variable operations and maintenance (O&M) costs are influenced by several external factors:

- Annualised capital costs ($\widetilde{CO}_{i,j}^{CAP}$) are uncertain because so are the equipment costs (which may be influenced by economies of scale) as well as investments in lines connecting new installations with the existing grid.
- Fixed operation and maintenance costs ($\widetilde{CO}_{i,j}^{FIX}$) are uncertain due to volatile fuel prices and labour costs.
- Variable costs ($\widetilde{CO}_{i,j}^{VAR}$) are subject to unpredictable maintenance tasks and fuel prices, among others.

Nominal values for these parameters were obtained by regionalising the average U.S. costs for each technology (i.e. CO_i^{CAPAVE} , CO_i^{FIXAVE} and CO_i^{VARAVE}) according to Eq. V-A36, Eq. V-A37 and Eq. V-A38, as described in section 5.7.1.3.7. In the case of the uncertain parameters, we follow a three-step approach by which we first fit triangular distributions considering the average parameters, then generate scenarios from them, and finally regionalise the value of each parameter in each scenario. Specifically, in the first step, the average parameters for each technology i (i.e. $\widetilde{CO}_i^{CAPAVE}$, $\widetilde{CO}_i^{FIXAVE}$ and $\widetilde{CO}_i^{VARAVE}$) are fitted to three triangular distributions in which the peak values c correspond to the nominal values (Table V-A1) and the extremes of the distributions (i.e. a and b) are obtained by disaggregating the nominal values on the same proportion as the min-max bounds published (EIA, 2015) for the total LCOE. In the second step, the scenarios are generated via sampling on the distributions of the 39 parameters (i.e. three parameters for each of the 13 technologies considered). Finally, in step 3, we regionalise the values obtained for each parameter in each scenario by means of Eq. V-A36, Eq. V-A37 and Eq. V-A38. As an example, Figure V-A13 depicts histograms of the scenarios generated for the 13 technologies after applying the regionalisation step.

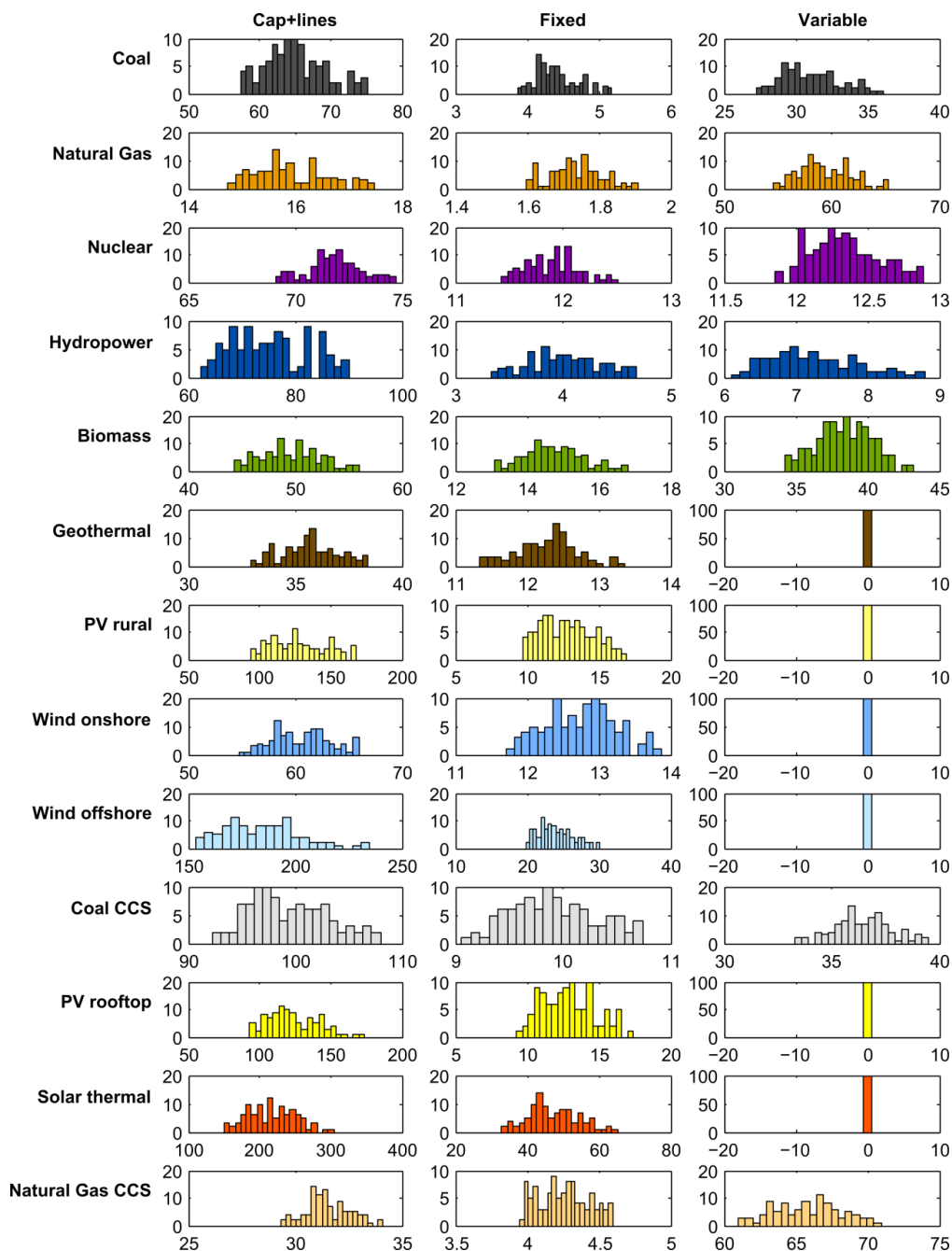


Figure V-A13 Scenarios for the disaggregated LCOE parameters (2012 US\$/MWh). Scenarios for the LCOE parameter are generated based on a triangular distribution. Triangular distributions are first fit from minimum, maximum and average 2012 values for the corresponding technologies, then a set of scenarios are generated for each parameter via Monte Carlo sampling and finally the value of each parameter in each scenario are regionalised to account for local differences.

Bound on imports from Canada

Electricity imports from Canada must lie below 5% of the total U.S. demand, which is consistent with the three-fold growth estimate that is expected (with respect to the current share of 1.8% (NERC, 2015)). However, this value is subject to new hydropower developments, grid reliability and new agreements and policies, among others. Therefore, we explore the influence of such bound by resorting to the stochastic parameter \widetilde{CTB} , which is assumed to follow a triangular distribution with a nominal value of 5% and with a support ranging from a minimum of 0% to a maximum of 7%. Figure V-A14 shows the scenarios generated for this parameter.

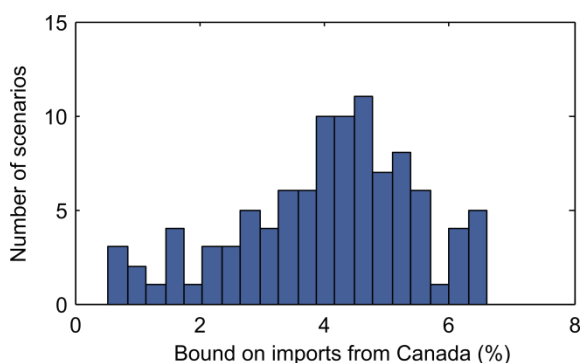


Figure V-A14 Scenarios for the upper bound on Canadian electricity imports (%). Scenarios for the CTB parameter is generated based on a triangular distribution.

Capacity factor

The capacity factor of a technology is subject to learning curves (in the case of immature technologies), efficiency improvements, unpredictable plant operation/maintenance as well as weather conditions (in the case of intermittent renewables), among others. We model this parameter as a stochastic ($\widetilde{CF}_{i,j}$) variable following a uniform distribution for each i - j pair. Specifically, we centre the distributions to the deterministic values and define the support (i.e. a and b in the uniform distribution) according to the standard deviation of historical data (EIA, 2016a). For states lacking data on some technologies, we use the average standard deviation among the different states, similarly as we did with the deterministic value of $CF_{i,j}$ (see section 5.7.1.3.6).

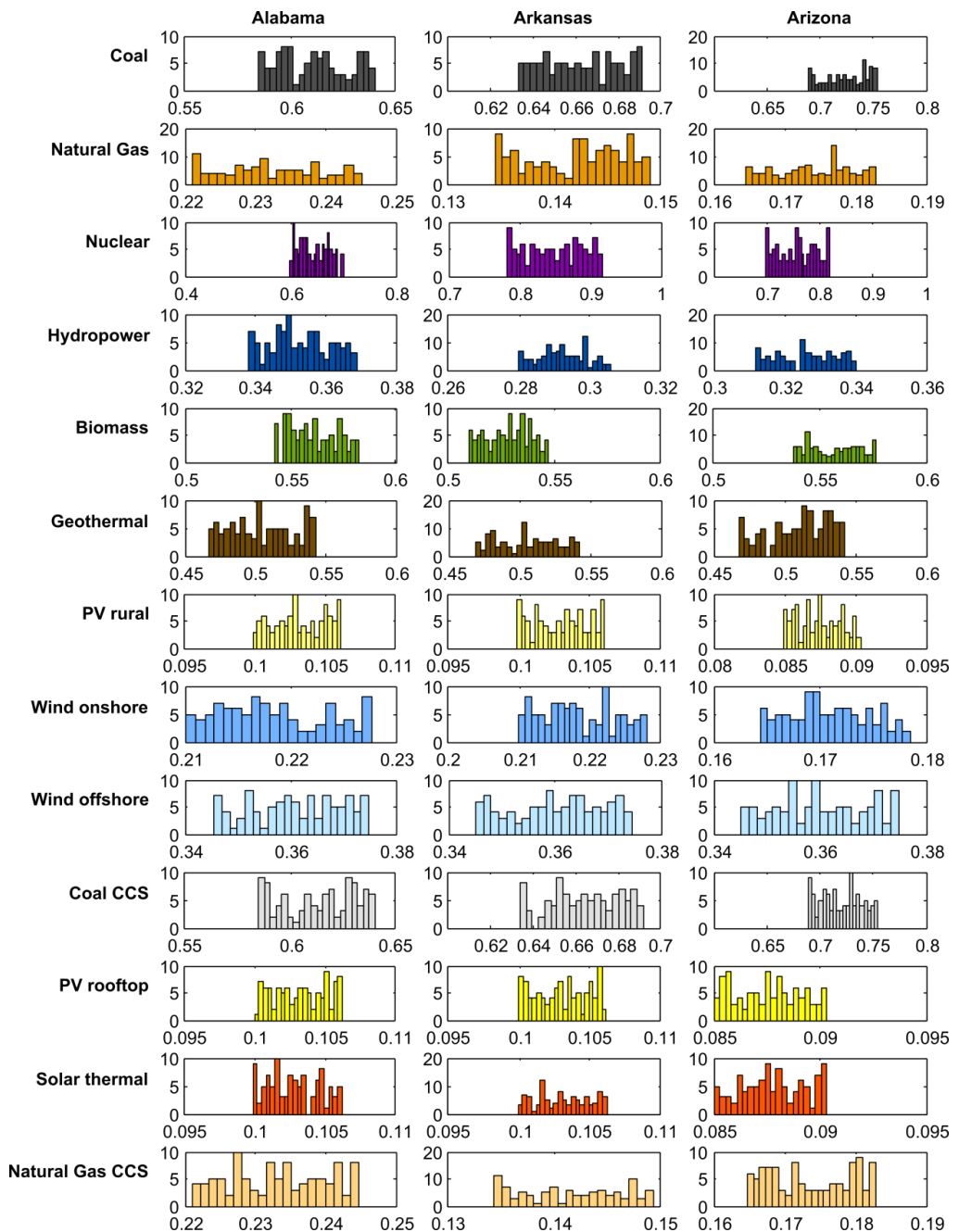


Figure V-A15 Scenarios for the capacity factor of electricity generation technologies. Sample of the scenarios for the CF_{ij} parameter in three states are generated by fitting to a uniform distribution centred at the deterministic value and with a variation as given by the standard deviation of historical data.

Carbon intensity

Carbon intensities depend on how plants are operated as well as on the composition of fuels, among other factors. An uncertain parameter, $\tilde{C}_{i,j}$, is thus defined which follows a uniform distribution centred around the deterministic value and with a support providing a variation of $\pm 30\%$. Note that by generating independent scenarios for coal with and without CCS, we are indeed modifying the % of CO_2 captured in CCS (i.e. it will not always be 90%, as assumed for the deterministic case, but rather depend on the scenario). The same happens for natural gas w/o CCS. Figure V-A16 illustrates the scenarios generated for the carbon intensity for emitting technologies in some of the states. Non-emitting technologies are excluded from the sensitivity analysis, that is, we consider that $C_{i,j} = 0$ for all of them in any scenario.

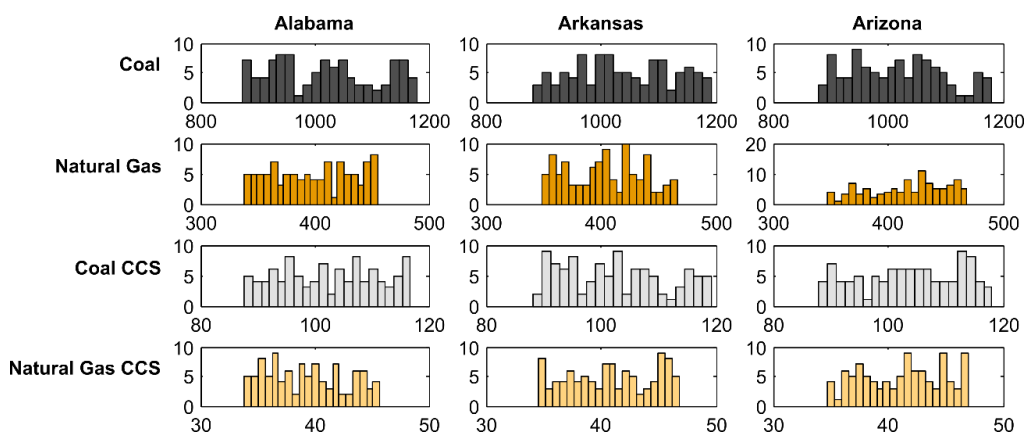


Figure V-A16 Scenarios for the carbon intensity (CO_2 kg/MWh). Sample of scenarios for the $C_{i,j}$ parameter in three states generated based on a uniform distribution.

Generation potential

Uncertainty in the generation potential, $\widehat{\text{GEN}}_{i,j}^{\text{POT}}$, stems mainly from poor weather forecasting (in the case of non-dispatchable renewables), discovering/depletion of fuel sources and technological development, among others. We approximate this stochastic parameter by fitting a uniform distribution assuming a support centred on the deterministic value with a variation of $\pm 30\%$. Therefore, $\widehat{\text{GEN}}_{i,j}^{\text{POT}} \sim U(0.7\text{GEN}_{i,j}^{\text{POT}}, 1.3\text{GEN}_{i,j}^{\text{POT}})$, which can be discretised in scenarios as

depicted in Figure V-A17.

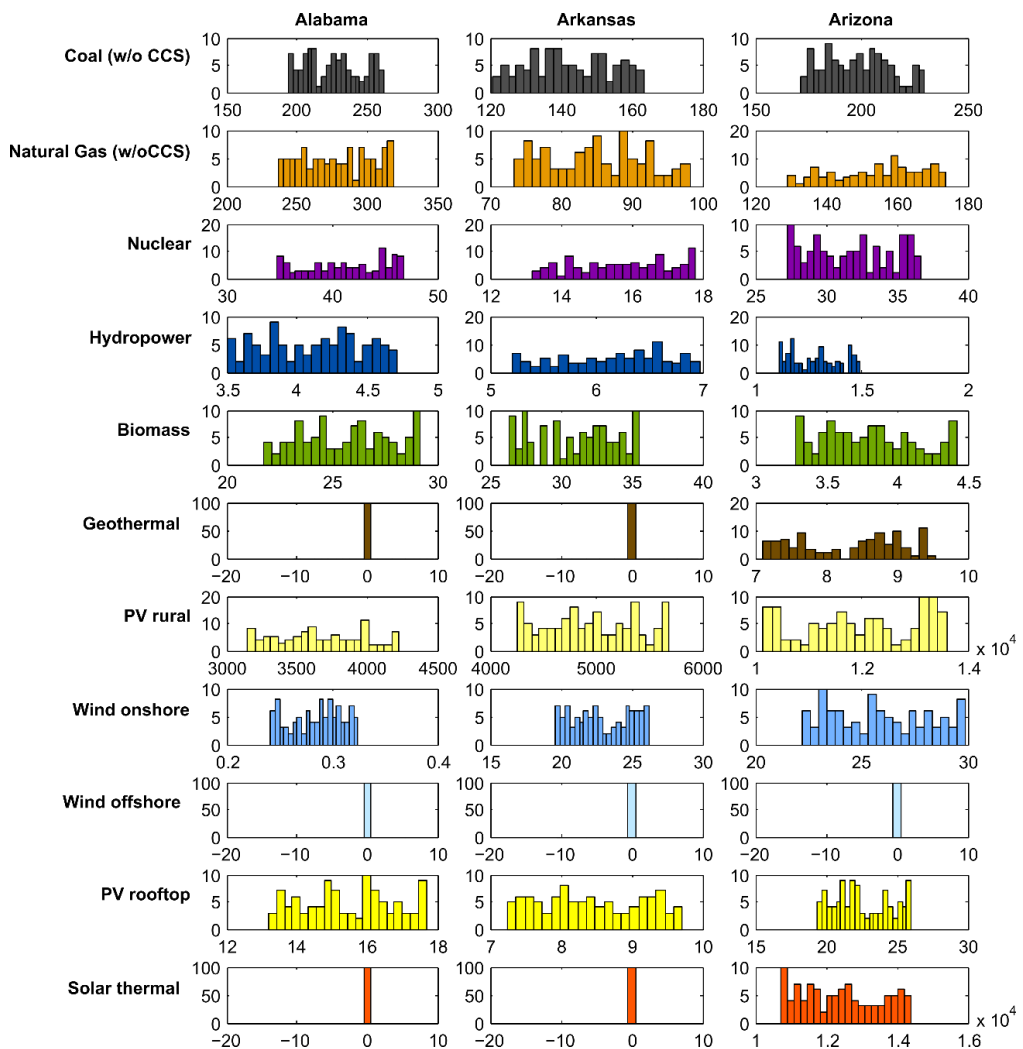


Figure V-A17 Scenarios for the generation potential (TWh/yr). Sample of scenarios for the $GEN_{i,j}^{POT}$ parameter in three states generated based on a uniform distribution.

Global generation potential

Natural gas is expected to play a key role in the close future. Proved reserves and technically recoverable resources (for shale gas, tight gas and offshore natural gas) described in the Reference case of the Annual Energy Outlook 2016 published by the EIA (EIA, 2016b) suggest that current generation with natural gas could be doubled in oncoming years. In light of this, we model the global bound on the

generation potential of natural gas as an uncertain parameter following a uniform distribution with a support between the baseline year generation and twice this amount (i.e. $\overline{GEN}_{\text{natural gas}}^{\text{POTGLO}} \sim U(\overline{GEN}_{\text{natural gas}}^{\text{POTGLO}}, 2\overline{GEN}_{\text{natural gas}}^{\text{POTGLO}})$). Figure V-A18 illustrates the scenarios generated for this parameter. Note that we only consider as uncertain the global potential for technology $i = \text{natural gas}$. The other potentials are kept at their deterministic values throughout the study.

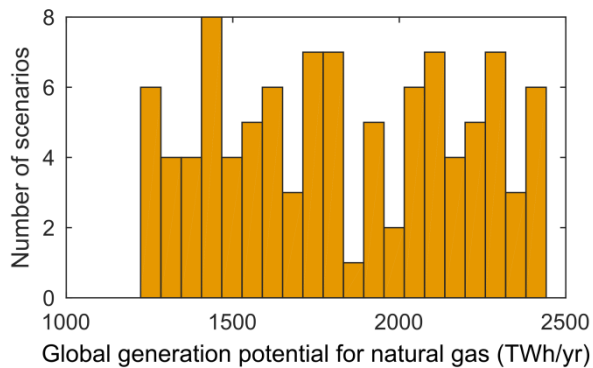


Figure V-A18 Scenarios for the global bound on the generation potential of natural gas (TWh/yr). Scenarios for the $\overline{GEN}_{\text{natural gas}}^{\text{POTGLO}}$ parameter are generated based on a uniform distribution.

5.7.2 Supplementary results

We next provide some results omitted from the main manuscript due to space limitations. First, in section 5.7.2.1 we provide the U.S. geographical breakdown of the non-cooperative optimal solution (A). Then, in section 5.7.2.2, we further describe consumption and production-based emissions/costs results and we discuss compensation rules aiming at spurring cooperation.

5.7.2.1 Optimal non-cooperative solution (Solution A)

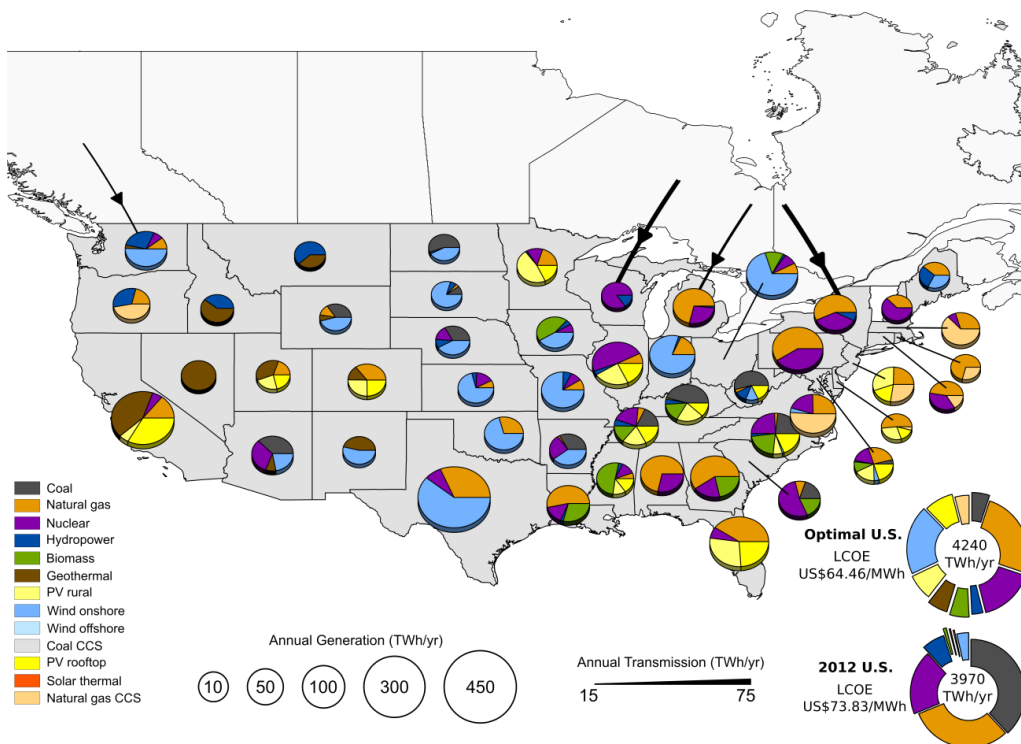


Figure V-A19 Geographical breakdown of the U.S. cost-optimal electricity system in solution A. The size of the pie charts is proportional to the electricity generation of each state (TWh/yr) whereas the slice colours represent the share of each technology. The global U.S. electricity generation portfolio for 2012 and for solution A are depicted (bottom right) together with the associated LCOE.

Solution A is obtained by minimising the total cost of electricity generation and forcing states to comply with their CPP target individually (i.e. parameter CS is set to zero, so all binary variables are zero as well). Note that this solution covers the demand in 2030, but its cost is expressed in 2012 dollars. In this solution no cooperation (i.e. target sharing or electricity trade) is allowed, and therefore states can only reduce their emissions by switching to cleaner energy mixes. Solution A leads to a total U.S. cost of electricity generation 4% below the base line (i.e. 2012) while simultaneously the CO₂ emissions are reduced almost double the CPP target (67% compared with the 35% required). Figure V-A19 shows the optimal electricity portfolio in each state without any form of cooperation among them. As can be

observed, CPP targets can be met individually without increasing the U.S. LCOE, which is slightly lower than in 2012 (i.e. US\$64.4/MWh compared to US\$73.8/MWh). Broadly speaking, in solution A, coal-fired power plants are almost phased out, while natural gas generation declines slightly and nuclear power is kept constant (as specified in the CPP). The share of renewables increases until representing a 47% of the total electricity demand. Economically competitive renewable technologies are deployed in many states. Namely, wind onshore increases substantially (from 3% to 20% of the total power needs), while solar PV (both at rural and rooftop scale) reaches almost 16% (from almost zero levels in 2012). States deploying these technologies complete their portfolios with back-up firm technologies based on coal, natural gas, geothermal and natural gas with CCS. These technologies ensure the system reliability under intermittency of sources. Geothermal and biomass resources are exploited until accounting for almost 6% (each) of the total electricity generation. Geothermal is largely implemented in western states (e.g. California, Nevada, Idaho, Utah and Montana), while biomass is employed in south eastern states (e.g. Louisiana, Mississippi and Georgia) as well as in Iowa and Ohio, among others. Besides deploying renewable resources, some states reduce their emissions by replacing coal by natural gas (e.g. Pennsylvania, Michigan, New York, Alabama and New Hampshire), while others implement carbon capture and storage technologies in natural gas-fired plants (e.g. Connecticut, Massachusetts, New Jersey, Oregon, Rhode Island and Virginia).

5.7.2.2 Further assessment of individual efforts: production vs consumption-based perspectives

5.7.2.2.1 Emissions and cost embodied in trade

Assessing the efforts every state makes in the cooperation only from a production-based perspective is arguably unfair since all the responsibility and the burden is allocated to electricity producers, which may be the states required to increase their generation for the sake of the overall gain (e.g. Oklahoma). Conversely, states displacing their facilities to other regions avoid the burden

attributed to the generation of their electricity demand, leading to ‘carbon leakage’. To shed further light on this, we consider the implications of adopting a consumption-based approach, which, unlike the territorial approach followed by CPP, assigns the responsibilities to consumer states, i.e. those that use rather than generate electricity. To this end, we quantify the CO₂ emissions and costs embodied in the electricity flows between the states in solution B (Figure V-A20) following the allocation method explained in Section 1.3 in Supplementary Information. Note that the amount of carbon (or costs) embodied in the flows is driven not only by the volume of the trade but also by the carbon intensity (or LCOE in the case of costs) of the electricity sources (Figures V-A21 and V-A22).

Allocation of emissions (Figure V-A20a) allows classifying states as net importers or net exporters of carbon emissions. The former release domestically less emissions than the amount emitted elsewhere in the U.S. to generate the electricity they consume. For the net exporters, this balance results in more emissions released locally than those associated with satisfying their own demand. Twenty nine states are net importers of emissions and 13 are net exporters, with four states not participating in electricity trade and one state importing only zero-carbon electricity from Canada. Within the first group, examples include Pennsylvania, Texas and New Jersey, while the exporters include Oklahoma, Florida, New York and Nevada. For most states that trade electricity, using the production and consumption perspectives results in a different level of emissions. In some cases, the mismatch between production and consumption emissions is marginal (Figure V-A20a and Figure V-A21a), as in Wyoming (0.4 more in the consumption-based approach). In others, it can be significantly higher, as in Pennsylvania (45.5 CO₂ Mt/yr more) and in Oklahoma (70.7 CO₂ Mt/yr less), evidencing that in some cases substantial emissions are traded between the states. Under the consumption-based approach, Oklahoma would be now released from any liability about the carbon embodied in its exports to the neighbouring states (i.e. final consumers), which would be held responsible for the emissions attributed to such trades.

Therefore, the consumption-based perspective provides a different picture of the efforts made by each state. However, it still fails to capture the behaviour of the state as a producer, thereby neglecting the potential efforts undertaken to reduce its carbon intensity. For instance, Colorado would be attributed the responsibility for the emissions embodied in its imports from Oklahoma, but it would not be credited for switching to a lower carbon mix (from a coal-intensive mix to a mix based on geothermal and solar).

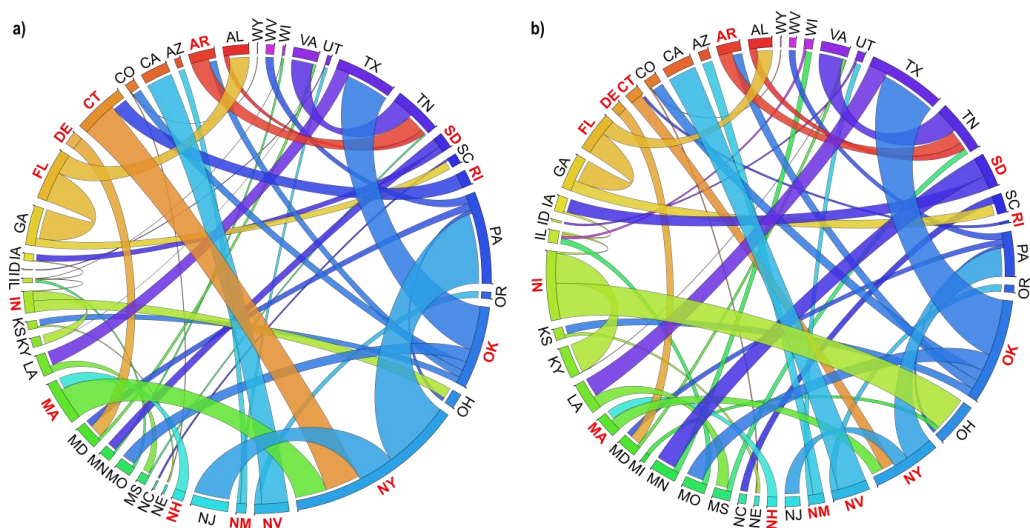


Figure V-A20 Emissions and costs embodied in the electricity trade under full cooperation (solution B in Figure V-1). Subplot V-A20a illustrates CO₂ emissions and subplot V-A20b the costs embodied in trade. In the chord diagrams, the states are denoted by coloured circle arcs, where the arc length measures the total emissions (subplot V-A20a) and costs (subplot V-A20b) of imports and exports traded. Each trade is represented by a chord whose thickness is proportional to the magnitude of the trade (in CO₂ Mt/yr in subplot V-A20a and in billion US\$/yr in V-A20b). Chords are coloured according to the origin of the trade (i.e. according to exporter state). States whose aggregated export chords take up less than 50% of their arc length, are net importers of emissions (subplot V-A20a) or of costs (subplot V-A20b), whereas the opposite holds for net exporters (which are depicted with red labels).

Similar to the emissions, next we allocate the total cost of electricity among the U.S. states (Figure V-A20b) to find out if monetary flows could compensate for the efforts made when cooperating. This allocation is equivalent to assuming that the importer state purchases electricity at generation cost (i.e. LCOE) rather than at market price, which will arguably be higher. We use the LCOE because predicting

future market electricity prices with accuracy is rather challenging due to their inherent volatility. This hampers the assessment of the future true economic contribution of each state in the cooperative solution.

The results show that in 32 states the cost of meeting their electricity demand is above the cost of their domestically generated electricity, while the opposite applies in 15 states. The mismatch in costs can be as low as in Wyoming (billion US\$0.2/yr higher in the consumption perspective) or as high as in Ohio (billion US\$10.5/yr more) and Oklahoma (billion US\$25.1/yr less). Therefore, allocation of costs from a consumption-based perspective reveals a totally different situation from that shown in Figure V-A4. For instance, Oklahoma, previously a penalised state because its production-based electricity cost increased through cooperation, would now receive a revenue for its electricity exports (see Figure V-A20b) that would place the state slightly above the diagonal in Figure V-A4. Conversely, Ohio, which gained from the cooperation, would incur extra costs through electricity imported from Michigan, Indiana and Pennsylvania. The same rationale can explain the different compensatory movements arising in other states, yet under this accounting we are still disregarding the individual contribution that each state makes as a producer to reduce the overall U.S. cost of electricity.

As seen, the production and the consumption-based accountings are complementary (Kander et al., 2015; Springmann, 2014; Steiner et al., 2014) and provide different insights into the contributions made by different states, to the extent that a single state may either benefit or be penalised, depending on the approach followed. At the U.S. level, the total amount of emissions embodied in the electricity trade represents 78% of the total electricity emissions released in the U.S., while the costs embodied in such trade reach 53% of the total cost of electricity generation in the country. Such large volumes of electricity flows emerge as a natural consequence of cooperation as trade favours the states with the most cost-effective resources.

5.7.2.2.2 Production and consumption-based accountings: breakdown by state

Cooperation among all U.S. states allows achieving the most cost-effectiveness mitigation; however, it entails an uneven distribution of efforts (both in terms of contribution to curb emissions and to reduce costs) which cannot be simply neglected. The exploitation of regions (i.e. states) with better abatement costs leads to two groups of states playing different roles: states acting as suppliers of electricity and states acting as recipients of electricity. The former increase the electricity generation by means of their low-cost and/or low-emitting technologies therefore suffering more from local burdens (but at the same time benefitting from the increase in the number of jobs, the associated tax share and enhanced energy security). The opposite holds for the latter group, whose members displace facilities abroad thereby avoiding the responsibility attributed to their electricity demand generation.

Due to the asymmetric distribution of efforts, some states can be either harmed or benefitted when moving from an individualist strategy to the cooperative one, which compromises the engagement of all states into the cooperation. Therefore, quantifying the contribution each state makes for attaining mutual gains provides valuable insight on how to credit/penalise them. However, each individual contribution changes greatly depending on whether the responsibilities are allocated to producers or to consumers which makes it necessary to assess the efforts considering both perspectives.

Thus, we quantify both production and consumption-based emissions and costs following the allocation method explained in Section 5.7.1.4 in this Appendix. The comparison between the traditional production-based approach and the consumption-based one provides further insight and better understanding on how responsibilities should be allocated among the parties involved. To shed further transparency on this issue, Figure V-A21 displays the breakdown by state of total

emissions and carbon intensities according to the production and consumption-based accountings, while Figure V-A22 shows the same comparison for the total and specific costs.

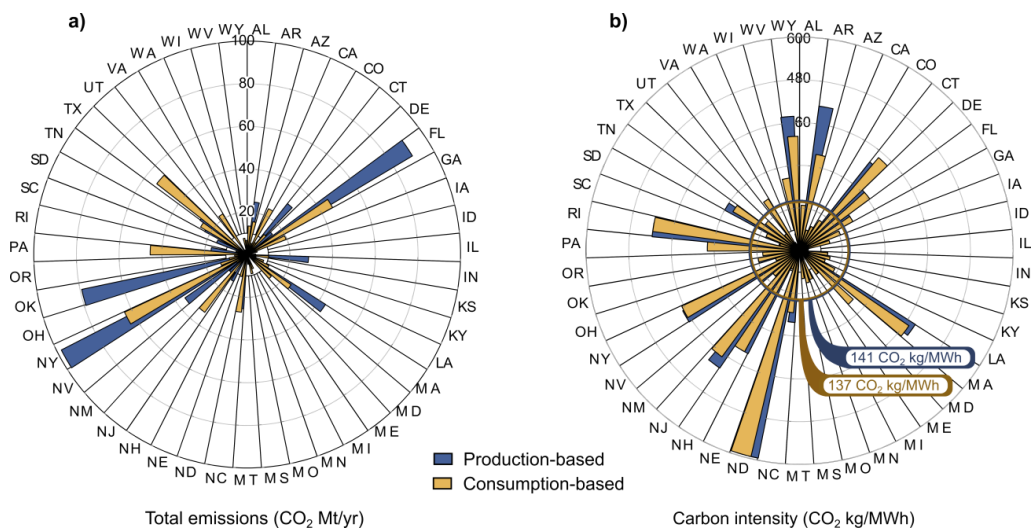


Figure V-A21 Comparison between production and consumption-based emissions in solution B by state. Subplot V-A21a displays the total emissions by state (in Mt CO₂) while subplot V-A21b displays the carbon intensity by state (expressed in CO₂ kg/MWh). Blue bars correspond to the production-based accounting while yellow bars correspond to the consumption-based one. Circumferences in subplot B depict average U.S. specific emissions following the same colour pattern as bars.

Total emissions (expressed in Mt CO₂) from the electricity generation vary greatly among U.S. states, regardless of the accounting system. This significant spatial heterogeneity is not only observed in the electricity generation (i.e. suppliers and recipient states) but also in the composition of the electricity mixes (i.e. lower and higher carbon intensities). As seen, there is a clear mismatch between the traditional production-based accounting and the consumption-based one at the state level, which evidences that substantial emissions are embodied in the electricity trades. The existence of this large discrepancy justifies the need of considering both perspectives in order to provide a more transparent picture of the “true” contributions made. Our results show that there are more states which are net importers of emissions (29) than net exporters of emissions (13). On a

production basis, most of the U.S. emissions in solution B correspond to a few states, with only eight states (i.e. New York, Florida, Oklahoma, Massachusetts, Nevada, Connecticut, Indiana and Arkansas) accounting for more than 70% of the total U.S. emissions. However, under the consumption-based perspective, those states are held responsible for only 30% of the total U.S. emissions evidencing the need to analyse the results following both accounting systems. For instance, Oklahoma acts as a supplier state in the partnership due to its lower abatement cost, producing 79.2 Mt CO₂ (third larger emitter in the U.S. partnership), while only 8.5 Mt CO₂ corresponds to its consumption (ranked as 21st larger emitter). Conversely, Texas, which does not appear as a top emitter in the production-based accounting, almost doubles its emissions from a consumption-based perspective (i.e. 27.4 Mt CO₂ according to the production-based and up to 53.8 Mt CO₂ in the consumption-based), thus becoming the second largest emitter (according to the consumption-based accounting). Even in the case of New York, which is by far the larger emitter from both perspectives, production and consumption-based emissions differ significantly, evidencing that both approaches complement each other and together provide a deeper understanding of the real contribution made by states towards curbing CO₂ emissions.

In subplot B we can see that carbon intensities (i.e. CO₂ kg/MWh) also show great variations among states (regardless of the accounting system). These are due to the differences in carbon intensities among the states' optimal electricity mixes. On a production basis, the largest carbon intensity corresponds to North Dakota, with a 55% coal-based electricity mix, followed by states deploying either coal-rich (e.g. Arkansas) or natural gas-rich (e.g. New Jersey, New York, Rhode Island or Massachusetts) portfolios. While most of these states are also among the top emitters on a consumption basis, some of them present significant differences between both accountings due to the emissions embodied in electricity trades. Production-based carbon intensities are above consumption-based ones in eight states, while 26 states show higher carbon intensities in the consumption-based

accounting and 13 states show the same carbon intensities in both accountings. Within the first group, we find states such as Arkansas, where the higher production-based emissions result from the combination of being a net exporter of electricity and deploying a high emitting electricity mix. Some other states within this group, like Wyoming, show lower carbon intensities as consumers because they import cleaner electricity with low embodied emissions. Within the second group (higher consumption-based carbon intensities), we find states such as Pennsylvania, which increase its consumption-based carbon intensity by importing electricity with high embodied emissions (e.g. importing large amount of electricity from the natural gas rich portfolio of New York). Finally in the last group (i.e. showing the same carbon intensities in both accountings), we find states which do not trade electricity at all (i.e. Maine, Montana and North Dakota); states which only export electricity (e.g. Florida, Indiana or Oklahoma); and states that import electricity with the same carbon intensity that the electricity they produce (e.g. Michigan only imports zero-emitting electricity from Canada and its mix is based on zero-emitting nuclear and hydropower).

Allocation of costs by state (Figure V-A22a) shows that, regardless of whether a production or consumption-based accounting system is considered, there is a significant variability among states. This is due to the different volumes of net generation among states and also to the spatial heterogeneity of the electricity cost. Production-based and consumption-based total costs differ greatly due to the large volume of electricity traded which in turn is translated in large monetary flows between suppliers and consumers of electricity (note that we allocate the cost of producing the electricity, which will presumably be lower than the market price of the electricity transferred). Results in subplot V-A22a show that in 13 states, the cost of electricity generation is above the cost of covering their electricity demand, while in 31 states the opposite situation occurs. On a production basis, more than 53% of the total U.S. generation cost in solution B is assumed by only 8 states (i.e. Florida, Indiana, Illinois, Oklahoma, California, Nevada, New York and Texas).

However, under a consumption-based perspective, this figure is reduced down to 33% which again evidences the need of considering both perspectives. Furthermore, for a single state, the mismatch between the total costs as a producer and as a consumer can be large, as for example in Oklahoma which presents production costs of US\$28.2 billion while its consumption costs are US\$3.0 billion (89.4% lower).

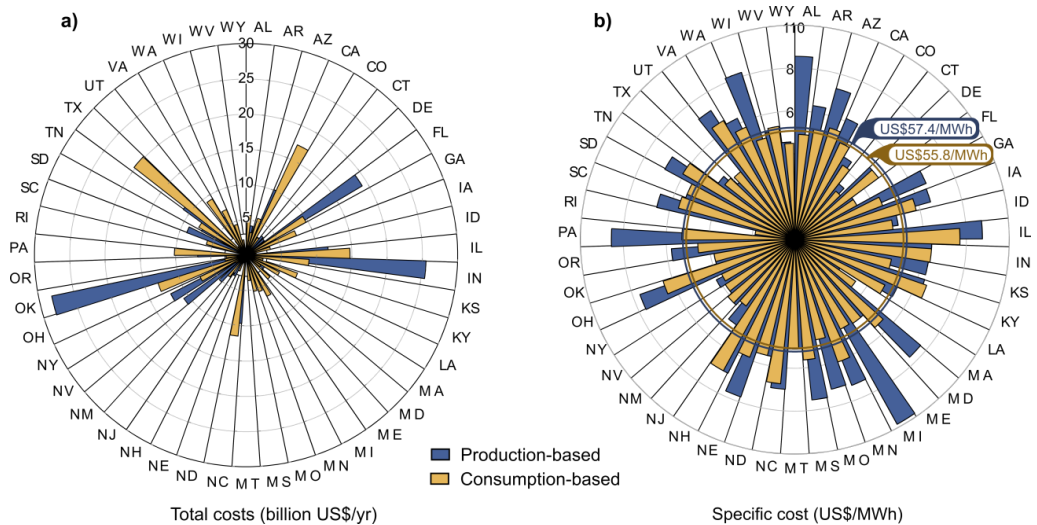


Figure V-A22 Comparison between production and consumption-based costs in solution B by state. Subplot V-A22a displays the total cost by state (in billion US\$) while subplot V-A22b displays the specific cost by state (expressed in US\$/MWh). Blue bars correspond to the production-based accountings while yellow bars correspond to the consumption-based accounting. Circumferences in subplot B depict average U.S. specific costs following the same colour pattern as bars.

The specific costs (i.e. US\$/MWh) are more equally distributed than carbon intensities (Figure V-A21b). Carbon intensities vary greatly among states since emissions are far below the target and therefore they play no significant role in shaping the optimal solution. In contrast, specific costs are more similar across the U.S. territory. This happens because technologies are selected mainly according to their economic competitiveness. Hence, the worst technologies (cost wise) are ruled out, with the ones being installed displaying similar average costs.

Results in subplot V-A22b show that the production-based specific costs lie above the consumption-based ones in 31 states (e.g. Michigan, Pennsylvania, Wisconsin, Alabama and Maryland), whereas the opposite holds in only four (e.g. specially Massachusetts and Rhode Island). Notably, most U.S. states reduce their specific costs in the consumption-based accounting, since the electricity they import is mainly produced in a few states with much lower specific costs. On the other hand, states where production-based unitary costs exceed consumption-based ones are not necessarily net exporters of electricity, because the monetary flows embodied in the electricity traded depend on both, the unitary costs and the volume of electricity exchanged (and the same applies to the net importers of electricity). For instance, Alabama is net importer of electricity (purchasing more electricity from the cost-effective portfolio of Florida than it sells to Tennessee). Besides, its production-based costs exceed the consumption-based ones, a mismatch that stems from the large difference in specific generation costs between Alabama and Florida (i.e. US\$94.0/MWh compared to US\$36.3/MWh, respectively; a 61.2% lower in Florida). Furthermore, we can identify 12 states in which the production and the consumption-based specific costs are the same. These are states which either trade no electricity at all or only export it. Note that, unlike what happened with the emissions, here Michigan presents lower costs from a consumption-based accounting than from a production-based one, because its imports from Canada are cheaper than its domestic generation.

5.7.3 *Sensitivity analysis*

In this section we present the results of the sensitivity analysis providing confidence intervals for the benefits from cooperation and analysing the behaviour of the optimal cooperative solution B when uncertainties are considered.

5.7.3.1 *Sensitivity of the benefits from cooperation*

In the main manuscript, we showed that the total U.S. cost of electricity generation can be reduced by 12% when all the states cooperate to curb CO₂

emissions. In order to provide confidence intervals for such benefits, we next explore how this figure varies when considering uncertainties. To this end, we recalculate solutions A and B following the procedure described in section 5.7.1.5. For each of the uncertain parameters, we provide the probability distribution of the model results (Figure V-A23) and identify the worst and best case scenarios (i.e. minimum and maximum benefits, respectively), which define the interval where the real benefits should fall.

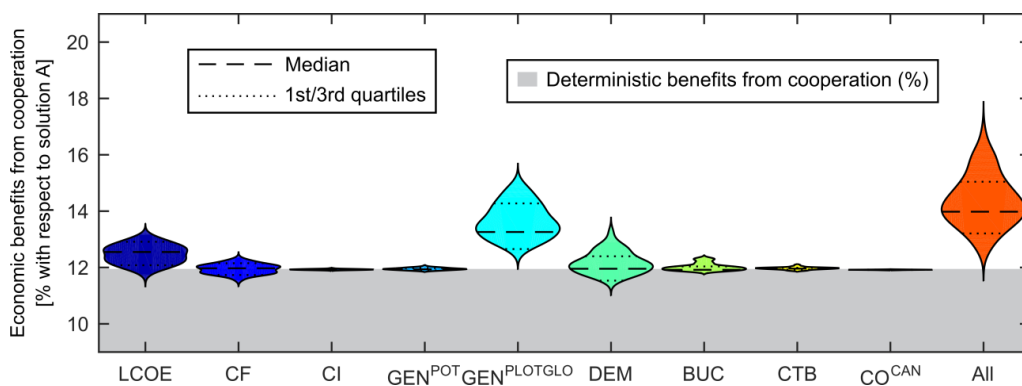


Figure V-A23 Sensitivity of the benefits derived from cooperation to the uncertain parameters. Each violin depicts the probability distribution of the difference between the U.S. cost in solutions B and A (expressed as a percentage) when uncertainty is considered in a given parameter(s) (indicated in the x axis). The width of the violin reflects the frequency (i.e. number of scenarios) of the solutions. Additionally, the benefit derived from cooperation in the deterministic case is also depicted for the sake of comparison.

We start by analysing the effects of single uncertainties (first nine violins in Figure V-A23), finding that there are four parameters whose uncertainty has little effect on the benefits of cooperation (i.e. similar savings as in the deterministic case are obtained regardless of the realisation of uncertainties). These are: (i) the carbon intensities (CI); (ii) the regional potential for electricity generation with each technology (GEN^{POT}); (iii) the amount of electricity traded with Canada (CTB); and (iv) the unitary cost of this electricity (CO^{CAN}). These results can be explained as follows. Carbon intensities show little influence on savings because emissions fall below the CPP targets in the optimal solution. Hence, technologies are mostly implemented according to their relative economic competitiveness. On the other

hand, changes in the state bounds on electricity generation impact very little on the results because these are in general high enough to not limit the installation of economically appealing technologies. Finally, parameters related to Canadian imports (i.e. bound on electricity imports and their unitary price) affect both solutions A and B in a similar manner, so the difference between both is always low. This is not surprising given that, firstly, deterministic solutions A and B already showed very similar Canadian imports (i.e. 197 vs 201 MWh) and, secondly, because Canadian imports represent a little share of the total U.S. cost (around 3% in both cases).

There are two parameters, namely the capacity factor (CF) and the coefficient for back up generation requirements (BUC), which show slightly higher influence on the benefits derived from cooperation, yet these are still small (i.e. between 11.3% and 12.6%, for the changes in the CF, and between 11.7% and 12.5% for variations in the BUC). Therefore, while they affect more the individual solutions A and B, the difference between both solutions remains very much alike since they are changed in similar proportions.

Conversely, the following parameters have stronger impact on the benefits that can be achieved when cooperating: (i) the LCOE of each technology; (ii) the electricity demand; and (iii) the global potential generation bound. For instance, when uncertainties are realised on the LCOE, savings can vary from as little as 11.3% to as much as 13.6%. Although these numbers are close to the deterministic 12%, they entail significant variations in benefits: from US\$1.8 billion less savings to US\$4.6 billion more. Note that scenarios for LCOE are not correlated, which means that costs for one technology can increase in one state but decrease in others. This penalises solution A more severely than B, since the latter can still resort to the most cost-effective technologies/states and use trade to supply electricity to less favourable regions.

Moreover, the DEM also shows a high influence on the savings that can be achieved, which range from 11.0% to 13.8% (i.e. from US\$2.6 less to US\$5.3 billion more than in the deterministic case). This is because the individualist strategy of solution A forces states with poor abatement costs to increase their generation to respond to a higher demand, thus severely worsening the U.S. costs. Conversely, in the cooperative solution B, regional advantages can still be exploited to supply economically appealing electricity thus cushioning the increase in the costs. Finally, the GEN^{POTGLO} parameter shows the biggest influence among individual uncertainties, leading to benefits from cooperation lying always above those in the deterministic case (i.e. from 12% to a maximum value of 15.7%). This happens because in all the scenarios the global bound imposed on natural gas resources is relaxed. This allows supplying the resource even to states where it is scarcer, thus increasing the share of the low-cost gas technology throughout the U.S. territory.

Finally, we analyse the effect of all the uncertainties simultaneously (case All in Figure V-A23). We find that benefits from cooperation can range from as little as 11.5% to as much as 17.9%, that is, from US\$1.2 billion less to US\$16.8 billion more than in the deterministic case. The sensitivity analysis therefore shows that cooperation can bring significant benefits even when uncertainties are considered, that is, uncertainties do not change the main insight obtained from the analysis. The median of the results is significantly shifted (i.e. from 12% in the deterministic case to 14% when uncertainties are considered). This mismatch might be caused by the uncertainty level of the global bound on natural gas, for which a more conservative value was established in the deterministic case.

5.7.3.2 Sensitivity of the full cooperative solution (Solution B)

Cooperation (i.e. solution B) allows bringing the U.S. electricity cost down to US\$248 billion and CO₂ emissions down to 607 Mt CO₂ when considering nominal parameters. In order to explore how these figures change in light of uncertainties, we next solve model B for the different scenarios and depict the resulting

distributions of costs (subplot V-A24a) and emissions (subplot V-A24b) in Figure V-A24.

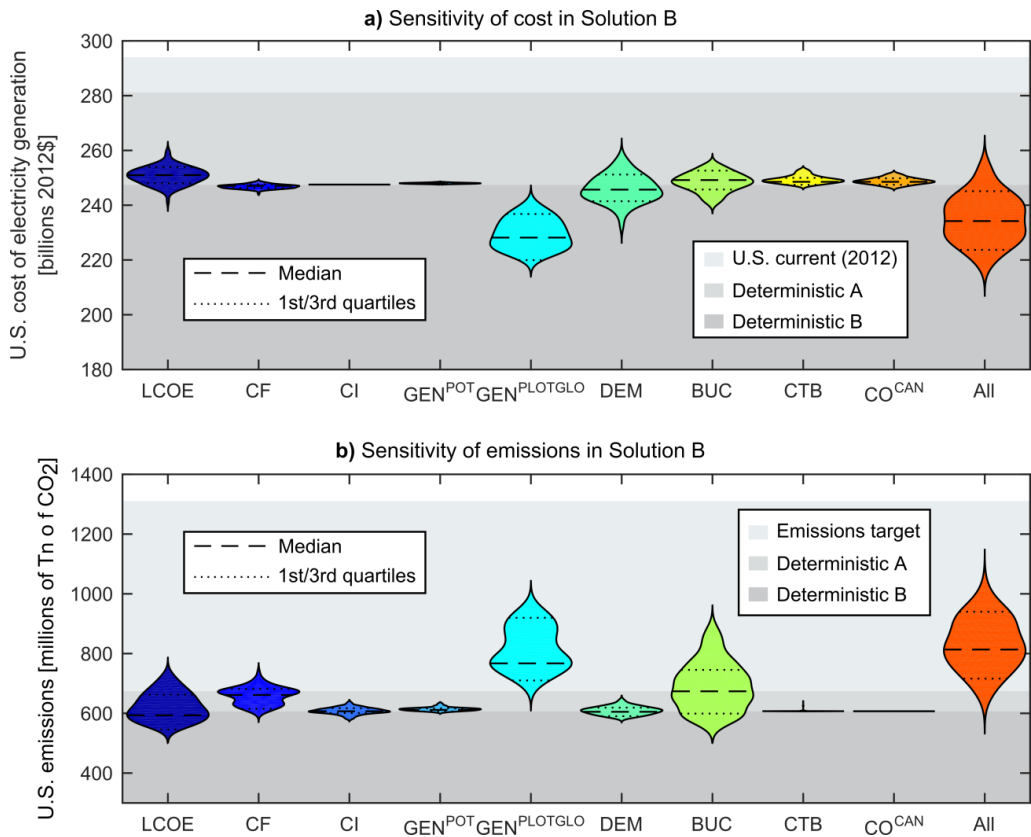


Figure V-A24 Results from the sensitivity analysis of solution B. Violin plots depict the distribution of the U.S. cost (subplot V-A24a) and emissions (subplot V-A24b) obtained when uncertainty is considered in the parameter indicated in the x axis (recall that only the cost is optimised). The width of the violin reflects the frequency (i.e. number of scenarios) of the solutions. The figure shows also the cost and emissions obtained for the deterministic parameters in solutions A and B, along with the U.S. cost in the baseline year (2012) and the CPP emissions target.

We first analyse how individual uncertainties affect the cost and emissions under full cooperation (i.e. solution B). As can be observed in Figure V-A24, the parameters with the strongest impact on the model outcome (both in cost and emissions) are LCOE, GEN^{POTGLO}, DEM and BUC. Particularly, GEN^{POTGLO} shows the biggest influence among the individual uncertainties, revealing that the total U.S. cost could be reduced by 13.7% comparing to the determinist case (i.e. US\$33.7

billion less). Furthermore, global emissions could increase by 72.4%, as a result of enlarging the share of natural gas in the overall electricity mix (recall that scenarios on GEN^{POTGLO} relax the global bound on natural gas-based resources). The total U.S. cost varies similarly when uncertainties in LCOE or DEM are considered (between -4.0% and +6.4%, and between -8.7% and +6.84%, respectively), yet the total emissions reflect a higher variation for the former (i.e. between -17.7% and +30.5%, compared to -6.5% and +9.1%). This can be explained as follows. In the deterministic solution B, emissions fall well below the CPP target (i.e. 70% reduction vs the 35% required). This occurs because the model decides to install technologies based only on their economic competitiveness, and some of the most competitive ones happen to show in turn lower carbon intensities. In such context, the order of the economic competitiveness of two technologies showing similar costs but very different CO_2 emissions can be switched when uncertainties are considered in the LCOE, thus significantly affecting the overall figure regarding the emissions. This does not happen when the uncertain parameter is the demand, since the economic competitiveness of the technologies remains the same. Finally, the uncertainty on the BUC affects more the emissions than the costs. Hence, the cost in solution B can vary $\pm 4.5\%$, while the emissions can either be reduced or increased significantly (i.e. from almost 17.7% reduction to a 58.8% increase). Recall that this parameter provides the amount of firm technologies required as back up for each MWh of intermittent renewables installed. Taking into account that the carbon intensity of firm technologies is in average higher than that of intermittent resources (which are all zero-emitting), it is not surprising that different values of BUC have a strong impact on the overall cleanness of the U.S. portfolio.

We then analyse all the uncertainties simultaneously (case All in Figure V-A24), noting that both costs and emissions show the most significant sensitivity among all the cases. As can be observed, the cost is lower than in the deterministic case in most scenarios (between -16.5% and +7.3%) while the opposite holds for the emissions (-12.6% and +89.6%), evidencing the high influence of GEN^{POTGLO} in these

results. Besides, in this case, as well as in general terms, the uncertainties affect more the distribution of emissions than that of the cost. This is due to the margin existing between emissions in the deterministic solution B and the target imposed by the CPP.

5.7.4 Nomenclature

5.7.4.1 Indexes

i	Technologies.
j	U.S. states.
k	Canadian regions.

5.7.4.2 Sets

CT	Set of coal-based technologies i .
IR	Set of intermittent (i.e. non-dispatchable) technologies i .
NGT	Set of natural gas-based technologies i .
NC_j	Set of Canadian regions k which are neighbours of state j .
NU_j	Set of states j' which are neighbours of state j .

5.7.4.3 Parameters

BUC	Backup capacity of dispatchable technologies required for every MW of non-dispatchable intermittent technologies.
$CAP_{i,j}^{CUR}$	Capacity installed with technology i in state j in the baseline year (i.e. 2012).
$CF_{i,j}$	Capacity factor of technology i in state j .
$CI_{i,j}$	Carbon intensity of technology i in state j .
CO^{CAN}	Unitary annual cost of electricity imports from Canada.
$CO_{i,j}^{CAP}$	Unitary annualised capital cost of technology i in state j .
CO_i^{CAPAVE}	U.S. average unitary annualised capital cost of technology i .
$CO_{i,j}^{FIX}$	Unitary annual fixed operating costs of technology i in state j .
CO_i^{FIXAVE}	U.S. average annual fixed operating costs of technology i in state j .

$CO_{i,j}^{VAR}$	Unitary annual variable operating costs of technology i in state j .
CO_i^{VARAVE}	U.S. average annual variable operating costs of technology i in state j .
\overline{COST}_j	Annualised cost of electricity generation in state j in the optimal solution.
CS	Number of states belonging to the partnership.
CTB	Upper bound on total electricity imports from Canada.
DEM_j	Electricity demand of state j .
$DIST_{j,j'}$	Distance between states j and j' .
$DISTCAN_{j,k}$	Distance between state j and Canadian region k .
DSF	Demand satisfaction factor.
\overline{EM}_j	Optimal production-based emissions of state j .
$GEN_{i,j}^{CUR}$	Electricity generation with technology i in state j in the baseline year (i.e. 2012).
$GEN_{i,j}^{POT}$	Potential generation with technology i in state j .
GEN_i^{POTGLO}	Potential generation with technology i in U.S.
H	Annual hours (i.e. 8760).
M1	Sufficiently large positive parameter.
M2	Sufficiently large positive parameter.
$TARG_j$	Target imposed by the CPP on the CO ₂ emissions of state j .
$TARG_j^{CI}$	Target imposed by the CPP on the carbon intensity of state j .
TLF	Trade losses factor (equivalent to 0.62% per 100 km).
$\overline{TRD}_{j,j'}^{ORIG}$	Electricity exported from state j' to state j in the optimal solution.
ω_j	Cost adjustment factor for state j .

5.7.4.4 Continuous variables

$CAP_{i,j}^{BU}$	Standard capacity installed of technology i in state j .
$CAP_{i,j}^{ST}$	Backup capacity installed of technology i in state j .
$CBCOST_j$	Consumption-based annualised cost of electricity consumed in state j .
$CBEM_j$	Consumption-based CO ₂ emissions of state j .

$COST_j$	Production-based annualised cost of electricity generation in state j .
$COST_j^{CAN}$	Annual cost of electricity imports from Canada.
$COST_j^{CAP}$	Annualised capital costs of electricity generation in state j .
$COST_j^{FIX}$	Annual fixed operating costs of electricity generation in state j .
$COST^{TOT}$	Total annualised cost of electricity generation in U.S.
$COST_j^{VAR}$	Annual variable operating costs of electricity generation in state j .
EM_j	Production-based CO ₂ emissions of state j .
$GEN_{i,j}^{BU}$	Backup electricity generation with technology i in state j .
$GEN_{i,j}^{ST}$	Standard electricity generation with technology i in state j .
$TRD_{j,j'}^{DEST}$	Electricity that state j imports from state j' (after losses).
$TRD_{j,j'}^{LOSS}$	Electricity losses in electricity trade between states j and j' .
$TRD_{j,j'}^{ORIG}$	Electricity exported from state j' to state j .
$TRDCAN_{j,k}^{DEST}$	Electricity that state j imports from Canadian region k (after losses).
$TRDCAN_{j,k}^{LOSS}$	Electricity losses in electricity trade between Canadian region k and state j .
$TRDCAN_{j,k}^{ORIG}$	Electricity exported from Canadian region k to states j .
YEM_j	Continuous variable that replaces the nonlinear product of the binary Y_j by the emissions level EM_j .

5.7.4.5 Binary variables

Y_j	Binary variable denoting whether state j belongs to a partnership (i.e. value equal to 1) or not (i.e. value equal to 0).
-------	---

5.7.5 References

Antweiler, W., 2016. Cross-border trade in electricity. *J. Int. Econ.* 101, 42–51.
doi:<http://dx.doi.org/10.1016/j.jinteco.2016.03.007>

Brooke, A., Kendrick, D., Meeraus, A., Raman, R., 1998. *GAMS—A User's Manual*. GAMS Development Corporation, Washington, DC.

Brown, J.A.G., Eickhoff, C., Hanstock, D.J., 2014. *Capacity and Balancing*

Options for the Design of Power Plant in the UK. A Study carried out for the Institution of Chemical Engineers.

CEA, 2015. Canada's electricity industry.

EIA, 2016a. Independent Statistics & Analysis. Energy Information Administration. Washington, DC.

EIA, 2016b. Annual Energy Outlook 2016 with projections to 2040.

EIA, 2015. Annual Energy Outlook 2015 with projections to 2040. Washington, DC.

EPA, 2015. Clean Power Plan for existing Power Plants. Environmental Protection Agency.

Fripp, M., 2012. Switch: A Planning Tool for Power Systems with Large Shares of Intermittent Renewable Energy. *Environ. Sci. Technol.* 46, 6371–6378. doi:10.1021/es204645c

Gross, R., Heptonstall, P., Anderson, D., Green, T., Leach, M., Skea, J., 2006. The Costs and Impacts of Intermittency: An assessment of the evidence on the costs and impacts of intermittent generation on the British electricity network.

Heuberger, C.F., Staffell, I., Shah, N., Mac Dowell, N., 2016. Quantifying the value of CCS for the future electricity system. *Energy Environ. Sci.* 9, 2497–2510. doi:10.1039/C6EE01120A

Kander, A., Jiborn, M., Moran, D.D., Wiedmann, T.O., 2015. National greenhouse-gas accounting for effective climate policy on international trade. *Nat. Clim. Chang.* 5, 431–435.

Law, A., Kelton, D., 2000. Simulation modeling and analysis. *Ser. Ind. Eng. Manag. Sci.*

Lilliestam, J., Bielicki, J.M., Patt, A.G., 2012. Comparing carbon capture and storage (CCS) with concentrating solar power (CSP): Potentials, costs, risks, and barriers. *Energy Policy* 47, 447–455.

Lopez, A., Roberts, B., Heimiller, D., Blair, N., Porro, G., 2012. US renewable energy technical potentials: a GIS-based analysis. NREL.

Marathe, R.R., Ryan, S.M., 2005. On the validity of the geometric Brownian motion assumption. *Eng. Econ.* 50, 159–192.

NERC, 2015. Potential Reliability Impacts of EPA's Proposed Clean Power Plan-Phase I. North American Electric Reliability Corporation. Atlanta.

Partnership, E.R., 2015. Managing Flexibility Whilst Decarbonising the GB Electricity System.

Pfenninger, S., Gauché, P., Lilliestam, J., Damerau, K., Wagner, F., Patt, A., 2014. Potential for concentrating solar power to provide baseload and dispatchable power. *Nat. Clim. Chang.* 4, 689–692.

Short, W., Sullivan, P., Mai, T., Mowers, M., Uriarte, C., Blair, N., Heimiller, D., Martinez, A., 2011. Regional energy deployment system (ReEDS). Contract 303, 275–3000.

Springmann, M., 2014. Integrating emissions transfers into policy-making. *Nat. Clim. Chang.* 4, 177–181.

Steininger, K., Lininger, C., Droege, S., Roser, D., Tomlinson, L., Meyer, L., 2014. Justice and cost effectiveness of consumption-based versus production-based approaches in the case of unilateral climate policies. *Glob. Environ. Chang.* 24, 75–87.

Tehrani Nejad M, A., 2007. Allocation of CO₂ emissions in petroleum refineries to petroleum joint products: a linear programming model for practical

application. *Energy Econ.* 29, 974–997.

U.S. Army Corps of Engineers., 2011. Civil works construction cost index system.

Usaola, J., 2012. Operation of concentrating solar power plants with storage in spot electricity markets. *IET Renew. power Gener.* 6, 59–66.

Chapter VI

Appendix

UNIVERSITAT ROVIRA I VIRGLI

CONTRIBUTION TO THE DEVELOPMENT OF MATHEMATICAL PROGRAMMING TOOLS TO ASSIST DECISION-MAKING
IN SUSTAINABILITY PROBLEMS

Àngel Galán Martín

VI. APPENDIX

5.8 List of publications

Click on the icons below to go to the author's profiles.



Author's ORCID: orcid.org/0000-0002-1209-0985

5.8.1 Research articles

- [1] [Á. Galán-Martín](#), C. Pozo, A. Azapagic, I. E. Grossmann, N. Mac Dowell, G. Guillén-Gosálbez. Time for global action: An optimised cooperative approach towards effective climate change mitigation. *Energy & Environmental Science*, 2017, DOI: 10.1039/C7EE02278F. Area: Environmental sciences (1 of 229/Q1) / Energy and fuels (1 of 99/Q1). Impact Factor: 29.518
- [2] [Á. Galán-Martín](#), P. Vaskan, A. Antón, L. J. Esteller, G. Guillén-Gosálbez. Multi-objective optimization of rainfed and irrigated agricultural areas considering production and environmental criteria: a case study of wheat production in Spain. *Journal of Cleaner Production*, 2017, Vol. 140, Part 2, 816-830. Area: Environmental sciences (24 of 229/Q1) / Environmental engineering (10 of 47/Q1). Impact Factor: 5.715
- [3] [Á. Galán-Martín](#), G. Guillén-Gosálbez, L. Stamford, A. Azapagic. Enhanced data envelopment analysis for sustainability assessment: A novel methodology and application to electricity technologies. *Computer & Chemical Engineering*, 2016, Vol. 90, 188-200. Area: Computer science (15 of 102/Q1) / Engineering, Chemical (22 of 135/Q1). Impact Factor: 3.024
- [4] A. Ewertowska, [A. Galán-Martín](#), G. Guillén-Gosálbez, J. Gavalda, L. J. Esteller. Assessment of the environmental efficiency of the electricity mix of the top European economies via data envelopment analysis. *Journal of Cleaner Production*, 2016, Vol. 116, 13-22.

Area: Environmental sciences (24 of 229/Q1) / Environmental engineering (10 of 47/Q1).

Impact Factor: 5.715

[5] Á. Galán-Martín, C. Pozo, G. Guillén-Gosálbez, A. A. Vallejo, L. J. Esteller.

Multi-stage linear programming model for optimizing cropping plan decisions under the new Common Agricultural Policy. *Land Use Policy*, 2015, Vol. 48, 515-524. Area: Environmental studies (10 of 100/Q1). Impact Factor: 3.089

5.8.2 Book chapters

[1] Á. Galán-Martín, G. Guillén-Gosálbez, L. Stamford, A. Azapagic.

Enhanced data envelopment analysis for sustainability assessment.

Computer Aided Chemical Engineering, 2016, Vol. 38, 817-822, ISSN: 1570-7946

5.9 Scientific conferences participations

5.9.1 Oral communications

[1] Á. Galán-Martín, G. Guillén-Gosálbez, L. Stamford, A. Azapagic. Novel data envelopment analysis approach for sustainability assessment: application to electricity generation technologies. *American Institute of Chemical Engineers "2016 AIChE Meeting"*. November 2016. San Francisco (California, United States). ISBN: 978-0-8169-1097-7

[2] Á. Galán-Martín, P. Vaskan, G. Guillén-Gosálbez, A. Antón Vallejo, L. Jimenez Esteller. *American Institute of Chemical Engineers "2015 AIChE Meeting"*. Multi-objective optimization applied to sustainable rain-fed and irrigated crop production: A case study of wheat production in Spain. November 2015. Salt Lake City (Utah, United States). ISBN: 978-0-8169-1094-6.

[3] Á. Galán-Martín, P. Vaskan, G. Guillén-Gosálbez, A. Antón Vallejo, L. Jimenez Esteller. *"13th Mediterranean Congress of Chemical Engineering"*. Multi-objective optimization applied to sustainable rain-fed and irrigated crop production: A case study of wheat production in Spain. October 2014. Barcelona (Spain).

5.9.2 Poster presentations

[1] Á. Galán-Martín, G. Guillén-Gosálbez, L. Stamford, A. Azapagic. Enhanced data envelopment analysis for sustainability assessment. *26th European Symposium on Computer-Aided Process Engineering*. June 2016. Portorož (Slovenia). ISBN: 978-0-4446-3444-3.

- [2] A. Ewertowska, A. Galán-Martín, G. Guillén-Gosálbez, J. Gavaldá, L. J. Esteller. *American Institute of Chemical Engineers "2015 AIChE Meeting"*. Assessment of the environmental efficiency of the electricity mix of the top European economies via data envelopment analysis. November 2015. Salt Lake City (Utah, United States). ISBN: 978-0-8169-1094-6.

UNIVERSITAT ROVIRA I VIRGLI

CONTRIBUTION TO THE DEVELOPMENT OF MATHEMATICAL PROGRAMMING TOOLS TO ASSIST DECISION-MAKING
IN SUSTAINABILITY PROBLEMS

Àngel Galán Martín



UNIVERSITAT ROVIRA I VIRGILI

Contribution to the development of mathematical programming tools to assist decision-making in sustainability problems

Impacts from human activities are exceeding the Earth's carrying capacity, which may lead to irreversible changes posing a serious threat to future human well-being and the environment. This situation calls for urgent and effective actions when facing ongoing and emerging sustainability challenges which help us to move towards a sustainable development.

This thesis focuses on two key structural transformations needed to reconnect the human development to sustained progress: the "sustainable food security transformation", through decoupling the intensification of agricultural production from unsustainable use of resources; and the "clean energy transformation", supporting the transition towards a more environmentally friendly economy. This thesis proposes sound and flexible mathematical programming tools to support sustainable decision and policy-making aiming at facilitating the transition towards a new era where the economic growth, the environmental stewardship and social progress coexist as key pillars of sustainable development.

